



Dipl. Ing. Wolfgang Richter

Surge Tank Design for Flexible Hydropower

DOCTORAL THESIS

to achieve the university degree of
Doktor der technischen Wissenschaften
submitted to

Graz University of Technology

Tutor

Univ.-Prof. Dipl.-Ing. Dr.techn. Gerald Zenz
Institute of Hydraulic Engineering and Water Resources Management

External Reviewers

Prof. Dr. Robert Boes, Eidgenössische Technische Hochschule, ETH Zürich
Prof. Leif Lia, Phd, Norwegian University of Science and Technology, NTNU Trondheim

Graz, February 2020

AFFIDAVIT

I declare that I have authored this thesis independently, that I have not used other than the declared sources/resources, and that I have explicitly indicated all material which has been quoted either literally or by content from the sources used. The text document uploaded to TUGRAZonline is identical to the present doctoral thesis.

Date

Signature

With love to
Ines, Sofie and Maja

ABOUT THE AUTHOR

Personal Data

Name: Wolfgang Richter

Education

- 2010 – 2020 Doctoral Programme in Engineering Sciences
Project and research assistant at the Institute of Hydraulic Engineering and Water Resources Management, Graz University of Technology
- 2013 (August) Outgoing – Research Cooperation with the Department of Hydraulic and Environmental Engineering, NTNU Trondheim, Norway
- 2000 – 2010 Diploma Studies – Civil Engineering, University of Innsbruck, Austria
Specialisation Modules: Hydraulic Engineering and Alpine Technologies; Sanitary Environmental Engineering
Diploma Thesis (in German) at Unit of Hydraulic Engineering: 3D-numerische Strömungssimulation von hydraulischen Rückstromdrosseln in Wasserschlässern; 3D-CFD simulation of hydraulic differential throttles in surge tanks [1]
Outgoing: Università La Sapienza, Facoltà d'Ingegneria, Roma, Italia, 09/2004 – 07/2005
- 1995 – 2000 Technical High School for Civil Engineering, Innsbruck, Austria

1.1 Journal Publications

Richter W., Knoblauch H. & Zenz G.; Surge Tank Design for Storage-Tunnels, in Wasserwirtschaft Extra S1, 2019

Richter W., Zenz G., Nicolet Ch.; Landry Ch., Vera Rodriguez J.C., De La Torre Abietar L.; Hydraulics of the Tail Race Surge Tank of Gouvães Pumped-Storage Hydropower, in: Wasserwirtschaft Extra S1, 2019

Richter W., Vereide K. & Zenz G.; Optimizing surge tank layout for highly flexible hydropower, in: Hydropower & Dams Volume 25 Issue 3, 2018

Richter W., Vereide K. & Zenz G.; Upgrading of a Norwegian pressurized sand trap combined with an open air surge tank, in: Geomechanics and Tunnelling (pg. 621-624, 2017

ABOUT THE AUTHOR

Richter W., Zenz G., Knoblauch H., Schneider J.; Surge tanks for high-head hydropower plants - Hydraulic layout - New developments - Wasserschläsler für Hochdruck-Wasserkraftanlagen - Hydraulische Auslegung - Neue Entwicklungen, in: Geomechanics and Tunneling 8, 1, S. 60 - 73, 2015

Richter W., Schneider J., Zenz G., Kolb S.; Degassing in a chamber surge tank (in German) Entgasung in einem Kammerwasserschloss Wasserwirtschaft No. 6 Pg. 37-45, 2012

1.2 Congress Proceedings and Co-author Publications

Vera J.C., Richter W., De La Torre L., Nicolet Ch.; Design of the tailrace surge tank of Gouvães Pumped Storage Hydropower Plant; Hydro Congress, Porto, October 2019

Berg E.T., Bårgard E.H., Lia L., Richter W.; Headrace tunnel used as short-term reservoir for hydropower; Proceedings of Hydro Congress, Porto, October 2019

Pikl F.G., Richter W., Zenz G.; Large-scale economic and efficient underground energy storage; Großtechnische, wirtschaftliche und effiziente untertätige Energiespeicher (in German and English), Geomechanics and Tunneling Vol.12, Issue 3, pg. 251-269 June 2019

Wachter St., Innerhofer G. jun., Gökler G., Werle L., Richter W., Schneider J., Zenz G.; Obervermuntwerk II, Surge Tank Krespa, from Theory to Practice (in German); Obervermuntwerk II, Wasserschloss Krespa, Von der Theorie zur Praxis, proceedings of Wasserbausymposium Graz, September 2018

Pikl F.G., Richter W., Zenz G.; Hydraulic accumulator as innovative energy storage for sector coupled energy supply; Wasserakku als innovativer Energiespeicher zur sektorgekoppelten Energieversorgung, proceedings of Wasserbausymposium Graz, September 2018

Pikl F.G., Staudacher E., Richter W.; (Publishing committee), Austrian National committee on Large Dams, Pumped storage Hydropower in Austria, book, July 2018

Pikl F.G., Richter W., Zenz G.; An innovative, electric and thermal coupled energy storage (in German); Ein innovatives, elektrisch und thermisch gekoppeltes Energiespeichersystem, Proceedings 15. Symposium Energieinnovation, TU Graz, 2018

Pikl F.G., Richter W., Zenz G.; Pumped storage technology combined with thermal energy storage – Power station and pressure tunnel concept, in: Geomechanics and Tunneling, pg. 611-619, 2017

Richter W., Knoblauch H., Zenz G.; Surge tank design in Austria: Dimensioning-philosophy for flexible hydropower, Proceedings of Hydro Conference, Seville 2017

ABOUT THE AUTHOR

Vereide K., Lia L., Havrevoll O. H., Jacobsen T., Richter W.; Upgrading of Sand Traps in Existing Hydropower Plants, Proceedings of Hydro Conference, Seville 2017

Richter W., Knoblauch H., Zenz G.; Surge tank design for storage-tunnels, Proceedings of the 19th International Seminar on Hydropower plants, Vienna 2016

Richter W., Knoblauch H., Zenz G.; Wasserschlossdesign für Stollenspeicher, Proceedings of the 18th Wasserbausymposium Oberrach TU München 2016

Richter W., Schneider J., Zenz G., Innerhofer G., Gökler G.; Wasserschloss Surge tank for Obervermuntwerk II PSH: demands, investigations, realisation (in German) Obervermuntwerk II: Anforderungen, Untersuchungen, Realisierung, proceedings of the 18th Wasserbausymposium Oberrach TU München 2016

Richter W., Zenz G., Vereide K.; Hydraulic design and modelling of large surge tanks, proceedings of the 12th International Conference on Pressure Surges, Fluid Transients and Water Hammer, Editor Arris Tijsseling, Pg. 745 – 759, Dublin 2015

Vereide K., Richter W., Zenz G., Lia L.; Surge Tank Research in Austria and Norway, in: Wasserwirtschaft 1 , S. 58 - 62, 2014

Vereide K., Lia L., Richter W.; Benefits of the Air Cushion Surge chamber for Alpine Hydropower Plants, proceedings of the 18th International Seminar of Hydropower Plants, Vienna 2014

Richter W., Vereide K., Schneider J., Zenz G.; Hydraulische, Ökonomische und Nachhaltige Optimierung von Triebwasserwegen für Hochdruckwasserkraftwerke, Proceedings 13. Symposium Energieinnovation, TU Graz, 2014

Zenz G., Schneider J., Richter W., Knoblauch H.; Hydraulic Aspects on the Design of Water Conduits, proceedings High Strength Steel Symposium, TU Graz, 2013

Richter W., Schneider J., Zenz G., Innerhofer G.; Hybrid Modelling and Development of a long Upper Chamber in a Surge Tank, proceedings of Hydro Congress, Innsbruck 2013

Richter W., Schneider J., Zenz G.; Ermittlung der Lufteintragstiefe eines Wasserfalls in einem Wasserschloss, proceedings of the 15th JUWI meeting of young hydraulic researchers. Graz University of Technology 2013

Richter W.; The Waterfall in a surge tank (in German) Der Wasserfall im Wasserschloss, proceedings of the 14th JUWI meeting of young hydraulic researchers. Technische Universität München 2012

ABOUT THE AUTHOR

Richter W., Dobler W., Knoblauch H.; Hydraulic and numerical modelling of an asymmetric orifice within a surge tank, proceedings of the 4th IAHR International Symposium on Hydraulic Structures, Porto 2012

Richter W., Schneider J., Zenz G., Kolb S.; Degassing of Air Bubbles in a Chamber Surge Tank, proceedings of the 2nd European IAHR Congress, Munich 2012

Richter W., Knoblauch H., Zenz G., Larcher M.; Modellversuch Wasserschloss Burgstall, proceedings of the Wasserbausymposium, Graz University of Technology, 2012

Richter W., Schneider J., Zenz G., Kolb S.; Physical model test of surge tank Atdorf (in German) Modellversuch Wasserschloss Atdorf, proceedings of the Wasserbausymposium, Graz University of Technology, 2012

Richter W., Knoblauch H., Zenz G., Larcher M.; Transient Modeltest of Surge Tank Reisseck 2, proceedings of 2nd IAHR Europe Congress Munich 2012

Richter W., Dobler W.; Hydraulic investigation of an orifice throttle with 3D-CFD (in German) Hydraulische Untersuchung einer Düsendrossel mit CFD-Simulationen und PIV-Messungen, proceedings of the 13th JUWI meeting of young hydraulic researchers, Hannover 2011

Richter W., Gabl R.; 3D-CFD simulation of hydraulic vortex throttles in surge tanks (in German) 3D-numerische Strömungssimulation von hydraulischen Rückstromdrosseln in Wasserschlossern, - Proceedings of 12th JUWI meeting of young hydraulic researchers, Stuttgart, 2010

1.3 Presentations and Speeches

Pumpspeicher Untertage; Regenerativer Strom gespeichert in der Tiefe; Österreichische Fachtagung für Photovoltaik und Stromspeicherung, (Author: *Pikl F.G.*), Vienna 6th November 2019

Design of the tailrace surge tank of Gouvães Pumped Storage Hydropower Plant; Hydro Congress, Porto, 13th – 16th October 2019

Hydraulics of the Tailrace Surge Tank of Gouvães Pumped-Storage Hydropower – at: Vienna Hydro, Vienna – Laxenburg, 14th – 17th October 2018

Obervermuntwerk II, Wasserschloss Krespa: Von der Theorie zur Praxis – co-speech with Innerhofer G. jun. at the Wasserbausymposium Graz University of Technology, 18th Sept. – 20th Sept. 2018

Upgrading of a Norwegian pressurized sand trap combined with an open air surge tank at the 66th Geomechanics Colloquium, Salzburg, 13th Oct. 2017

ABOUT THE AUTHOR

Surge Tank Design in Austria: Dimensioning-philosophy for flexible hydropower, at: Hydro Conference, Seville, 10th October 2017

Pumped Storage Hydropower Combined with Heat Storage (in German) Pumpspeicherkraftwerk mit Wärmespeicher, at: Renexpo Interhydro, 8. Internationale Kleinwasserkraftkonferenz, Salzburg, Austria. 24 Nov. 2016

Surge Tank Design for Storage-tunnels, at: 19th International Seminar on Hydropower Plants, Vienna, Austria 10.Nov. 2016

Wasserschloss Obvermuntwerk II; Surge tank Obvermuntwerk II PSH, at the 18th Wasserbausymposium, Wallgau, Germany, 29. Jun. – 01. Jul. 2016

Combined Pumped Hydropower and heat storage, at the 14th Symposium Energieinnovation, Graz, Austria 10.-12. Feb. 2016

Value of Pumped Storage Hydropower at the 14th Symposium Energieinnovation, Graz, Austria 10.-12. Feb. 2016

Surge Tank model test with PIV at: Dantec Fluid Measurements - Workshop. on: 30.09.2015

Hydraulic design and modelling of large surge tanks, at the 12th International Conference Pressure Surges - BHR. Dublin on: 18.11.2015

Hydraulische, Ökonomische und Nachhaltige Optimierung von Triebwasserwegen für Hochdruckwasserkraftwerke; Hydraulic, economic and sustainable optimization of pwer waterways for high-head hydropower plants, at the 13th Symposium Energieinnovation, on: 13.02.2014

Druckluftwasserschlämmer für alpine Hochdruckwasserkraftanlagen; Air cushion surge tanks for alpine high-head hydropower plants at: Internationales Symposium Wasser- und Flussbau im Alpenraum. Zurich am: 25.06.2014

Behaviour of Long Chambers in Surge Tanks at the 18th International Seminar on Hydropower Plants. Vienna, Austria, 26.11.2014

Hybrid Modelling and Development of a long Upper Chamber in a Surge Tank, at the Hydro Conference, Promoting the Versatile Role of Hydro. Congress, Innsbruck on: 07.10.2013

Evaluation of air bubble intrusion of a waterfall into a surge tank (in German) Ermittlung der Lufteindringtiefe eines Wasserfalls in einem Wasserschloss, at the 15th JUWI meeting of young hydraulic researchers, on: 31.07.2013, Graz

ABOUT THE AUTHOR

Degassing of Air Bubbles in a Chamber Surge Tank, at the 2nd IAHR Europe Congress. TU München: 27.06.2012, Munich

Physical model test of surge tank Atdorf (in German) Modellversuch Wasserschloss Atdorf, at the Wasserbausymposium - Wasser - Energie - Global denken - lokal handeln: 12.09.2012, Graz

Hybrid Modeling of a Large Surge Tank, at the 17th International Seminar on Hydropower Plants, Laxenburg: 21.11.2012

Hydraulic Investigation of an orifice throttle with CFD simulations and PIV measurements (in German) Hydraulische Untersuchung einer Düsendrossel mit CFD-Simulationen und PIV-Messungen, at the 13th JUWI meeting of young hydraulic researchers, Hannover on: 03.09.2011

3D-numerische Strömungssimulation von hydraulischen Rückstromdrosseln in Wasserschlässern (in German), at the: 12th JUWI meeting of young hydraulic researchers, Stuttgart on: 11.08.2010

1.4 Projects/Surveys and Investigations - Selection

Gouvães, pumped storage hydropower, head race surge tank – physical model test

- Development of a Johnson differential surge tank
- Physical, 1D-numerical and 3D-numerical investigation of the hydraulic design
- Throttle design loss evaluation

Obervellach II, Hydropower plant

- 1D-numerical simulation of the storage-tunnel
- Numerical simulation of the sand trap, and the surge damping reservoir

Imst-Haiming, Hydropower plant

- 1D-numerical investigation of hydraulic power waterway, surge tank, balancing reservoir

Gouvães, pumped storage hydropower, tailrace surge tank – physical model test

- Physical and numerical investigation of the hydraulic design

Obervermuntwerk II, pumped storage hydropower, surge tank - physical model test

- Physical and numerical investigation of the hydraulic design of a differential throttle
- Physical and numerical investigation of the overall surge tank design and hydraulic check of final design
- Research regarding waterfall air intrusion depth

ABOUT THE AUTHOR

Atdorf, pumped storage hydropower, surge tank – physical model test

- Numerical investigation of the hydraulic design of an orifice
- Physical and numerical investigation of the overall surge tank design and hydraulic check of final design
- Research for waterfall – air intrusion and de-aeration of the lower chamber

Reisseck II, pumped storage hydropower, surge tank *Burgstall* – physical model test

- Physical and numerical investigation of the hydraulic design of a differential throttle
- Physical and numerical investigation of the overall surge tank design and hydraulic check of final design

Reports, Hydraulic investigations:

- Several surge tank design concepts for projects
- Water hammer simulations for high-head hydropower projects including reversible pump turbines
- Hydraulic design of a cavern storage system as a lower reservoir for a pumped storage scheme
- Run-of-River high-head hydropower scheme with long pressure tunnels,
- 1D-numerical investigation, applied research

Lectures (Tutor)

Hydraulic Engineering Basics (Bachelor)

- Hydraulic Engineering
- Supervision of Bachelor projects
- Laboratory courses

Hydraulic Engineering Advanced (Master)

- Hydraulic Engineering (High-head hydropower plants design)
- Numerics in Hydraulics
- Supervision of Master projects
- Supervision of Master thesis

1.5 Supervised Master Theses

Boehler C. (2019); Case study of an Underground Pumped Hydro Storage for the city of Graz Supervisors: *Knoblauch H., Richter W., Pikel F.G.*

Mauko G. (2019); Water hammer simulation for Tonstad HPP upgrade
Supervisors: *Knoblauch H., Richter W.* (ongoing)

Brener M. (2018); Historical development of pressure tunnel design in Austrian (in German) Historische Entwicklung des Druckstollenbaus in Österreich
Supervisors: *Zenz G., Richter W., Pikel F.G.*

Forsthofer Ch. (2018); 3D-CFD Simulations of a channel that acts as a retention basin between two hydropower plants (in German) Strömungsuntersuchungen eines als Ausgleichsspeicher wirkenden Anschlusskanals zwischen zwei Wasserkraftwerken
Supervisors: *Zenz G., Richter W.*

Sterner L. (2018); 3D-CFD simulations for Tonstad surge tanks upgrade
Supervisors: *Zenz G., Richter W.*

Pikel F.G. (2017); Combination of the pumped storage hydropower technology with thermal energy storage (in German) Kombination der Pumpspeichertechnologie mit thermischer Energiespeicherung
Supervisors: *Zenz G., Richter W.*

Mlinar J. (2017); Pumped storage hydropower in Austria
Supervisors: *Zenz G., Richter W.*

Hatz K. (2017); Hydraulische Optimierung der Querausleitung der Ulmendrainagen des Semmering-Basistunnel (in German)
Supervisors: *Zenz G., Richter W.*

Wagner A. (2017); Hydraulische Ausgestaltung eines Ein-/Auslaufbauwerks für ein Pumpspeicherkraftwerk (in German)
Supervisors: *Lehmann B.* (TU Darmstadt), *Richter W.*

Hambaumer K. (2017); Shifting and storing renewable energy by pumped-storage hydropower plants for the power system in Germany (in German)
Supervisors: *Knoblauch H., Richter W.*

Kaiser A. (2017); Hydraulic investigation of a tailrace tunnel for a pumped-storage power plant at the Danube
Supervisors: *Zenz G., Richter W.*

Fally S. (2017); Druckstoß in Rohrleitungen (in German)
Supervisors: *Zenz G., Richter W.*

ABOUT THE AUTHOR

Koch M. (2016); 3D-Numerische Simulationen der hydraulischen Verlustbeiwerte der asymmetrischen Drossel im Wasserschloss Krespa (in German)

Supervisors: *Zenz G., Richter W.*

Daka E. (2015); Analysis of a hydraulic surge tank model.

Supervisors *Zenz G., Richter W.*

Maierhofer K. (2015); Computational fluid dynamics modelling of large, shallow water reservoirs.

Supervisors: *Zenz G., Muschalla D. and Richter W.*

Ingmar Nopens and Daan Van Hauwermeiren, (Gent University)

Urach T. (2015); Investigations at the physical model test of the surge tank Krespa of the Obervermuntwerk II pumped storage power plant (in German).

Supervisors: *Zenz G., Richter W.*

Ruetz M. (2014); Particle Image Velocimetry at the physical model test of the surge tank Krespa (in German).

Supervisors: *Zenz G., Richter W.*

Wechtiitsch R. (2014); Modelling of a storage-tunnel (in German).

Supervisors: *Zenz G., Richter W.*

1.6 Invention Idea

The principle concept of combined electrical and heat storage concept by means of a closed loop pumped storage plant containing water that can be heated up to 90°C. The aim is to balance and shift electrical energy by pumped storage and additionally store summer heat in the water reservoir for usage in winter to allow a sustainable combining and double utilisation of two mature energy storing technologies. Presented 10.02.2016 at Energy Innovation Congress, Graz. Title: Combined Pumped Hydropower and Heat Storage (Pumpspeicherkraftwerk mit Wärmespeicher – Konzeptstudie). Describing a case study for the City of Graz. Initiation of the master thesis [2]) and the research for the dissertation of Píkl [3] [4] . ICOLD Innovation Award 2018 by Píkl [5]. Thanks to the encouraging and outstanding work of Franz Georg this issue could be followed up and is being seriously discussed to take an important part for a sustainable energy system transformation.

ABSTRACT

Surge tanks are structural components that allow safe and flexible operation of water conduits with pressurized flows that contain significant water inertias for power generation in high-head hydropower plants and pumped storage hydropower plants. Surge tanks allow safe and flexible controllability of the hydraulic machines and reduce the impact of pressure surges.

The ongoing and demanded transition of the energy system towards a renewable energy system requests for capable and sustainable renewable energy production and vast energy storage systems, utilising minimal resources by maximising the economic output. Hydropower schemes are built increasingly larger and more flexible in sense of power capacity. This aspect demands for several issues for improved surge tank design.

Several specific surge tanks were tested by means of 1D and 3D-numerical simulations as well as physical model tests. A specific large surge tank facility was investigated and compared with prototype measurements. The focus of the investigations is the hydraulic design of surge tanks with respect to the mass oscillation, discussing and stating a safety philosophy to provide robust facilities. Special focus of the work are waterfalls in surge tanks, that occur due to water outflow of upper chambers. These may intrude considerable amounts of air into the water, what needs to be controlled. The development of a specific waterfall-damping device is investigated on the basis of a physical model test and the realised prototype. Storage-tunnel surge tanks and semi-air cushion surge tanks as further improvements for surge tank design are investigated. Hydraulically optimized surge tanks show minimised excavation volumes and low coefficients of inertia for water hammer reflections. They are very robust and constructed without moving parts for operation, to allow safe and effective maintenance. To dampen the mass oscillation for large surge tanks for flexible hydropower schemes, passive differential effects such as hydraulic throttles and upper chamber effects show high effectiveness for safe and economic designs.

KURZFASSUNG

Wasserschläsler sind hydraulische Bauteile, die einen sicheren und flexiblen Betrieb von Hochdruckwasserkraftwerken und Pumpspeicherkraftwerken mit Druckstollen bei signifikanten Wassermengen ermöglichen. Effektive Wasserschläsler ermöglichen eine sichere Steuerung der hydraulischen Maschinen und verringern die Amplituden von Druckstößen.

Der Umbau des Energiesystems zu einem auf erneuerbare Energiequellen basierenden Systems erfordert leistungsfähige und nachhaltige Erzeugung erneuerbarer Energie, sowie die Speicherung großer Energiemengen und leistungsfähiger Netzstabilisierung bei minimalen Ressourcenverbrauch und maximaler ökonomischer Nutzbarkeit über eine lange Lebensdauer. Wasserkraftwerke werden immer größer und flexibler in Bezug auf Leistung- und Energiespeicherkapazität konzipiert.

Es wurden spezifische Wasserschläsler von großen Wasserkraftanlagen mittels 1D- und 3D-numerischer Simulationen sowie physikalischer Modellversuche untersucht. Ein spezifisches Wasserschloss wurde mit Messungen im Prototyp verglichen und validiert. Der Schwerpunkt der Untersuchungen liegt auf der hydraulischen Auslegung von Wasserschläsler im Hinblick

auf die Massenschwingung und einer adäquaten Druckstoßreaktion. Es wird eine Sicherheitsphilosophie für eine robuste Auslegung von Wasserschlössern diskutiert und vorgeschlagen. Ein besonderer Schwerpunkt der Arbeit sind die Untersuchungen zur Beherrschung von Wasserfällen in Wasserschlössern, die aus dem Abfluss von oberen Kammern in Kammerwasserschlössern entstehen, und welche erhebliche Luftmengen in Wasserschlösser einbringen können. Anhand physikalischer Modellversuche und des realisierten Prototyps wird die Entwicklung eines spezifischen Wasserfalldämpfungselements untersucht und verifiziert. Speicherstollen Wasserschlösser und Semi-Luftdruck Wasserschlösser werden als weitere Verbesserungen als Wasserschlosskonstruktionen untersucht und vorgeschlagen. Hydraulisch optimierte Wasserschlösser weisen ein minimiertes Volumen und niedrige Trägheitskoeffizienten auf. Sie sind sehr robust und ohne bewegliche Teile für den Betrieb konstruiert, und ermöglichen eine sichere und effektive Wartung. Um die Massenschwingung in Wasserschlössern für große und flexible Wasserkraftanlagen zu dämpfen, erweist sich die Optimierung der Differentialeffekte durch hydraulische Drosseln und Oberkammereffekte als besonders effektiv.

PROLOGUE

This present doctoral thesis represents the envelope and the distillate of applied surge tank research and publications of the author between the years 2008 and 2019. It was chosen to use the form of a monograph by presenting the work in terms of a handbook. Surge tanks are unique structures and depend on specific boundary conditions, thus, this doctoral thesis approaches to highlight the general and the specific design aspects of surge tank design. The goal is to discuss and emphasise via a holistic approach the surge tank research that has been done. It contains some essential outcomes from supervised Master theses, dealing with the research issue. The suggestions and proposals in relation to the Master theses are distinguished in the text.

The aim of the present work is to highlight and collect the findings during the various physical and numerical studies of surge tanks, three transient physical small-scale model tests of large surge tanks for pumped storage projects and the investigations for a large Norwegian surge tank are investigated and discussed as pilot cases in this work. Additionally, the goal is to underline the outcome of relevant literature as well as the link to comprehensive publications associated with the issue of surge tank design. The work aims to gap interdisciplinary questions and to lay the basis for further research on presented surge tank proposals such as the semi-air cushion surge tank and the storage-tunnel surge tank.

ACKNOWLEDGEMENTS

Working with water and energy is a very thankful and delighting activity. I am very thankful to my family for having a wonderful childhood high up in the Austrian Alps with full experimental freedom on brooks and mountain streams feeling the magic and helpfulness of water serving for joy and human wealth. I heartily thank my parents and my family for all the support during my whole life. I am very proud and happy for having an own family, thanks so much to my wonderful wife Ines and my fabulous daughters Sofie and Maja.

I thank all my great friends in Tirol for the fantastic time. I heartily thank my wonderful friend *Kaspar Vereide* for all the great surge tank exchange, thoughts, discussions, co-conferencing, teamwork and team researching. I am very grateful to learn much about Norway and its culture, the technical history and its indispensable role for a sustainable energy system transformation in Europe. I am very thankful for the established surge tank research exchange with Assoc. Prof. *Kaspar Vereide*, Assoc. Prof. *Elena Pummer* and Prof. *Leif Lia* from NTNU Trondheim, including the integration in numerous Master theses about special surge tank investigations and several surge tank seminars conducted with students from Graz University of Technology and NTNU Trondheim. Special thanks are dedicated to the numerous colleagues that I had the chance to work with over the times. In addition, I am glad to have the chance to study the oscillation behaviour and upgrading aspects for a large hydropower scheme such as *Tonstad* in southern Norway. I thank my friend *Wolfgang Dobler* for the great surge tank collaboration for my first years at the institute in Graz, and *Gabriele Harb* for all the enthusiastic hydraulic engineering talks. I am grateful to *Markus Larcher* for having many fruitful discussions as well as the constructive collaboration for the *Burgstall* surge tank project. I thank very much the team from Illwerke engineering and the team for the kind cooperation at the *Atdorf* surge tank investigations. I thank very much the colleagues from TIWAG for the great collaboration on numerous high-head hydropower applied research projects. Especially I gratefully thank *Robert Reindl* for the supervision of the diploma thesis about the surge tank simulations of various power plants that has triggered my personal appreciation for surge tanks and the eager to dig deeper into this interesting issue.

The applied research work of the author in collaboration with others has led to several improvements and developments described in this present work, such as the waterfall-dampening device for surge tank *Krespa* at *Obervermuntwerk II*, the idea of a semi-air cushion surge tank as general application and in special for *Tonstad* surge tank upgrade. In addition, a storage-tunnel surge tank design was developed to utilise storage-tunnels that can have free surface flow or pressurized flow conditions improving several purposes.

Thanks to the interdisciplinary scientific environment at Graz University of Technology. I am very grateful about the engaged work of my colleague *Franz Georg Pikel* on underground pumped hydro and combined pumped hydro.

I thank very much Prof. *Gerald Zenz* for the great working environment and the kind supervision of this thesis. I am very grateful for the constructive cooperation in the surge tank projects with *Helmut Knoblauch* and *Josef Schneider* and all the other wonderful colleagues that have been accompanying and this path with me in Graz.

ACKNOWLEDGEMENTS

I am very thankful for all the master students generating very valuable work and outcomes regarding the issues of surge tanks, pumped storage plants and the energy transition.

I am very thankful for the external review work and the valuable feedback of Prof. *Robert Boes* from ETH Zürich and Prof. *Leif Lia*, from the Norwegian University of Science and Technology, Trondheim.

Thanks to all persons I could collaborate, communicate and brain-gain with.

I thank Prof. *Weinberger* at the University of Innsbruck for the most inspiring lecture of my career, that was: *Astronomy for all students*, by. I learn about the statistically rule of thumb proof that: The earth, with its habitable atmosphere and its complex living creatures is an absolute exception in the universe and very most likely the only one of its kind in the whole galaxy (that alone contains ~100 billion solar systems). Thus, we need to take care and do our best to preserve the book of life. One thing we can do is to adapt the energy system by a fundamental transition towards a fully renewable supply.

CONTENT

ABOUT THE AUTHOR	i
1.1 Journal Publications.....	i
1.2 Congress Proceedings and Co-author Publications	ii
1.3 Presentations and Speeches	iv
1.4 Projects/Surveys and Investigations - Selection	vi
1.5 Supervised Master Theses	viii
1.6 Invention Idea	ix
ABSTRACT	10
KURZFASSUNG	10
PROLOGUE.....	11
ACKNOWLEDGEMENTS.....	12
CONTENT	14
ABBREVIATIONS	18
LIST OF SYMBOLS	19
DEFINITIONS	20
1. INTRODUCTION	22
1.1 Problem Outline – Hypothesis.....	22
1.2 Goal and Objectives	22
1.3 Research Methodology	23
1.4 Outline of the Thesis.....	23
2. ENERGY ASPECTS	24
2.1 Electrical Energy Situation in the Alpine Region.....	24
2.2 Storage Demands for High Shares of Renewable Power	29
2.3 High-Head and Pumped Storage Hydropower	35
2.4 Combined Pumped and Thermal Energy Storage	42
2.5 Machinery Concepts.....	43
3. FUNDAMENTALS AND STATE OF THE ART	45
3.1 General Aspects	45
3.2 Historic Aspects	45
3.3 Purposes of the Surge Tank.....	46

CONTENT

3.4	Design Criteria	50
3.4.1	Surge Tank Requirements	50
3.4.2	Maximum and Minimum Oscillation	54
3.4.3	Stability Criterions of Surge Tanks	54
3.5	Surge Tank Design in Austria	59
3.6	Surge Tank Prototype Development for Large Schemes	65
3.7	Hydraulic Safety Design Philosophy	67
3.8	Roughness Considerations	69
3.9	Complex Surge Tank Concepts	73
4.	SURGE TANK CASE STUDIES	76
4.1	Atdorf – Tailrace Surge Tank.....	77
4.2	Burgstall – Tailrace Surge Tank	80
4.3	Krespa - Headrace Surge Tank	82
4.4	Tonstad - Headrace Surge Tank.....	85
5.	INVESTIGATION METHODS	87
5.1	Physical Model Tests	88
5.1.1	Froude Similarity Law	89
5.1.2	Euler Similarity Law	90
5.1.3	Reynolds Similarity Law	90
5.1.4	Weber Similarity Law	91
5.1.5	Physical Throttle Model	91
5.1.6	Physical Full Model.....	96
5.1.7	PIV Measurements	99
5.1.8	Small-Scale Model for Water Hammer	100
5.2	1D-Numerical Simulations	101
5.2.1	Mass Oscillation	102
5.2.2	Water Hammer	105
5.2.3	Stability Simulation	106
5.2.4	Surge Tank Inertia	107
5.3	3D-Numerical Simulations	108
5.4	Hybrid Modelling – Physical Model Test and 3D-CFD	110
5.5	Prototype Measurements	112
6.	RESULTS AND DISCUSSION	113

CONTENT

6.1	Load-case Scenarios	113
6.1.1	Headrace Surge Tanks	114
6.1.2	Tailrace Surge Tanks	116
6.2	Surge Tank Lining.....	118
6.3	Air Cushion Surge Tanks	121
6.3.1	Existing Air Cushion Chambers for Alpine Adaptions	124
6.3.2	Proposed Possible Arrangement of Alpine ACST	124
6.3.3	Challenges with Air Cushion Surge Tanks	126
6.4	Surge Tank Upgrade.....	127
6.4.1	Case Study of Surge Tank Upgrade.....	127
6.4.2	Attached Additional Chamber	129
6.5	Semi-Air Cushion Surge Tank Proposal.....	131
6.5.1	General Proposal of Semi-Closed Surge Tanks	136
6.5.2	Design Process of Semi-Closed Surge Tanks	139
6.5.3	Thermodynamic Effect	140
6.6	Storage-Tunnel Surge Tank	141
6.6.1	Storage-Tunnel Surge Tank Operation	142
6.6.2	Stability Criterion for Storage-Tunnel Surge Tanks	146
6.6.3	Case Study Simulation for a Storage-Tunnel Surge Tank	146
6.6.3.1	Stability Criterion	146
6.6.3.2	Simulation of the Storage-Tunnel Surge Tank.....	147
6.7	Surge Tank Details	151
6.7.1	Throttle Design	151
6.7.2	Orifice Throttle	152
6.7.3	Differential Orifice Throttle.....	153
6.7.4	Differential Vortex Throttle	155
6.7.5	Aeration Shaft	156
6.7.6	Flow Direction Aspects for Throttle Losses	158
6.7.7	PIV Measurements of a Throttle	159
6.7.8	Long Upper Chambers - Hydraulic Behaviour	165
6.8	Waterfalls in Surge Tanks	170
6.8.1	Air Bubble Entrainment	172
6.8.2	Numerical Simulation of Waterfalls	174

CONTENT

6.8.3	Criterion of Similitude of Air Intrusion.....	177
6.8.4	Terminating Velocity of Air Bubbles	177
6.8.5	Methods for Determining the Air Penetration Depth	178
6.8.5.1	Equation of <i>Clanet and Lasheras</i>	178
6.8.5.2	Experimental Air Intrusion Depth by Ervine and Falvey	179
6.8.5.3	3D-Numerical Simulation of Waterfalls.....	180
6.8.5.4	Hydraulic Froude Scale Model.....	180
6.8.5.5	PIV Measurements of Air Intrusion Depth.....	183
6.8.6	Air Detrainment in 3D-numerical Multi-phase Simulation Approach.....	186
6.8.7	Waterfall-Dampening Device.....	188
6.9	Surge Tank Commissioning.....	192
6.10	Prototype Measurements at Krespa Surge Tank.....	193
7.	SUMMARY AND OUTLOOK.....	198
8.	BIBLIOGRAPHY	201
	LIST OF FIGURES.....	218
	LIST OF TABLES.....	225

ABBREVIATIONS

ACST	Air cushion surge tank
CAES	Compressed Air Energy Storage
CAPEX	Capital Expenditure
CFD	Computational Fluid Dynamics
CST	Chamber surge tank
EEX	European Energy Exchange
ENTSO-E	European Network of Transmission System Operators
EROI	Energy Return on Energy Invested
ESOI	Energy Stored on Energy Invested
ESD	Emergency shutdown
FEM	Finite element method
GHG	Greenhouse gas
HPP	Hydropower Plant
HW	Headwater
IFM	Inductive Flowmeter
IWB-TU	Institute of Hydraulic Engineering and Water Resources Management (Graz Technical
GRAZ	University)
LC	Load-case
LCOD	Levelized cost of delivery
LCOE	Levelized cost of electricity
LCOS	Levelized cost of storage
LCh	Lower chamber of a surge tank
m.a.A.	Meters above Adriatic Sea-level
MOC	Method of characteristic
MRHT	Modified Rational Heat Transfer (method)
MT	Physical model test (hydraulic small-scale test)
MW	Mega Watt
m w.c.	Meter water column
NTNU	Norwegian University of Science and Technology, Trondheim Norway
OVW I	Obervermuntwerk I HPP – stage between Silvretta reservoir (upper) and Vermunt reservoir (lower)
OVW II	Obervermuntwerk II PSH, new pumped storage hydropower stage between Silvretta reservoir (upper) and Vermunt reservoir (lower)
P2G	Power to Gas
PID	Proportional – Integral – Derivative Controller
PIV	Particle image velocimetry
PSH	Pumped Storage Hydropower
PT	Pressure Tunnel
PV	Photovoltaic
Q	Discharge
RANS	Reynolds Average Navier Stokes
RES	Renewable energy sources
RES-E	Renewable energy sources - electricity
SST	Shear stress turbulence model
ST	Surge tank
TSO	Transmission system operator

LIST OF SYMBOLS

$a_{,0}$	Distance between the surge chamber roof and the water level in a surge chamber with vertical walls and a horizontal roof	[m]
A	Cross sectional area	[m]
A_i	Internal flow section area	
A_{ST}	Cross sectional area of the open-air surge tank shaft	[m ²]
$A_{SV,AIR}$	Cross sectional area according to Svee criterion, air cushion surge tanks	[m ²]
A_{SV}	Cross sectional surge tank shaft area according to Svee criterion for tailrace and headrace systems	[m ²]
A_T	Cross sectional area of the pressure tunnel	[m ²]
A_{TH}	Cross sectional area according to Thoma criterion	[m ²]
D_i	Internal diameter	[m]
D_{jet}	Jet diameter entering a water surface	
D_T	Diameter Pressure tunnel	[m]
E_k	Kinetic energy	[J], [Nm], [Ws]
E_p	Potential energy	[J]
H	Head, gross head	[m a.s.l], [m]
H_o	Mean reference head at turbine	[m]
H_B	Air bubble penetration depth	[m]
H_G	Gross head	[m]
h_{HL}	Head loss	[m]
$h_{HL,0}$	Head loss in the pressure tunnel at reference discharge	[m]
h_v	Local hydraulic loss	[m]
h	Height	[m]
K_M	Manning number	[s/m ^{1/3}]
K_S	Equivalent sand grain roughness	[mm]
K_{ST}	Strickler roughness	[m ^{1/3} s ⁻¹]
L	Length	[m]
N	Rotational speed	[rpm]
N_{11}	Unit speed factor	[-]
Nm^3	Normal cubic meter (air volume at atmospheric pressure)	[m ³]
Q_o	Reference flow rate at turbine	[m ³ /s]
Q_d	Design discharge	[m ³ /s]
Re	Reynolds number	[-]
T	Torque	[Nm]
T_{11}	Unit torque factor	[-]
T_a	Mechanical inertial time constant of the rotating masses	[s]
T_c	Closing time	[s]
T_L	Length of pressure tunnel	[m]
T_r	Water hammer reflexion time	[s]
T_W	Hydraulic inertial time constant for the water conduit	[s]
J	Inertia of the rotational mass	[kgm ²]
P_{max}	Full power output	[W]
$P_{z,0}$	Pressure of air cushion, steady-state condition	[N/m ²]
P	Power	[W]
Q	Discharge	[m ³ /s]
Q_{11}	Unit discharge factor	[-]
V	Volume	[m ³]

DEFINITIONS

α_0	Distance between the surge chamber roof and the water level in a surge chamber with vertical walls and a horizontal roof [m]	[m]
f	Friction factor equivalent to λ	[-]
m	Mass	[kg]
mwc	Meter water column	[m]
n_{11}	Unit speed factor	[-]
n	Polytropic exponent	[-]
p	pressure	[Pa]
s	second	[s]
u_B	Terminating velocity of a single bubble	[m/s]
v	Velocity	[m/s]
$v_{T,0}$	Velocity in Tunnel at reference discharge	[m/s]
v_{jet}	Jet velocity at water surface	[m/s]
α	Friction coefficient	[s ² /m ⁵]
α_{jet}	Opening angle of a waterfall jet dissipating in the water	[°]
η	Efficiency	[-]
γ	Specific weight of water	[N/m ³]
λ	Friction coefficient	[-]
ρ	Density	[kg/m ³]
ν	Kinematic viscosity	[m ² /s]
σ	Surface tension	[N/m]
σ_1	Maximum principal rock stress	[Pa]
σ_3	Minimum principal rock stress	[Pa]
ω	Angular speed	[s ⁻¹]

DEFINITIONS

This chapter defines crucial and new words for the present work:

Ancillary services	Services to provide stable and secure grid operation beyond generation and transmission such as frequency control, spinning reserves or operating reserves.
Borda mouthpiece	Thin cylindrical extension at an orifice throttle to enhance the differential loss factor ratio.
CCD	Charge-Coupled Device; sensor in the digital high-speed camera
Crown throttle	Throttle device at the crown of a chamber for the purpose to trap air and create an air cushion with delayed air release.
Hydraulic transients	High- and low frequency oscillations in pipe systems. High frequency transients are meant to be pressure pulse induced by water hammer events. Low frequency transients are meant to be mass oscillations also called surge tank oscillations or U-tube oscillations. These secondary oscillations are triggered by the fact of the free surface in the surge tank. The free surface is needed to

DEFINITIONS

	counteract and mitigate the water hammer effects. For best functionality, low inertia values of the surge tank are pursued.
Fixed speed PSH	Pumped storage hydropower plants with machine units that are operating solely at a fixed rotational speed.
Flexible PSH	Flexible pumped storage hydropower defines schemes with machine units that can be switched quickly and continuously between pumping and turbine mode, such as schemes utilising variable speed technology with a full size converter or schemes with ternary machine units.
Storage-tunnel surge tank	Novelty of this dissertation. A surge tank enabling a proper use of pressurized water conveyance tunnels that act as storage facility for a HPP. Development made during this dissertation and discussed for application, (see chapter: 6.5).
Walch's limit	The intersection of the crack water table and the internal pressure along the pressure tunnel – defines the need of watertight lining.
Waterfall-dampening device	Developed novelty of this dissertation by the author in cooperation with Illwerke AG to dampen the air bubble intrusion for the surge tank Krespa for <i>Obervermuntwerk II</i> PSH, (see chapter: 6.8.7).
Semi-closed surge tank respectively Semi-air cushion surge tank	Novelty of this dissertation. A surge tank device using a crown throttle and small deaeration pipe for the purpose of trapping air for delayed de-aeration and filling of significant water volume of the crown region of a lower expansion chamber to create a differential effect for mass oscillation dampening, (see chapter: 6.5 and 6.5.1).

1. INTRODUCTION

1.1 Problem Outline – Hypothesis

Surge tanks are well proven structural facilities for hydropower plants with sometimes complex hydraulic behaviour. New high-head schemes and especially new pumped storage schemes are built with significantly increased demands regarding installed capacity and flexibility. Since pumped storage schemes allow very long-life times and provide efficient electric storage as well as grid stabilizing services these facilities are indispensable for the ongoing energy transition towards higher shares of renewables. For providing safe operation conditions surge tanks must be constructed in a different manner as they were in the past. Larger installed capacities demand for higher discharges and thus show higher inertias in the pressure tunnels that is directly affecting the surge tank design. Quick operational changes between different operation modes demand for safe and economic structures with innovative solutions. Surge tank research for hydropower plants has been going on since the early days of hydroelectric developments. Due to this long period some facts may become difficult to trace. The thesis of the Svee stability criterion for tailrace tunnels was developed at the author's institute but not known. Other questions are such as:

- How to best integrate numerical simulation tools in the surge tank design process?
What makes sense, what are the limits and what can the future bring?
- How can the differential effects in the surge tank be efficiently utilised for further improvements?
- What are the effects of a waterfall in a surge tank? How can the air bubble intrusion be mitigated?
- What are the differences of turbine operation and pump operation in sense of demands for the surge tank design?
- What are the aspects and state of the art regarding air cushion surge tanks and the properties regarding flexible hydropower operation?

Energy systems and the electric system in specific is facing challenging times and a time of a momentum giving the chance for investments in sustainable hydro infrastructure.

1.2 Goal and Objectives

The aspects of developing new and larger high-head hydropower schemes ask firstly for a comprehensive literature review of various solutions and findings from the past and secondly for new design solutions for specific hydraulic questions. The literature gives valuable information about experience from existing plants and highlight issues to be considered for new developments. The goal of this doctoral thesis is to combine relevant knowledge from literature with new design aspects. The aim is to show new concepts to improve the surge tank operation by minimizing construction efforts. The design of storage-tunnel surge tanks is discussed that allow flexible operation for tunnel utilised as reservoirs.

INTRODUCTION

The technical novelties developed with major contribution by the author and described in the present thesis are:

- The waterfall-dampening device investigated in the model test and approved in the prototype pumped storage power plant
- The concept design of a storage-tunnel surge tank
- The proposal of principal layout of air cushion surge tanks for Alpine locations
- The proposal of a semi-closed surge tank design

Some aspects are indeed already known, however due to a lack of a general recent textbook about surge tanks these facts are collected and outlined.

The present thesis also highlights general energy aspects in relation to the energy transition and the important role of pumped storage hydropower.

In respect to the associated issues of surge tanks and pumped-storage hydropower schemes to the energy transition a main chapter is dedicated to the aspects of the energy system and the possible valuable contribution of pumped-storage hydropower. In the opinion of the author, it is vital for each energy participant to derive and understand the raw numbers of the energy system and to reflect the vital value of hydropower and pumped storage hydropower in specific.

Owed to a personal research cooperation of the author with NTNU, Trondheim the question of what can be learned from different aspects of hydropower and surge tank design in Norway and Austria is significantly influencing the present work and reflects the aspects of closed surge tanks, unlined water conduits and the issues of surge tank upgrade.

1.3 Research Methodology

The investigations are done by means of physical model testing and numerical simulations. Surge tanks are studied for recent new pumped storage schemes that are already in operation. The physical small-scale tests are conducted in the hydraulic laboratory of Graz University of Technology. 1D-numerical simulations are made to simulate and investigate mass oscillation and pressure surges events to improve surge tank design developments. Free surge pipes elements are used and tested to mix pressurized flow and free surface flow for surge tanks. 3D-numerical simulations are conducted to investigate 3D flow behaviours such as for hydraulic throttles and to outline its utilisation for investigating waterfall events and the specific filling of surge tanks.

1.4 Outline of the Thesis

Chapter (2) gives an overview of the aspects related to the electrical energy system as well as the electrical storage need as a major demand for the energy transition. Specifically, the value of pumped storage schemes is discussed. In Chapter (3) the general aspects related to surge tanks are described. Chapter (4) describes the surge tank case studies that are the basis for the investigations. The methods are expressed in Chapter (5). The results and the discussions of the investigations and the surge tank specific design aspects are described in Chapter (6). The summary of the present work as well as the outlook for further research and developments are given in Chapter (7).

2. ENERGY ASPECTS

This chapter briefly describes the general aspects of the electrical energy situation, highlighting the storage and flexibility options with the focus on pumped storage hydropower. The value of flexible operation of hydropower plants is tightly bound to surge tank design since these structures control flexible machine operation. The vast extension of electrical storage will play a crucial role in the energy transition towards the increased utilisation of renewable electricity sources since the new renewable energy sources such as wind and solar are fluctuating. Pumped storage hydropower plants are very sustainable and high flexible facilities for high efficient and vast electricity storage as well as for providing grid services.

2.1 Electrical Energy Situation in the Alpine Region

Electrical energy is among others one of the most important energy sources for modern societies. The electrical energy system has grown massively over the last 130 years after many inventions during the 19th and 20th century have made it possible to produce, supply and use electrical energy in a vast manner. On the European continent, a comprehensive interconnected and densely meshed electrical system has been constructed. Redundancies by hardware design make this system one of the most reliable energy system in the world. The connection is both its secret of success as well as the challenge for present and future operation. The grid design results from the early days of the breakthrough of the AC current system after the successful 170 km long power transmission from a hydropower plant in *Lauffen am Neckar* to Frankfurt am Main in Germany in 1891 and the exploitation of economic hydro sources [6]. Several large-scale boundary conditions are current challenges that change the demands of the power industry, such as the European market liberalisation process, the German *Energiewende* with its vast transition from conventional energy production towards a renewable energy based supply, other political aspects in association of European harmonisation processes.

It has to be recognized that the market design as well as the European power generating system are in a constant changing process. The market design in the end only tries to match the physical production with the consumers' needs and is not designed to support any vast energy transition. The transition to the goals of low carbon power production in the European Union is stated in the EU Energy roadmap 2050 [7].

To understand the electrical system and its boundary condition the nine paradigms are listed in the following from *Stigler* (2008) [8]:

1. Grid bounded

The highly meshed and interconnected power grid of very large areas reduces reserve capacities and guarantees a high security of supply.

2. Wire-bounded

Such as natural gas and long-distance heating, the electrical energy needs a longitudinal physical infrastructure to conduct the energy. To avoid multiple investments only one electrical supply company is responsible for a certain zone and thus, it is a natural monopoly.

3. Total system-bounded

The overall electrical system consists of production – transmission – distribution – consumption. Because of the ongoing liberalization process in Europe resulting in efforts for decartelisation well-engineered regulation frameworks are required. A secure operation of the grid requires that large zones are controlled by transmission system operators (TSOs) that also have access to the production facility.

4. Marginally storable of electrical energy

The crucial characteristic of electrical energy is its lack of its direct storability. Since this is not possible in an important manner, the production has to fulfil the needs at each specific point in time. The capacities have to be designed to meet the requirement of maximum demand. Appropriate reserve capacities have to be provided to guarantee continuous power supply. This led already at the beginning of the electrification to the establishment of international aggregations of power grid suppliers. In Europe: the ENTSO-E. Especially the transmission grids can minimize the reserve capacity of a single electricity entity. In combination with the high capital intensity the aim is to fulfil best possible system usage.

5. Capital-intense

All technical parts of power production and distribution show a high capital-intensity. In combination with the paradigm of long-living and the bondage to grid, wire and system the energy related structures are only slowly adaptable compared to other industries. Also the energy consumer with its multiple amount of installed power can only adapt slowly to different boundary conditions. This simultaneity factor plays a major role in the decentralisation process of the Energiewende when many producers, formerly consumers, produce with a high grade of simultaneity at the end of the supply system. The supply system was designed to fulfil the requirements regarding a low simultaneity factor.

6. Long development time

Projects regarding the power industry show usually a long period of preliminary lead time. The construction of power plants may take from first drawing to the completion from 5 – 20 years. Power lines might take even longer due to increasing public participation processes and extensive environment impact assessments.

7. Long-living

The power industry shows high values regarding long operation times of the facilities.

8. Consumer demands versus production constraints

For renewable energy sources (RES) such as Water, Solar and Wind a problem between the supply offer (production) and the time of demand appears. Especially at run-of river power plants, solar and wind power plants the energy is produced at times, at which the source is available. This results in a need of additional requirements. In Austria the high-head hydropower plants with reservoirs fulfil the demand of power peaking and shift the production from the high run-of season to the low run-of season in winter. An increasing level of RES production requires increasing measures to balance the production and the need in terms of peaking and short term as well as long term shifting. In addition, also an increased need to stabilise the grid is related to the intensified production of fluctuating energy resources.

ENERGY ASPECTS

9. Electrical energy can be produced from all primary energy sources

Electrical energy is a secondary energy source. Therefore, it can be produced and derived from all primary energy sources. This allows a high rate of diversification to guarantee the supply. Because of the mechanical generation of electrical power primary sources with direct mechanical energy offer high values of efficiency. Thermal and solar energy production show significantly lower values of generating electrical energy.

Energy exchanges in Europe and in the world allow trading with electricity. Products and prices differ from each market place, market environment and market design. Energy markets utilise the coupling between the physical production and the physical demand and are constantly adapted to changing environment of the production and the demand response in order to allow secure energy supply. This adaption process is currently visible in the vast and accelerated energy transition towards an increased renewable production, as well as in the wake of delayed transmission line constructions such as in Germany that has finally led to the marked split between Austria and Germany in 2018.

In the following examples from the Energy Exchange in Leipzig, Germany (EEX), in terms of markets for dynamic demand [9] are given:

- Energy Markets
 - EEX day-ahead (D-LU, F, A, CH)
 - EEX spot intraday 1-hour (D-LU, F, A, CH)
 - EEX spot intraday 15-minutes (D)
 - PV for own consumption (D)

- Load Markets
 - Primary control – activation and deactivation Time ≤ 30 Seconds
 - Secondary control – activation and deactivation Time ≤ 5 Minutes
 - Tertiary control – activation and deactivation Time ≤ 15 Minutes
 - (Capacity Markets)

In ENTSO-E Grid about 3000 MW are reserved for primary control. Each year its size is evaluated. Germany has to provide about 700 MW for primary control [10]. In Germany each generating unit with a nominal capacity ≥ 100 MW has to be capable of supplying primary control power for at least 2 % of the nominal power of the unit [11].

ENERGY ASPECTS

Figure 2-1 shows the time margins of grid control activities. The electrical grid frequency in Europe is 50 Hz. This frequency is constantly fluctuating. A frequency band of 0.2 Hz up to 50.2 Hz or down to 49.8 Hz is the desired range for the shared grid of the Continental Europe Synchronous Area. In a range of 0.02 Hz no counteraction is taken. The goal frequency may vary for different regions. Above this margin primary control is linearly activated up to the maximum available primary control. It is activated within 30 seconds. The purpose of the primary control is to stabilise the grid frequency. If the deviation of the target frequency persists the secondary control is activated. This is achieved within a time range of 5 minutes. Primary as well as secondary control are activated automatically by the TSO. The next higher stage of control is the tertiary control of minute reserve. Tertiary control has to be activated in a time range of up to 15 minutes. Spinning reserves in the grid related to inertia are very quickly activated. This grid stability reserve is not yet a value that can be traded. The inertia reserves are stabilising values of the generator based electric production by rotating masses. PSH equipped with electronic converters can provide a multiple amount of its physical inertia by providing virtual inertia [12].

Figure 2-1 indicates the areas of the advantage of the fast responding property of HPP or PSH. By reason or utilisation of heavy mass generators inertia is provided. Depending on the design of the HPP or PSH, it can provide highly valuable primary and secondary control. A highly flexible PSH has the additional advantage to provide negative ranges of primary and secondary control for pumping mode.

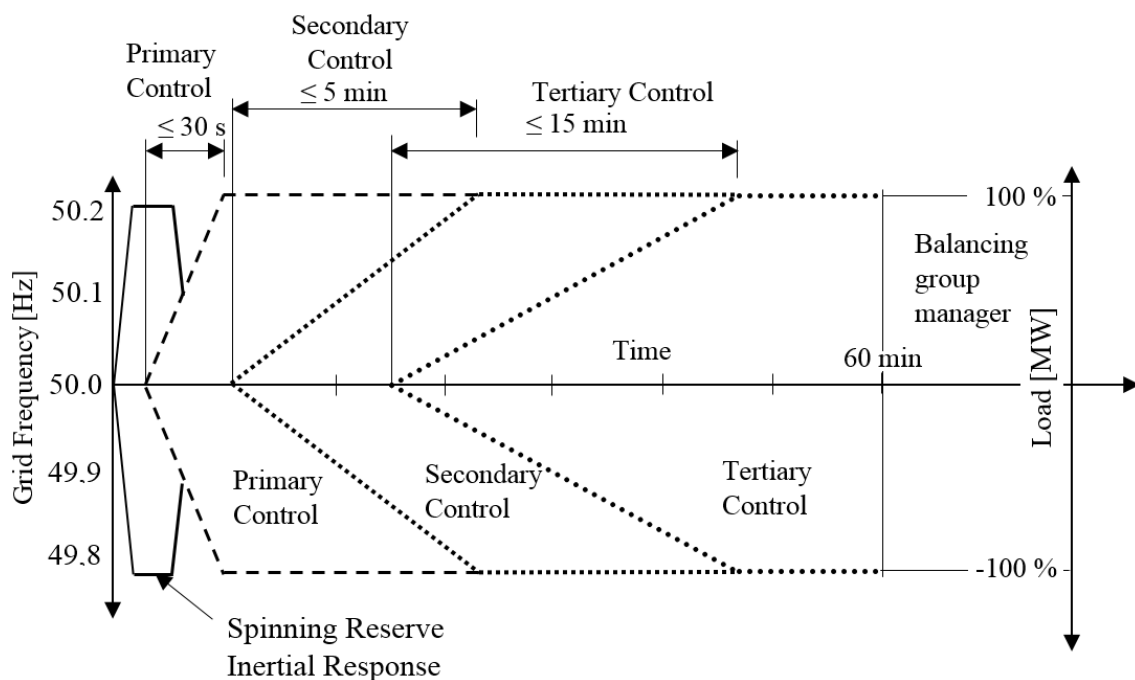


Figure 2-1: Frequency control stages to stabilise the electrical grid, times to provide the pre-approved 100 % of the power (*Richter*, information from [9], [10])

ENERGY ASPECTS

The value of highly flexible hydropower plants is the ability to deliver positive load (generating mode) within very a short time. PSH can also retain electricity to store the energy for later use. Current PSH reach up to 70 % to 80 % of cycle energy efficiency, whereas large PSH and flexible PSH schemes reach higher values [13] [14]. Table 2-1 show the available dynamic market options at EEX.

Table 2-1: Examples of dynamic market options at EEX [9]

	Direction of power	Daily us of plant	Modulating	Reaction rate	Maximum call duration
Primary Control	pos. & neg.	Plant must operate permanently, throttled 24 h	Continuous	High (15s), usually only possible when plant is already running	1 week (hydro plants 4 h)
Secondary Control	pos. & neg.	Plant must operate permanently, throttled 24 h	Discrete levels	Fast launch possible (30 s to 5 min) or system is already running	12 to 60 hours
Tertiary control (Minute reserve)	pos. & neg.	Plant must operate permanently, throttled 24 h	Discrete levels	Start in 15 minutes	4 hours
Day-Ahead	Purchase or sale pos.	Low, demand occurs on many days	no	Only at scheduled times, performance within 15 minutes	Min. 1 hour
Intraday hours	Purchase or sale pos.	Low, demand occurs on many days	no	Few hours to 45 minutes before performance scheduled	Min. 1 hour
Intraday 15-minute	Purchase or sale pos.	Low, demand occurs on many days	no	Two hours to 45 minutes before performance scheduled	Min. 15 minutes
PV self-consumption	negative	Low, demand occurs often	no	Two hours to 45 minutes before performance scheduled	Min 15 minutes
Capacity market	positive	Plant must be shut down until it is called	no	Low, several hours or days to service delivery	Day up to weeks

Ancillary services (see chapter definitions) need to be prequalified in order to be considered [11], since the switching time is crucial, the surge tank has to be designed to fulfil the requirements for the pre-qualification. High flexible PSH also can provide negative regulation power thus; the switching times between generating-mode and pumping-mode are significantly influencing the surge tank design.

2.2 Storage Demands for High Shares of Renewable Power

Electrical energy storage is a vital need for a successful energy transition towards increasing shares of fluctuating renewable sources. The economic benefit is driven by minimizing the energetic and the material demands for constructing and operating storage facilities. To evaluate the energetic cost of energy generation the EROI (energy return on invested) factor is used [15]. The EROI factor describes the ratio between the energy output of the facility over the lifetime divided by the energy demand to construct the generation facility and the energy input for maintenance. The higher the ratio the more energy is generated and thus describes the positive impact on the economy and its resource efficiency. Hydropower has the highest EROI since it is by far the technology with the longest lifetime compared even with nuclear or fossil energy generation [16]. *Atlason and Unnthorsson (2015)* [17] describe the EROI numbers in case of the large hydropower scheme *Kárahnjúkar* in Iceland by comparing the input energy of the construction that was about 1.4 TWh with an annual output of 4.6 TWh. In its target lifetime the scheme will reach an EROI value significantly of over 100 [-] showing the energetic advantage of hydropower compared with other generating technologies. The EROI value may also be called Energy Payback Ratio (EPR), for hydropower the mean payback ratio is with about 200 [-] by far the highest output compared to other renewable or fossil energy production [18]. Figure 2-2 shows the evaluation of the EROI values for various energy resources, obviously hydro power shows by far the highest values compared to other technologies [19]. This aspect is can also be concluded to improved prosperity and quality of life for various regions utilising hydro power [20], also in association with the historical economic development of the Alpine regions [6].

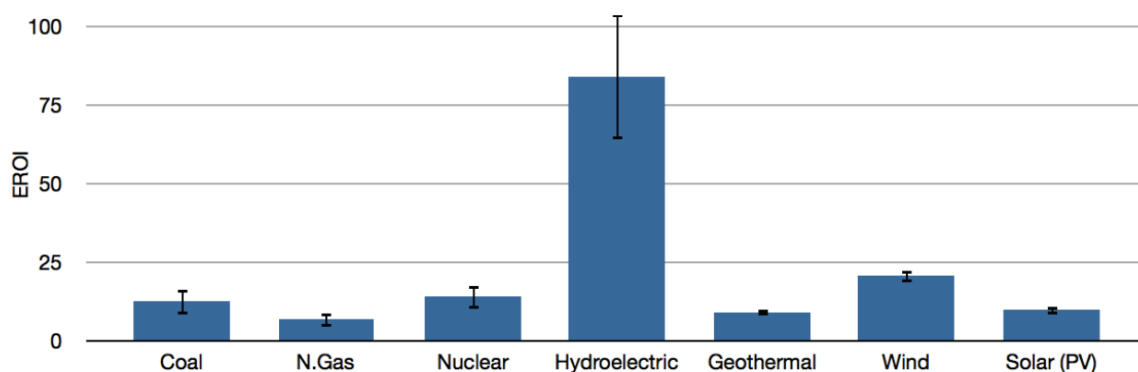


Figure 2-2: “Mean EROI (and standard error) values for known published assessments of electric power generation systems (Note: the ranges of the values are much greater than the standard error). Values derived using known modern and historical published EROI and energy analysis assessments and values published by Dale (2010)” [21], (figure from Lambert et. al. [19])

In sense of energy storage, the same concept is applied with the ESOI value (energy stored on invested) to compare the energy that is stored over lifetime needed divided by the energy needed to build and aggregate the storage device including maintenance energy input. Especially a long lifetime and high specific storage amounts are main aspect for high ESOI factors. *Barhart and Benson (2013)* [22] describe the vital importance of reducing the energy demands for energy storage systems. The studies carried out to compare the values of different energy storage technologies and show the supremacy of the storage schemes in the underground (geologic)

ENERGY ASPECTS

such as PSH and CAES. Figure 2-3 shows that all electro-chemical and possible hydrogen storages show significant lower ESOI values than geologic storages compared with PSH. In combination with the efficiency that is much higher for Li-Ion batteries than for hydrogen, Li-Ion batteries have an economic advantage compared to fuel cells for mobile devices such as cars despite their lower ESOI value as the authors conclude [22]. In sense of stationary storages, it can be concluded that PSH storage facilities are sustainable and economic investments for future energy systems.

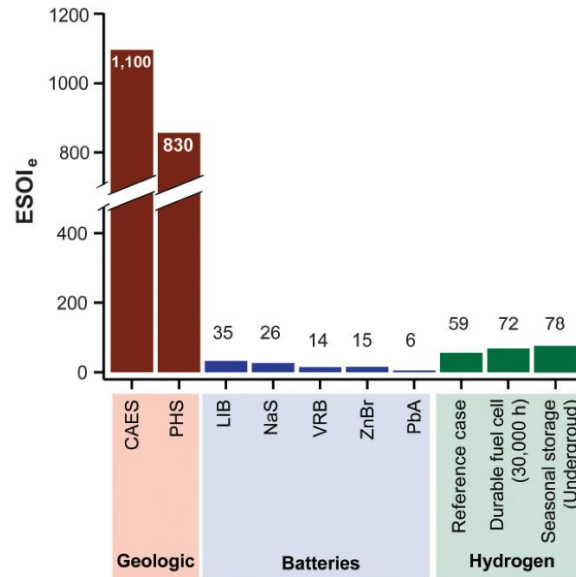


Figure 2-3: ESOI_e ratios of energy storage in geologic, battery LIB (lithium-Ion), NaS (sodium sulphur), VBR (vanadium redox), ZnBr (zinc-bromine) flow batteries, (PbA (lead-acid)), and regenerative fuel cell systems (figure from [23])

In the study of *Hambaumer* (2017) [24] a comprehensible approach was developed to investigate the ideal storage demand for a German electricity system with high shares of variable renewable electricity. Germany was found to be an ideal case since it shows already high installed capacities of PV and wind generation that could be extrapolated with expansion factors balancing wind and solar. The study concludes that even with high shares of renewables in Germany and electricity storage option with pumped storage hydropower the overall costs would only be slightly higher compared to the fossil fuel-based generation. Costs of CO₂ were not taken into consideration, and also other simplifications were made. Indeed, it is known that pumped storage hydropower demands for land use and this aspect is more and more difficult to overcome.

Research from *Pikl et. al.* (2019) [25] shows that new and fully underground pumped storage plants are very compatible with conventional pumped storage hydropower and thus it can be concluded that the underground solutions are superior also taking other advantages next to the topographic independence into account such as no sedimentation and ecological benefits.

ENERGY ASPECTS

The approaches of *Hambaumer* [24] were used by the author to study the storage demands of 100 % renewable electricity generation in Germany for the six basis years from 2012 to 2017 wherein the domestic German electricity demand was extrapolated to 100 % renewable generation including hydro, biomass, wind and solar. Wind and solar were extrapolated with upgrading factors that would allow a best balance between pumping and generating mode, since wind and solar show a very different production pattern. The other energy sources were kept at the basis years' level.

Figure 2-4 shows the result in terms of electrical storage demand with ideal efficiency and ideal transmission. The artificially extrapolated years 2014 to 2017 show a comprehensive storage demand fluctuation. The explicit domestic electric storage for Germany is difficult to predict since the fluctuation is variable and stochastic. The light blue line represents the ideal storage filling. This storage demand line is derived by the accumulated difference between the renewable production and the demand to balance this via energy extraction (pumping mode) and energy input (generating mode) concerning the energy demand of the grid. An ideal grid is assumed. The factors given in Figure 2-4 describe a needed expansion of the renewable production of wind and solar to reach 100% renewable electricity production related to the concerning year.

The storage line can be shifted in order to adjust the balance. Each year is different and economic storage and economic electricity supply will need energy trading. Thus, it can be concluded, that a save and economic future electricity system demands for a high capacity grid and increased efforts in interconnectors.

Such approaches seem to be very helpful to sustain in the energy storage discussion defining the decisions for the transition and to show differentiated needs in sense of power supply in kW and energy supply in kWh, both in positive (production) and negative (storage charging) direction.

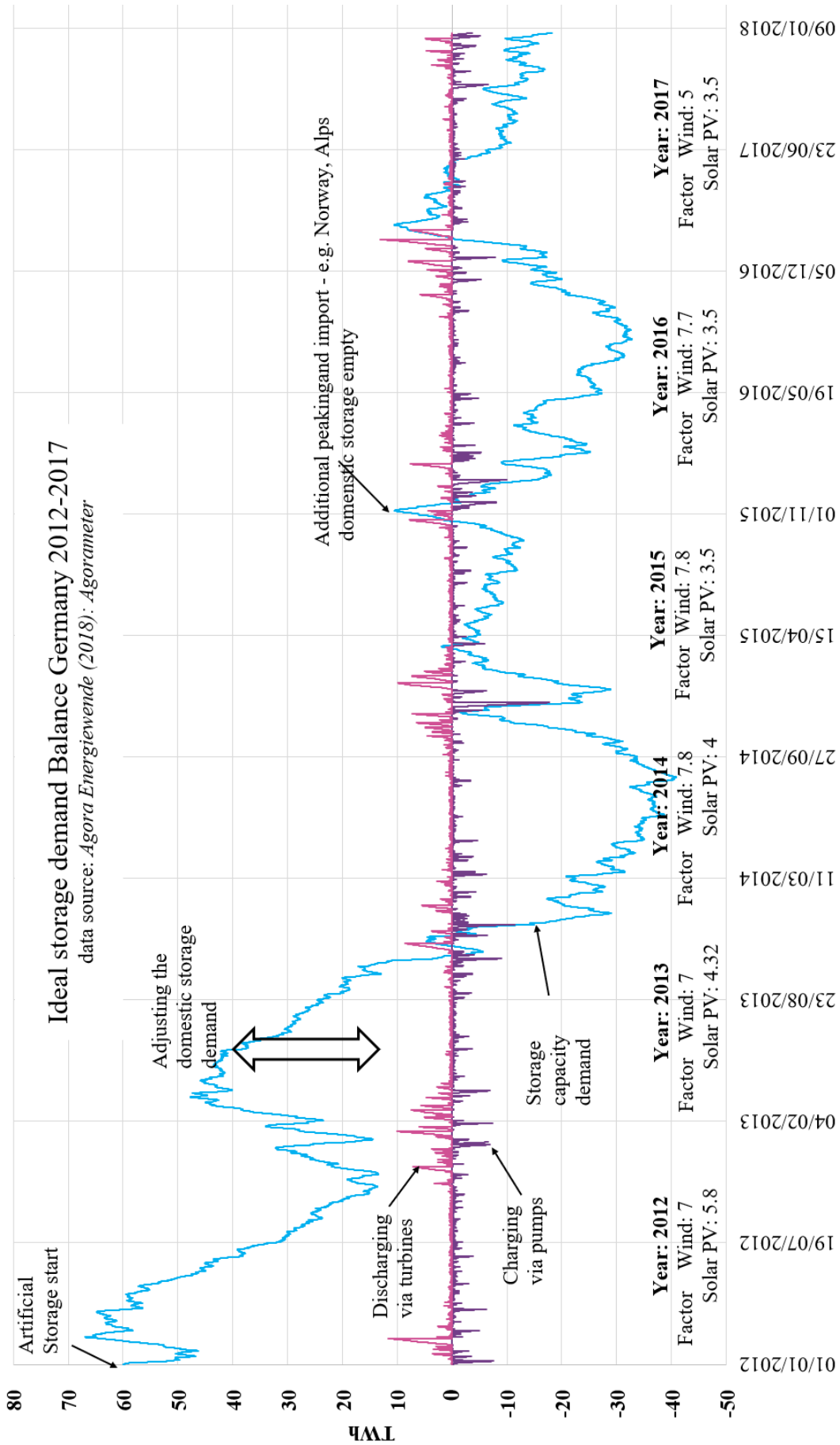


Figure 2-4: Ideal electrical storage demand with PSH of extrapolated 100 % power production in Germany with basis years 2012 to 2017 (*Richter*, data from: [26])

ENERGY ASPECTS

Very clearly visible are the alternating peaks of storage charging and the peaks of storage discharging in the winter season.

The major challenge for increase solar and wind energy harvesting is, that times with high wind is generally followed by times with low wind production. Usually effect takes place at seasons with lower sun radiation in the winter time. The high and low wind production times may occur over several weeks. This effect is a major argument for the demand of large and high capacity storage facilities. This stochastic but high capacity storage demand is crucial for the electrical storage sizing evaluation. Figure 2-5 shows a detail of the storage demand extrapolating two winter seasons based on the basis years 2015 to 2017. Between October of the extrapolated year 2015 external energy sources must balance the demand, before storage is filled, reaching maximum filling in August to 32 TWh for the shown approach. From September to February, the storage is fully emptied and demands external filling:

Analysis show, that a well-managed balance between wind and solar production may be key for best efficient system and storage costs.

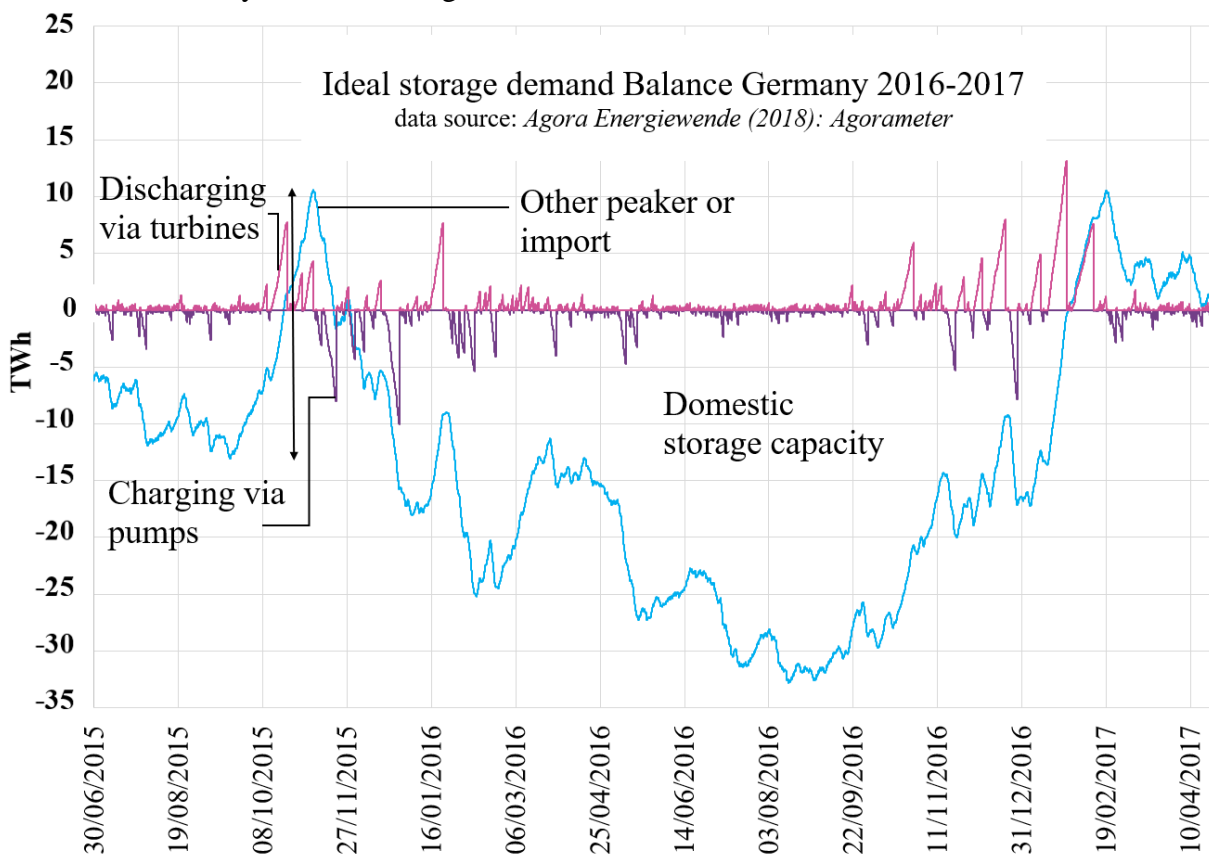


Figure 2-5: Ideal electrical storage demand with PSH of extrapolated 100 % power production in Germany with basis years 2016 to 2017, detail (Richter, data from: [26])

Figure 2-6 visualises the generation capacity demands for the extrapolated 100 % renewable storage with idealised turbine generation and pumping mode for Germany. Obviously, a misbalance between the demand of charging capacity and the demand of discharging capacity for the extrapolated case is visible with significantly higher demand on specific charging capacity (peak demand of pumping).

The relation to flexible surge tank design is given due to the aspect that pumped storage schemes can provide high capacity and highly flexible energy storage for a vast energy transition.



Figure 2-6: Ideal power capacity demand for PSH equivalent storage demand of extrapolated 100 % power production in Germany with basis years 2012, to 2017 (Richter, data from [26])

2.3 High-Head and Pumped Storage Hydropower

High-head hydropower can generate electricity from potential energy of water. Thus, with even low discharges utilised at high-heads significant energy can be generated. High potential energy is at the same time high internal pressures. These pressures need to be technically handled in order to provide high material strength to confine the stresses or counterbalance the internal pressure with stable rock-mass overburden. The latter option allows concrete lining or unlined pressure tunnels. The significance of high-head hydropower plants (high-head HPP) is the ability to provide electrical energy very quickly and in a large amount. In addition to generating electric energy it can also store energy by pumping water up to the upper reservoir at a higher altitude. High-head HPPs with installed pumps are pumped storage hydropower (pumped-storage HPP). Other abbreviations such as PSP (pumped storage plants) or PSH (pumped storage hydropower) are be used. In the present work the abbreviation PSH is used. Pumped storage hydropower schemes are one of the most efficient opportunities to store electric energy. At plants with an optimised hydraulic design about 20 % to 30 % of the initial energy will be dissipated during a total cycle of pumping (energy consumption) and generating (energy production), depending on hydraulic design of the plant, the machinery and especially the length of the power water conduits. Other technologies such as power to gas and back to power might lose about 70 % or even more of the initial energy [27].

Figure 2-7 shows the hydraulic electric storage capacity in Austria and an operation band for maximum and minimum filling rates between the years 1998 and 2012. The maximum energy that is stored in Austria is about 3200 GWh (without the storages of the Austrian federal railway). This represents about 4.6 % of the annual demand of electricity. PSH can store about 1350 GWh of electrical energy in Austria, taking the upper reservoir content into account [28]. With additional inflow, the high-head HPPs produce about 9000 GWh in Austria [29]. This is about 13 % of the annual electricity demand.

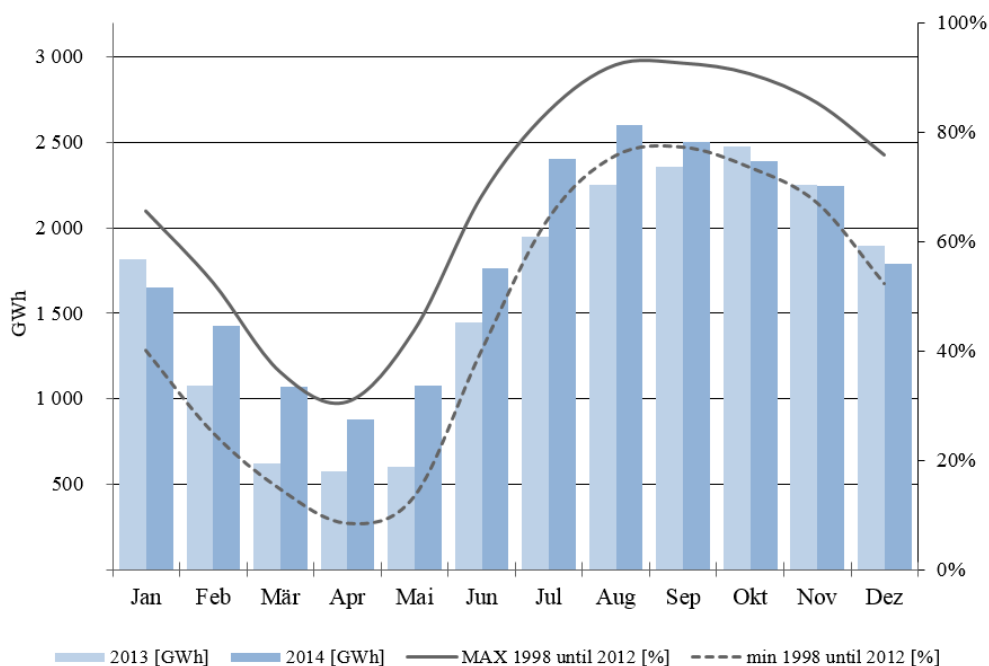


Figure 2-7: Storage capacity in Austria [GWh] and filling level of the hydro storage [%], (from E-Control, Austria)

ENERGY ASPECTS

Economic aspects of energy storage may be compared by the specific investment costs. The most used value to compare has been the specific value €/kW in official communication. Also discussed in this chapter are investment costs related to specific costs of storage €/kWh. To generally compare the cost of energy storage, the number; levelized cost of storage LCOS has been established [30]. Several approaches for LCOS are being proposed. This number highly depends on the full cycle between charging and discharging and considers the degradation and the lifetime. Still variables for the different storage technologies are vague and may result in questionable results. Figure 2-8 shows the specific investments in €/kW and the gross head for recent pumped storage schemes (selection). Most schemes utilise existing reservoirs and contain new structures such as hydraulic waterways, caverns, machinery etc. The construction costs of the dams are included and are inflation-adjusted to the year 2018. By its prototype nature the cost of PSHs vary in its specific aspects such as:

- Site specifics, such as geology, accessibility, infrastructure availability
- Grade of flexibility – machinery concept
- Length of power waterways and surge tank demand
- Accessibility

The construction of new reservoirs increases the cost of new schemes, but also significantly increases the value due to new storage capacity, as well as new water diversions for new open loop pumped hydropower schemes.

Boundary conditions of the plant in the associated figures (Figure 2-8 to Figure 2-9) below:

- PSH *Kopswerk II*; Upper reservoir considered; ternary machine units
- PSH *Baixo Sabor*; lower reservoir considered - Upper has 1 km^3 Water storage
- PSH *Limberg II*; half of the reservoir considered since sharing with *Limberg I*; fixed speed pump turbines
- PSH *Linthal*: Upgrade of upper reservoir; variable speed units
- PSH *Nante de Drance*: Dam heightening; variable speed units
- PSH *Atdorf*: Cancelled project
- PSH *Obervermuntwerk II* incl. dam costs *Silvretta*, *Biel* and *Vermunt*; ternary machine units
- PSH *Reisseck II* incl. dam costs *Großer Mühdorfer See*, *Gößkar* fixed speed pump turbines
- PSH *Feldsee* incl. dam *Wurten* fixed speed pump turbines
- PSH *Gouvães* incl. dam and 65 % of *Daivões* HPP costs (lower reservoir); fix speed pump turbines
- PSH *Tianhuangping II* - very short power waterway

ENERGY ASPECTS

Figure 2-8 shows the relation between specific capital cost related to the installed capacity in €/kW versus the head. No clear correlation can be identified since the schemes show very specific aspects.

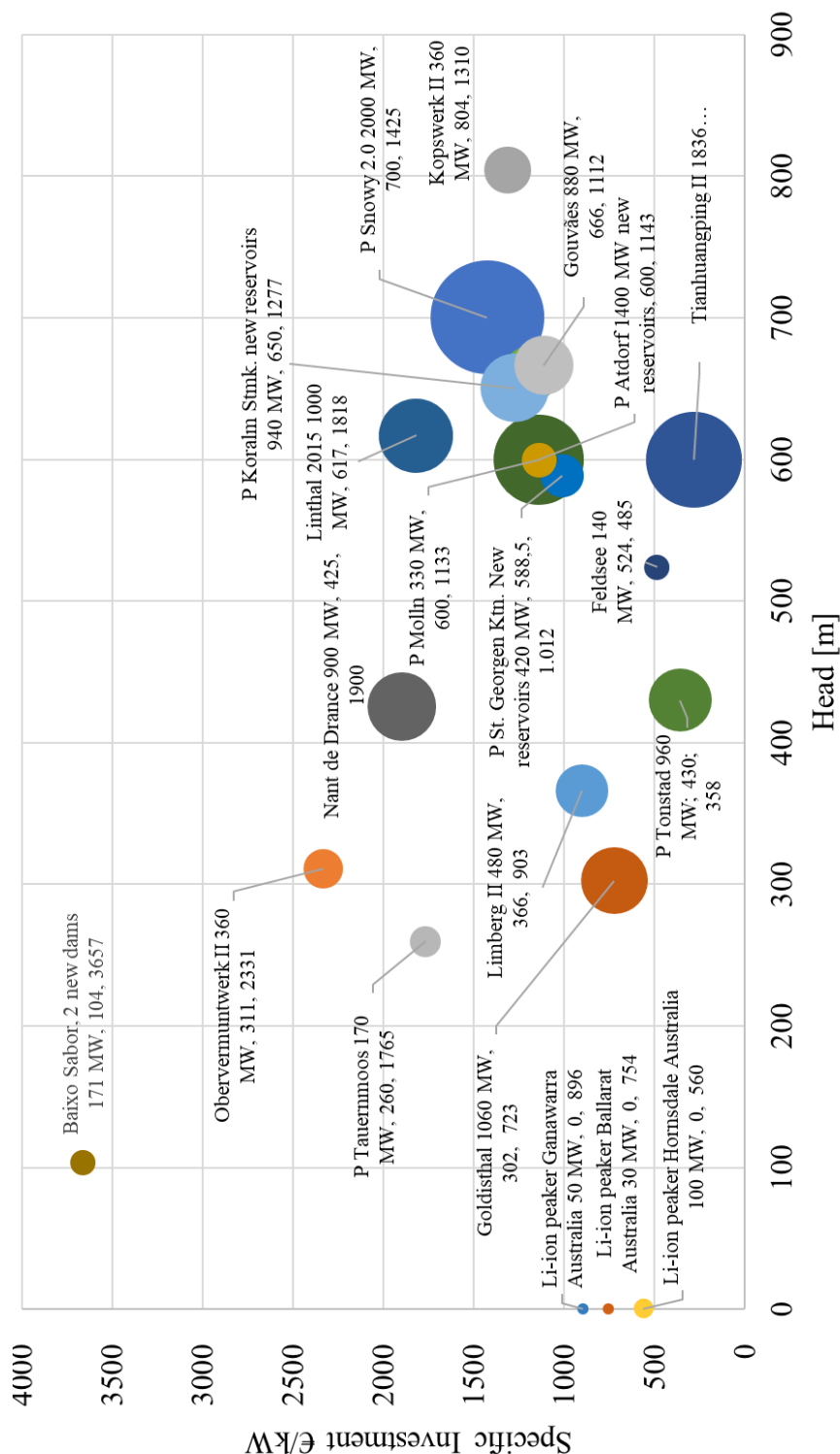


Figure 2-8: Specific capacity investments [€/kW] and gross heads [m] for selection of recent pumped storage schemes (P) project in planning, (figure and data collected by *Richter*)

ENERGY ASPECTS

Figure 2-9 shows the specific investment on energy storage in €/kWh versus the specific costs of installed capacity in €/kW. Both values are specific capital expenditure (CAPEX) values, expressing specific investment costs.

It is visible that recent li-ion battery parks in Australia with specific investment costs of about 600 €/kW for installed power are relatively cheap compared to pumped storage hydropower. But with 450 €/kWh to over 700 \$/kWh of storage investment costs, the li-ion battery parks show very high expenses in comparison with pumped storage hydropower. Even with pumped storage hydropower schemes requiring new dams and reservoirs li-ion storage demands for multiple amounts of the specific investment costs for storage. The unit price of battery storage in US\$/kWh is projected to be around 200 [\$/kWh] in 2030 due to improved battery factories and more lithium mines serving for the world market [31]. Other sources project a price of about 150 US\$/kWh for [32]. But even with this outlook pumped storage hydropower will need much less investments to realise efficient electricity storage, even if new dams are constructed or even if built fully underground as shown by *Pikl et. al.* [25]. Due to relatively low costs for installed power capacity it is obvious that batteries have been increasingly used as short term peaker for grid stabilisation in production direction (positive regulation) and energy withdrawal (negative regulation). Thus, batteries may make sense to be used for providing auxiliary services but only limited for specific energy storage.

The storage costs can be expressed by the Levelized Cost of Storage (LCOS), in contrast to the specific CAPEX values above. This LCOS value is being developed in relation to the well-established value of Levelized Cost of Electricity (LCOE) for new power generation units. It reflects the final cost to store one kWh of electrical energy. Applying the LCOS values for pumped storage hydropower it can be shown that it is the most cost-effective technology. Even for li-Ion in 2030 the storage will cost in the range of 0.2 €/kWh while storage via pumped hydro can be below 0.1 €/kWh [30].

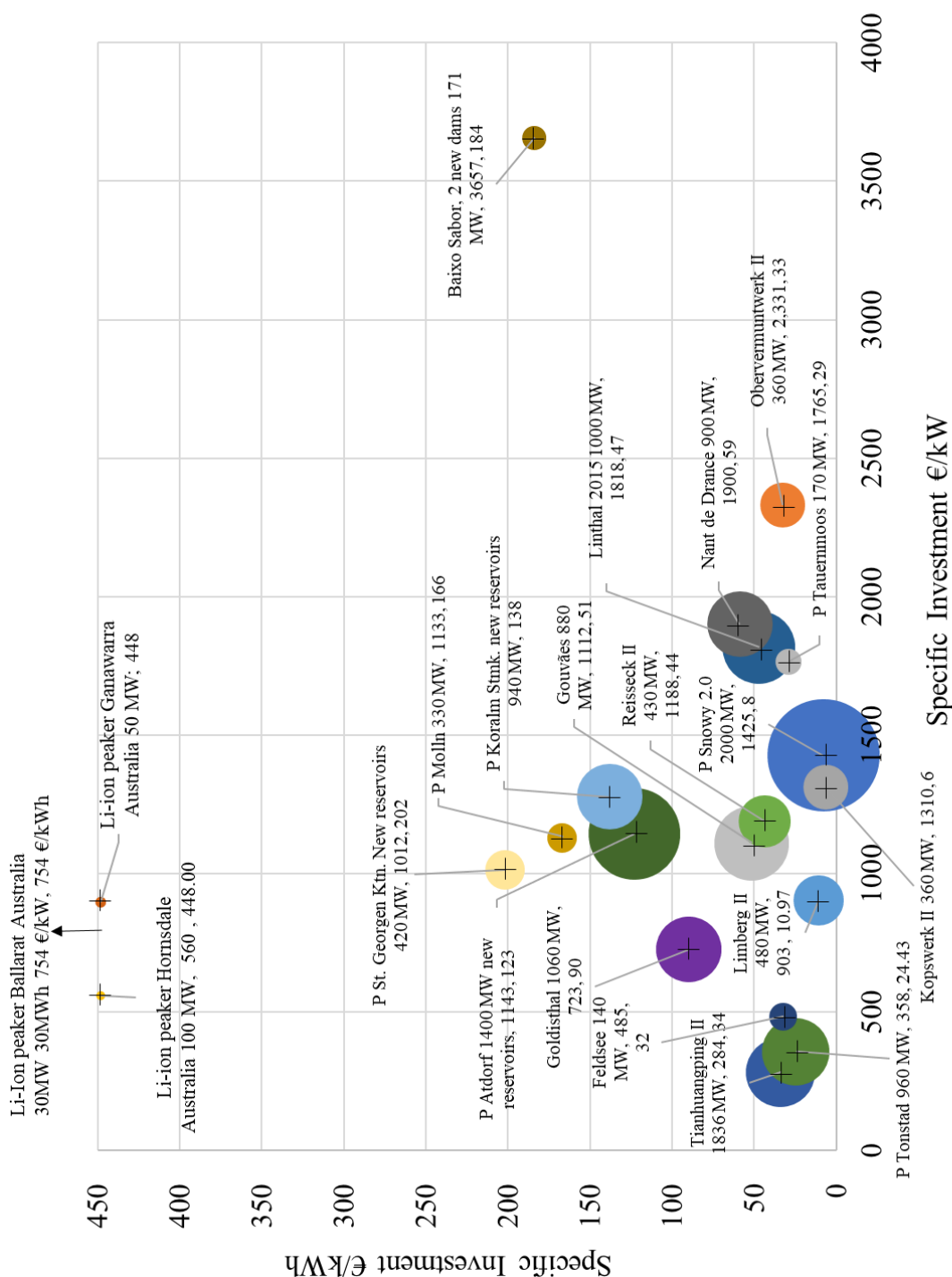


Figure 2-9: Specific investments €/kW versus €/kWh for selection of recent pumped storage schemes, (P) projects in planning, (figure and data collected by Richter)

Generally, it is difficult to compare pumped storage hydropower schemes in detail by simple numbers. The plants are unique in their design. Due to boundary conditions given by nature, such as very site-specific aspects as different tunnel dimensions in various geological surroundings, systems with no surge tank (*Feldsee*, *Project Tauernmoos*, *Project Kühtai II*) or with one surge tank (*Limberg II*, *Obervermuntwerk II*), and schemes with headrace and tailrace surge tanks (*Reisseck II*, *Project Snowy 2.0*, *Kopswerk II*).

ENERGY ASPECTS

In addition, the flexibility provided by the plants for the electrical system supply is very different and capital intensive that is implied in the specific costs. The figures show highly flexible plants such as *Kopswerk II* and *Obbervermuntwerk II* and schemes including the variable speed technology [33] such as *Nant de Drance* and *Linthal 2015* [34].

The significant cost drop of lithium-ion batteries has risen a lively discussion about how this type of electro-chemical storage will affect the energy storage development.

Figure 2-8 and Figure 2-9 show the investment cost position of Li-Ion batteries in 2019. It can be concluded that installed power for grid regulation purposes is economic, but bulk energy storage is expensive compared to pumped hydro. Li-ion battery lifetimes depend strongly on temperature with best conditions at around 25°C [35]. For vehicles, battery application for different models and manufacturers an average warranty time of 8 years or 100 000 miles with 70 % capacity degradation is given [35]. However, besides the price evolution of batteries, what will very likely be decreasing in the next years, strategic and limiting aspects in association with rare elements [36].

A lively discussion is proposing the power to gas (P2G) technology to convert power to hydrogen H₂ and further to methane CH₄ as a way to store large amounts of energy. But one has to consider that several conversion processes show significant amounts of efficiency losses and thus lead to high costs while pumped hydro has high efficiency for very long periods of time. P2G H₂ and P2G CH₄ are significantly more expensive than pumped hydro in various studies [37] [31] and the study from *Agora Verkehrswende et.al. (2018)* visualises the large efficiency losses of P2G in comparison with electricity-based systems [27]. Table 2-2 compares qualitatively the aspects of Li-ion batteries with pumped storage hydropower, advantages are highlighted in green. The qualitative indication matrix clearly shows the advantage of pumped storage hydropower. The aspects of pumped storage hydropower that may be challenging can be solved by fully underground pumped storage hydropower eliminating the need of topography and increasing the licensing procedure [25]. The underground pumped hydropower storage is also comprehensively described by *Pickard (2012)* [38].

Table 2-2: Qualitative comparison matrix between Li-ion batteries and PSH

	Li-ion batteries	Pumped storage hydropower
lifetime	7–10 years [39]	50-60 years of machinery >100 years civil structures
Investment cost of storage	→ 256-500 €/kWh future prognosis/prediction → 150 - 200 US\$/kWh in 2030 battery packs	→ 20 to 50 €/kWh upgrade existing reservoirs → ≥ 120 €/kWh with new reservoirs
Qualified for vast storage	Short term storage	Short-, mid- and long term
Qualified for multipurpose use	Only electric storage	May provide additional use of the water
Cycling stability – efficiency over time	Decreases	Remains constant
Topographic independent	Yes	Needs elevation
Pollution	Toxic when burns	Uses water
Critical resources	Several rare earth metals needed	Vastly available resources

ENERGY ASPECTS

Flexible to grid infrastructure	Can be placed to existing grid	May need new connections
Time of realisation	Very quickly	5-10 years – if long public and environmental procedures are necessary - 20 years
Response time full power	Very fast	Fast
Power control in charging mode	Very flexible	If flexible PSH
Inertia service	No inertia	Rotating mass

Table 2-3 lists the advantages of pumped storage hydropower regarding grid stabilisation and bulk energy storages after a report from Argonne National Laboratory [40].

Table 2-3: Advantages of pumped storage hydropower [40]

1	<i>“Inertial response</i>
2	<i>Governor response, frequency response, or primary frequency control</i>
3	<i>Frequency regulation, regulation reserve, or secondary frequency control</i>
4	<i>Flexibility reserve</i>
5	<i>Contingency spinning reserve</i>
6	<i>Contingency non-spinning reserve</i>
7	<i>Replacement/supplemental reserve</i>
8	<i>Load following</i>
9	<i>Load levelling/energy arbitrage</i>
10	<i>Generating capacity</i>
11	<i>Reduced environmental emissions</i>
12	<i>Integration of variable energy resources (VERs)</i>
13	<i>Reduced cycling and ramping of thermal units</i>
14	<i>Other portfolio effects</i>
15	<i>Reduced transmission congestion</i>
16	<i>Transmission deferral</i>
17	<i>Voltage support</i>
18	<i>Improved dynamic stability</i>
19	<i>Black start capability</i>
20	<i>Energy security”</i>

Especially the point of inertia is crucial for an electrical grid since it is instantaneous response that does not need to be started up by a response controller. This is a major advantage in comparison to batteries. Even though batteries may react in milliseconds the controller need to react faster and this encounters challenges of the grid wide reaction in order to prevent instabilities.

2.4 Combined Pumped and Thermal Energy Storage

In order to meet the requirements of decarbonisation of the energy systems all sectors have to gain efficiency. The thermal sector with heating and cooling requires significant amount of energy. Far distance heating and cooling systems are found to be the most efficient and sustainable systems to provide thermal resources to cities and urban areas. Approaches to decarbonise this thermal sector efficiently need seasonal heat storages. Underground thermal energy storages (UTES) may provide a resource efficient and environment friendly technology [41]. Water physically provides a very high specific heat capacity of $4190 \text{ J kg}^{-1}\text{K}^{-1}$. Thus, 1 m^3 of water using a temperature spread of 90° allows to store heat energy of $377.1 \text{ MJ} \underline{\underline{=}} 104.7 \text{ kWh}$. Subsequently large water volumes can store large volumes of thermal energy. The combination of pumped storage and cavern thermal energy storage may combine efficiently the storage of electricity and thermal energy since both energy storage systems use large volumes of water. In order to overcome even the negative aspects in Table 2-2 the solution may be the utilisation of fully underground pumped storage hydropower plants. Also, the direct combination of seasonal thermal storage and efficient electricity allows to harvest the friction as a significant energy input to increase the overall efficiency and the thermal charging. Friction is usually not usable and a loss of energy by producing heat. If the medium water is additionally a heat storage this heat loss can be utilised. The combination technology of electricity storage and heat storage within fully underground pumped storage hydropower plants is described by *Pikl et. al.* (2019) [25]. Additional heat pumps or secondary systems may be needed to fulfil the demands of district heating functionality [25].

2.5 Machinery Concepts

This chapter gives a brief introduction to machinery concepts used for high-head hydropower plants and pumped storage hydropower in specific. Machinery concepts may have significant impact on the demands for the surge tank design. Pumped storage hydropower plants utilise in contrast to conventional hydropower plants a reverse flow direction by pump operation. If pumps are somehow disconnected to the grid and suddenly lose the motor power, they are *tripped*. Due to this, the flow may reverse in the pressure shaft very quickly, even much quicker as guide vanes close, subsequently demanding quick acceleration to withdraw water out of the headrace surge tank. The main surge tank aspect in this respect is to overcome the inertia of the surge tank. An example of not sufficiently functioning surge tank inertia is studied by *Nicolet et. al.* (2015) [42].

Ternary machine units may influence the surge tank design by the ability of the machinery of very flexible operation as for the case study headrace surge tank *Krespa* for *Obervermuntwerk II* PSH [43] [44] [45]. For high-head schemes equipped with Pelton turbines surge tanks have the advantage that the closing of these machines can be slower due to the quick reaction of deflectors. In general, the surge tank follows the possibilities and demands of the machinery equipment. Details for Austrian pumped storage hydropower schemes are given in the comprehensive book *Pumped Storage Hydropower in Austria* [28]

The high-head HPP generate power whereas PSH additionally draw electricity from the grid to feed pumps and store electric energy as well as allow negative grid regulation if flexible PSH. Different following types of turbines with pumps are available:

- Single stage pump turbine (up to about 700 m head), and double stage pump turbines (higher than 700 m head) advantage: compact machine units, disadvantage: compromises in flexibility
- Vertical ternary machines (Pelton turbine – motor generator – Pump)
 - Tailwater of the turbine as atmospheric outlet (PSH *Malta main stage*, PSH *Rosshag*, PSH *Häusling*).
Advantage: high flexibility possible and optimised hydraulic design of turbine and pump.
Disadvantage: large vertical construction height, challenge with downstream regulation height.
At the PSH *Lünerseewerk* from 1958 the construction size of the vertical ternary units is very compact due to the placing of a booster basin to provide pre-pressure for the pumps. At this specific plant the pre-pumps to provide filling of the booster basin from outlet reservoir are directly run by Pelton turbines.
 - Tailwater of the turbine under pressurized air (*Kopswerk II* PSH)
Advantage: Head until drawdown level of tailwater reservoir utilisable, full range of pump regulation due to hydraulic short circuit, compact vertical construction size, very high flexibility.
Disadvantage: Higher investment cost and additional demands for air cushion facility.

ENERGY ASPECTS

- Horizontal ternary machines (Francis turbine – motor generator – pump) (*Obervermuntwerk II* PSH)
 - Advantage: Very high flexibility, specific optimised hydraulic design of pump and turbines.
Disadvantage: Large cavern size demand.
- Variable Speed pump turbines (PSH *Nant de Drance*, PSH *Linthal 2015*, Project PSH *Kühtai II*)
 - With full size frequency converters (advantage; no dewatering necessary, adaption to high variations in heads, increased flexibility in pumping and generating mode).

A very comprehensive machine unit design is applied at the pumped storage scheme *Ranna* from 1954 utilising the Danube river as lower reservoir with the serial combination of Francis with Kaplan turbines that optimise the usable head variations in water levels of the Danube [28].

The machinery concepts influence the surge tank design significantly since high flexible machine units that allow quick changes between pumping and generating mode additionally stress the power water ways and thus, demand for robust design of surge tanks. In addition, the trend to more flexible operation increases the likability of extreme resonance cases that need to be captured by the surge tank design.

3. FUNDAMENTALS AND STATE OF THE ART

This chapter describes the general aspects in association with surge tanks and the historical background and well as the general needs for the for the surge tank design.

3.1 General Aspects

The increasing installation of renewable energy sources (RES) such as wind and solar power is a challenging task for the integration into the electrical grid since the energy production and the energy demand does not occur at the same time. Since electric energy is not directly storable, this shift in time and power is the challenge. A well-proven solution is given by the utilisation of pumped storage hydropower plants (PSH). Thus, the demand for new PSH is growing since it is the most efficient technology to provide a time shift of electrical energy [31]. Many PSH projects consist of long conveyance tunnels due to topographic boundary conditions. In order to guarantee an optimized operation of a PSH or a flexible high-head HPP surge tanks play a crucial role in the operability.

Surge tanks are very site specific and usually unique structures are developed for a specific hydropower scheme. An understanding of the tools to evaluate surge tanks as well as the hydraulic behaviour have a significant importance for an optimized design.

The recent surge tank research by the author consists of the hybrid application of physical model tests in combination with numerical simulations in order to capture various hydraulic phenomena. New requirements due to increasingly flexible energy sources are changing the design of HPPs and PSH. Especially for grid control it is vital to deliver or retain large amounts of power very quickly. This steep gradient of power supply may be given by the sun rise and sun set over a large region that produces vast amounts of electricity with grid scale solar power infrastructure.

This present work bridges the interdisciplinary point of views of current boundary conditions of modern hydropower plants. The surge tank facility is a linking element of civil, mechanical and electrical engineering. It has to be designed to fulfil the requirements of all these technical fields. The civil works' aim is to build the surge tank and the total pipe system as economic as possible by high construction quality to allow a long operation time. The mechanical engineering is interested in an undisturbed, optimized and well-controllable operation without hydraulic effects such as cavitation of the turbines, pumps and closing devices. The electrical engineering sets margins for allowed frequency disturbance and requirements from the electrical grid. Since the kinetic energy of the conveyance system is transferred to pressure forces and pressure pulses at shifting or regulation operations the hydraulic transient behaviour of the system has crucial importance. The surge tank placement allows for independent distances between a reservoir and a power-producing unit.

3.2 Historic Aspects

Since the very beginning of the construction of water conveyance systems, surge tanks have been used to distribute the water from the aqueducts to the main consumer units. The placing at the end of the aqueducts was to mitigate the water hammer effects of the pressurized pipes that were used after the surge tank to the consumer units. In the ancient city of *Pergamon*, a

high-pressure pipe with an internal pressure of 17.5 bar was constructed to overcome a valley in a pressurized pipe to supply water for a monastery. Before the water entered the pressurized pipe after a long free surface conduit, a surge tank was constructed. It was built in 1200 B.C. and was minimum in operation for 380 years [46].

The sophisticated Roman water transportation and distribution systems had surge tanks, the so called; *castellum dividicum* as close as possible to the final consumers. The German word *Wasserschloss* is directly associated to the Latin description. For modern hydropower systems surge tanks were established linked to the vast electrification of industry and society, beginning around the 1880s.

Modern surge tank research has been a constant task in hydropower development since the late 19th century and since surge tanks are key facilities for successful operation of hydropower schemes dealing with significant pressurized inertias. The constant improvement and increase in size of hydropower plants and pumped storage schemes demands for constant surge tank improvements.

3.3 Purposes of the Surge Tank

Surge tanks were already built to enable hydraulic long pipeline systems in ancient civilizations in the Middle East. They were placed at the end of aqueducts before the distributions pipes to ensure a safe operation for a long period of time. For ancient surge tanks the used material were heavy and well assembled stone blocks [47]. Modern material and construction technology underground allow for even higher loadings as in ancient times to make modern high-head hydropower systems possible [48]. Variations in flow velocity resulting by opening and closing actions of valves or machine units are generating positive or negative pressure surges (water hammer) according to the specific velocity gradient. Significant differences in transient flow characteristics can occur depending on the type of the machine unit. Surge tanks are applied to protect the tunnel system against excessive positive or negative pressures. Negative pressure is limited by the atmospheric pressure but overstressing this limit may result in extreme water hammer events due to the collapse of macro cavitation [49]. In addition to the hydraulic constrains, the coupling of the high-pressure pipeline to the electricity grid via the electromagnetic field in the generator, with its condition of frequency-stable operation, has a feedback effect on the hydraulic system. This must be considered with the requirements of machine regulation to prevent resonance effects. In cases of electrically isolated operation such as for grid rehabilitation the stability aspect is crucial. Also, if hydropower plants are providing energy for large single consumers such as aluminium plants the stability aspects are crucial. This condition leads to a required minimum cross-section (stability cross-section) of the riser shaft in the surge tank [50].

A typical high-head hydropower plant water conveyance system consists of a long pressure tunnel, a surge tank and a most direct possible steel lined pressure shaft (penstock) to the machine units. The headrace tunnels of high-head schemes contain large quantities of water under significant pressure. This inertia generates considerable kinetic energy in operation controlling the volume demand for the surge tank. Due to control actions of the power plant, the kinetic energy is either generated (starting/accelerating) or dissipated (closing/throttling). Hydraulic communication in the power waterway creates pressure waves, which propagate through the water with the speed of sound. Since this communication takes some seconds in the

long pipe systems, regulation actions may cause unfavourable interference. The placing of a surge tank allows a hydraulic separation of the power waterway into two pressurized systems between free surface reservoirs. The pressure shaft system from the units to the surge tank enables a rapid reaction in this water pipe and is accelerated or decelerated according to machine demand. In the second pipe system between the surge tank and the reservoir, the water mass oscillates with frequencies in a range of minutes. High-frequency pressure waves communicate in the entire water conduit between the two free water surfaces (reservoir and surge tank) and the units respectively closing facilities. The kinetic energy is expressed by pressure energy in the pressure shaft according to the flow gradient. This generates the dynamic pressure surges (water hammer) in the pressure shaft. Subsequently the surge tank reflects the pressure waves at the free surface and counteracts with discharge to fulfil the demand of initial pressure wave. The surge tank reacts to improve hydraulic reactions with a rise or fall of the water level by charging or discharging water. Due to the separation of the pressurized pipes, the pressure tunnel basically reacts to the given pressure in the surge tank. Theoretically, a linear pressure behaviour between the pressure at the surge tank base and the water surface in the reservoir is assumed. Since the pressure pulses divide at the branch to the surge tank equivalent to area (one part enters the surge tank, the other continues to the reservoir), water hammer interference may occur in pressure tunnels [51]. Taking the water hammer interference into account, it is crucial to ensure that no section of the tunnel experiences a critical negative pressure that could lead to cavitation with the danger of column separation [49]. During the mass oscillation, the kinetic energy of the pressure tunnel is converted into potential energy by up-surge and down-surge in the surge tank. The energy enabling the dampening is dissipated by hydraulic losses such as friction and local losses (throttle loss). In particular, modern PSHs with high requirements for flexible operation demand for more stringent requirements on the design of surge tanks and pipe systems. Rapid loading and unloading ramping times increase the velocity gradient and thus the pressure gradient in the pressure tunnel and other parts of the plant. Plants are much more strained by flexible operation of increased starts and stops as it was the case before the massive expansion of wind and solar generation by the energy transition. A common type of machine unit is the pump turbine, which can be operated both as pump and turbine. Ternary machine units can specially be optimized for each mode of operation and allow effective hydraulic short circuits to fully control pump operation for a wide range (e.g. *Kops II* PSH and *Obervermuntwerk II* PSH). This type of machine unit demands larger caverns as for pump turbines. With compact pump turbines, the resistance of the magnetic field of the generator vanishes suddenly in case of a load rejection. The turbine accelerates to the runaway speed. Depending on the characteristics of the machine, this hydraulic behaviour leads to a short-term reversal of the flow direction, which may occur a few seconds after the load rejection and generates very high-pressure loadings. In case of generating mode, this leads to increasing pressure on the headrace side and to decreasing pressure on the tailrace side. This must not lead to separation of the water column (macro cavitation). In case of a sudden collapse of the cavity, very large pressure surges can occur, even higher than the Joukovsky hammer that is normally assumed as a maximum as reported by *Bergant et. al.* [49]. Pressure surge reflection in the surge tank is considered as the collaboration of pressure surge generation in the turbines and other devices as well as the water mass acceleration in the surge tanks. The water mass acceleration in the surge tank itself is considered in the modelling of surge tanks with an additional inertia term.

Surge tanks become necessary for high-head HPPs with pressure tunnels, when a certain acceleration time demand is exceeded. Regarding a rule of thumb this is about 1 km to 2 km in plan view depending on the head. The surge tank provides an intermediate water reservoir with free surface that enables the proper regulation of the power plant machinery [50]. Pressure pulses are reflected at the free surface and decrease the design criteria of internal pressure of the pressure tunnel. The kinetic energy in the pressure tunnel is transferred to potential energy in the surge tank rather than to deformation energy, which would be generated by the water hammer phenomenon. Surge tanks have to store the amount of water that is necessary to bridge the inertia of the pressure tunnel when starting the turbines at the most unfavourable point in time. This can for example be right after a previous shut down after the water has already filled the surge tank and is reaching its point of highest kinetic energy of the backflow to the reservoir. Surge tanks are designed not to overflow at any time and not to completely drain.

This ability to capture the mass flow demands a certain size of chambers and shafts of surge tanks. The size of the surge tank is mainly governed by the amount of water and the friction losses in the pressure tunnel. In order to enhance the dampening effect throttles can be placed at the base of the surge tank or at the end of the lower chamber. The throttles additionally dissipate hydraulic energy by creating backflow regions in the pipe. The aim is to optimise the loss behaviour of the throttle without negatively influencing its behaviour regarding the water hammer and machinery. No moving elements in the surge tank should be used during operation to avoid any malfunction, especially if intended to establish or enhance a differential effect of the surge tank itself. Since the surge tank is a major protecting device for the power plant this aspect ensures a very robust behaviour and thus is an important aspect for the safety philosophy. For air cushion surge tanks improvement, a closing device solution is proposed by *Ødegaard and Vereide* (2018) [52] to place this in combination with the static throttle functionality. In this case the element is used for inspection of the pressure tunnel only to avoid the release of pressurized air from the air cushion. Such moving parts are possible in the same manner as for closing devices if malfunction is prevented by redundant precaution measures.

Usually, a single flow direction might allow for a large loss. In this case asymmetric orifice throttles might be used. Such devices show a ratio of about two to three between the losses regarding the two flow directions.

Thoma (1910) [50] describes that the earlier discovered phenomenon of water hammer pulses, that has caused some severe damages, was tried to be mitigated with several measures such as flywheels or bypass structure to mitigate the water hammer pressure at a fast closing event. Even small pressurized air cushions were used to reduce the water hammer effect introduced by *Michaud* (1878) [53]. Pelton turbines provide deflectors that separate the runner from the high velocity water jet, this allows any given closure law of the machine closing valve mitigating water hammer and reducing maximum rotating speed of the generator. But according to *Thoma* [50] some historic hydropower plants with tunnel systems could not ensure a proper turbine regulation. This lack of speed regulation is related to the pressure communication of the turbine and the reservoir. For a certain delay of time response, the regulation of the turbine may get unstable. To ensure a functional self-regulation of turbines the surge tank with an open surface was found to fulfil these requirements.

Figure 3-1 illustrates the dependencies and actions of the surge tank on the hydraulic system of a power plant. The surge tank is a vital part of the hydraulic pressurized power waterway system

to allow turbine and pump functionality and mitigates water hammer, but the surge tank creates secondary hydraulic aspects such as the mass oscillation that defines the gross size of the surge tank. The suggested stability criteria are shown depending on headrace system, tailrace system or air cushion surge tank system.

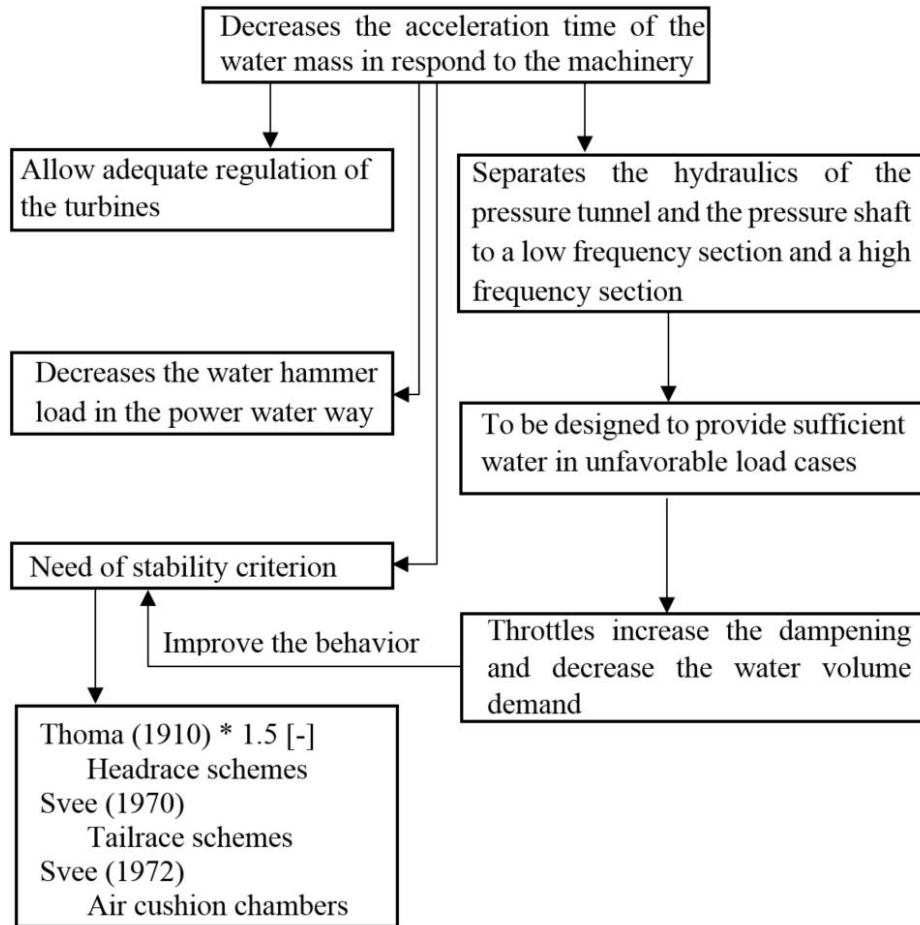


Figure 3-1: Purposes and dependencies of surge tank design

Johnson (1908) [54] first describes the functionality and the design criteria of surge tanks as well as a geometrical optimisation by introducing a differential effect with an internal small riser pipe in the surge tank itself. The concept of the Johnson differential surge has been widely implemented in hydropower and pumped storage plants in various forms. Examples can be found at the HPP *Prutz-Imst* in Austria [55], in the positioning of the riser inside the main shaft for large pumped storage schemes in the U.S. such as the *Castaic* pumped-storage plant in California (1050 MW) [56], or the differential headrace surge tank for *Gouvães* pumped storage plant in Portugal (880 MW).

3.4 Design Criteria

This chapter briefly describes the needs of a surge tank and common approaches to derive the design values.

3.4.1 Surge Tank Requirements

A main question is; when is a surge tank required for a high-head hydropower plant? The simplest answer is; if a long pipe connects the reservoir and the power unit. To give more precise information the water acceleration time constant is used (3-6).

The energy of the water is transferred from pure potential energy in the reservoir to partly of kinetic energy and potential energy in the pipe. The utilised energy for high-head HPPs can be expressed by power P [W], depending on the main factors discharge Q [m³/s] and head h [m]. Each conveyance system is to be viewed as an energy balancing system.

Equation (3-1) describes the potential Energy (E_p). Equation (3-2) describes the kinetic Energy (E_k) and the power equation (3-3) defines the main dependencies of how the capacity of the hydropower plant is derived. The main values are the discharge Q [m³/s] and the head H [m]. The head is already applied as the net head (gross head minus all local and continuous hydraulic losses of the conveyance system) thus, the efficiency η [-] is only related to the machinery units. One has to note that the machine efficiency is a function of various machine parameters showing its optimum at certain boundary conditions.

$$E_p = m g H \text{ [J]} \quad (3-1)$$

$$E_k = \frac{1}{2} m v^2 \text{ [J]} \quad (3-2)$$

$$P = \rho g Q H \eta \text{ [W]} \quad (3-3)$$

According to the first law of thermodynamics - conservation of energy - the system always tends to balance the internal energy. Regarding the fact that the conduit system containing water and pipe elements is an elastic system, all increments misbalances in energies are communicating. This communication is utilised via longitudinal pressure waves (incremental water hammer pulse). These travel with the speed of sound. In a water conduit system embedded by hard rock or steel pipes, the value can be approximated by 1000 m/s to 1200 m/s, however the velocity may decrease significantly when using a more elastic material. In contrast in free surface flow systems the energy information is traveling by free surface waves. The velocity of this propagation can be assumed at about 10 m/s. If placing a surge tank to separate a power conduit into two pressure pipe systems this factor of 100 [-] comes into action and separates the power waterway into the high frequency part with the water hammer oscillation and the low frequency part with the surge tank oscillation or mass oscillation (Figure 3-2). But it has to be noted that also between the surge tank and the reservoir a pressure wave is traveling with the speed of sound to communicate between the surge tank and the reservoir. This aspect of pressure wave travelling time difference is a design challenge for storage-tunnel surge tanks (see chapter:6.6). In the pipe part between the turbine and the surge tank the kinetic energy is transferred to internal pressure and in the pipe section between the surge tank and the reservoir mainly to potential energy related to the surge tank filling height. A complete transformation

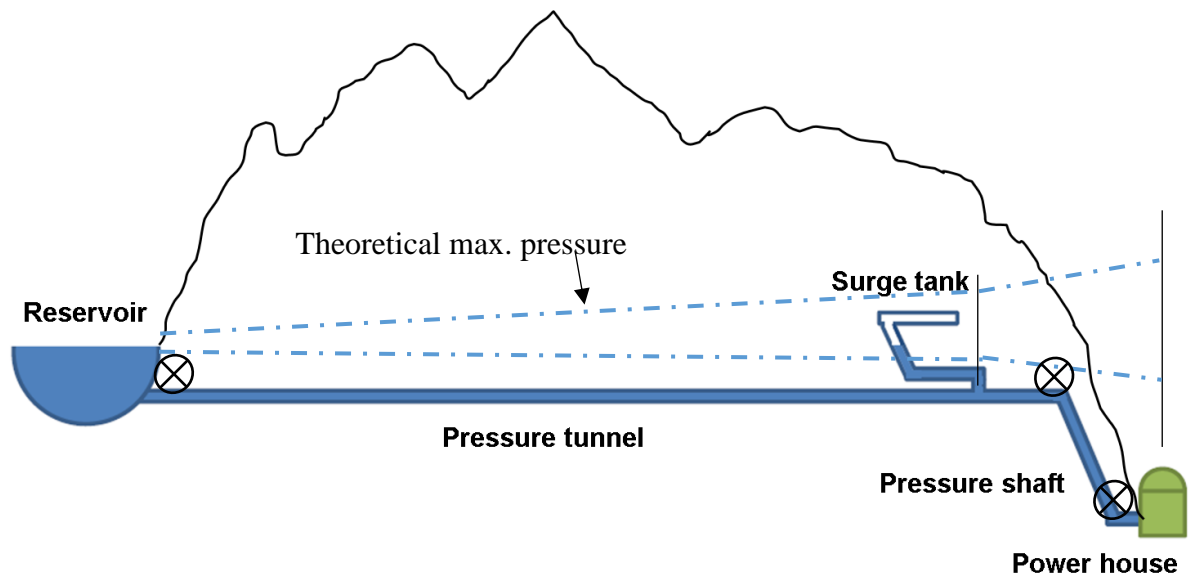
FUNDAMENTALS AND STATE OF THE ART

of kinetic energy to internal pressure leads to the equation of Joukovsky (3-4). The Joukovsky equation is an important estimation to assume the maximum water hammer and also the mitigated water hammer taking the closing time into account that is slower as the reflexion time (3-5). Column separation or macro cavitation by creating full flow section cavitation must be avoided. This may lead to even higher water hammers as the Joukovsky value [49]. Safe design of surge tank device is the key facility avoiding this aspect.

$$\text{Joukovsky Equation: } \Delta h = \pm \frac{a}{g} \Delta v \quad (3-4)$$

$$\Delta h \sim \pm \frac{a}{g} \Delta v \cdot \frac{T_r}{T_c} \quad (3-5)$$

The surge tank divides the power waterway into two separate pressurized hydraulic sections. For a usual design layout of high-head hydropower plants this interruption will be placed at the transition of the slightly inclined long headrace tunnel with relatively low pressure and the steeply inclined pressure shaft with the high-pressure section. This separation into two pressurized flow sections by an intermediate free surface is the reason for the mass oscillation. Figure 3-2 indicates the sections created by the surge tank placing.



Reservoir	Surge tank oscillation	Water hammer oscillation
Small, size depending oscillation	Low frequent mass oscillation	High frequent Pressure pulse oscillation

Figure 3-2: General layout of a high-head hydropower plant with headrace surge tank system, indicating the oscillation regimes (Richter [57])

FUNDAMENTALS AND STATE OF THE ART

Figure 3-3 shows a schematic longitudinal section of underground works for a pumped storage scheme with a vertical shaft concrete lined [58]. The maximum and minimum pressure lines visualise the effect of the surge tank. Due to a throttle at the headrace surge tank the maximum pressure at the surge tank base may be above the free surface level (Figure 3-3) for most unfavourable design case. As a rule of thumb, the pressure peak of the throttle loss is suggested to the maximum water surface level in the surge tank.

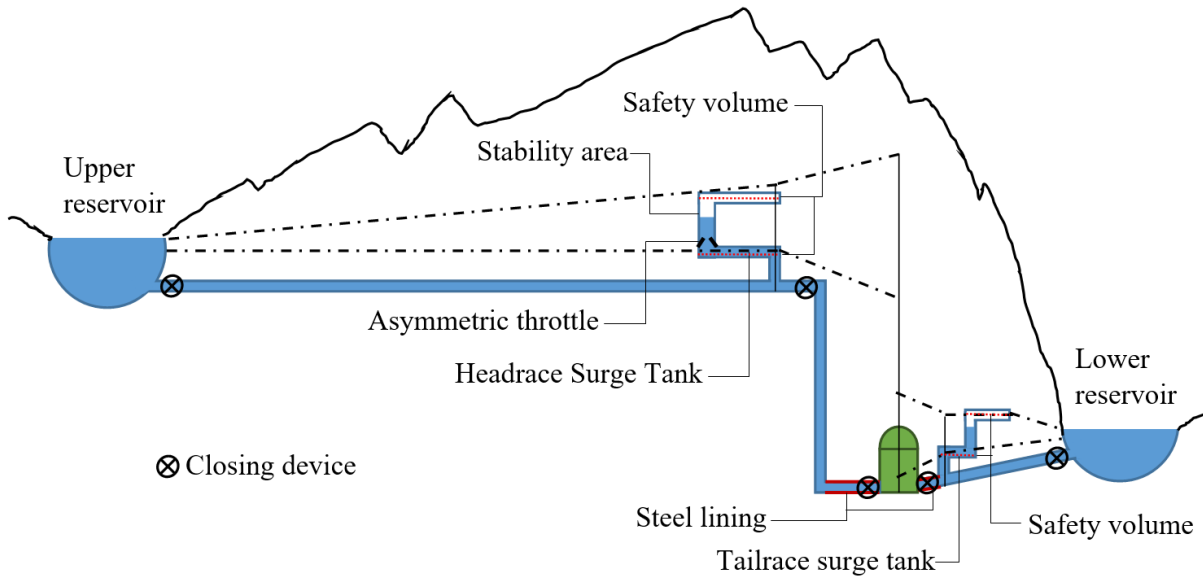


Figure 3-3: Longitudinal section of generic pumped-storage hydropower scheme with chamber surge tanks

Equation (3-6) gives the time constant of hydraulic inertia depending on the length of the power waterway and the flow section area. This hydraulic inertia time constant influences together with the inertia of the rotating mass (3-7) the demand of a surge tank.

$$T_W = \frac{Q_0}{g H_0} \sum_i^n \frac{L_i}{A_i} \text{ [s]} \quad (3-6)$$

Q_0	...	Reference flow rate at turbine
H_0	...	Mean reference head at turbine
L_i	...	Length of pipe section
A_i	...	Cross-sectional area of pipe section

Equation (3-7) leads to the inertia time constant for the rotational masses including all associated masses on the shaft with the generator and the turbine [59] [60].

$$T_A = J \frac{\omega^2}{P_{max}} \quad (3-7)$$

J	...	Inertia of the rotating mass
ω	...	Angular speed
P_{max}	...	Full power output

The inertia of the rotating masses act as dampening to the oscillation of the hydraulic system. Thus, for stable operation and mitigated pressure fluctuations the rotational time constant should be significantly larger as the water inertia time constant Equation (3-8) [61].

$$\frac{T_A}{T_W} > 6 \quad (3-8)$$

This aspect leads to the conclusion that either the mass of the generator is high or the water mass in the penstock is low for best transient and stability behaviour. This factor can be influenced by short and wide penstocks to minimize the water inertia constant. This aspect has led to investigations of *Mader* (1990) [62] study an ideal control power plant applying a closed surge tank. Thus, the minimized inertia of the penstock is an important argument of using closed surge tanks or vertical shafts from the surge tank as direct as possible to the machine cavern. The aspect of direct shafts is also discussed by *Schleiss* (2013) to improve economic aspects of pumped storage projects [58].

Low values of hydraulic inertia subsequently correspond with low water hammer pressures and thus improves the dynamic design of hydropower schemes.

3.4.2 Maximum and Minimum Oscillation

For an estimation of the maximum up-surge and minimum down-surge of unthrottled surge tanks the equations (3-9) and (3-10) are given in literature [63]. The amplitude is measured from the idle state of the water level in the surge tank. However, these formulas do not replace comprehensive numerical transient analyses.

$$z_{\max} = v_{T,0} \sqrt{\frac{A_T L_T}{g A_{ST}}} - 0.6 h_{HL,0} \text{ [m]} \quad (3-9)$$

$$z_{\min} = -v_{T,0} \sqrt{\frac{A_T L_T}{g A_{ST}}} - \frac{h_{HL,0}}{8} \text{ [m]} \quad (3-10)$$

$h_{HL,0}$... Head loss in the pressure tunnel at steady-state flow [m]
 $v_{T,0}$... Velocity in the pressure tunnel at steady-state flow

3.4.3 Stability Criteria of Surge Tanks

To avoid instability in a surge tank separated water conduit system the stability criterion was established [50]. This criterion was adapted to be multiplied by a safety factor of 1.5 to 1.8 [-] according to empirical investigation of *Jaeger* [64]. The criterion of Thoma is used for surge tanks in headrace systems such as shown in fig. (3-2).

$$A_{TH} = \frac{Q_0^2}{2g A_T} \frac{L_T}{h_{HL,0} H_0} \text{ [m}^2\text{]} \quad (3-11)$$

A_{TH} ... Minimum cross-sectional area by the Thoma criterion [m²]
 A_T ... Cross section area of the pressure tunnel [m²]
 L_T ... Length of the pressure tunnel [m]
 H_0 ... Head at steady-state discharge with Q_0 [m]

Additionally, a headrace system stability criterion equation (3-12) was derived by *Svee* including the velocity height in the pressure tunnel [65]. This formula can be applied for headrace as well as for tailrace surge tank systems. The velocity head has a destabilizing effect on surge tanks in headrace tunnels. This aspect represents analytically the empirical safety factor of *Jaeger*.

$$A_{SV} = \frac{L_T A_T}{2 \cdot g \cdot \left(\frac{h_{HL,0}}{v^2} + \frac{1}{2g} \right) \cdot (H_G - h_{HL,0})} \cdot \frac{1}{\left(1 + \frac{q_0 \cdot \Delta\eta}{\eta_0 \cdot \Delta q} \right)} \quad (3-12)$$

A_{SV} ... Cross sectional area according to the Svee criterion in headrace systems [m²]
 $\Delta\eta/\Delta q$... Variation of turbine efficiency over discharge (if 0: constant efficiency)
 H_G ... Gross head [m]

Example: Transient 1D-numerical stability simulation for high-head HPP:

Table 3-1: Data of example high-head HPP.

$P = 91 \text{ MW}$	$D_T = 5.1 \text{ m}$
$L_{\text{Headrace}} = 12\,300 \text{ m}$	$K_{ST} = 85 \text{ m}^{1/3}/\text{s}$
$Q_d = 83 \text{ m}^3/\text{s}$	$\eta = 0.9 [-]$
Shaft surge tank case depended cross section	$H_0 = 123.4 \text{ m}$
$1.0 \times \text{Thoma area} = 84.3 \text{ m}^2$	$H = 144.7 \text{ m}$
$1.5 \times \text{Thoma area} = 126.5 \text{ m}^2$	

Figure 3-4 visualises the power start-up of the turbine within 1000 s by a given linear output set point to 91 MW. The output power is then kept constant as it is the demand for unfavourable stability boundary conditions. In relation to the surge tank shaft size with Thoma factor 1.0 [-] respectively Thoma factor 1.5 [-] the machine discharge is plotted. The Thoma factor 1.0 [-] leads to an oscillating discharge while a surge tank shaft size with Thoma factor 1.5 [-] is leading to a constant machinery discharge. Accordingly, Figure 3-5 shows the oscillation behaviour in the surge tanks itself for constant power output for unfavourable boundary conditions.

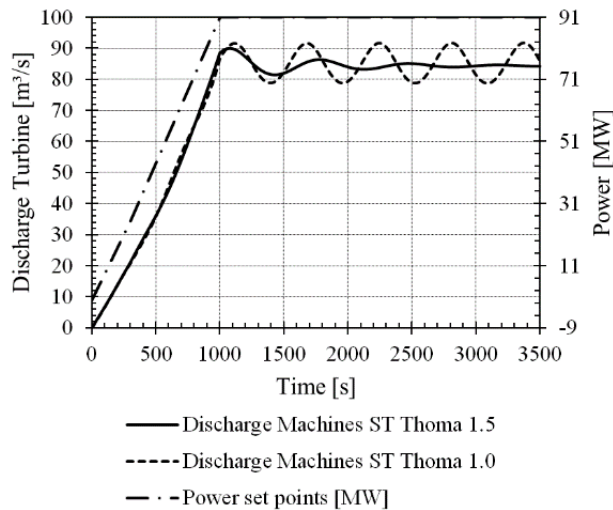


Figure 3-4: Turbine discharge for ST with Thoma 1.0 and 1.5 shaft size

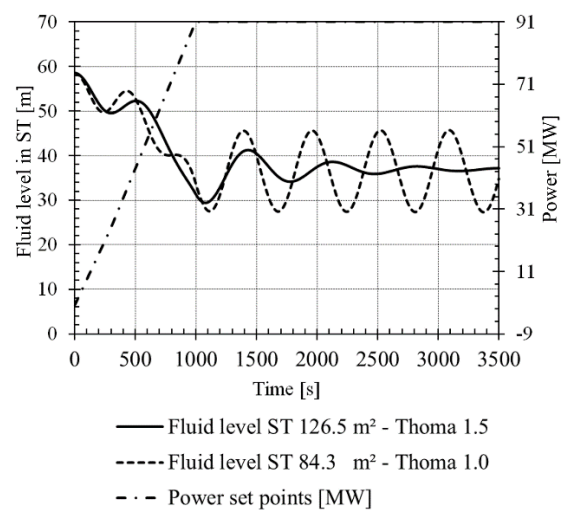


Figure 3-5: Shaft oscillation in ST with Thoma 1.0 and 1.5 shaft size

If the surge tank is equipped with an additional throttle, the stability behaviour can be improved, as shown in Figure 3-6 in addition to Figure 3-5. This positive effect of throttling was also shown by [66].

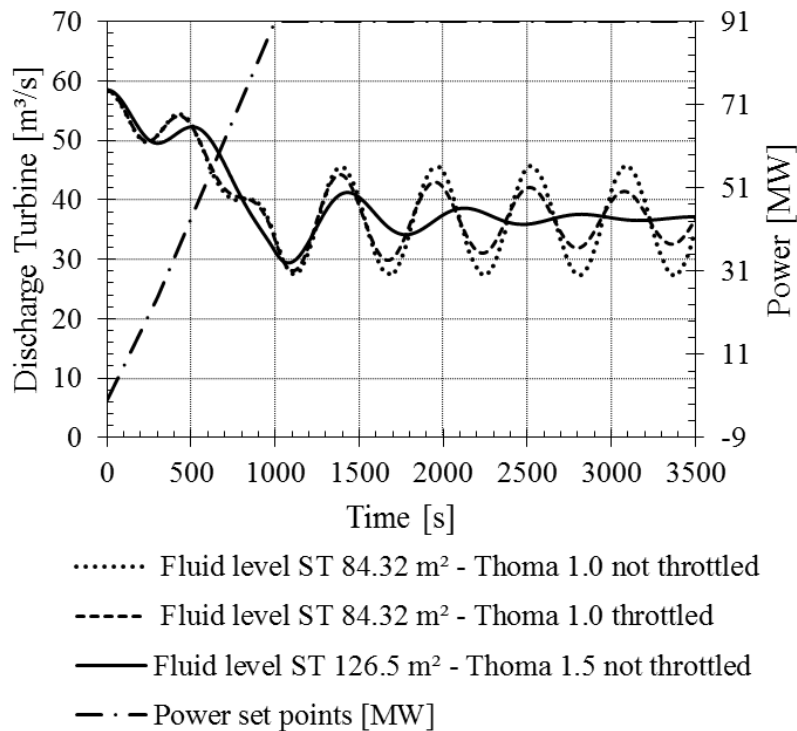


Figure 3-6: Turbine discharge for ST with Thoma 1.0 [-] not throttled and throttled and a not-throttled Thoma 1.5 [-] shaft size

Tailrace systems with surge tanks show a stabilising effect regarding the velocity height. The stability criterion of surge tanks in tailrace systems is expressed regarding [65] and visualised in Figure 3-7. It shows the deviation of Thoma criterion and Svec criterion adapted to a tailrace pressure tunnel with open air shaft surge tank. One can notice that the shaft size demand decreases the shorter the length of the tailrace tunnel. For tunnels with a length up to about 2 000 m significant reduction in demanded stability area can be reached by applying the Svec criterion.

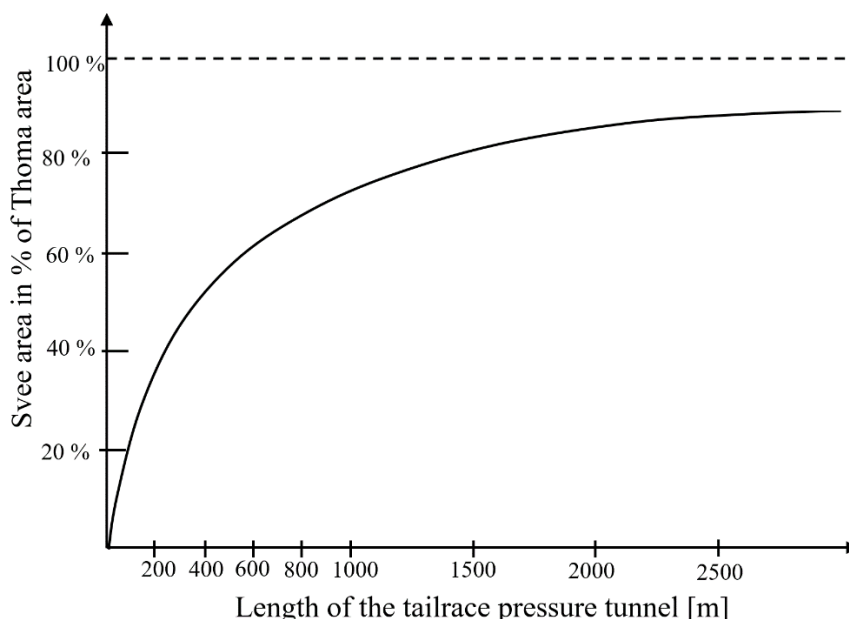


Figure 3-7: Comparison of Svee stability area to Thoma stability area for tailrace conduit systems [65]

Equation (3-13) describes the stability criterion regarding air cushion chambers as firstly defined by *Svee* [67]. The stiffness of the surge tank is defined by a necessary air volume. This finding, published in 1972 allowed the construction of the first air cushion surge tank in Norway 1973 for *Driva* power plant that can be operated in islanded grid with an aluminium plant [68]. The main advantage was to overcome the steep rock formations with an economic design for this particular case and was the basis for further air cushion surge tanks, mainly in Norway.

$$A_{AIR} = A_{SV} * (1 + n * \frac{P_{Z,0}}{\gamma * a_0}) \quad (3-13)$$

- n ... Polytropic exponent [-]
- $P_{Z,0}$... Pressure of air cushion, steady-state condition [N/m²]
- γ ... Specific weight of water [N/m³]
- a_0 ... Distance between the surge chamber roof and the water level in a surge chamber with vertical walls and a horizontal roof [m]

The polytropic coefficient defines the thermodynamic state between isotropic ($n=0$) and adiabatic ($n=1.4$) behaviour. For isotropic state the thermal energy is fully transferred to the surrounding rock, for adiabatic state it is kept within the compressed air cushion.

The thermodynamic behaviour of air cushion surge tanks is described by the polytropic equation [69].

$$pV^n = \text{constant} \quad (3-14)$$

FUNDAMENTALS AND STATE OF THE ART

p	...	Pressure [Pa]
V	...	Volume [m ³]
n	...	Polytropic exponent [-]

Regarding the right choice of the polytropic exponent it was shown by *Vereide* [70] that for quick transients appearing in surge tanks the adiabatic constant with $n=1.4$ [-] is feasible. These quick transients appear for usual power plant operations that result in mass oscillations and water hammer oscillations. For closed surge tanks in the range from 1000 m³ to 120 000 m³ of volume (covers the range of Norwegian ACST) the thermodynamic behaviour is confirmed to be adiabatic [70]. For slow transients in surge tanks, when heat exchange into the adjacent rock can be anticipated, the Modified Rational Heat Transfer method (MRHT) was developed [71]. Such slow transients are encountered e.g. for changing reservoir level.

The effect of brook intakes on the mass oscillation and the surge tank stability are studied at NTNU in Trondheim for Norwegian high-head schemes, that are usually consisting of comprehensive water conduit systems [72]. Further investigations of the stability of closed surge tanks can also be found in *Chaudhry et.al.* (1985) [73].

3.5 Surge Tank Design in Austria

This chapter describes general designs of surge tanks in large Austrian high-head hydropower plants and pumped storage schemes. Hydropower exploitation utilising high-head schemes has a long tradition in Austria due to the location in the Alps with a favourable precipitation situation and existing glaciers as additional historic water storage that amplify the production during the melting season. The Austrian topography demands significant tunnel lengths and differential chamber surge tanks were often used due to less outbreak volume than shaft surge tanks. Figure 3-8 shows the development of large high-head schemes in Austria with its installed capacity (P), the turbine (TU) and pump (PU) discharge and the internal diameter (D) of the pressure tunnel. Also listed is the planned, but recently cancelled pump storage station *Atdorf* in the German Black Forest. This specific surge tank was also part of the applied hydraulic research at the hydraulic laboratory at Graz University of Technology conducted with the engagement of the author. Figure 3-8 demonstrates the continuous trend to increase capacities with the maintenance of existing facilities and the schemes currently under construction.

After the first hydropower plants were constructed, along with the development of electrical energy in the 1880s, Austria encountered several highs and lows of high-head and pumped storage hydropower development. The historic development is crucial to recognise since the power plants are mostly still in operation. The philosophical background of the hydropower development is tightly bound to the economic success of the Alpine countries and the success of the electrical grid as proposed by *Miller v.* [6]. The structural and hydraulic robustness of surge tank design is seen very much in association with the historic background.

Figure 3-8 indicates the first large high-head schemes constructed in the western mountainous parts in the 1920s providing vast amounts of energy but exporting much of it to Germany [74]. General development plans to exploit the hydraulic resources were performed in the 1920s that has paved the way for many constructions in the 20th century. During World War II several constructions were continued following the technology established in the decades before. Forced labour was significantly used at that time [75]. The timeline indicates the peak construction from the mid-1960s to the 1980s correlating with peak oil prices after the oil price shock in the 1970s [76]. Low oil prices in the 1990s [76] and the European liberalization of electrical markets in the 1990s [77] as well as the low oil price during that period including the millennium years may explain the stopped development of high-head schemes and pumped storage plants in Austria. After the millennium, only large pumped storage plants were constructed newly. Trend lines show the increased values of installed capacity along with increased discharges and diameters. It can be expected that in the future the values of new pumped storage schemes will increase even further as Figure 3-8 indicates with logarithmic scaling. The further increase in design does not automatically mean that also the surge tank design can be continued as known, this is the gap the present doctoral thesis is approaching to bridge.

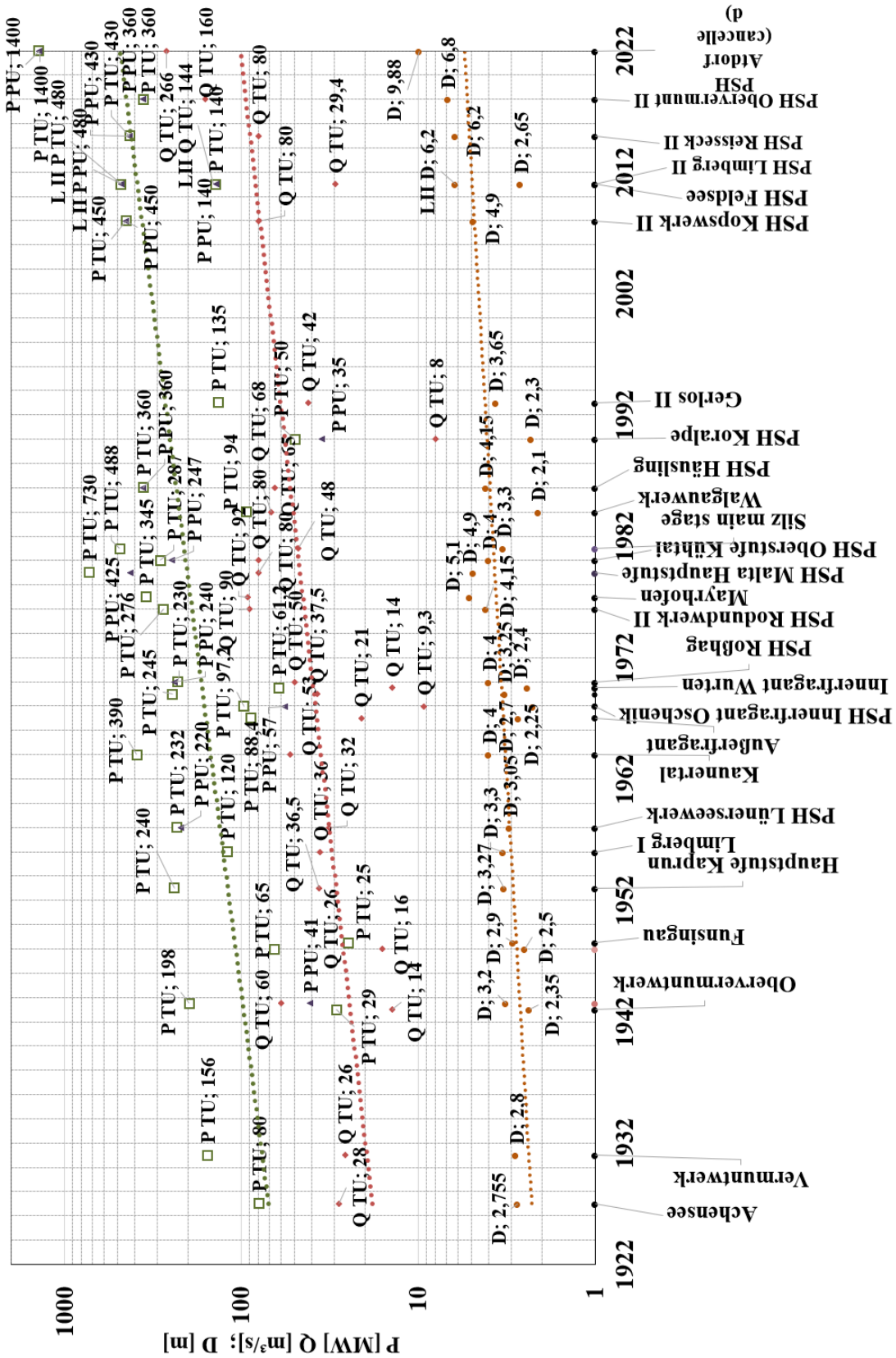


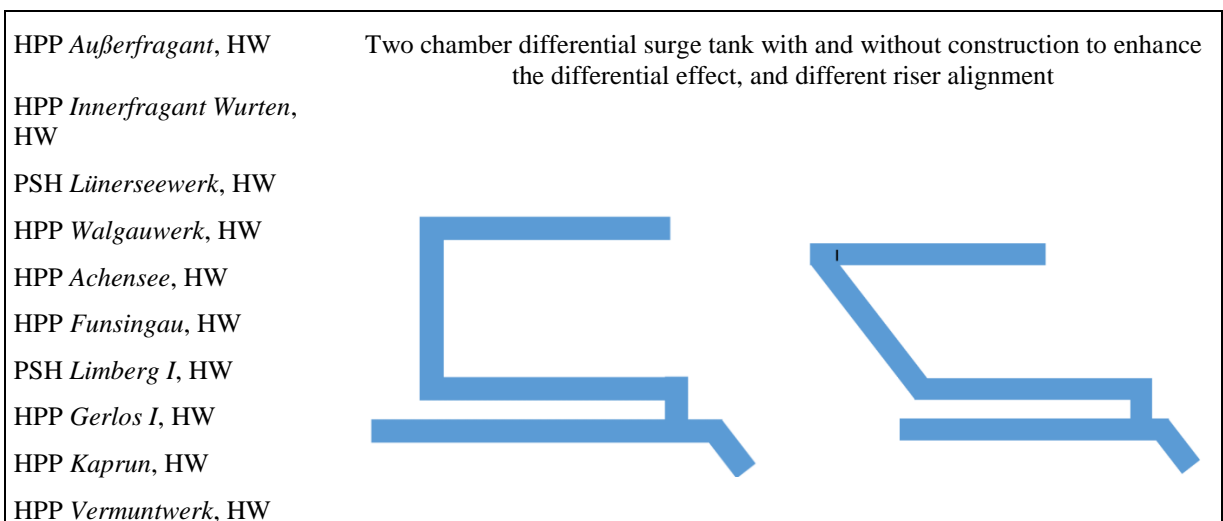
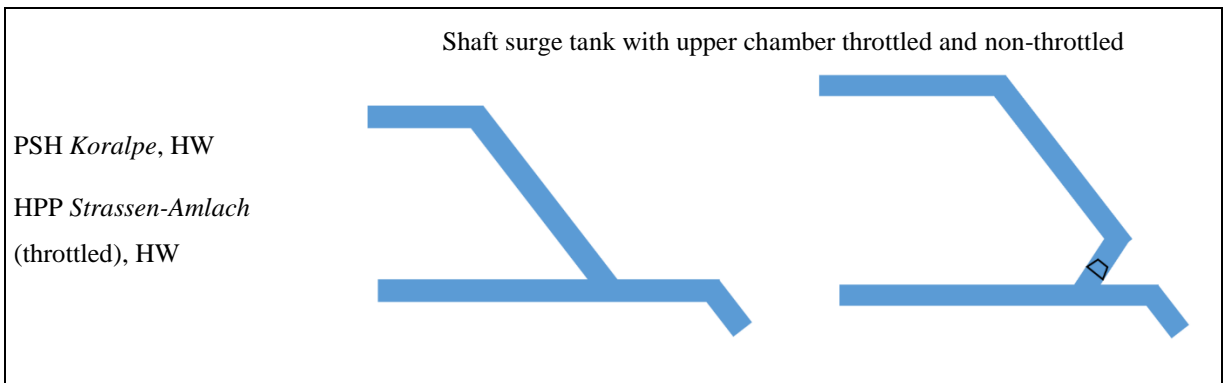
Figure 3-8: Large high-head and pumped storage schemes in Austria, development of power (P), design discharge (Q) and diameter of headrace tunnels (D) along one hundred years, as well as the planned Atdorf PSH scheme in Germany (Richter, data collection from [29])

FUNDAMENTALS AND STATE OF THE ART

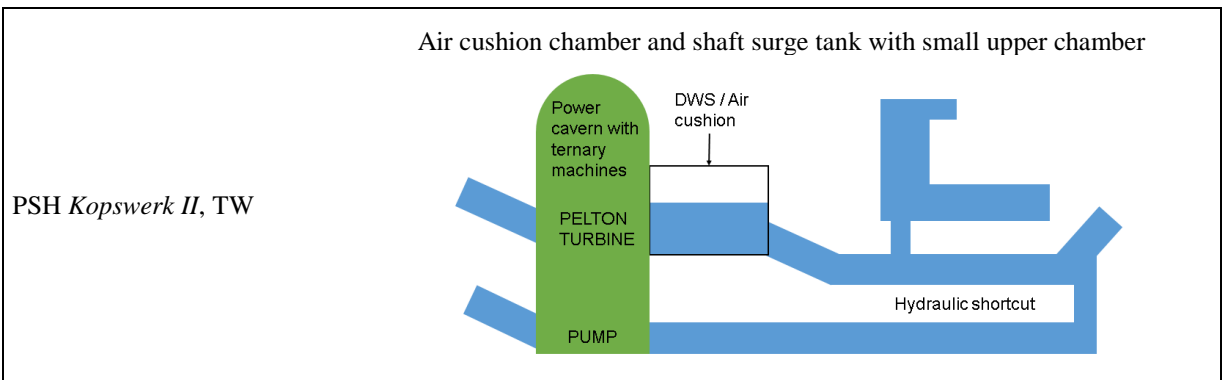
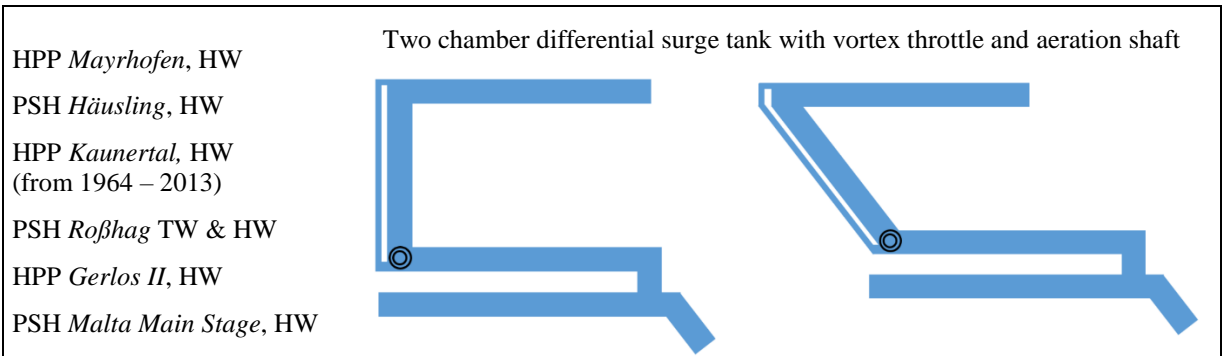
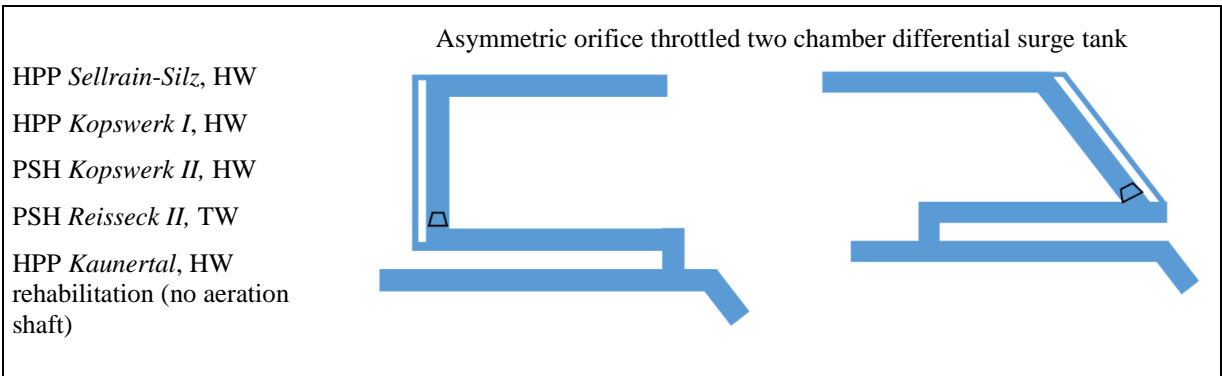
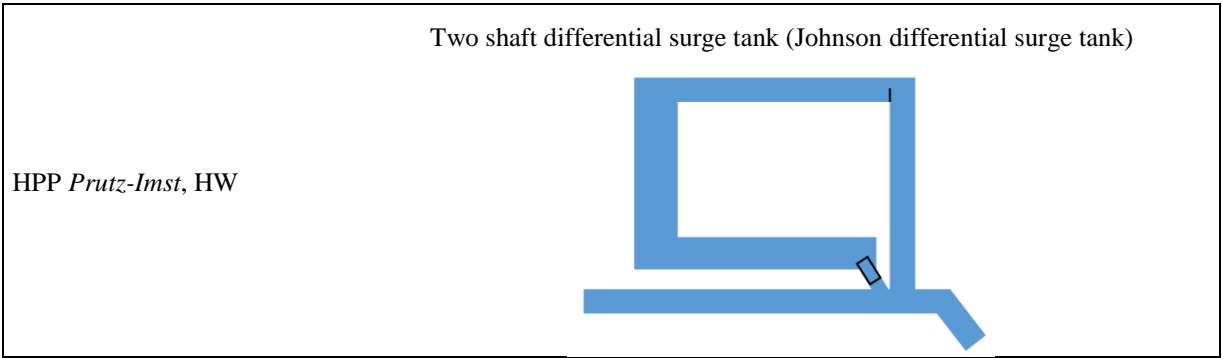
Table 3-2 gives an overview of surge tank types constructed in Austria in large high-head schemes and additionally the specific surge tank of the *Atdorf* project in Germany. One particular feature of the surge tanks in Austria is the frequent use of throttles and the significant use of chamber surge tanks with mostly two chambers. Another surge tank application designed in Austria is a complex arrangement of the tailwater system with two surge tanks: a compressed air surge tank as Pelton turbine tailwater and an open-air shaft surge tank connected to the pressurized tailwater tunnel, utilised at the highly flexible pumped storage hydropower scheme *Kopswerk II*.

Table 3-2: HPPs in Austria and the planned *Atdorf* PSH scheme in Germany with their schematic surge tank concepts (selection), (*Richter* [57]) (modified)

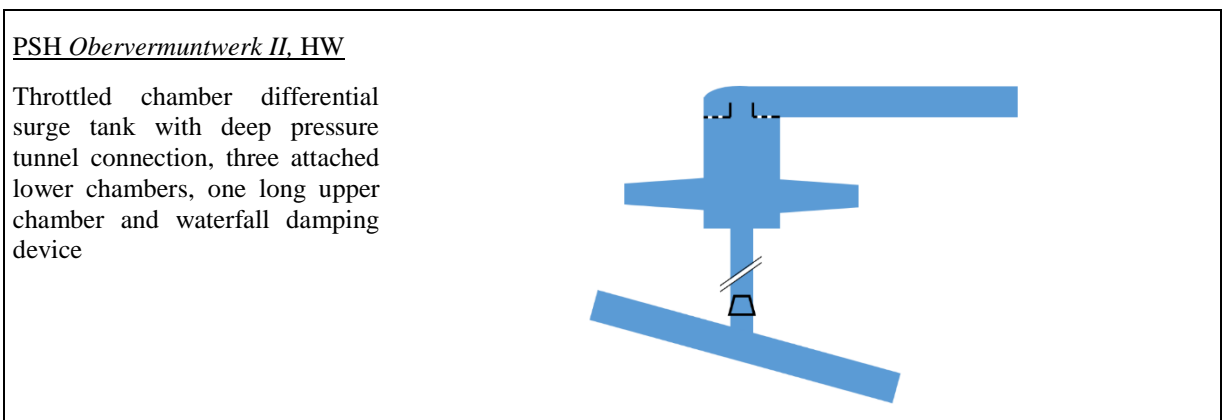
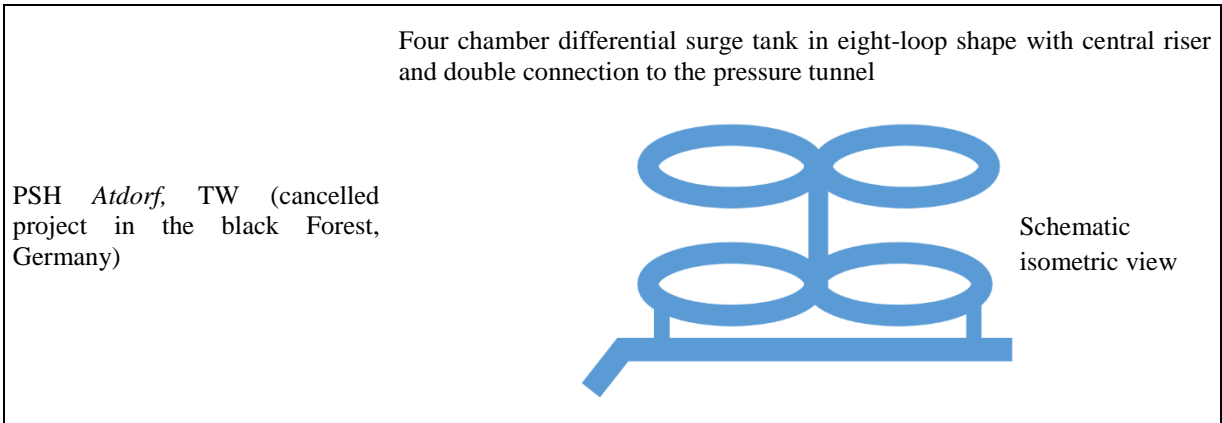
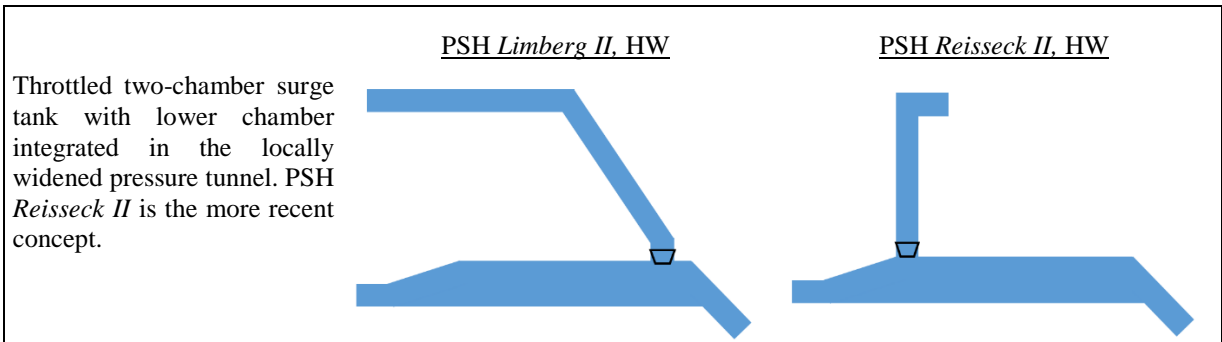
PSH <i>Kühtai</i> upper stage, HW	
HPP <i>Obervermuntwerk</i> , HW	
PSH <i>Rodundwerk I</i> , HW	
PSH <i>Rodundwerk II</i> , HW	No surge tank Because of direct reservoir connection by pressure shaft
PSH <i>Innerfragant-Oschenik</i> , HW	
PSH <i>Feldsee</i> , HW	



FUNDAMENTALS AND STATE OF THE ART



FUNDAMENTALS AND STATE OF THE ART



FUNDAMENTALS AND STATE OF THE ART

The driving inertia of the mass oscillation is represented by the water mass in the pressure tunnels that may reach 100,000 t of water and significantly more (Figure 3-9). With over 600,000 t water mass the Atdorf project utilises a huge amount of water, representing a significant inertia that needs to be controlled by the surge tank. Thus, the surge tank of this particular project utilises these large chambers to provide the necessary amount of balance water for the oscillation.

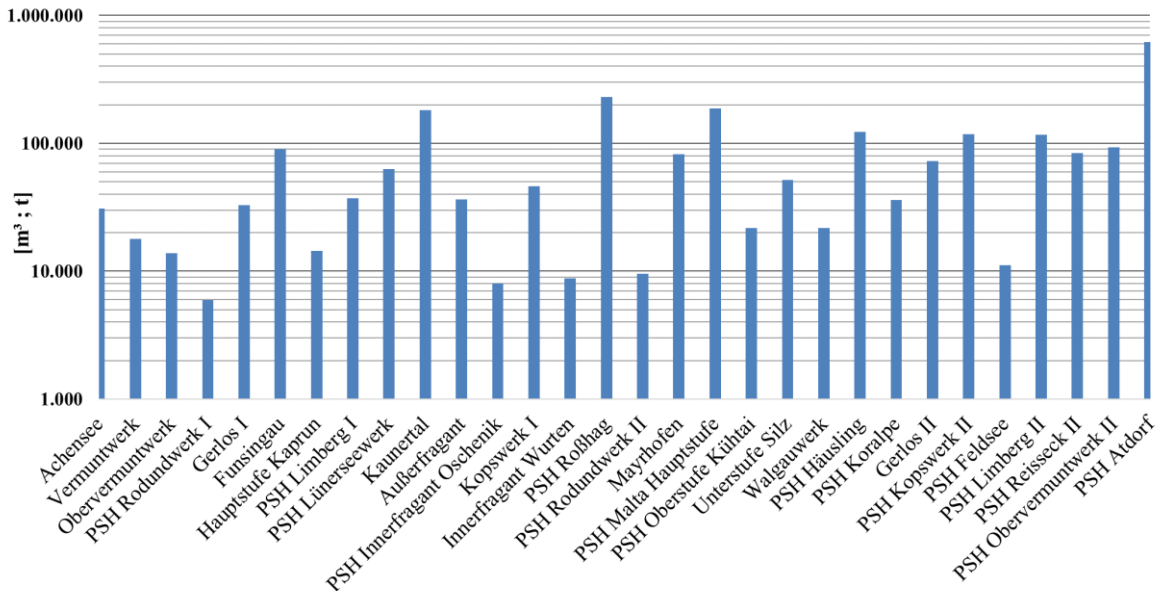


Figure 3-9: Internal water volume of pressure tunnels in selected Austrian and the planned PSH *Atdorf* in Germany schemes, chronological from left to right (*Richter*, data from [29])

3.6 Surge Tank Prototype Development for Large Schemes

Surge tank design is crucially influencing operation and construction of hydropower and pumped storage schemes. Surge tanks need an access to open air if not designed as closed surge tanks (air cushion surge tanks). Access tunnels help to decouple construction processes and allow additional accesses to penstock and pressure tunnel. For decoupling of the construction process the shaft surge tanks may be connected by an additional horizontal connection tunnel providing also space for throttle placement [44].

For large unique high-head schemes or pumped storage plants the surge tank design may not be possible applying “off the shelf” design guidelines or “copy paste” from other projects. Unique schemes may demand for unique solutions. As an example, the highly flexible pumped storage power plant *Kopswerk II* (525 MW_{Tu}, 450 MW_{Pu}) is discussed: Commissioned in 2008, it is still the world’s most flexible pumped storage scheme due to hydraulic shortcut, ternary machine concept and the special surge tank design. A two-chamber differentially throttled headrace surge tank and a combined air cushion and shaft surge tank in the tailrace system were developed. The air cushion chamber also provides the tailrace free surface chamber for the Pelton turbines allowing to operate and utilise the water between the capacity level and the draw-down level of the lower reservoir [78] [79] [80]. One of the main hydraulic and machinery designers *Mader* has made his dissertation about the mass oscillation of closed surge tank of a grid controlling high-head power plant in 1990 [62]. The closed air cushion surge tank was additionally placed directly in front of the machines to maximise the hydraulic response of the system. In his thesis Fortran routines were developed and merged to a 1D code utilised to develop several complex schemes such as PSH *Obervermuntwerk II* and PSH *Rellswerk* at Illwerke AG. In 1996 a dam heightening at a Swiss power plant with Pelton turbines was reported to be solved by utilising a compressed air free surface outflow [81]. In 2004 the construction for PSH *Kopswerk II* started and which was finished in 2008. This developing background visualises that comprehensive and well-functioning schemes may take several years to be developed by variant iteration processes. Also, the hydraulic design for PSH *Obervermuntwerk II*, a highly flexible pumped storage scheme was started about 7 years before construction began in 2014 and the first unit was in operation in June 2018. The aim of this discussion is to visualise the need and the value of long-term design processes. This approach can be seen at many comprehensive high-head schemes in Austria constructed in the 20th century. Between the idea, the design and the construction sometimes even decades were needed. Due to unique opportunities of the water resource exploitation, complex schemes needed to be developed to best use the given head and inflow. This approach results in reliable energy infrastructure serving for many decades.

FUNDAMENTALS AND STATE OF THE ART

An optimised surge tank solution influences the whole power plant functionality and also improves the construction process since the surge tank is an access point if connected to the surface. Thus, a multi-problem issue has to be solved. The goals of a well-integrated design can be defined with the aspects of:

- Hydraulic stability – can be found in terms of discrete application of formula or 1D stability simulations
- Best hydraulic performance – in combination with constructability
 - Differential effect
 - Minimised reaction time of surge tank system
 - Resonance load-cases at most unfavourable condition
 - No air in the pressure tunnel system
 - Minimised volume demand
 - Sufficient water hammer protection against cavitation
 - Best dampening of water hammer reflection by ideal inertia coefficient
- Constructability and best integration in the construction process – in combination with the whole system
 - Access of the surge tank
 - Decoupling of construction processes
 - Combination of how to improve construction of pressure shaft, pressure tunnel
- Minimised maximum pressure for system load – in combination with best hydraulic performance
- Maximised minimum pressure for system operation – in combination with best hydraulic performance and danger of cavitation
- Additional improvements of the whole system by combining issues such as the closing devices

For increasingly large hydropower schemes with large pipe diameters and lengths additional aspects are relevant for the surge tank design such as:

- The Attachment of multiple chambers to a main shaft
- Complex aeration and de-aeration of the chambers
- Waterfall aspects
- Aspects of inertia for water hammer mitigation, especially for pumped storage plants

These large-scale power plants are the main focus of the present thesis. The requirements of new flexible and large schemes may demand improved design approaches. It is a nonlinear, multi-variable optimisation problem – thus it demands for an iteration process, that takes some time but influences significantly cost and performance of a power plant.

3.7 Hydraulic Safety Design Philosophy

Surge tanks must not harm structures and lives; thus, they should not overflow and should not completely drain for any possible operational load-case event. Surge tanks need to provide stable operation of the powerplant. The surge tank has to be designed and checked for the most unfavourable water hammer event in order to prevent column separation in the water conduit and to mitigate high-pressure fluctuations and amplitudes.

For the construction of the hydropower plant *Kaunertal* in 1964 load-cases with loading, unloading and reloading were established and are since then standard design cases for surge tank layouts in Austria [82]. This means that the hydraulic machines are loaded and unloaded in succession at the most unfavourable time points in the simulations of the power plant. Later it was proven by *Heigerth* [83] that it cannot be amplified to infinity. For shaft surge tanks 1st load → unload, 2nd load → unload and a 3rd load → emergency shut down is sufficient to cover the infinity of succeeding loading events if the set-points are chosen at a most unfavourable time step regarding to the discharge of the water in the tunnel. The set-point finding is still suggested to be done manually with a 1D-numerical simulation software. Figure 3-10 shows a reloading in resonance after unloading for a generic case with conservative assumptions, the amplified tunnel discharge is clearly indicated. Figure 3-11 shows a load-case with three times loading in resonance with a following emergency shut-down for a generic shaft surge tank system. Additional amplification after the first reloading is very low and will asymptotically lead to no more additional amplification. If security facts are considered for the simulation, a sufficient and desirable design load-case is given for a 2nd loading followed by an emergency shut down. This load-case has to be considered as an important water hammer load-case [83].

Multiple loading cases are carried out at maximum and min. reservoir levels to define maximum filling and minimum emptying level of the surge tank as well as maximum and minimum pressure at the surge tank base.

Figure 3-10 visualises the principle of a multiple loading event for loading, unloading and reloading at unfavourable time points regarding mass oscillation.

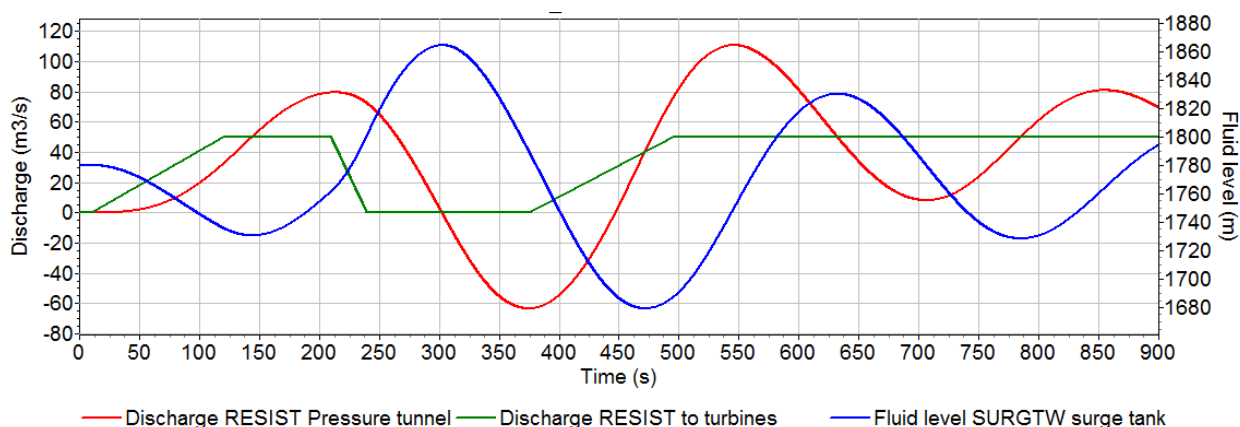


Figure 3-10: Reloading after start-up and unloading, idealised 1D-numerical simulation of a generic system with rigid column simulation, without water hammer capturing (*Richter* [55])

If the units are unloaded and reloaded for more than two times the additional amplification is limited and thus, it is sufficient to consider one reloading event at the most unfavourable time after previous unloading [83]. For chamber surge tanks with an upper chamber differential effect additional loading loops even show a decreased amplification.

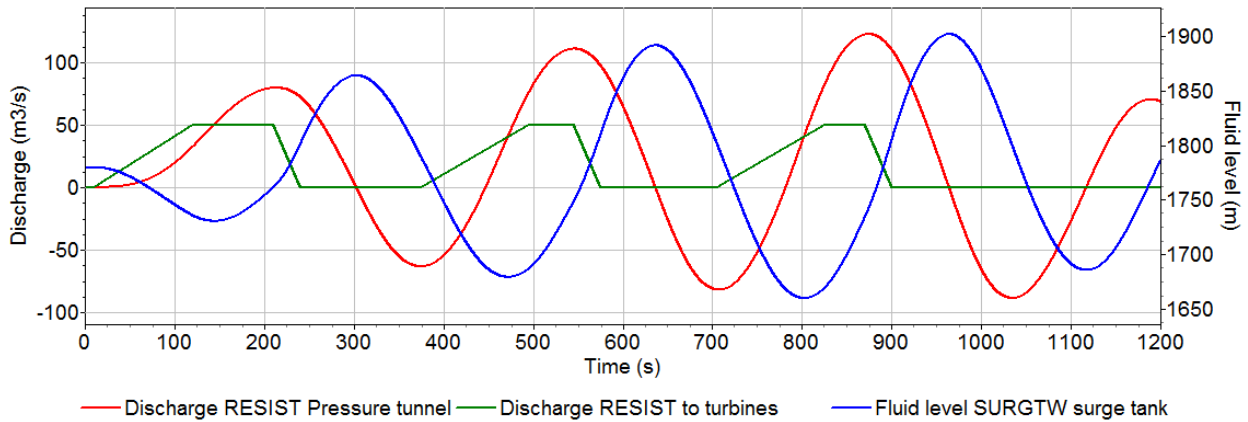


Figure 3-11: Resonance load-case – multiple loading cases, idealized 1D-numerical simulation of a generic system representing with rigid column simulation, without water hammer capturing (*Richter* [55])

The lack of these considerations may have led to failures in the past such as reported by *Dahlbäck* 2015 [84] on a flooding of a machine cavern by overflow of the tailrace surge tank. While the resonance case may lead to considerably larger surge tanks it allows for safe operation and long term functionality that may even cover margins for future operational expansions. The safety concept also includes a conservative choice of the pressure tunnel friction loss factor.

Unfavourable differences in proposed design friction values to observed ones were reported e.g. for HPP *Kárahnjúkar*, Iceland [85] or the *Lesotho Highlands Water Project* [86]. For both cases the friction was less as predicted, which is fortunate for the aspects of energy loss but also have the consequence of higher kinetic energy in the water conveyance system that need to be safely under control by surge mitigating structures. These specific cases also highlight the importance of research on friction related issues.

For resonance or multiple loading and unloading load-cases a rather smooth pipe friction leads to most unfavourable oscillation results. Thus the friction factor has to be assumed sufficiently smooth for the surge tank simulations (see chapter 3.8).

3.8 Roughness Considerations

For a single turbine mode full shut down a low friction factor generates the highest up-surge in the headrace surge tank and thus represents the most unfavourable load-case. For single turbine mode start-up a high friction factor generates a deep down-surge in the headrace surge tank. For a resonance load-case with multiple loading and reloading events a low friction factor is key for a conservative approach regarding the surge tank design. This accounts for headrace surge tanks as well as for tailrace surge tanks. Friction values found by measurements of existing pressures tunnels depend significantly on lining concepts such as in-situ concrete lining, segmental lining or unlined pressure tunnels. Friction factors may be differently implemented in 1D-numerical simulations, either a non-dimensional friction factor [f] or equivalent sand grain roughness [K_S]. Measurements at pressure tunnel may also be available in terms of the Strickler value [K_{ST}]. Thus, value conversions may be necessary The Strickler value K_{ST} is equivalent to 1/Manning number $1/K_M$.

$$\alpha = \frac{L}{K_{ST}^2 \cdot A^2 \cdot R_{Hyd}^{\frac{4}{3}}} \quad (3-15)$$

α ... Friction coefficient [s^2/m^5]
 K_{ST} ... Strickler friction factor [$m^{1/3}/s$]
 R_{Hyd} ... Hydraulic radius [m]

$$h_{HL} = \alpha \cdot Q^2 \quad (3-16)$$

h_v ... Local hydraulic loss [m]
 Q ... Discharge [m^3/s]

$$K_{ST} = \frac{1}{K_M} \quad (3-17)$$

K_M ... Manning friction factor [$s/m^{1/3}$]

Equation (3-18) describes the Darcy-Weisbach friction formula for friction loss in pipe flow the friction factor λ [-] derived by the Colebrook-White formula (3-19).

$$h_{HL} = \lambda \cdot \frac{L}{D_i} \cdot \frac{v^2}{2g} \quad (3-18)$$

λ ... Friction coefficient [-]

$$\frac{1}{\sqrt{\lambda}} = -2 \cdot \log \left(\frac{2,51}{R_e \sqrt{\lambda}} + \frac{K_S}{3,71 D_i} \right) \quad (3-19)$$

FUNDAMENTALS AND STATE OF THE ART

Figure 3-12 shows the approach of a table to convert Strickler friction factor to Darcy friction factor and equivalent sand grain roughness by applying goal seek function to match the friction losses for both equation (3-15) and (3-19). There is no analogue equation to convert the roughness factors for this purpose. Table 3-3 shows an example of applying the table approach for a friction factor variation for a pressure tunnel with smooth concrete liner (cast in-situ with steel framework), using the Strickler values as basis. The conversion may be necessary to apply available friction values to the 1D numerical software, that usually request either friction value λ [-] or equivalent sand grain roughness K_S [mm].

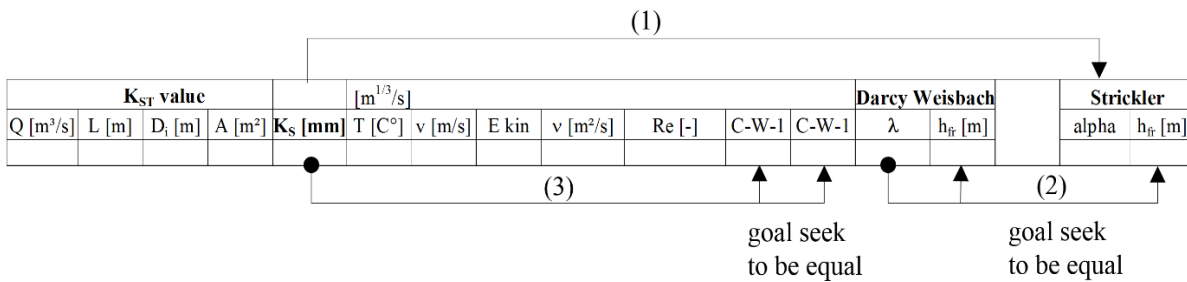


Figure 3-12: Table approach to convert Strickler friction into Darcy friction factor and sand grain roughness

Table 3-3 shows the table approach to compare friction values of tunnel section with different friction factors to compare the boundary conditions.

Table 3-3: Friction value conversion Strickler (K_{ST} [m^{1/3}/s])– Darcy Weisbach (f or λ [-]) – equivalent sand grain roughness (K_S [mm]) after Colebrook-White

conservative value for design with additional distinguished local losses in layout																	
K _{ST} value				100 [m ^{1/3} /s]										Darcy Weisbach		Strickler	
Q [m ³ /s]	L [m]	D _i [m]	A [m ²]	K _S [mm]	T [C°]	v [m/s]	E kin	v [m ² /s]	Re [-]	C-W-1	C-W-1	λ	h _{fr} [m]	alpha	h _{fr} [m]		
160	5000	7.3	41.85	0.015	20	3.82	0.74	1.00E-06	27 850 918	12.479	12.479	0.00642	3.276	0.0001	3.276		
conservative value for design if no distinguished local loss are used																	
K _{ST} value				90 [m ^{1/3} /s]										Darcy Weisbach		Strickler	
Q [m ³ /s]	L [m]	D _i [m]	A [m ²]	K _S [mm]	T [C°]	v [m/s]	E kin	v [m ² /s]	Re [-]	C-W-1	C-W-1	λ	h _{fr} [m]	alpha	h _{fr} [m]		
160	5000	7.3	41.85	0.065	20	3.82	0.74	1.00E-06	27 850 918	11.231	11.231	0.00793	4.044	0.0002	4.045		
realistic value - in-situ concrete lining steel forms																	
K _{ST} value				85 [m ^{1/3} /s]										Darcy Weisbach		Strickler	
Q [m ³ /s]	L [m]	D _i [m]	A [m ²]	K _S [mm]	T [C°]	v [m/s]	E kin	v [m ² /s]	Re [-]	C-W-1	C-W-1	λ	h _{fr} [m]	alpha	h _{fr} [m]		
160	5000	7.3	41.85	0.134	20	3.82	0.74	1.00E-06	27 850 918	10.607	10.607	0.00889	4.535	0.0002	4.535		
realistic value of prefabricated segmental lining																	
K _{ST} value				78 [m ^{1/3} /s]										Darcy Weisbach		Strickler	
Q [m ³ /s]	L [m]	D _i [m]	A [m ²]	K _S [mm]	T [C°]	v [m/s]	E kin	v [m ² /s]	Re [-]	C-W-1	C-W-1	λ	h _{fr} [m]	alpha	h _{fr} [m]		
160	5000	7.3	41.85	0.367	20	3.82	0.74	1.00E-06	27 850 918	9.733	9.734	0.01056	5.385	0.0002	5.385		

For large diameter pipes and high Reynolds numbers there is evidence that friction values might be about 5 %-10 % even below those obtained by the Moody / Prandtl / White / Colebrook / Nikuradse smooth pipe law. The reason is that slight swirl flow is present over long flow distances [87].

Jaeger (1977) [88] recommends for cast in situ concrete lining to use smooth friction ($K_{ST} = 85$ to 95 [$m^{1/3}/s$]) values for opening load-cases and rough values for closing events ($K_{ST} = 70$ to 75 [$m^{1/3}/s$]). As a recommendation of this present thesis and an analysis of literature, it can be concluded to use the smooth friction numbers for resonance load-cases simulations. For cast in situ concrete lined tunnels it is recommended to apply the smooth line approach for the simulations as given in the empirically derived formula (3-20) and (3-21) recommended by *Jaeger (1949)* [89] based on various comprehensive measurements on water conduit tunnels [90]. *Jaeger (1949)* recommends to reduce the obtained k_{ST}^* value by 2 %-7 % to get a realistic friction loss. However, two contrast consequences of friction loss predictions may be considered by applying a safety approach:

- 1) An increased tunnel friction assumption for energy production prediction
- 2) A reduced tunnel friction for resonance surge tank oscillation simulations

$$\lambda^* = 0.0032 + 0.221 \text{Re}^{-0.237} \quad (3-20)$$

$$K_{ST}^* = \frac{1}{R_{\text{hyd}}^{1/6}} \sqrt{\frac{8g}{0.0032 + 0.221 \text{Re}^{-0.237}}} \quad (3-21)$$

Measurements at the prototype and recalculations of *Obervermuntwerk II* have also revealed that very smooth conditions in the pressure tunnel are present [45] and that the safety philosophy worked out well. The results also lead to the discussion that the usual approach to sum local hydraulic losses of bends, restrictions and diversions is imperfect since the given numbers in the literature are taken into account the full developing length that may not be given in a prototype power plant when the local losses are discrete and summed up consequently. Instead, the real superposition shows a hydraulic influence that may lead to possibly lower friction losses that need to be reflected in the safety approach. The *Obervermuntwerk II* hydraulic design applies an overall conservative and very successfully applied design philosophy described by *Dich and Barwart (2017)* [91]. It can be concluded and recommended that for surge tank resonance oscillation simulations the hydraulics of the whole power waterway is to be calculated including all local losses and friction losses separately. The local losses are determined regarding empiric or best practice values following literature such as *Idel'chik (1994)* [92] or *Miller (1990)* [93] or other specific publications. The friction losses need then to follow the very smooth approach following *Jaeger 1949* [89]. Local losses might interfere each other and even interfere with friction losses, especially for high Reynolds numbers and large tunnel diameters. Thus, an exact pre-evaluation of the final friction is always a guess and should be chosen carefully applying specific safety values to lower the losses for resonance mass oscillation simulations.

FUNDAMENTALS AND STATE OF THE ART

Figure 3-13 shows the friction value range of various tunnel lining materials in Strickler value K_{ST} [$m^{1/3}s^{-1}$] [94]. A significant difference is given for precast segmental concrete liners with or without filling gaps and various holes. If using a filler material, it is important to consider traps to catch particles that are likely to fall off during operation period. Unlined tunnels show a very wide range of friction, depending on the excavation method. From very rough for drill and blast to very smooth for hard rock TBM boring. The unlined tunnel values in the figure were adapted by the authors project experience. Various design approaches for unlined tunnels are given in literature such as [95]. The unlined pressure tunnel design is extensively applied in Norway [96]. Sediment traps are placed usually after the surge tank or even at and before the surge tank, to trap grains transported to the machines [97] [98]. Unlined tunnels with gravel on the invert may also be paved with asphalt to improve the friction behaviour [99]. This gravel put on the invert was used as road during the construction and for the reasons of significant time consumption for the cleaning it was not removed to allow quicker commissioning. The unlined tunnels were thus designed with low flow velocities and sand traps. Higher friction can be easily encountered by larger diameters of the pressure tunnel in the design phase [100].

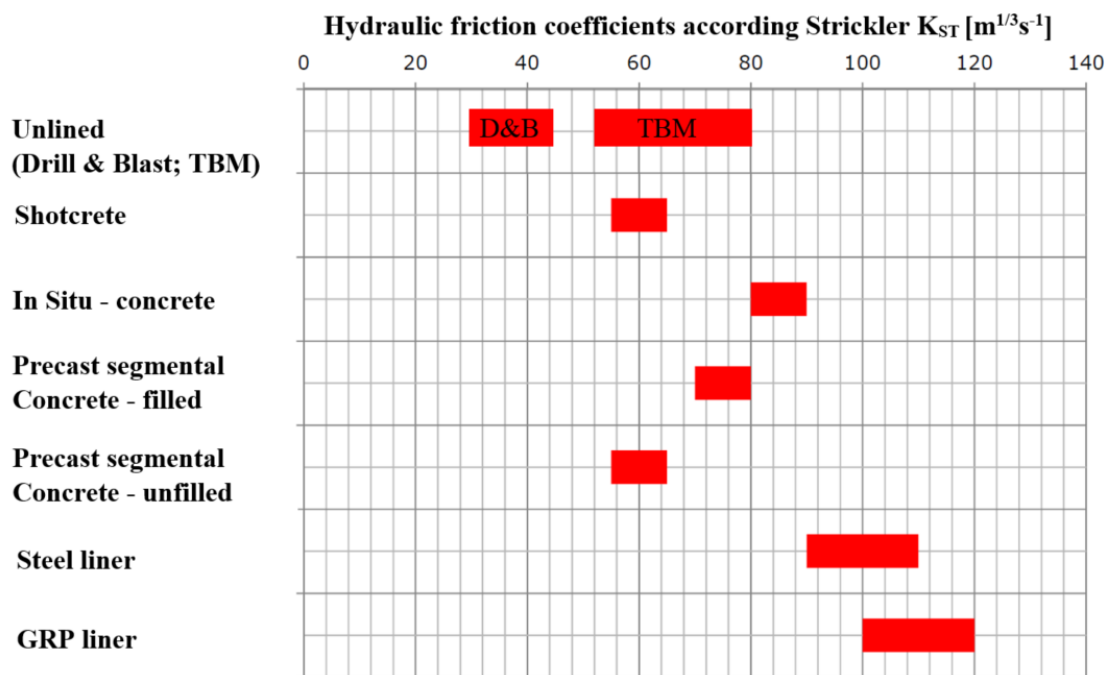


Figure 3-13: Typical friction coefficients for tunnel and shaft liners in Strickler value k_{ST} [$m^{1/3}s^{-1}$] (source: lecture script A. *Vigl* 2018, modified)

3.9 Complex Surge Tank Concepts

Simple surge tanks such as unthrottled shaft surge tanks may be a first approach for designing a surge tank concept. For large hydropower or pumped storage hydropower schemes simple shaft surge tanks may show significant drawbacks due to high demand of volume that is associated with the demands for optimised minimum and maximum level. For highly flexible high-head schemes a size factor of 2-3 [-] needs to be considered to capture multiple switching events generating resonance effects as a result of investigated high head schemes for the present thesis. The idea of differentiating between a quick riser directly connected to the pressure tunnel and a main riser that is in throttled connection to the pressure tunnel was developed in the early stages of the 20th century by *Johnson* [101]. In the literature, these surge tanks are still often referred to as Johnson surge tanks. Johnson proposed a differential surge design to improve the dynamics of the surge response on the mass oscillation. Figure 3-16 shows a generic Johnson differential surge tank. This type of surge tank provides a quick pressure response in the surge tank after machine or valve action, which leads to a fast acceleration or deceleration of the water mass in the pressure tunnel. The simple principle is: The quicker the response of the surge tank, the smaller the volume needed in the surge tank. The stability criterion is considered by ensuring that the sum of the section area of all risers is sufficiently large. An impressive Johnson surge tank was constructed in Austria for the *Prutz-Imst* run-of river high-head scheme, in operation since 1956 (Figure 3-17).

In addition, other throttled surge tank types function as differential surge tanks such as:

- Throttled shaft surge tanks
- Throttled chamber surge tanks

Figure 3-14 visualises a generic and general layout of a shaft surge tank with connection structure that can be throttled or unthrottled.

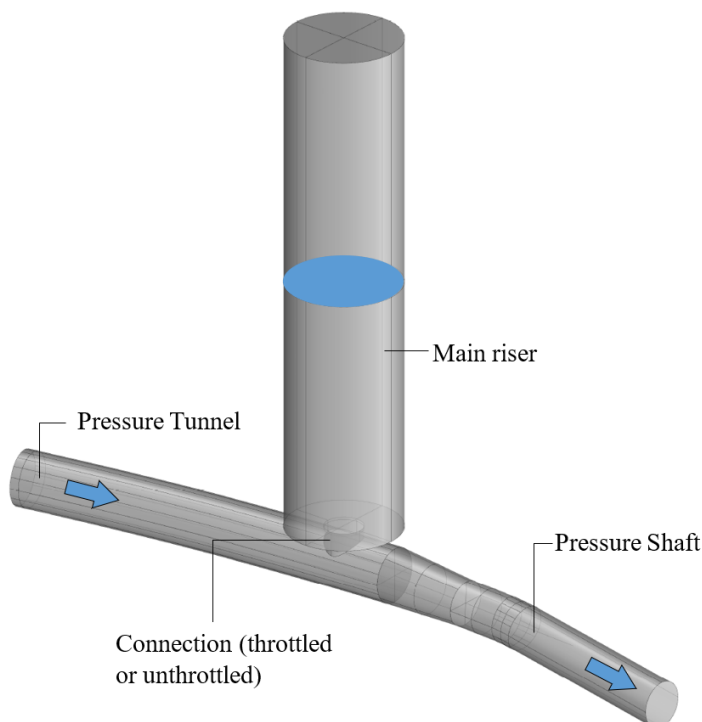


Figure 3-14: Generic shaft surge-tank design

Throttled chamber surge tanks additionally increase the differential effect by flow separation at the outflow of the upper chamber. This has been often enhanced by installing weir structures with higher outlet restriction at backflow. The flow through lower chamber design allows sufficient deaeration of the water that is intruded by a waterfall. Usually throttles are placed at the transition from the lower chamber to the main riser (Figure 3-15).

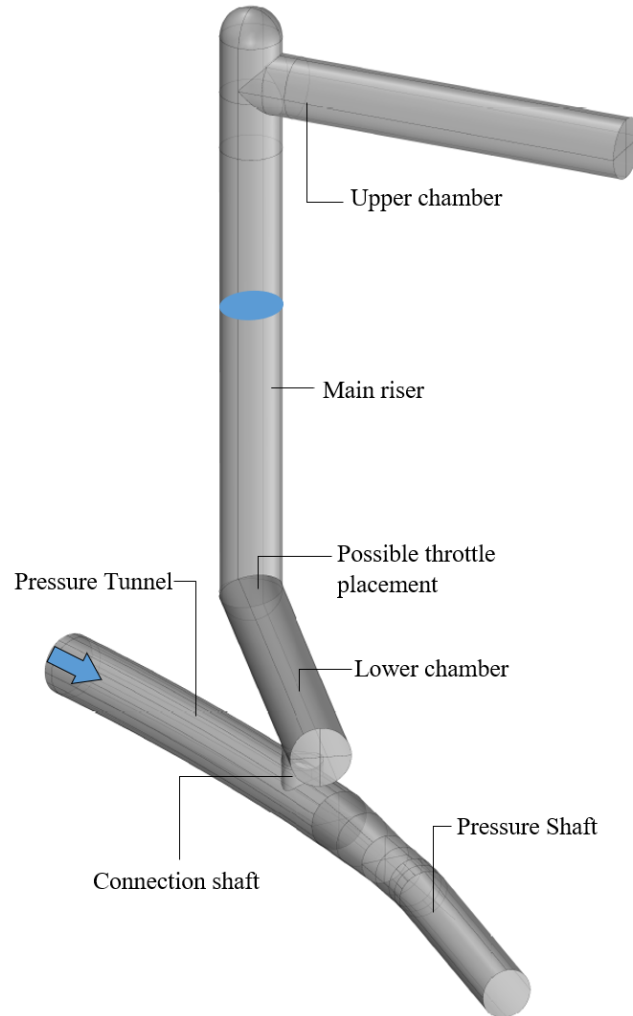


Figure 3-15: Generic chamber surge tank design

Higher discharges and higher heads may demand for new hydraulic and structural challenges for the surge tank. Flexible pumped storage and high-head schemes with discharges of more than 150 m³/s and long pressure tunnel systems may face additional demands. In these cases, the principle of differential surge tanks offers major advantages for design and operation. The main benefits can be summed as:

- Reduced excavation volume
- The lower and upper chamber can be used to adjust the operational range, maximum head for pumping, minimum head for generating mode
- Quick response during water hammer events
- Robust throttle design
- Placing of the gate inside the surge tank
- Mitigating air intrusion caused by waterfall events in the surge tank

The Johnson surge tank shown in Figure 3-16 consists of:

- Riser shaft with high-head gate for emergency closing of pressure tunnel or maintenance
- Aeration shaft to allow emergency closing of the gate and for maintenance access
- Differential riser to provide water storage
- Hydraulically asymmetric orifice throttle
- Upper basin that is connected open to air
- Weir structure to maximise head in gate shaft and to prevent backflow with waterfall
- Lower chamber to control the maximum down-surge in the riser shaft

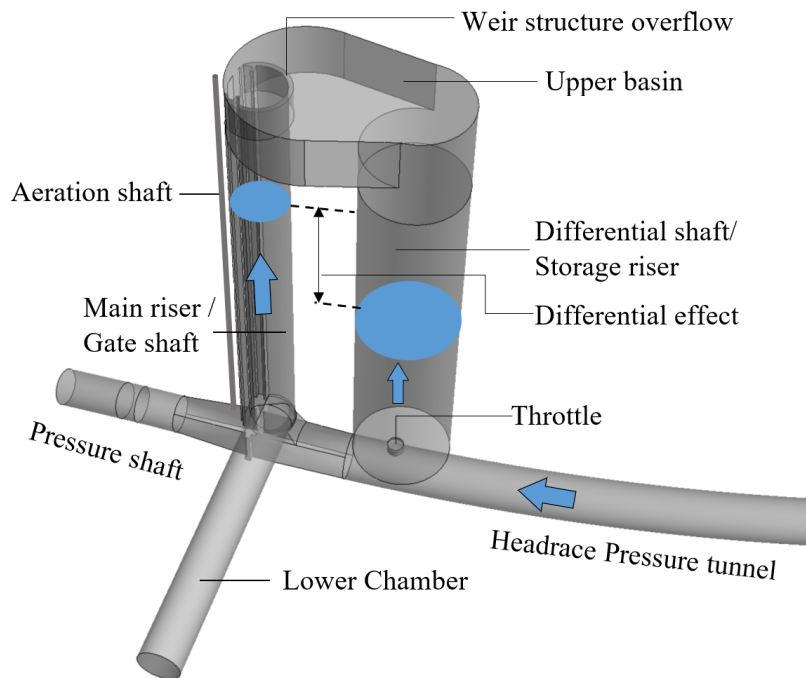


Figure 3-16: Generic Johnson differential surge tank design (Richter [102])

Figure 3-17 shows the sophisticated Johnson surge tank for the HPP *Prutz-Imst* in Austria with integrated gate in the main riser and aeration shaft as well as the differential shaft and the weir structure in the upper chamber that prevents backflow into the main riser and thus air intrusion.

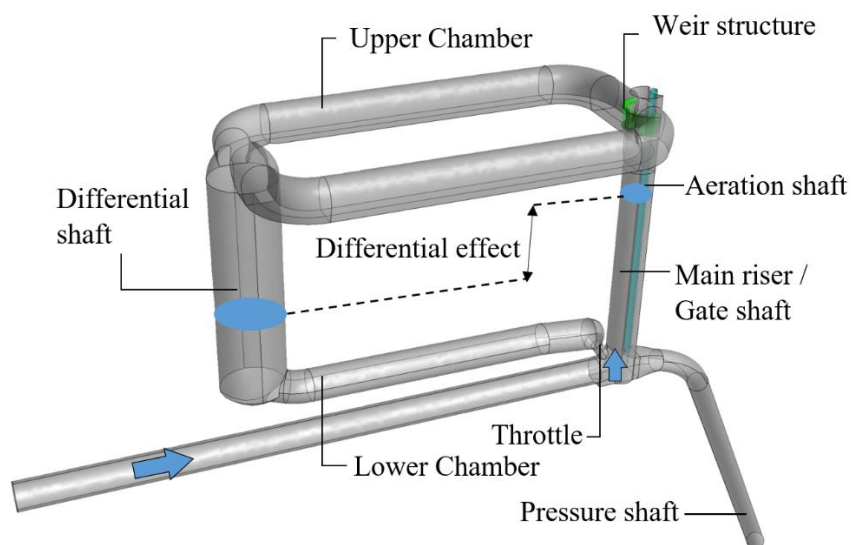


Figure 3-17: Johnson differential surge tank at *Prutz-Imst* HPP in Austria (Richter [102])

4. SURGE TANK CASE STUDIES

This chapter describes the hydraulic investigations for the surge tanks performed during this dissertation time as applied research projects. Relevant outcomes and developments are described in various chapters. The surge tank studies are listed in chronological order as investigated at the hydraulic laboratory at Graz University of Technology:

- The tailrace surge tank of *Atdorf* PSH 1400 MW in southern Germany (suspended project), located in the Black Forest, Germany.
- The tailrace surge tank *Burgstall* of the *Reisseck II* PSH with 430 MW, in operation since 2016, located in Carinthia, Austria.
- The headrace surge tank *Krespa* of *Obervermuntwerk II* PSH with 360 MW, commissioned in 2018, located in Vorarlberg, Austria.
- The headrace surge tank for *Tonstad* HPP with 960 MW in Norway.

The investigated surge tanks are part of new pumped storage hydropower plants except the *Tonstad* surge tank, that is part of an existing, high capacity and highly productive high-head hydropower plant.

1D- and 3D-numerical simulations were conducted for the listed case studies. For the surge tanks *Atdorf*, *Burgstall* and *Krespa* Froude scaled physical model tests in the hydraulic laboratory were conducted. For the surge tank *Krespa*, prototype measurements conclude the validation of the hydraulic investigations. Each project shows its specific demands and purposes. All mentioned surge tanks demand for best possible flexibility of the associated power plant or energy storing facility. The surge tanks *Burgstall* and *Krespa* were equipped with differential throttles to improve the hydraulic behaviour of the mass oscillation. The surge tank *Atdorf* utilises unique 8-loop shape chambers. The long upper chamber behaviour was studied for the surge tanks *Atdorf*, *Burgstall* and *Krespa*. Significant waterfall cases were investigated for the surge tanks *Atdorf* and *Krespa*, for the surge tank *Krespa* a specific waterfall-dampening device was developed to mitigate air intrusion. 3D-numerical multiphase simulations were conducted for the surge tanks *Atdorf* and *Krespa* to evaluate the air bubble behaviour. The surge tank *Tonstad* utilises very specific pressurised sand traps, that are not specifically part of the thesis. This surge tank is a mainly unlined construction and was investigated for a potential upgrade of power and discharge. This upgrade was researched to be utilised by semi-air cushion surge tanks as a new concept for surge tank design, in order to improve the overall behaviour and the differential effect for optimised volume use. All the beauty of the investigated surge tanks is finally hidden underground as part of sustainable energy infrastructures.

4.1 Atdorf – Tailrace Surge Tank

A physical model test and 3D-numerical as well as 1D-numerical simulations were performed to study the hydraulic behaviour of the tailrace surge tank of the project *Atdorf* pumped storage scheme in Germany [103]. The whole project was finally cancelled in 2017. However, this surge tank pilot case was intensively studied and is an important basis for this present thesis, highlighting the issues of waterfall prevention and the aspects of large water volumes in chambers. The significance in this pilot case (Figure 4-1) are the:

- 8-Loop shape, both for lower and upper chamber design
- Double connections to the pressure tunnel
- Large dimensions of the pressure tunnel
- High volume demand of the surge tank
- Significant differential effect of the upper chamber
- Large waterfall event
- Air-water investigations
- Water hammer reflection – as driving parameter for placing [104]

Figure 4-1 shows the schematic longitudinal section of the *Atdorf* pumped storage hydropower plant, indicating the long tailrace tunnel and the placing of the tailrace surge tank. The pressure tunnel is inclined outwards to the lower reservoir, allowing an economic emptying by bypassing the lower reservoir into the Rhine River.

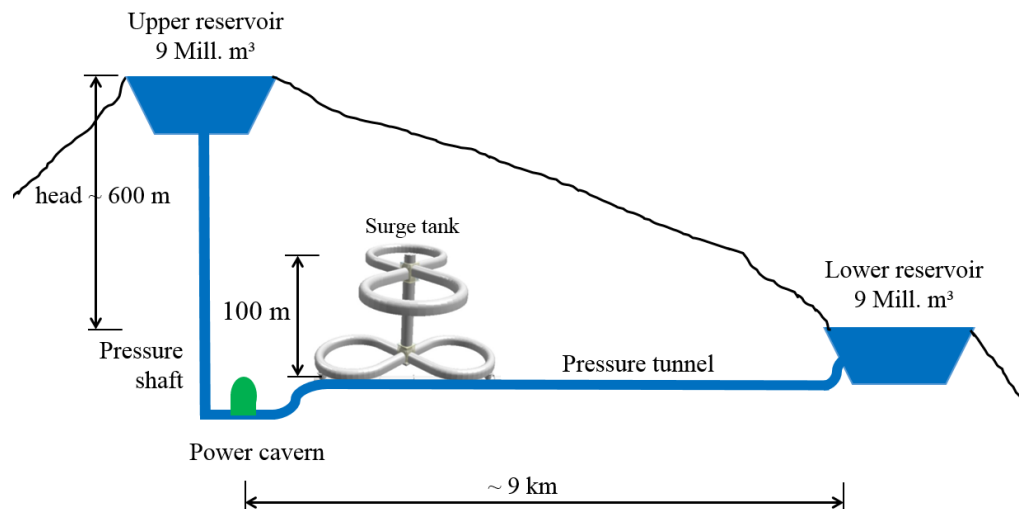


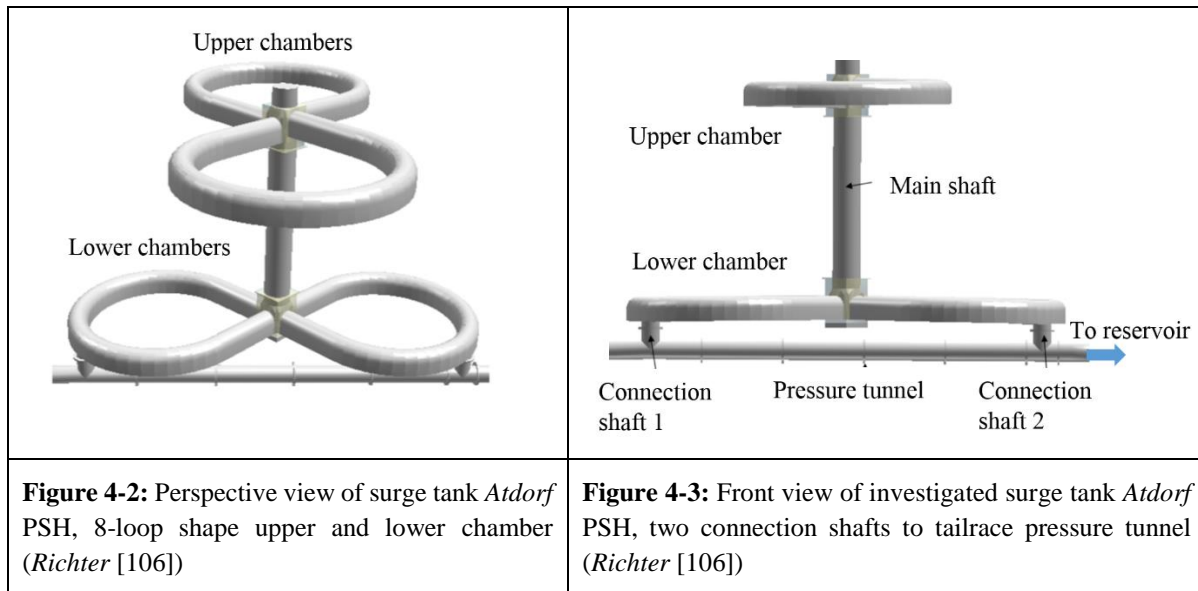
Figure 4-1: Schematic section of the *Atdorf* pumped storage hydropower plant, not to scale (Richter [105])

SURGE TANK CASE STUDIES

Table 4-1: Key numbers of *Atdorf* PSH

Installed capacity pumps and turbines	1400 MW
Head	~ 600 m
Machine concept	6 pump turbines with asynchronous motor generator
Energy content	13 GWh
Pressure tunnel: length, diameter	7800 m, $D_i = 9.8$ to 11 m
Design discharge	$Q_{Tu} = 267 \text{ m}^3/\text{s}$, $Q_{Pu} = 204 \text{ m}^3/\text{s}$
Physical model test Froude scale factor	1:40

Figure 4-2 and Figure 4-3 show the principle design of the 8-loop shape tailrace surge tank. The design of the 8-loop shape was developed by the planners of the project and has went through several steps of development. The model test was carried out in two stages since the initial design with a single connected main riser demanded an improvement because a massive waterfall was intruding significant amount of air, creating unfavourable free surface flow in the pressure tunnel. The suggested solution was, that the lower chamber was linked by two connection shafts to the pressure tunnel that allows a sufficient degassing length of air bubbles in the lower chamber.



SURGE TANK CASE STUDIES

Figure 4-4 indicates the total net volume demand of the structure of 132 400 m³ and the symmetric volume demand of the lower chambers and upper chambers. The spiral inclination (helix) of the four separate chambers as it was the outcome of the design process of the project planners. An earlier design concept showed three unconnected branches with dead ends [104]. Hydraulically the inclination is needed both for the de-aeration of the crown of the lower chamber and for the emptying of the upper chamber. Figure 4-5 shows the plan view of the 8-loop chamber and for the emptying of the upper chamber. Figure 4-5 shows the plan view of the 8-loop shape surge tank.

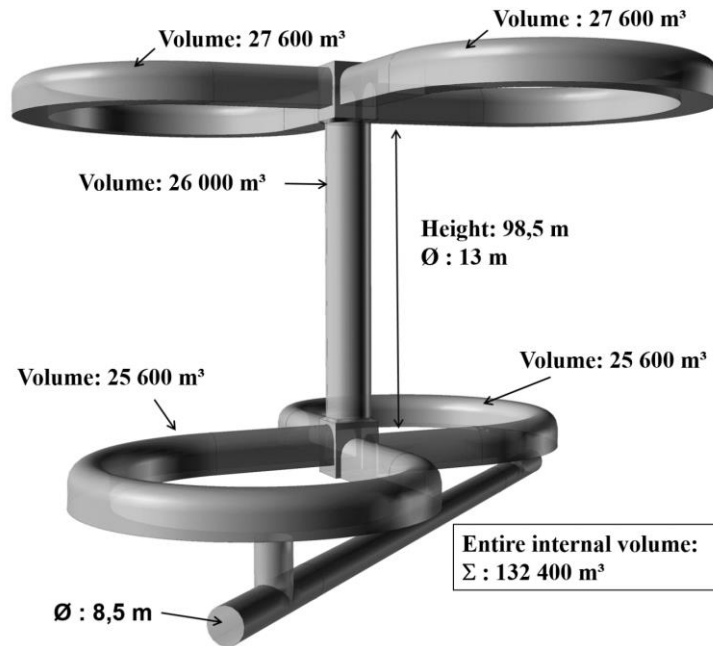


Figure 4-4: Perspective view of the final *Atdorf* surge tank design with internal volume (*Richter* [106])

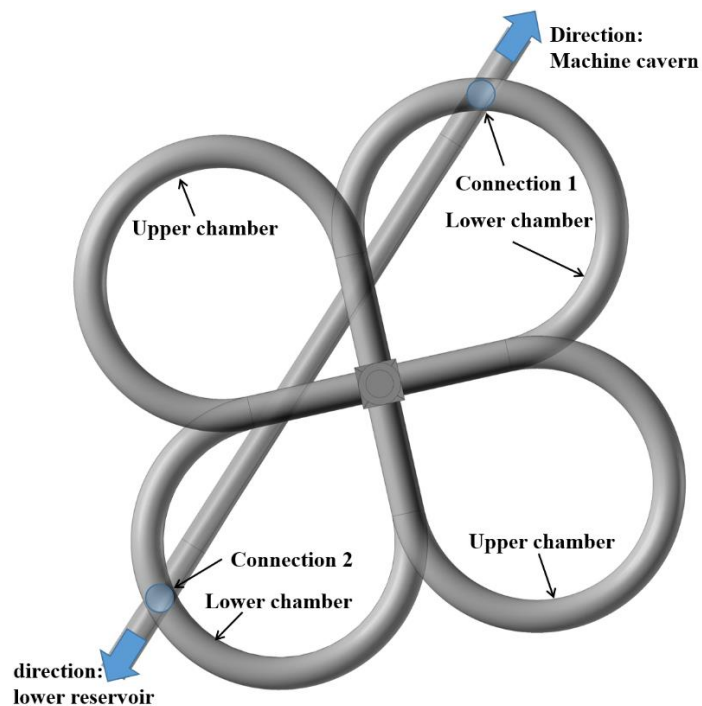


Figure 4-5: Top view of the final *Atdorf* surge tank design, indicating orientation and connection shafts

4.2 Burgstall – Tailrace Surge Tank

Physical model tests for the tailrace surge tank *Burgstall* of the pumped storage hydropower plant *Reisseck II* of the Verbund Hydropower company were conducted to check the overall hydraulic behaviour and to test the hydraulic differential throttle [107]. Figure 4-6 shows the surge tank *Burgstall* within the hydraulic scheme of the power plant schemes *Reisseck II* and *Malta Main Stage*, explaining also the capacity levels (C.L.) and drawdown levels (D.L.) of the reservoirs. Figure 4-7 visualises the geometry of the tailrace surge tank in specific.

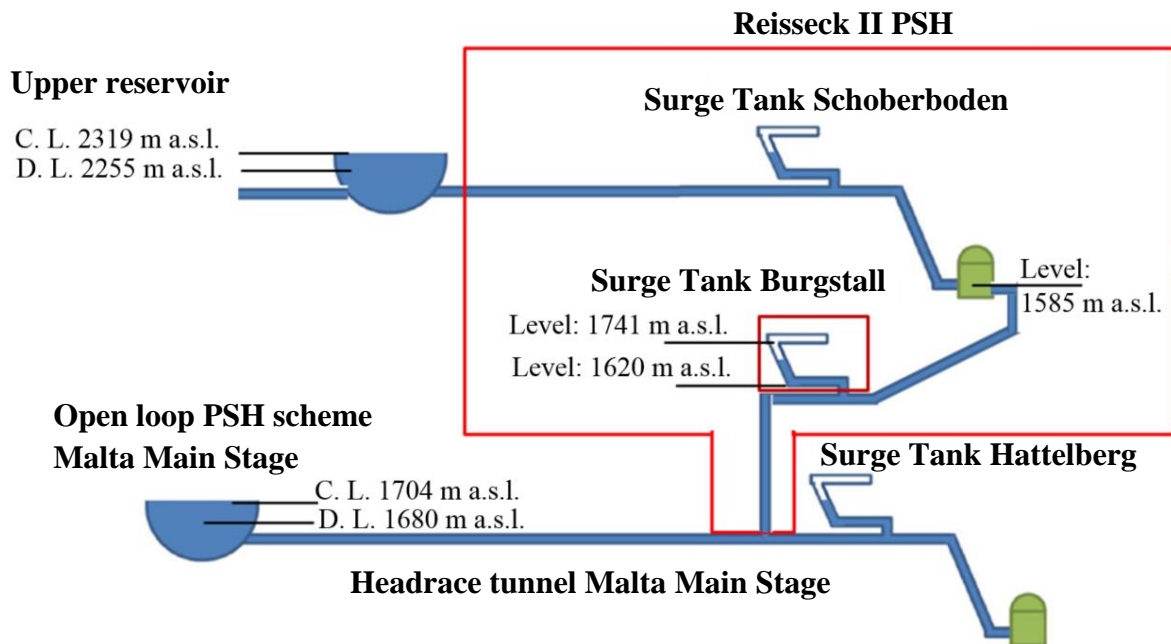


Figure 4-6: Systematic position of the *Burgstall* tailrace surge tank in the *Reisseck II* scheme (Richter [107], modified)

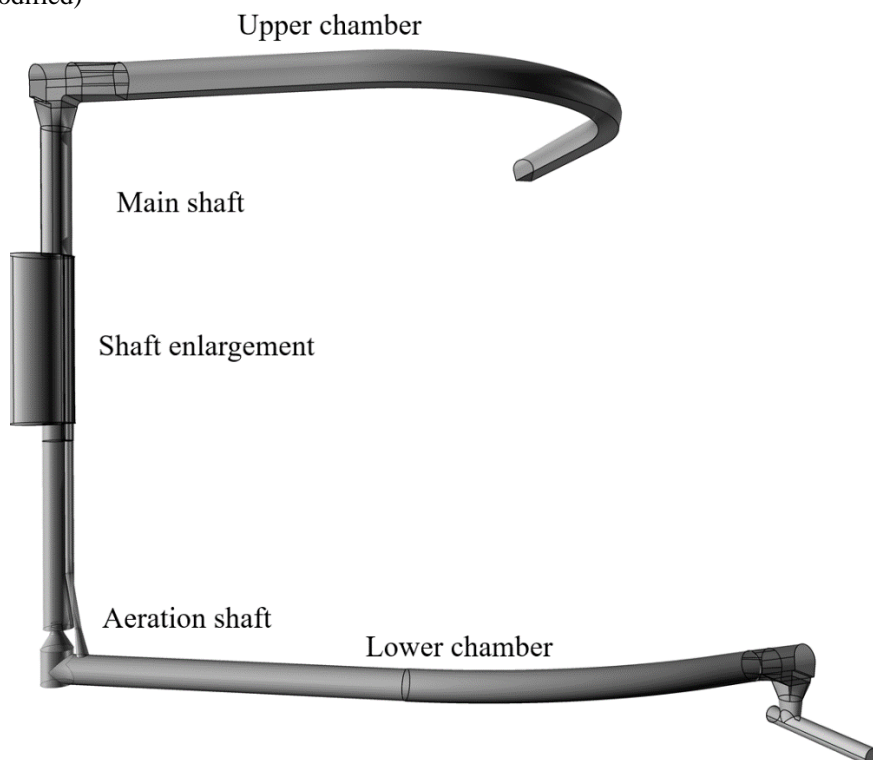


Figure 4-7: 3D geometry of the *Burgstall* tailrace surge tank (Richter [107])

SURGE TANK CASE STUDIES

Table 4-2: Key numbers of *Reisseck II* PSH [28]

Installed capacity pumps and turbines	430 MW
Head variation	551 m – 639 m
Machine concept	Two pump turbines
Pressure tunnel tailrace: length, diameter	$L = 9765$ m, $D_i = 4.4 - 4.9$ m
Design discharge in turbine and pump mode	$Q_{Tu} = 80$ m ³ /s, $Q_{Pu} = 70$ m ³ /s
Physical model test Froude scale factor	1:25

A differential throttle is placed at the bottom of the main riser to improve the mass oscillation in the chamber surge tank *Burgstall*. The up-surge is gradually restricted, while the down-surge is restricted very abruptly creating a higher flow contraction by a Borda mouthpiece. This part of the throttle at highest contraction is additionally equipped with an outside chamfer to improve the creation of a down-surge contraction jet for dissipation.

Figure 4-8 shows the connection detail of the main riser with the lower chamber and the throttle. The aeration shaft is attached by a conical widening into the lower chamber. This aeration shaft is integrated into the circular main riser excavation profile.

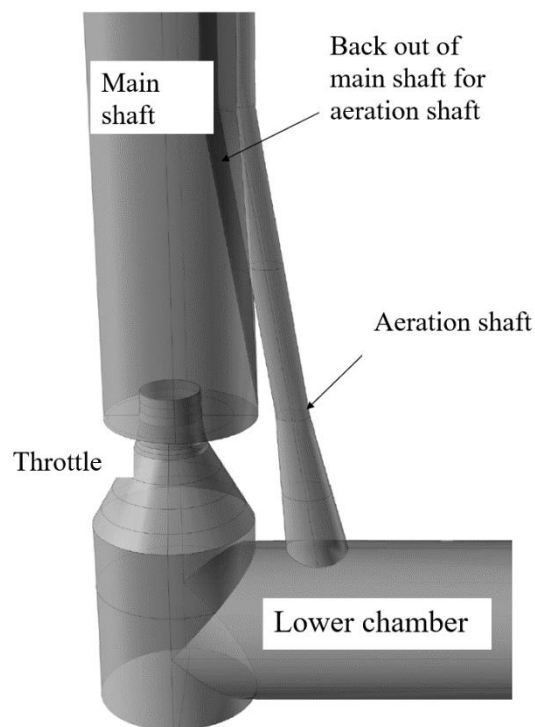


Figure 4-8: Main shaft connection detail of the differential orifice throttle of *Burgstall* tailrace surge tank (Richter [107])

4.3 Krespa - Headrace Surge Tank

The surge tank *Krespa* of the *Obervermuntwerk II* pumped storage hydropower scheme (Figure 4-9) was hydraulically checked in terms of physical model tests for the overall behaviour and the differential throttle properties. Numerical studies were conducted to generate boundary conditions for the transient small-scale tests and to identify associated hydraulic behaviour.

Table 4-3: Key numbers of *Obervermuntwerk II* PSH [28]

Installed capacity pumps and turbines	360 MW
Head variation	240.7 m – 308.7 m
Machine concept	Two ternary machine units horizontally aligned pump, Francis turbine and torque converter
Pressure tunnel: length, diameter	$L = 2552 \text{ m}$, $D_i = 6.8 \text{ m}$
Design discharge in turbine and pump mode	$Q_{Tu} = 150 \text{ m}^3/\text{s}$, $Q_{Pu} = 100 \text{ m}^3/\text{s}$
Physical model test Froude scale factor	1:30

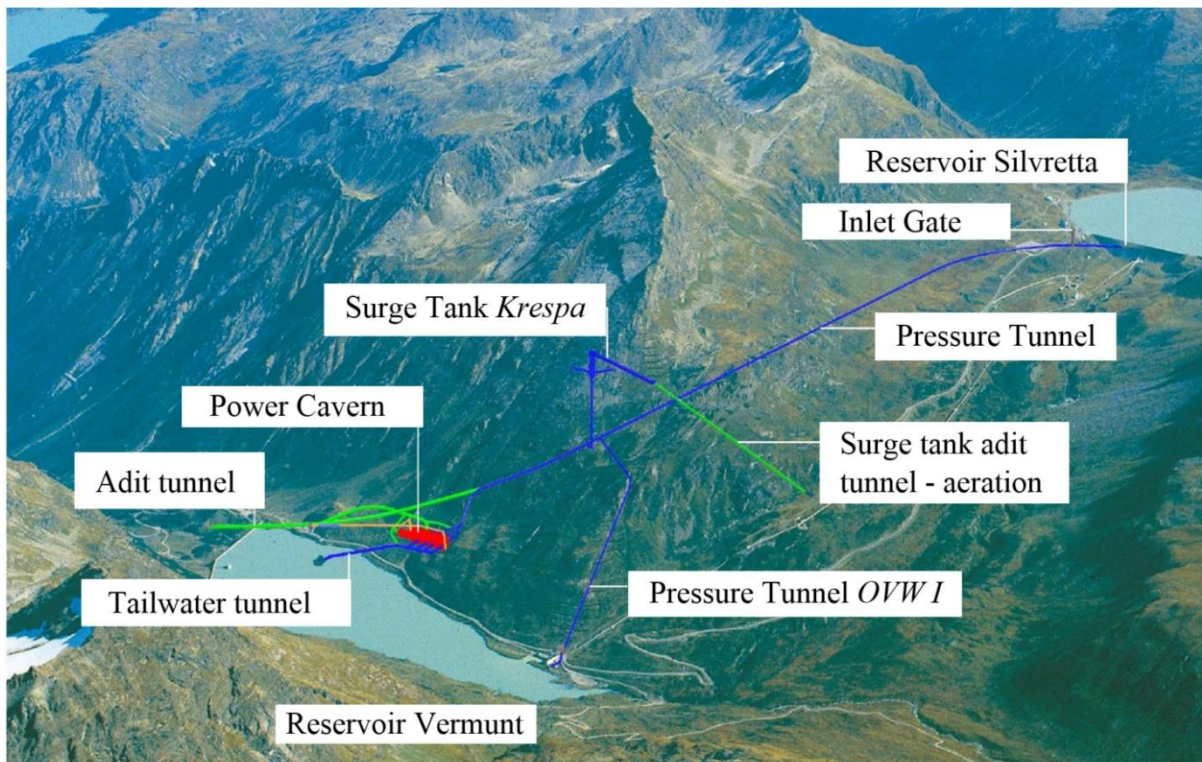


Figure 4-9: Visualisation of pumped storage scheme of the PSH *Obervermuntwerk II* [45] (modified)

SURGE TANK CASE STUDIES

The surge tank *Krespa*, visualised in Figure 4-10 consists of a high connection shaft, a $D_i = 17$ m main shaft, three attached lower chambers and a long upper chamber. The main riser is in direct hydraulic connection to the vertical shaft to provide minimum inertia values for water hammer reflection. Subsequently, the upper chamber causes waterfall issues that are addressed in the hydraulic research for this specific facility. A waterfall-dampening device was designed and developed to mitigate the air bubble intrusion into the main shaft to avoid air bubble migration into the pressure tunnel.

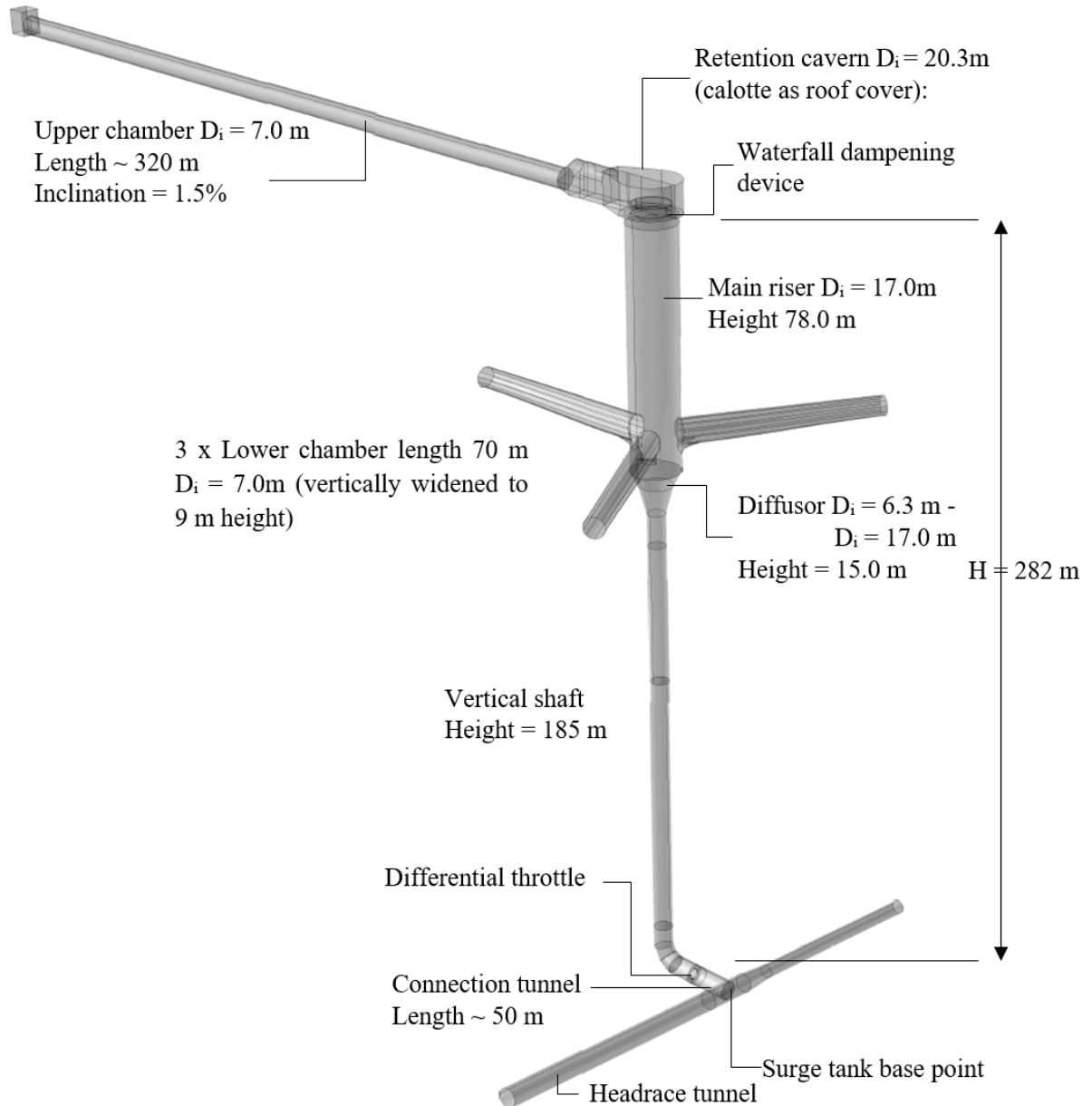


Figure 4-10: Visualisation of the *Krespa* surge tank (Richter [44], modified)

SURGE TANK CASE STUDIES

Preliminary studies of the surge tank were elaborated at Illwerke AG, investigating a closed surge tank or a surge tank with conventionally attached lower chamber with main shaft at its end; both studies were not followed for the final design, described by *Meusbürger and Gökler* 2014 [108]. Figure 4-11 and Figure 4-12 show the different water hammer reflection behaviour in comparison to the various lower chamber respectively main riser attachment. A flow-through attached lower would negatively affect the water hammer reflection and water mass reaction on flow changes due to the longer distance and the higher inertia of the lower chamber to be accelerated (Figure 4-11). These aspects would result in higher water hammer loads and fluctuations onto the conduits and the machines. In addition, the controllability of the units may suffer. Thus, a directly attached main riser, as utilised for *Krespa* PSH improves the surge tank reaction for water mass acceleration demands and the controllability of the units (Figure 4-12). This aspect leads to the research question of how the waterfall from the upper chamber influences the air bubble intrusion into the pressurized system, which led to the development of a waterfall-dampening device. The final design of this feature constructed and successfully tested in 2018 at prototype.

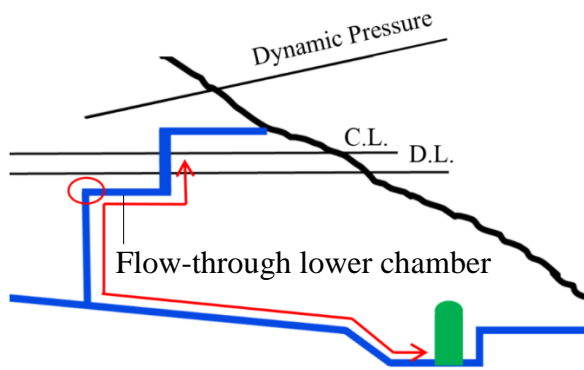


Figure 4-11: Water hammer reflection if flow-through lower chamber – initial variant

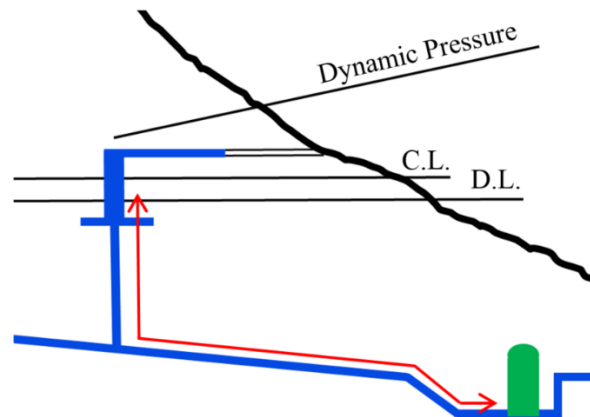


Figure 4-12: Water hammer reflection with direct shaft – final solution

4.4 Tonstad - Headrace Surge Tank

The *Tonstad* HPP is the power plant with the highest electricity production in Norway with about 3.8 TWh/a. It is part of the *Sira-Kvina* scheme located in the south-west of the country. *Tonstad* power plant utilises the watershed of the *Sira* and *Kvina* river and operates as a controllable high-head run-of-river power plant. Due to long and complex headrace tunnel system and high water discharge a large surge tank structure is operated. The headrace tunnels are unlined with a gravel invert from the construction. The sediments from the tunnel and other sources are trapped in a pressurized sand trap directly after the surge tank shafts. The surge tanks are a key facility to handle the large water inertias of the system in order to allow acceleration and deceleration. The original layout was not specifically considered resonance load-cases; thus, the lower chambers are quite small and designed as start-up chambers. Increased demand for flexible operation for grid balancing is challenging the power water way and especially the surge tanks. Issues of the flexible operations are reported by *Vereide et. al.* (2015) [109].

The *Tonstad* surge tank was studied and discussed herein regarding its upgrade possibilities. The upgrade of this surge tank in specific would allow more discharge and higher flexibility for the scheme. Additionally, the pressurized sand traps were investigated for improved operation [98]. This aspect is not described in the present work.

Such upgrade options may be the case for other surge tanks designed for operation cases that would follow the demands physical demands before the vast integration of solar and wind sources into the power grid. Figure 4-13 visualises the complex power waterway with brook intakes and the two main reservoirs *Ousdalsvann* and *Homstølvann*.

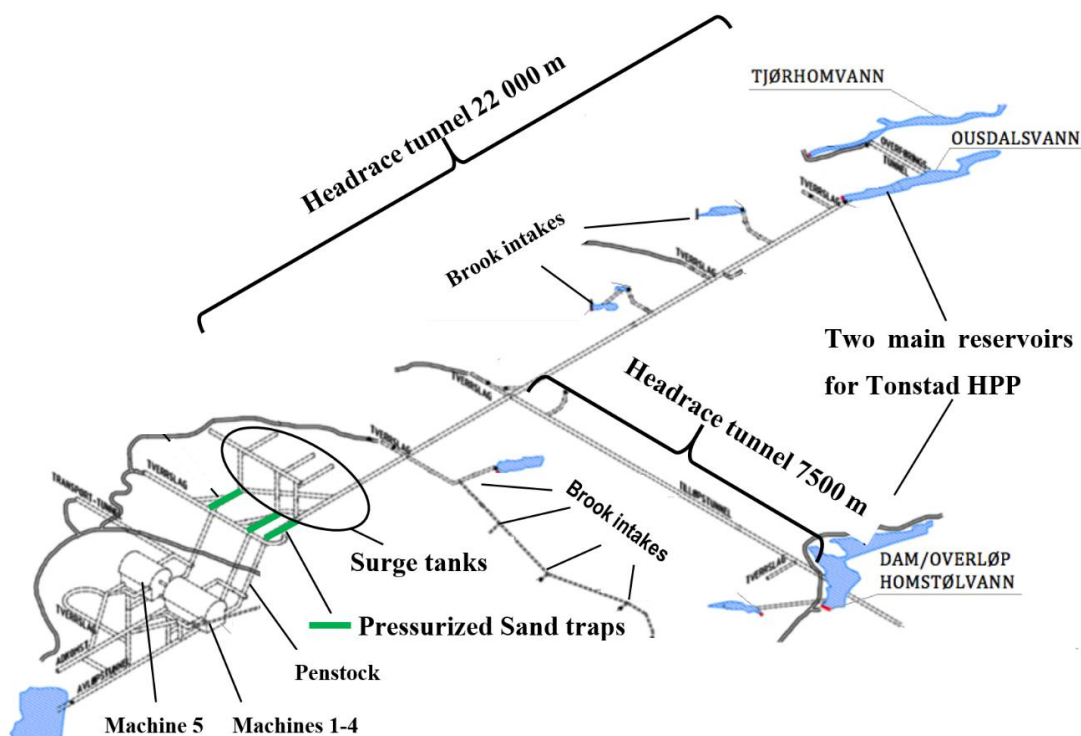


Figure 4-13: General layout of *Tonstad* HPP scheme in southern Norway [98], (source: *Sira-Kvina*)

SURGE TANK CASE STUDIES

Table 4-4 shows the key numbers of the *Tonstad* high-head hydropower plant.

Table 4-4: Key numbers of *Tonstad* HPP (source: *Sira-Kvina*)

Installed capacity	960 MW
Head variation	430.3 m – 450.1 m
Machine concept	Five Francis turbines
Main headrace tunnels length and flow section area	L = 16000 m, $A_i = 66 \text{ m}^2$ L = 7500 m, $A_i = 57 \text{ m}^2$ L = 6000 m, $A_i = 100 \text{ m}^2$
Design discharge	$Q_{Tu} = 240 \text{ m}^3/\text{s}$

Figure 4-14 shows the geometry of the three surge tank structures of *Tonstad* HPP, except the gate section, that are concrete lined all other parts of the surge tank are unlined. The pressure shaft is steel lined.

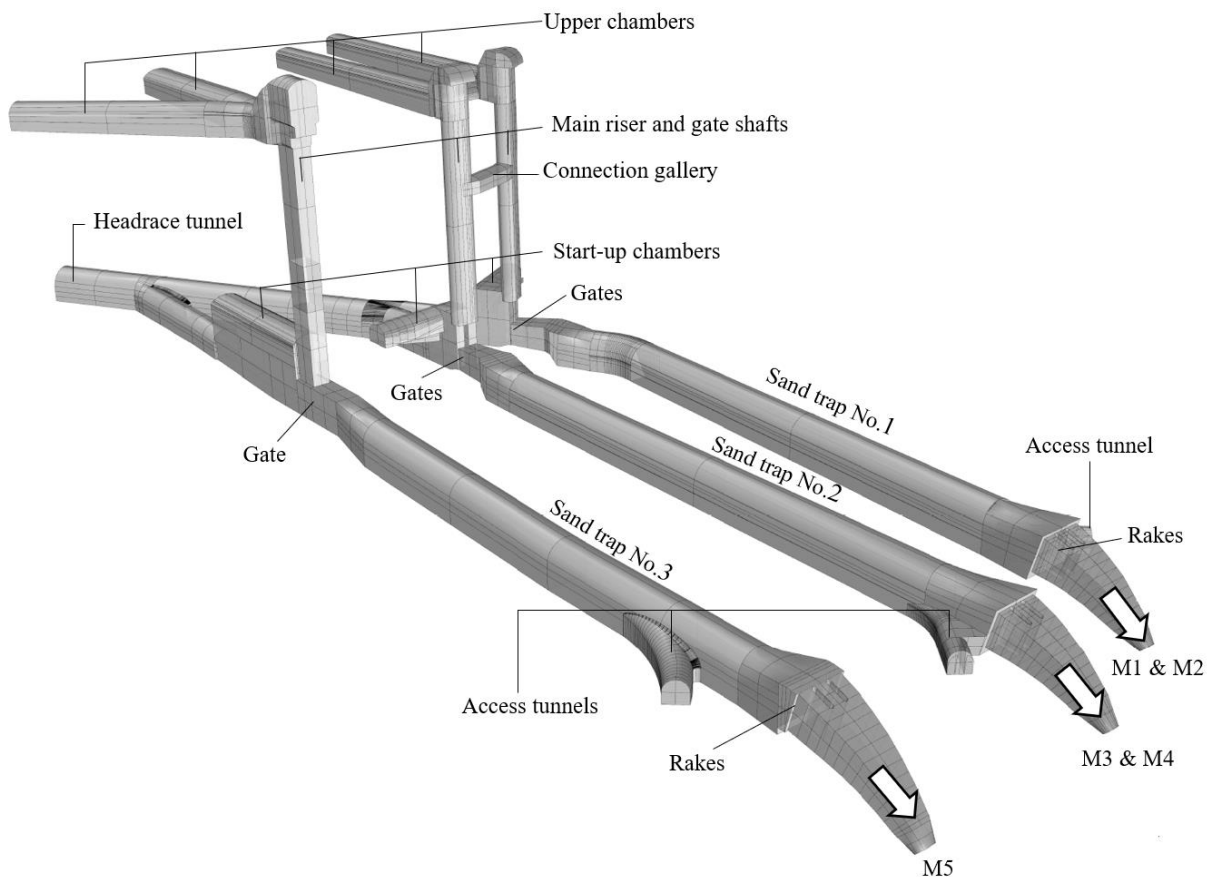


Figure 4-14: *Tonstad* surge tank, perspective view (Richter, 3D model by Sterner [110])

5. INVESTIGATION METHODS

This chapter describes the approaches for investigating the transient and multiphase phenomena of surge tanks for hydropower schemes conducted within this thesis. The methods are listed such as:

- Physical small-scale model tests in the hydraulic laboratory:
 - Throttle model test – small-scale partial surge tank representation
 - Surge tank model – small-scale full surge tank representation
 - PIV-measurements
 - Small-scale model with water hammer
- Numerical simulations:
 - 1D-numerical simulations
 - Mass oscillation
 - Water hammer
 - Stability simulations
 - Surge tank inertia aspects
 - 3D-numerical simulations
 - Throttle loss evaluations
 - Swirl flow evaluations
 - Waterfall evaluations
 - Surge wave investigation in upper chamber
- Hybrid modelling applying numerical and physical approaches
- Prototype measurements

Figure 5-1 visualises the multi modelling approach for interacting numerical simulations with physical small-scale model tests to optimise and develop new parts of hydraulic systems such as the waterfall-dampening device.

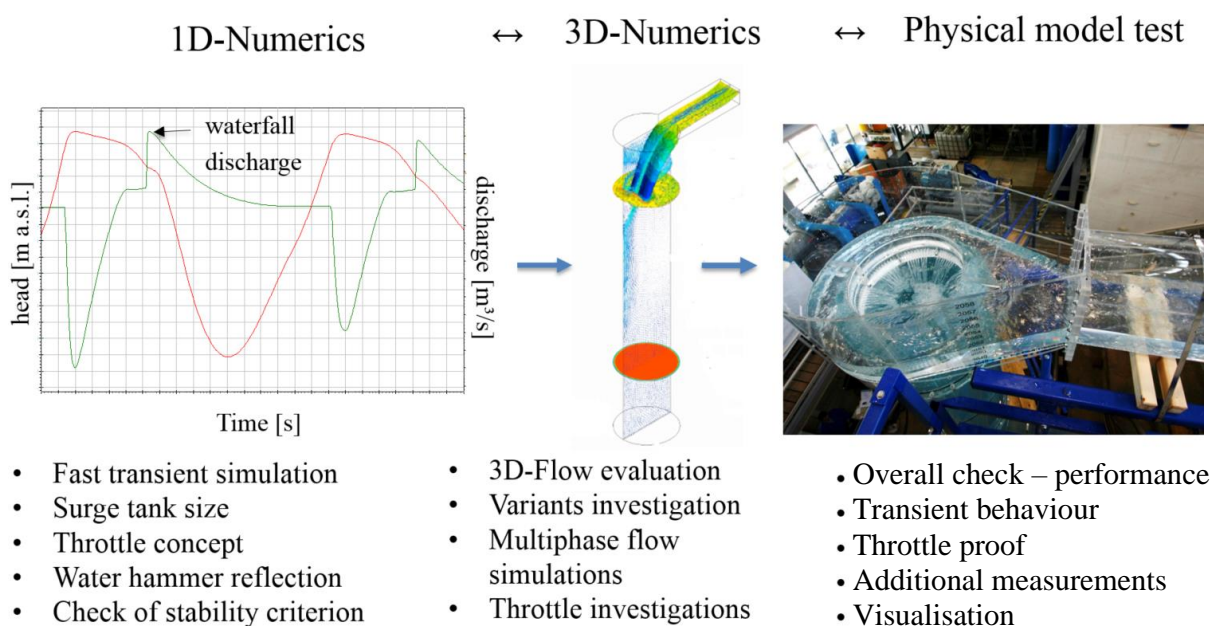


Figure 5-1: Investigation evolution of hybrid modelling for waterfall aspect (1D-numerical simulation *Wanda*, 3D-CFD *Ansys CFX*)

5.1 Physical Model Tests

Physical model tests are an important tool for hydraulic research and were conducted in the hydraulic laboratory, to check:

- The overall flow behaviour in a surge tank facility and
- The detail design structure such as a hydraulic throttle design
- Efficient variant studies to optimise structural details considering transient hydraulic

Physical model tests have the advantage to fully resolve hydraulic phenomena in a scaled geometry and to visualise transient events, such as they appear in surge tanks. A challenge for multiphase observations is, that only one explicit hydraulic value is scaled in respect to the chosen scaling law [111]. The chosen approach for the investigated full model surge tanks of this work was the Froude law of similitude to resolve the free surface flow phenomena [111]. Special multiphase challenges such as air bubble behaviours in surge tanks were investigated additionally and needed special attention due to the effects of the Froude scale model tests. Air bubbles terminate faster in the model as supposed to, regarding the scaled velocity. Therefore, 3D-numrical simulations and theoretical approaches were chosen to highlight these multiphase aspects. Comprehensive model law descriptions for comparison are given e.g. by *Kobus (1984)* [111]. Table 5-1 shows the relevant dimensionless numbers for hydraulic models in association with surge tanks. The approach of applying the similarity laws are, to generate the same dimensionless numbers for the prototype scale and for the model test scale. To achieve this by a given length scaling factor, the other physical boundary values are modified, such as the velocity or the fluid itself. Throttle model test may also be conducted with air as fluid to obtain a loss factor, as done for the differential surge tank orifice throttle for *Sellrain-Silz HPP* [112].

Table 5-1: Dimensionless numbers for hydraulic model tests

Dimensionless Numbers	Forces ratio	Expression
Froude number	Inertia / Gravity	$\frac{v}{\sqrt{g L}}$
Euler number	Pressure / Inertia	$\frac{p}{\rho v^2}$
Reynolds number	Viscous / Inertia	$\frac{v L}{\nu}$
Weber number	Inertia / Surface tension	$\frac{\rho v^2 L}{\sigma}$

- L ... Characteristic length, typically pipe diameter [m]
- ρ ... Density of the fluid [kg/m³]
- p ... Pressure or pressure drop respectively head loss [Pa]
- v ... Velocity [m/s]
- ν ... Kinematic viscosity of the fluid [m²/s]
- σ ... Surface tension [N/m] – of water (0.072 N/m)

5.1.1 Froude Similarity Law

For free surface flows, gravity is the most significant force that influences the flow. The hydraulic model test investigations for chamber surge tanks are therefore operated according to Froude's similarity law. This similarity means that the ratio of inertial and gravitational forces is the same in the prototype and in the model, allowing a geometrically similar replication of the water level. The ratio of inertial and gravitational forces is described by the Froude number. This equilibrium between model scale and prototype scale is the most important similarity law for modelling of free surface flows.

$$Fr_R = \frac{F_P}{F_M} = 1 \quad (5-1)$$

Index [R] Relation [P/M]

Index [P] Prototype

Index [M] Model

$$Fr = \frac{v}{\sqrt{gL}} \quad (5-2)$$

Defining the scale number L_R with the ratio of the lengths in prototype to the lengths in the model ($L_R = L_P / L_M$), the other relevant hydraulic transfer functions result according to the following relationships:

$$\text{Length: } L_R = \frac{L_P}{L_M} \quad (5-3)$$

$$\text{Area: } A_R = \frac{A_P}{A_M} = L_R^2 \quad (5-4)$$

$$\text{Velocity: } v_R = \frac{v_P}{v_M} = L_R^{1/2} \quad (5-5)$$

$$\text{Time: } t_R = \frac{t_P}{t_M} = L_R^{1/2} \quad (5-6)$$

$$\text{Discharge: } Q_R = \frac{Q_P}{Q_M} = L_R^{5/2} \quad (5-7)$$

5.1.2 Euler Similarity Law

For flows that are predominated by pressure and inertia forces, the viscosity and the gravitational terms can be neglected. Thus, the Euler number describes the relation between the pressure or pressure drop versus the inertial forces.

$$\frac{p_M}{\rho_M v_M^2} = \frac{p_P}{\rho_P v_P^2} \quad (5-8)$$

5.1.3 Reynolds Similarity Law

The Reynolds number is one of the most important numbers in fluid dynamics describing the ratio of viscous forces to inertia forces. For flows with low Reynolds numbers the viscous forces are predominant while they can be neglected for flows with high Reynolds numbers. In pipe flows the viscous influence is crucial in the near wall region thus the Reynolds number is important for the friction loss aspects comparing model test with prototype testing.

Equation (5-9) defines the similarity law regarding the Reynolds number.

$$\frac{v_M L_M}{\nu_M} = \frac{v_P L_P}{\nu_P} \quad (5-9)$$

L ... Characteristic length such as the pipe diameter [m]

$$\text{Length: } L_R = \frac{L_P}{L_M} \quad (5-10)$$

$$\text{Area: } A_R = \frac{A_P}{A_M} = L_R^2 \quad (5-11)$$

$$\text{Velocity: } v_R = \frac{v_P}{v_M} = L_R^{-1} \quad (5-12)$$

$$\text{Time: } t_R = \frac{L_R}{v_R} = L_R^2 \quad (5-13)$$

$$\text{Discharge: } Q_R = v_R \cdot A_R = L_R \quad (5-14)$$

Since the model diameters are smaller by the model scale factor, the model test velocity needs to be higher by the scaling factor to obtain the same Reynolds number. For the hydraulic model tests of the pilot case studies this was not possible. It would have demanded very velocities and thus pressures to be provided by the pumps. To overcome this issue, an approach of extrapolating the model test Reynolds number up to the prototype Reynolds number is utilised. Therefore, the testing procedure is to run the model test for several discharges and measure the loss factor in relation to the Reynolds number. These measurements are interpolated by a quadratic polynomial that is extrapolated to the desired Reynolds number. This procedure is described by *Klasinc et.al.* [113].

5.1.4 Weber Similarity Law

For hydraulic phenomena that are influenced by surface tension effects, the similarity law after Weber is important to be applied. For hydraulic model tests utilising water as fluid, the surface tension is the same for prototype and model test. Surface tension forces can be neglected in prototype size since they are very small. But model tests are significantly scaled, thus the surface tension may have an important effect, this can be for example regarding the formation of air core swirling flows. Those may occur at inlet structures to pipelines or turbines that may transport unwanted air into the pressurized system. To fully represent this phenomenon, the Weber number must be equal in the prototype and model test by modifying any of the variables (equation (5-15)). Such swirling flows may occur at inlets with free surfaces whereas the inlet represents a restriction in the flow such as orifices of surge tanks connecting to pressure tunnels.

$$\frac{\rho_M v_M^2 L_M}{\sigma_M} = \frac{\rho_P v_P^2 L_P}{\sigma_P} \quad (5-15)$$

5.1.5 Physical Throttle Model

The physical model tests regarding the throttle loss evaluation are conducted at a specific test rig with controllable water discharge to generate the highest possible Reynolds numbers. A full Reynolds number equality between the model and the prototype scale was not possible to be created for the investigated surge tanks. In this chapter the throttle model test with the scale factor 1:30 for the *Krespa* surge tank is described. The test rig for throttle evaluations was adapted to the specific demands including the attached pipes and shafts. The throttle loss is influenced by the complete geometry in the vicinity of the flow restriction that creates the flow dissipation. Figure 5-2 shows the model test setup to evaluate the *Krespa* differential throttle within a closed water circle.

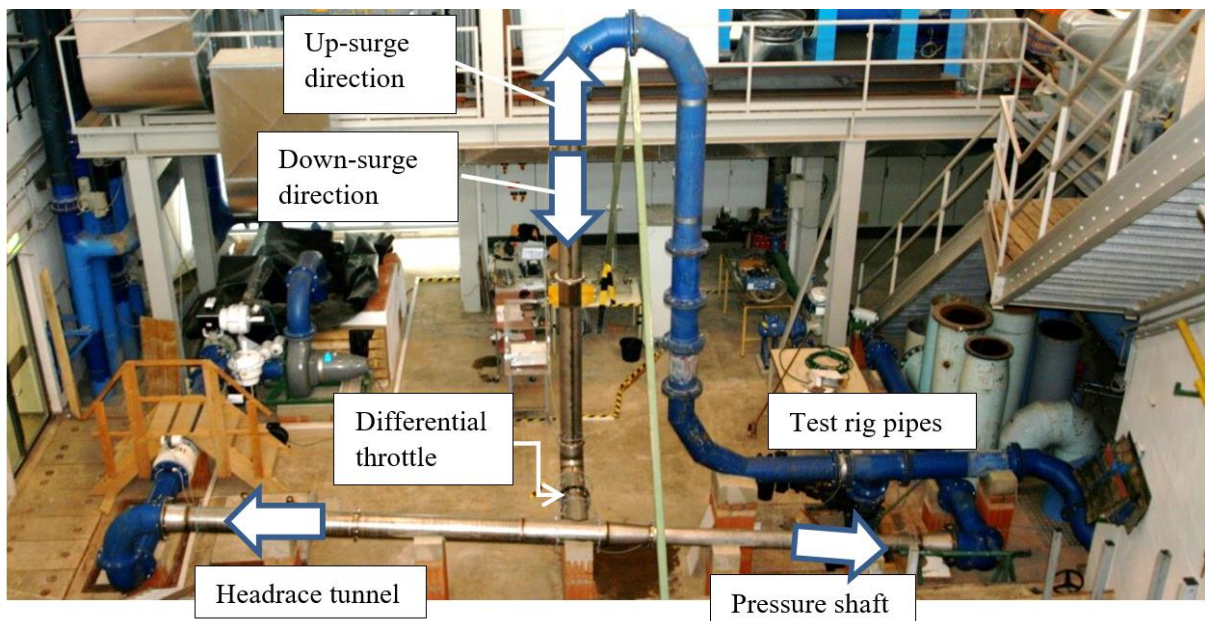


Figure 5-2: Model test rig for differential throttle evaluation of *Krespa* surge tank (Richter [45], modified)

INVESTIGATION METHODS

Figure 5-3 shows the detail of the throttle placement in the connection tunnel for the Krespa throttle model test.

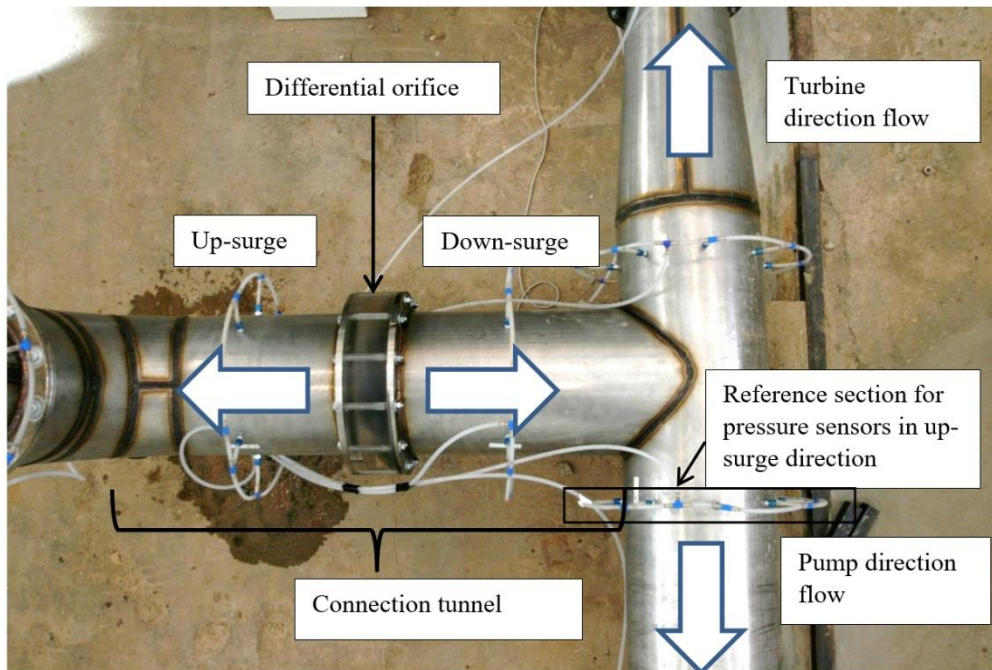


Figure 5-3: Pressurized model test setup for differential throttle evaluation of *Krespa* surge tank (Richter [114], modified)

To extract the singular loss of the throttle, the friction loss of the pipe has to be subtracted from the continuous friction loss observed in the model test. Figure 5-4 shows the different losses associated with the measurement of the pressure drop caused by the flow. All singular losses such as the conical bend, the differential throttle and the T-junction are combined in the throttle loss. All continuous losses such as the friction losses in all associated pipes have to be subtracted. The friction losses are depending on the Reynolds number. The local losses are independent of the Reynolds numbers above a certain value of $Re=10^4$ [-] to $Re=10^5$ [-] in the outflow pipe [115], [92]. In a study by *Koch* it was found that $Re=10^6$ [-] are recommended to be used to achieve Reynolds number independent local losses [116]. This aspect is very helpful for scaled throttle tests because it is possible to achieve this Reynolds numbers range, while it is not possible to achieve the prototype Reynolds numbers in pressure tunnels that may be even above $Re=10^7$ [-].

The approach that is applied for this thesis is the determination of the friction losses based on the material friction subtracted from the measured difference head loss by extrapolating the model test discharge to mitigate the Reynolds dependency of the friction loss, as described by *Klasinc et. al.* [113].

The throttle loss is generated by hydraulic dissipation after the flow contraction by internal friction. The length of the dissipation zone is crucial to generate the local loss. The used approach is the length of 15 times the pipe diameter (15 D). This value was found to give a reasonable development to reach a most fully developed turbulent flow pattern. This is crucial to convert between 1D approach after a 3D flow effect such as a hydraulic throttle.

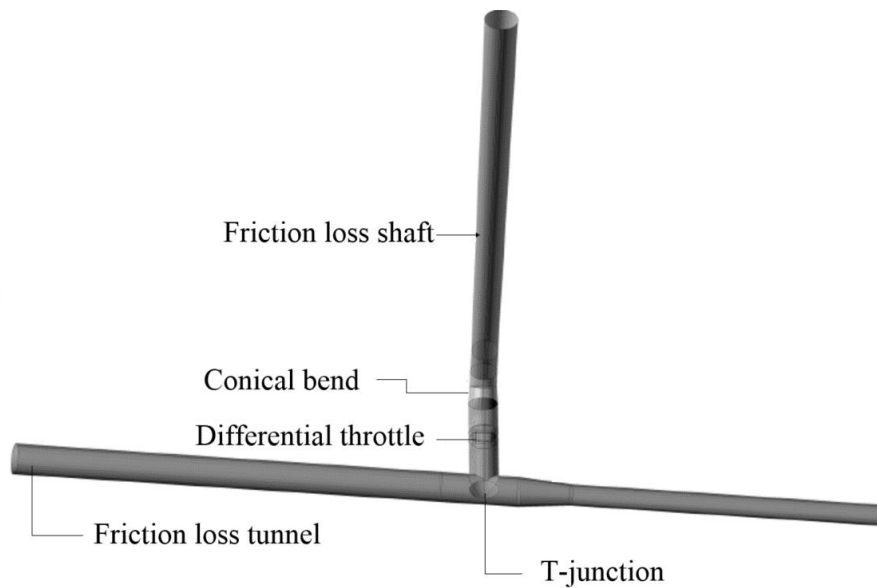


Figure 5-4: Hydraulic losses in surge tank connection with differential throttle (*Richter* [114], modified)

Figure 5-5 visualises the connection tunnel detail with the throttle and the T-junction, the arrows indicate physical boundary conditions for 3D-numerical simulations.

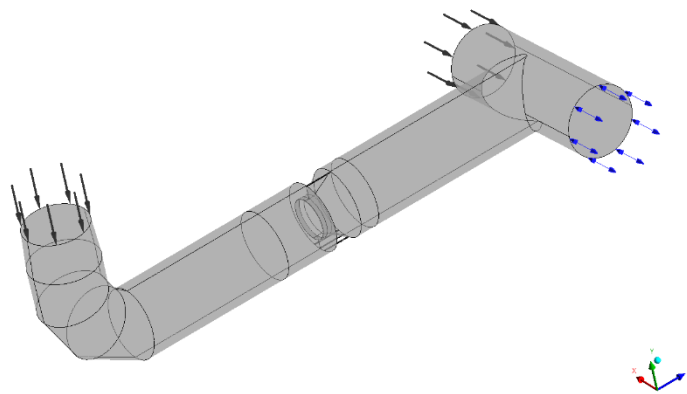


Figure 5-5: Detail of the connection tunnel with the T-junction, the differential throttle, the conical bend

To evaluate the differential loss factors both the up-surge discharge and the down-surge discharge were measured in the most dominant direction (Figure 5-6 and Figure 5-7 for the *Krespa* surge tank). Since the mass oscillation happens between the free surface in the surge tank and the reservoir, this is the reference flow direction to be damped by the throttle.

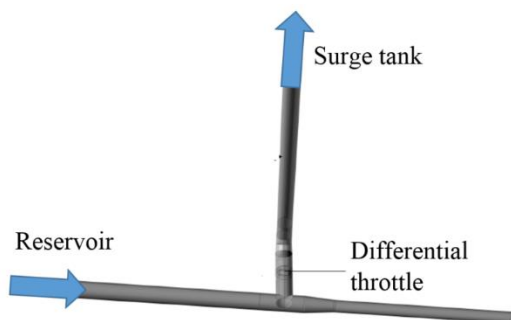


Figure 5-6: Up-surge loss discharge (*Richter* [114], modified)

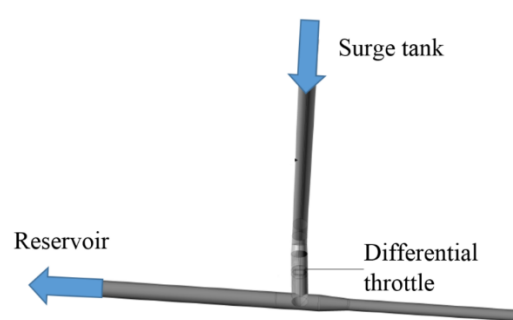


Figure 5-7: Down-surge loss discharge (*Richter* [114], modified)

INVESTIGATION METHODS

Figure 5-8 visualises the concept of the dissipation creation after the obstacle that is assumed to demand for 15 D. Full recovering of the flow pattern may demand even longer distances, but this is assumed to be but is suggested to be considered by conservative safety concepts. Figure 5-8 shows a principle of the 1D flow approach. For real pipe systems, local losses of bends, diameter changes or valves are considered discretely but may interact in the prototype. These effects need to be covered in the safety concept of assuming smoother pipe conditions for the surge tank oscillation.

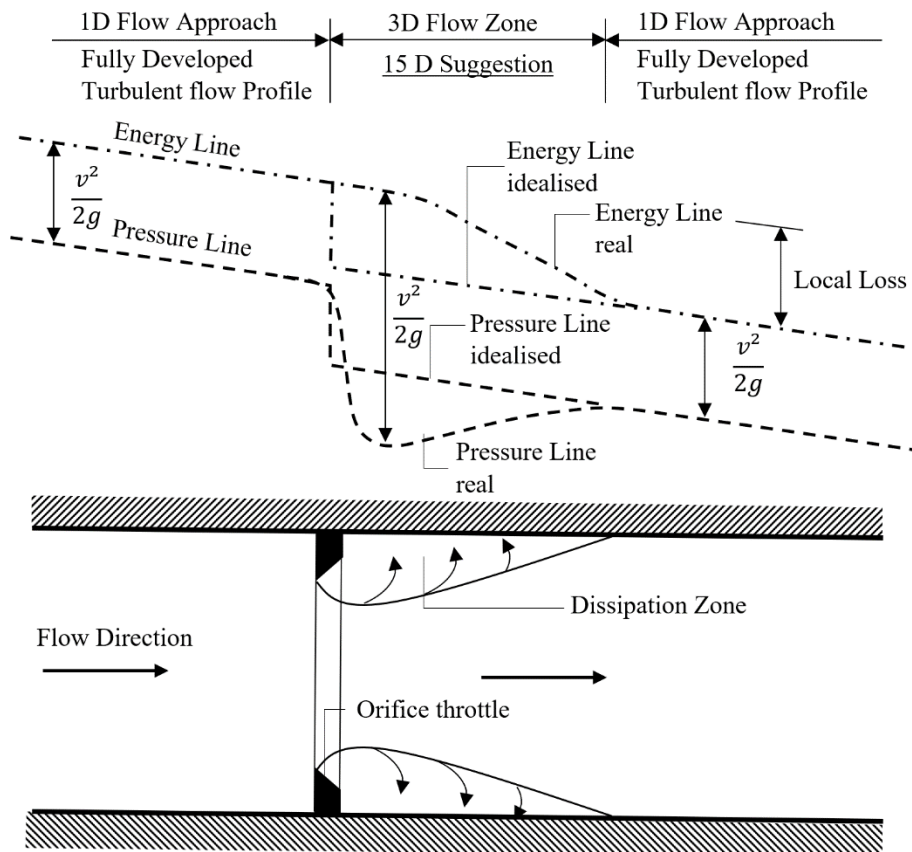


Figure 5-8: Local loss visualisation, 3D-flow zone, 1D approach flow zone (Richter after [115])

Figure 5-9 shows the measurement sections for the throttle measurement pilot case of the *Krespa* surge tank. The up-surge loss factor was measured by the differential pressure between measuring sections PT 1 to ST 2. This allows most developed turbulent flow pattern at the measure section PT 1 before the complex 3D-flow section with the throttle and a redeveloped flow pattern at the measuring section ST 2 after the dissipation zone. The down-surge loss was measured by pressure difference between section ST 1 to PT 2, with the opposite flow and opposite location of the dissipation zone. Also, the disturbed inflow of the test rig pipes was considered and tranquilised by flow straighteners. The tests were evaluated by measuring the differential pressure both by direct pressure sensors and differential pressure transducers. It was found that the latter measuring technique is suggested for measuring local losses such as for hydraulic throttles, since one single value is computed. Additionally, the differential pressure transducers were calibrated by a calibration facility (90 cm water column) before each run.

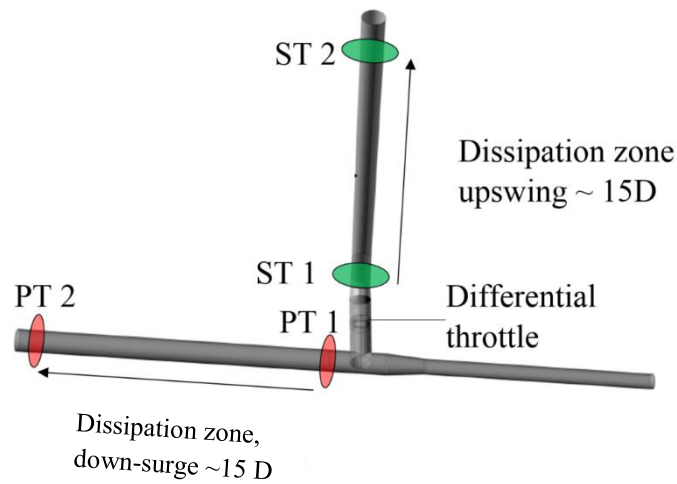


Figure 5-9: Measurement sections and dissipation zone, PT (pressure tunnel), ST (surge tank), (*Richter* [114], modified)

The throttle may be constructed in one piece using stainless steel (Figure 5-10 and Figure 5-11) or out of acrylic glass with a steel designed Borda mouthpiece. Acrylic glass has the advantage of easier adaption possibility of the geometry to adjust the diameter during the physical test phase. Figure 5-10 shows the assembling of the detail model investigating a differential throttle. The main riser was modelled as a pipe that is connected to the throttle in the figure. Figure 5-11 shows the section cut through the differential throttle, indicating the down-surge direction and the up-surge direction. The Borda mouthpiece is an important detail to enhance the down-surge loss value. The thinner this is constructed the higher the local loss due to the contraction.



Figure 5-10: Differential orifice throttle small-scale model, (picture: *Richter*)

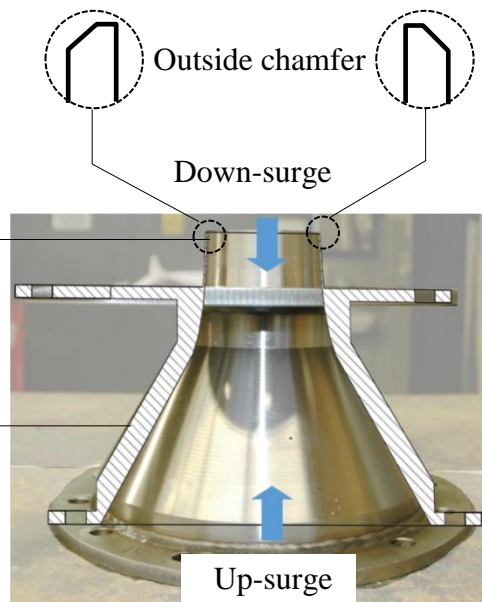


Figure 5-11: Section cut of asymmetric throttle for physical test (figure and picture by *Richter*, [107] modified)

5.1.6 Physical Full Model

Surge tanks are very site-specific structures with individual hydraulic demands, thus 3D-flow visualisation provide valuable information of the functionality. For specifically large surge tank developments, it may be indispensable to carry out small-scaled physical model tests. During the compilation of the present work, physical model tests were conducted for several pumped storage power plants, such as:

- *Reisseck II* PSH, tailrace differential chamber surge tank *Burgstall*, scale 1:25
 - Full model in acrylic glass
 - Detail model for throttle evaluation in stainless steel, scale 1:25
- *Atdorf* PSH, tailrace chamber surge tank, scale 1:40,
- *Obervermuntwerk II* PSH, headrace differential chamber surge tank *Krespa*, scale 1:30
 - Full model in acrylic glass
 - Detail model for throttle evaluation in stainless steel, scale 1:30
- *Gouvães* PSH, tailrace differential chamber surge tank, scale 1:25 (not part of this thesis)
- *Gouvães* PSH, headrace differential shaft surge tank, scale 1:25 (not part of this thesis)

The full model physical tests were constructed in acrylic glass and operated in Froude scale similitude law. The detail throttle model tests were operated with higher pressure to achieve higher Reynolds numbers to capture the local loss of the throttle (see chapter 5.1.5). Figure 5-12 visualises the procedure of how the physical model test was cut out of the entire hydraulic system. A transient 1D-numerical simulation was performed of the entire hydropower system. This included the specific characteristics respectively a $Q(t)$ approach of the machine units. The latter approach is less precise in terms of water hammer, but provides sufficient accuracy for mass oscillation representation as a result of the present case studies. The most important aspects are the ramping times of both in the generating and the pumping mode. The pressure tunnel representation was applied in the physical model tests by the 1D-numerical simulations. The transient inflow and outflow parameters to the surge tank were exported from the 1D-numerical simulation results and were converted to the scaled discharge to be governed by the PID for transient flow.

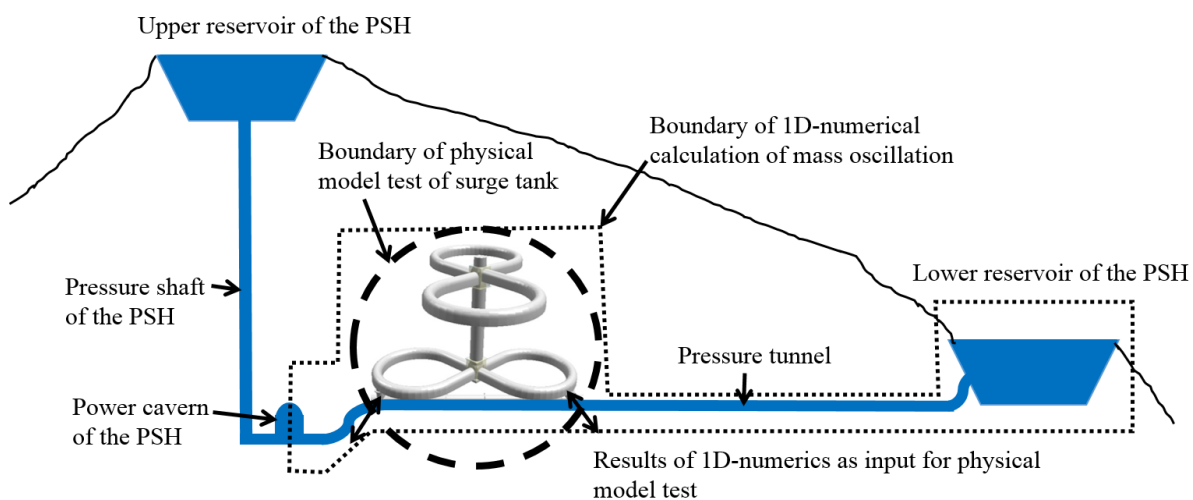


Figure 5-12: Scheme of a PSH design, boundary of 1D-numerical simulation, boundary of physical model test simulation for the *Atdorf* surge tank, (*Richter* [106])

INVESTIGATION METHODS

Figure 5-13 shows the plan view of the model test arrangement of the *Atdorf* surge tank in the hydraulic laboratory. The model test flow was fed from two sides, directly representing the transient flow of the machines as well as the transient behaviour in the tailrace pressure tunnel. The control valves are governed by the PID controller. The model pump, equipped with a frequency converter, is specifically added to the test rig to ensure quick reaction of the outflow. The frequency is adjustable to especially calibrate the peak outflows in case of pump trip events.

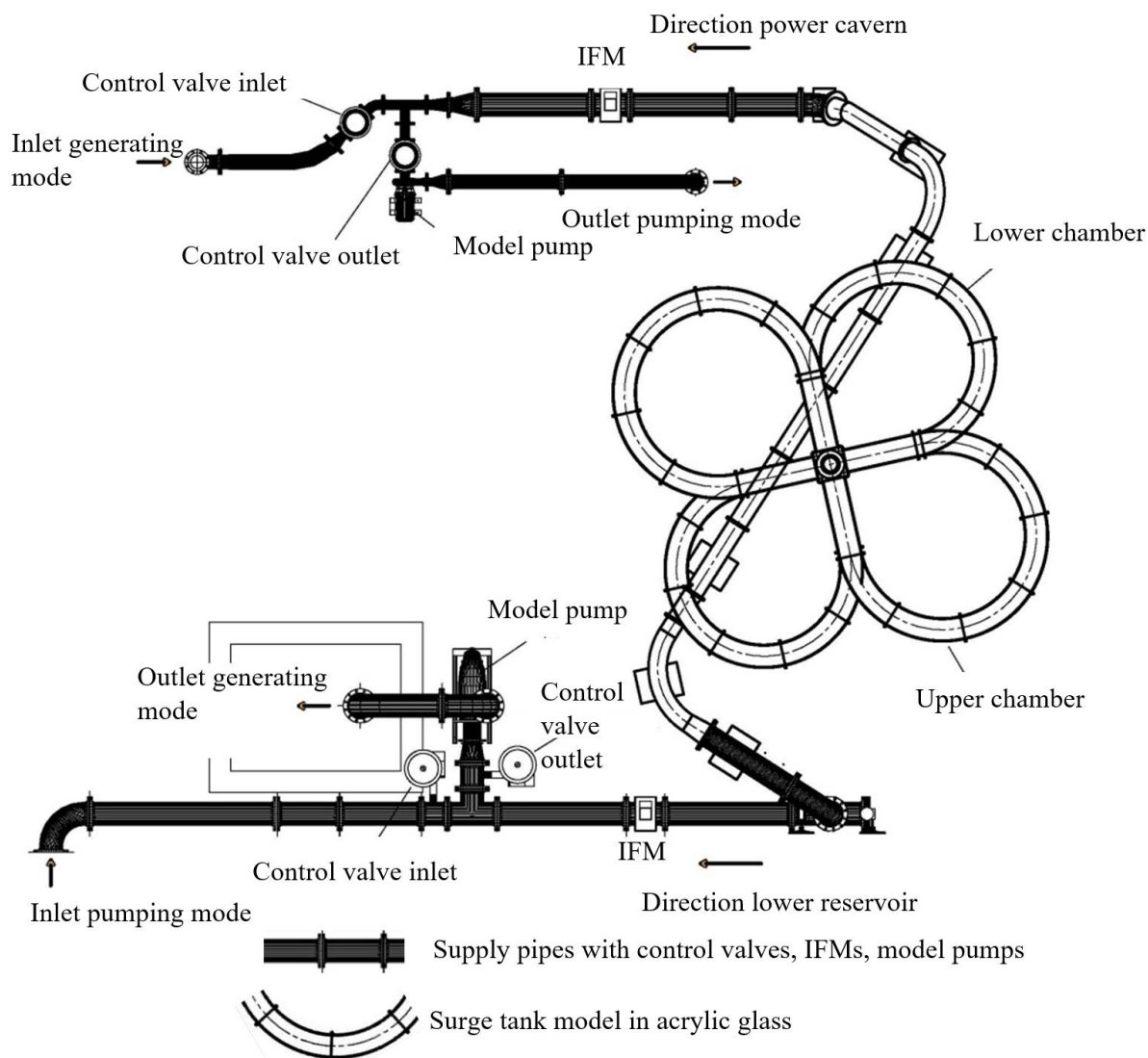


Figure 5-13: Ground view of model test setting of PSH *Atdorf* surge tank investigation, (drawing by Lazar [105], modified)

INVESTIGATION METHODS

Figure 5-14 visualises the result of a prototype 1D-numerical simulation with discharge into and out of the surge tank. Figure 5-15 visualises the transformation of the prototype discharge to the model test scale 1:25. The peak at 600 s in the prototype, respectively 125 s in the model valve represents the specific discharge peak due to a full turbine load rejection.

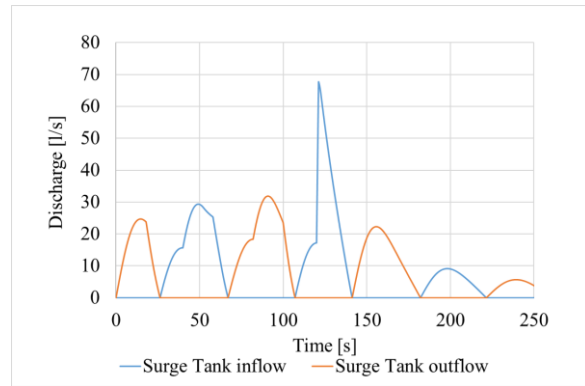
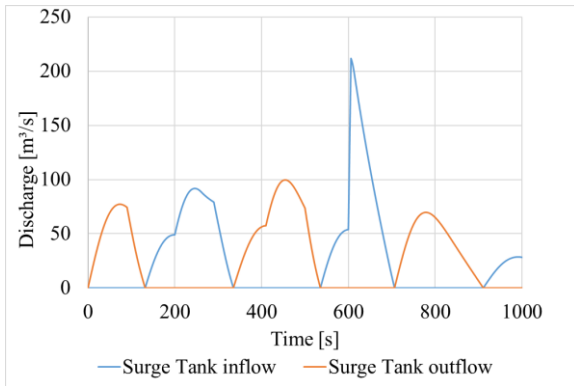


Figure 5-14: Prototype discharge at surge tank base

Figure 5-15: Model test discharge at surge tank base

Figure 5-16 shows the comparison of input target discharge and measured discharge of the IDM in model test scale in the control software of the test rig (*LabVIEW*). In the particular case the violet line represents the outflow of the surge tank as target values for the outflow valve, the yellow line represents the target input for the inflow valve to the surge tank. The white line is the measured discharge of the IDM. One may recognize a constant time shift between the white line and the input parameters. This aspect is related to the control loop time delay between measured discharge, PID process and valve reaction. Thus, this delay only shifts the starting time. It can be concluded that the system may become more dynamic and more difficult to adjust when more than a single valve per flow direction is placed. The adjusting parameters are given by the PID governor itself and the tuning of the laboratory pumps and the outflow pump of the surge tank test rig.

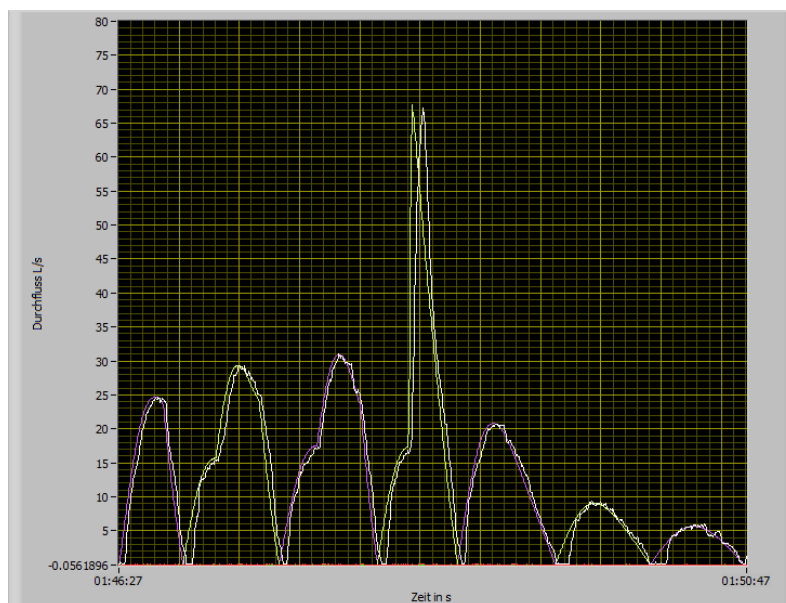


Figure 5-16: Input discharge target compared with measured discharge at surge tank base at specific model test scale factor 1:25

INVESTIGATION METHODS

The physical small-scale model tests were applied by Froude similitude law, substituting the pressure tunnel by transient 1D-numerical input as described above. This allows relatively highly scaled models. The *Atdorf* surge tank with scale factor 1:40 was accurately resolved. *Vereide* (2016) [70] utilised a small-scale model with the pressure tunnel representation to investigate the behaviour of air cushion surge tank. Additionally, the scaling effect of the pressurized air was utilised by placing the surge tank at a high point to adjust the scaling effects of the mass oscillation and the air representation [117]. For modelling the closed surge tank for the *Kopswerk II* pumped storage hydropower plant, *Larcher et. al.* (2006) utilised a separate enlarged air tank to model the transient air cushion behaviour in association with the mass oscillation [118]. For stability analysis of a tailrace surge tank with physical small-scale model tests, *Svee* (1970) [65] fully applied the pressurized tailrace tunnel in the physical hydraulic modelling approach.

5.1.7 PIV Measurements

Particle image velocimetry (PIV) measurements were used to investigate the details of a surge tank facility such as the flow patterns in a throttle or specific pipe arrangements. PIV measurements were applied in combination with physical model tests. The advantage of the PIV approach is that flow velocities and specific flow patterns are made visible and can be used to calibrate and validate 3D-numerical simulations. Figure 5-16 briefly describes the PIV principle: A pulsed laser spans a light sheet to define the investigated flow section. Perpendicular to this section a high-speed camera is located (e.g. with CCD chip). The high-speed camera shoots triggered pictures coupled to the laser pulse. The flow to be investigated may be additionally fed with seeding particles such as polyamide that can follow the flow, also in acceleration zones. *Dobler* (2012) [119] investigated the use of natural seedings for. Two images with a defined time delay plot the tracked seeding as lighted dots. Via a correlation algorithm the particles define the velocity vectors for the full section area. A particular throttle flow, investigated with PIV is described in chapter 6.7.7.

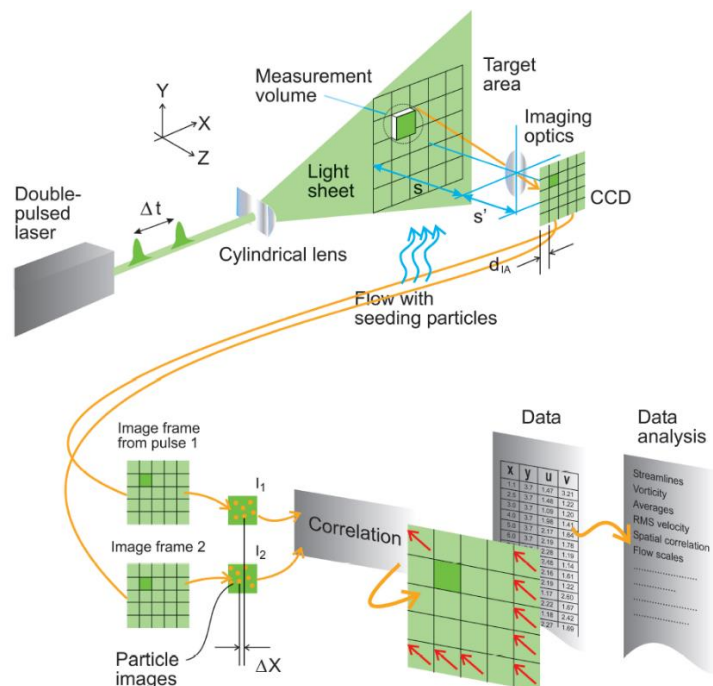


Figure 5-17: Principle of PIV (*Dantec Dynamics*)

5.1.8 Small-Scale Model for Water Hammer

The small-scale surge tank model is used to simulate the mass oscillation, as well as to measure the water hammer pressure. Figure 5-18 shows the small-scale test facility in the laboratory. The system consists of a reservoir with a diameter of 0.5 m, a sharp-edged inlet, a connection pipe, a pressure tunnel pipe ($D_i = 0.0209$ m), T-piece, a pressure shaft pipe ($D_i = 0.03$ m) and a closing valve. The upper end of the T-piece is connected to the surge tank. Via a valve the surge tank connection can be adjusted in its diameter and also totally closed.

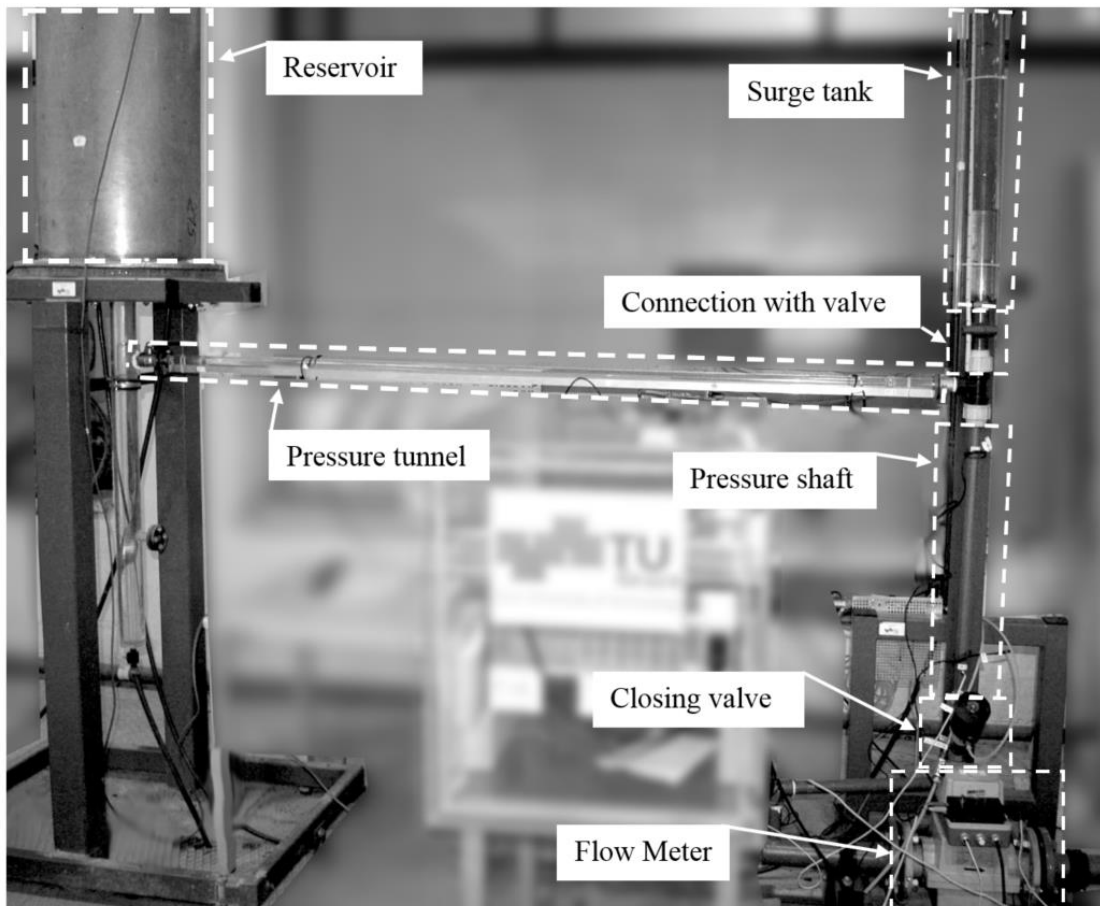


Figure 5-18: Small-scale surge tank model with reservoir, pressure tunnel, pressure shaft, surge tank and outlet valve (Richter)

The facility is compact and thus, capable to visualise the mass oscillation directly as well as the water hammer phenomena (overpressure and sub-atmosphere) by high frequency measurement equipment. The visualisations are used for teaching purposes. Pressure surges can be up to over 10 bar in the small facility with 0.5 l/s discharge generating a Joukowsky hammer directly in front of the valve representing the turbines. Manual valve closings at the outlet of the reservoir are used to visualise the effects of macro cavitation and the associated pressure surges.

5.2 1D-Numerical Simulations

The development of computers, comprehensive numerical schemes and software utilising the codes for transient hydraulic simulations have made it possible to simulate complex hydraulic schemes in an appropriate manner. Before establishing the first transient simulations software in Austria in the 1970s, stepwise derivations for low frequency mass oscillations needed to be made by hand. Several graphical approaches were developed by *Prášil* (1908) [120], *Schoklitsch* (1923) [121], *Gardel* (1957) [122] and others.

For the high frequency water hammer problem graphical methods were developed by *Schnyder* [123] and *Bergeron* [124] and very widely used as *Schnyder-Bergeron* method. Other than this, an analytical method by *Jaeger* (1933) [125] was proposed among other techniques before inventing numerical methods in combination with increasing computational capacities.

The mass oscillation problem for shaft surge tanks can also be modelled quite simple in *Excel*. Due to its transient character, every time step needs to be calculated stepwise. Especially for resonances load-cases this was very time consuming in former times and needed the support of good preliminary approaches. Modern 1D-numerical water hammer software allows to compute complex hydraulic schemes in reasonable time. Still, the surge tank development demands experience and numerous simulations of variants to capture all possible unfavourable oscillation and water hammer issues in a finally combined simulation taking the elastic water column and the machinery specifics into account. 1D-numerical simulations require most accurate transformation of the 3D-flow into a 1D-numerical model applying the available empiric approaches of local and longitudinal losses and channel flows.

1D-numerical simulations herein were conducted mostly with the software *WANDA* [126] and *SIMSEN* [127]. The reasons to use these packages are described as following:

WANDA uses the method of characteristics (MOC) for water hammer evaluation [69]. It provides several modules to simulate liquid flows with transient pump representation, gas flows, it allows to add control elements and to simulate heat distributing systems. **WANDA** provides robust elements and various tools to model complex surge tank designs and arrangements. Especially, the free surface flow pipe elements allow comprehensive modelling of the flow transitions of pressurized flows and free surface flows in surge tanks. The free surface flow conduit element is capable of slow filling and draining processes. It also can be used to directly predict wave heights or wave reflection on walls. The element treats the air above the free surface in a way that it can leave or enter freely without causing pressure surges. But, the air is not freely leaving in prototype surge chambers. It might be trapped at the crown. One may notice that this aspect is more conservative in the simulation of lower chambers. Thus, the prototype is modelled on the safe side.

For a long upper chamber modelling as described below, the best inclination was evaluated accurately with the 1D approach and was confirmed by the physical model test. The optimised inclination allows in that case to minimise the gross volume of the chamber.

This is crucial to model flow separations at upper chambers influencing the differential effect of the upper chamber and the economic design of large chamber surge tanks.

SIMSEN uses the hydroacoustic impedance method [128]. With this approach also electrical systems with the flow of electricity and elements associated with this can be simulated the same way as hydraulic pipe systems. Thus, this approach allows for a combination with electric system simulations in the same model. *SIMSEN* provides various methods of programmable control elements and supports all major hydraulic turbines and wind turbines or tidal turbines to be modelled. The comprehensive representation of hydro turbines and pumps as well as pump turbines with their four-quadrant characteristics field is vital to accurately predict water hammer behaviours in power waterway systems (see chapter 5.2.2). Surge tank elements in *SIMSEN* provide inertia factors that are crucial for water hammer reflection and comprehensive differential surge tank elements. Since the version 3.2.2 of this software it also provides free surface flow conduits.

The placing of a surge tank divides the power waterway into two pressurized hydraulic sections interrupted by the free surface of the surge tank. The part of the high-pressure section from the machine units to the surge tank is water hammer predominant and the section from the surge tank to the reservoir is dominated by the mass oscillation. The aim of the interruption by the surge tank is the splitting of the inertia. The smaller inertia supposed to be in the section directly attached to the machine units to improve their controllability. Still significant water hammer pulses may be recognised in the pressure tunnel, depending on the surge tank inertia. High inertia of surge tanks to be accelerated are increasing the amplitudes of water hammer in the pressure tunnel. No macro cavitation is allowed to occur, since this would create a severe secondary pressure surge by a sudden collapse [49].

Steps to develop the surge tank as done for the present work:

- 1) 1D-numerical simulations by means of rigid column approach for detailed check of mass oscillations. The advantage of rigid column simulations is the reduced time demand, which is crucial for efficient variant checks and the manual setting of most unfavourable time points for loading and unloading in terms of amplifying the system.
- 2) Combined simulations of water hammer and mass oscillation, as well as the check of most unfavourable machine emergency closings and pump trips, causing maximum and minimum pressures in the power waterway systems.

5.2.1 Mass Oscillation

The mass oscillation behaviour is the predominant flow phenomena, defining the needed size of the surge tank. It is driven by the water mass in the pressure tunnel in its reaction to the needs of the units. Thus, the surge tank volume is a function of the pressure tunnel dimensions and significantly influenced by the friction parameters of the tunnel. For resonance load-cases the lower limit of the friction value is the most unfavourable to be applied [1]. For quick simulation results, some software allow to apply the rigid column method for mass oscillation simulation. A mass oscillation simulation approach is comprehensively described by *Giesecke et. al.* [63].

INVESTIGATION METHODS

Figure 5-19 visualises the 1D-numerical representation of the *Krespa* surge tank case study including the modelling approach of the waterfall-dampening device. The upper chamber is modelled with $D_i = 7.0$ m and 311 m long free surface pipe element. This modelling type allows the representation of flow separation due to outflow characteristics of the upper chamber. Thus, it is possible to investigate the mass oscillation events to detect waterfall intensity and the most unfavourable boundary conditions of the waterfall (Figure 6-74). The important aspect of the free surface flow behaviour modelling is to capture the retardation effect of the upper chamber regarding the mass oscillation of the entire power waterway. For large surge tank designs with long chambers this has a significant impact on the economical surge tank design. Since the chamber is filled by a surge wave this kinetic energy needs to be dampened evenly to utilise the given volume as best as possible. A simplified chamber simulation with area/height modelling underestimates the impact of waves. The size of the surge tank should be large enough including safety, but not significantly too large in order to be economic.

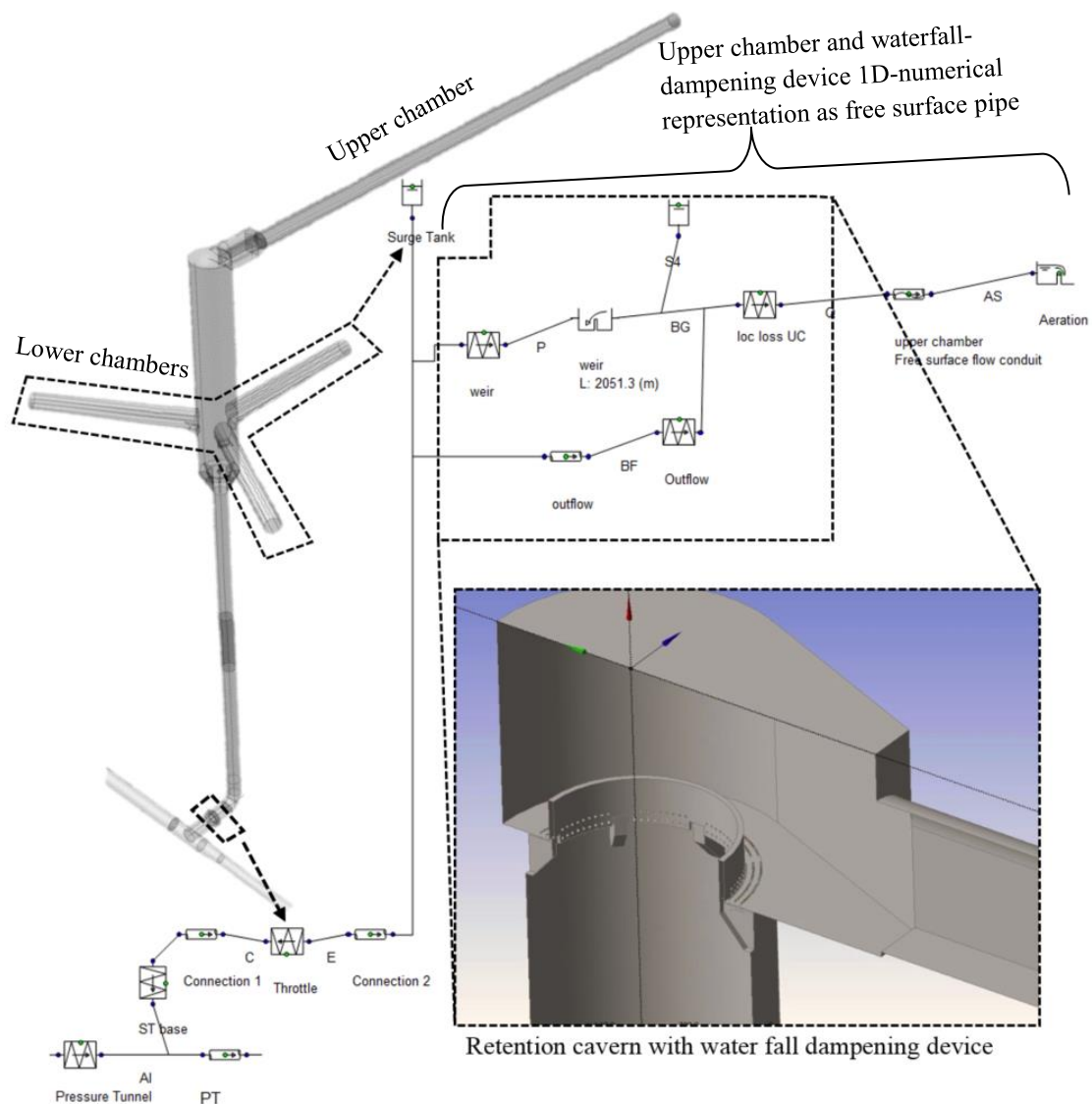


Figure 5-19: 1D-numerical model of *Krespa* surge tank with waterfall-dampening device in WANDA, (Richter [114])

INVESTIGATION METHODS

Figure 5-20 shows the typical representation of a chamber in a surge element with height-dependent area. Chambers for surge tanks are usually recommended to be inclined to allow both de-aeration on the ceiling and sufficient water outflow on the invert. Only horizontal section cuts of the 3D geometry can generate accurate input parameters for the 1D-numerical representation. Figure 5-21 depicts the horizontal section cuts of the lower chamber tunnel for 2 % inclined crown and 1 % inclined invert. This lower chamber has a very compact geometry with a L/A_{ave} ratio of 1.48 [-].

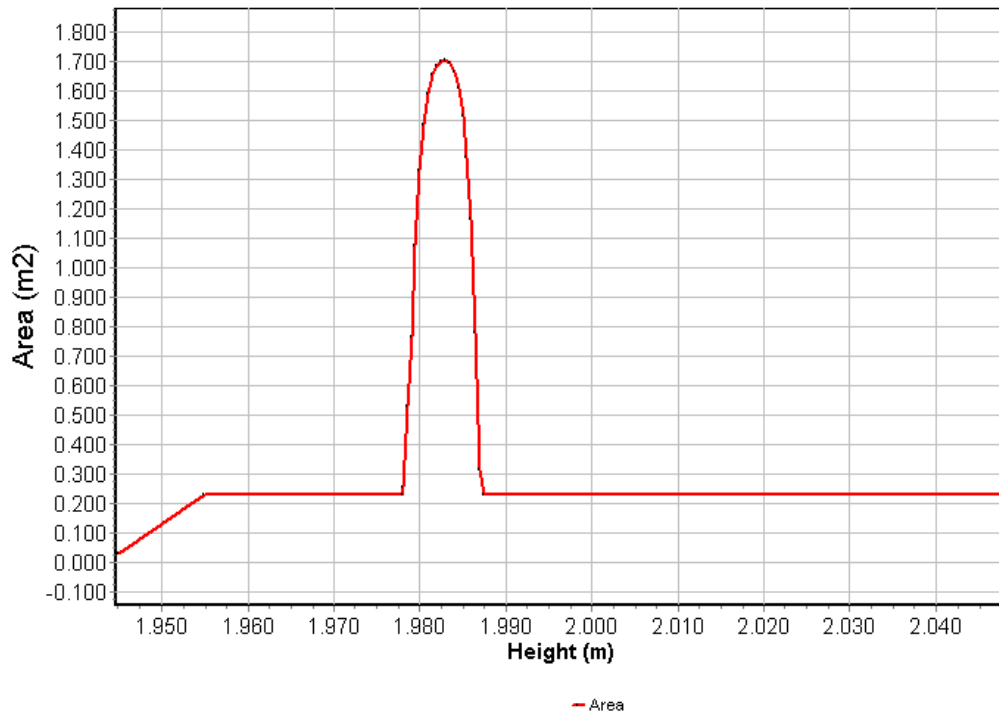


Figure 5-20: 1D representation (area/height) of compact lower chamber in *Wanda* (Richter [114])

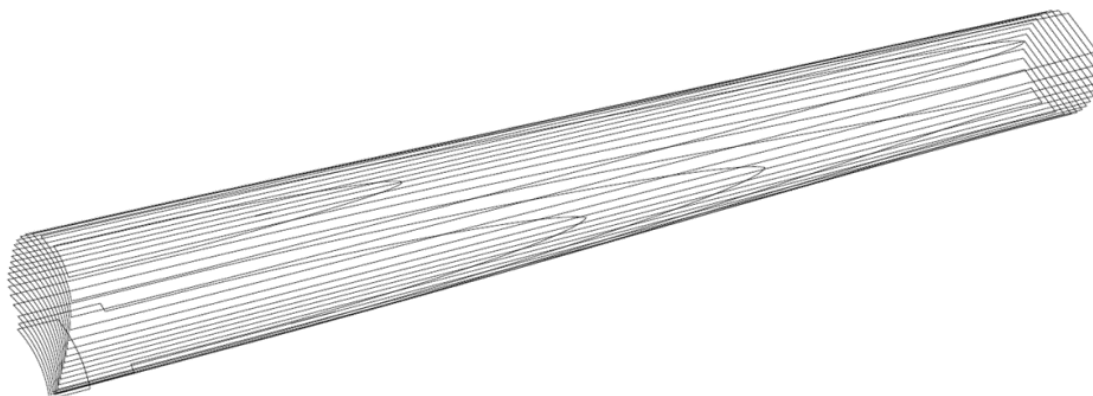


Figure 5-21: 3D geometry with horizontal section cuts of a lower chamber (Richter [114])

5.2.2 Water Hammer

Transient water hammer simulations may utilise either the impedance method or the method of characteristics (MOC) [69] within a numerical software. The simulations are applied in an explicit numerical scheme. Crucial boundary conditions for surge tank behaviour are the hydraulic behaviour of the machines in case of load rejections in generating mode or pump trips in pumping mode. Both force the water mass to a quick counter reaction. Since pump turbines are represented by four-quadrant characteristics based on complex hydraulic effects [129] the implementation of hydraulic machines has to satisfy this request. A well confirmed approach can be utilised with *SIMSEN* [128].

The four-quadrant characteristics field describes the behaviour of a pump turbine for all flow condition between pump operation and turbine operation. Additionally, the brake operation and a reverse pump effect may occur. Figure 5-22 shows a typical four-quadrant field of a pump turbine by *Ješe et. al.* (2019) [130]. The typical important instability zone marked as turbine brake, this shows the characteristic S-shape instability. The challenge is, that this region is not clearly defined in this representation. A vertical line may have three intersection points, that is not straightforward to an appropriate value reading. Thus, an adequate transformation of the region is indispensable, that can be found at for example at *Nicolet* (2007) [128].

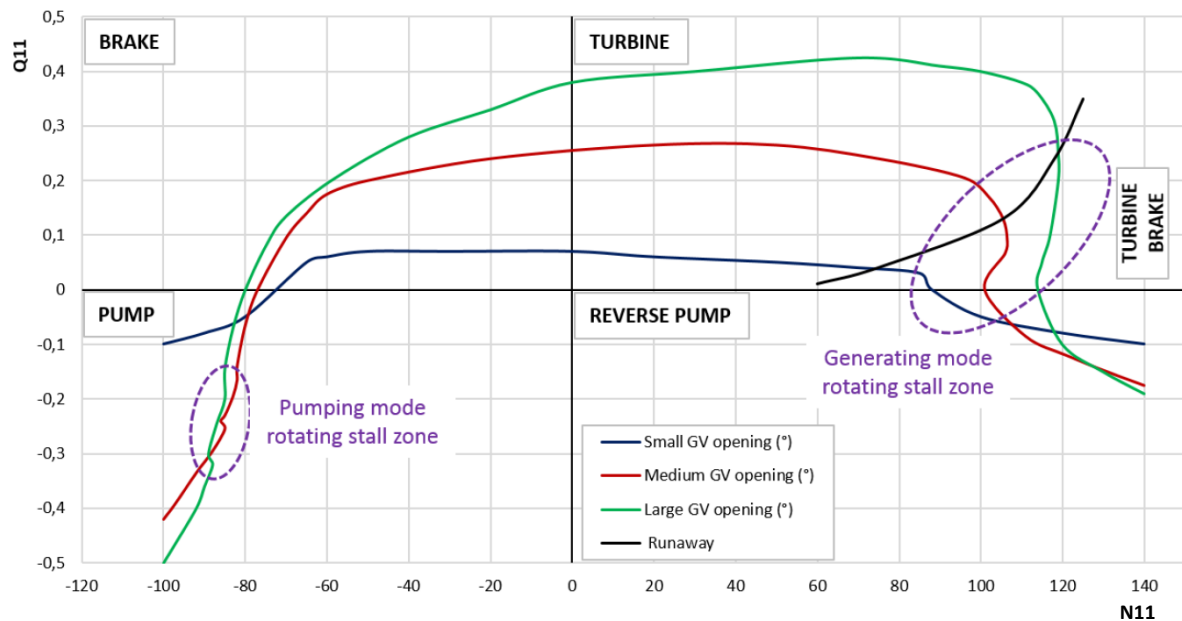


Figure 5-22: Typical Four-quadrant field characteristics with marked zones of instability, *Ješe et. al.* (2019) [130]

Q11	...	Unit discharge factor, $Q11 [-] = Q/D_{ref}^2 H^{0.5}$
Q	...	Discharge [m ³ /s]
D _{ref}	...	Diameter reference [m]
H	...	Head [m]
N11	...	Unit speed factor = $N D_{ref} / H^{0.5}$
N	...	Rotational speed [rpm]
GV	...	Guide vane

INVESTIGATION METHODS

Figure 5-23 from *Zuo et. al. (2016) [131]* visualises the two cases at which the instability zone in turbine mode plays a role; the synchronisation at start-up and the load rejection. The blue line is indicating the load rejection that shows the direct flow path to no-flow and even into the quadrant “Reverse Pump” with a reverse flow. This behaviour can be defined as self-blocking of the flow and even pushing some water back up, as if it would be in pump mode. These instabilities are linked to complex 3D flow vortices in the runner blade as investigated by *Guggenberger et. al. [129]*. However, the quick flow blocking at load rejection may define the design water hammer for the hydraulic system in the headwater and the tailwater, and requires an appropriate guide vane closing.

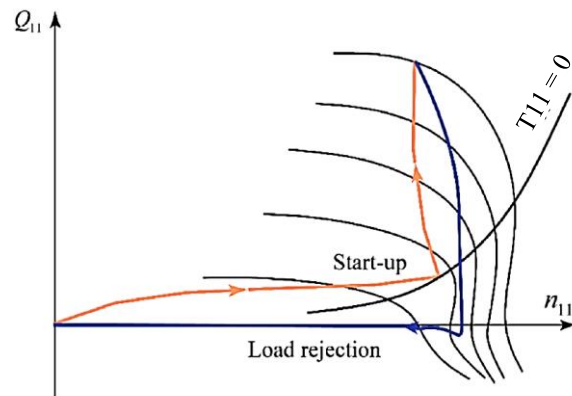


Figure 5-23: Effect of the S-shape zone for start-up and load rejection *Zuo et.al. (2016) [131]*

T11 ... Unit torque factor, $T11 = T/D_{ref}^3 H^{-1}$
T ... Torque [Nm]

5.2.3 Stability Simulation

1D-numerical simulations allow a check of the surge tank stability criterion. The above-mentioned software packages allow different approaches of the stability check application. The Norwegian software *LVTrans* [132] is designed for stability checks in islanded grids. *SIMSEN* and *Wanda* allow stability checks utilising control elements for applying different approaches to check the requirements of a grid standard or an implementation of the energy equation (5-16). This approach allows a power governed loading and unloading as well as constant operation at full load utilising the minimal possible head for the design case. The equation governs the discharge via a PID controller element while the head is directly computed in the simulation and reflects the head variation of the surge tank oscillation. If the surge tank oscillation is dampened for this case the system is hydraulically stable.

$$P = \rho \cdot g \cdot Q \cdot H \cdot \eta = const \quad (5-16)$$

5.2.4 Surge Tank Inertia

The consideration of the water inertia in the simulation of surge tanks may not be included in standard elements in 1D-numerical simulation software. For the mass oscillations, the inertia does not play a significant role. But for the water hammer reflection it may play a significant role for certain surge tank design or load-cases. Especially for cases when long and slightly inclined surge tank elements have to be suddenly accelerated.

Sudden events are usually given at emergency shutdowns or load rejection when high gradient water hammer pressure waves have to be mitigated quickly and the water in the surge pipe is either in no motion or needs to reverse for the flow direction. The effect is worsened by long connection tunnels, small diameter and long lower chambers. In addition, orifices have a negative impact, but not as significant as small horizontal pipes. A comparison from *Nicolet, et. al.* (2015) [42] of an incident at the *Avče* pumped storage hydropower plant by 1D simulation has proven this fact. This has shown the importance of considering the inertia in the surge tank. The paper of *Nicolet* also states that a calibration of additional 30 % increase of the inertia was necessary to fit with measurements.

The surge tank *Avče* is interesting since not only the inertia was obviously not considered, but also no physical test of the surge tank was conducted. It resulted in a dangerous situation in a case of pump trip and insufficient water volume [133]. After the construction and the findings of the transient issues two model test solutions were investigated. A small aeration pipe was found to improve the system and was adapted to the construction [133]. A more reliable solution with an extra shaft and sufficiently low inertia and additional volume was not considered due to higher costs [134].

5.3 3D-Numerical Simulations

3D-numerical simulations, also noted as 3D-CFD simulations for computational fluid dynamics, may improve significantly the design of surge tanks due to the possibility to identify potential problems that have to be studied with physical model tests. For surge tanks it is possible to perform 1D simulations or 3D-numerical simulations. Following aspects were studied with 3D-numerical simulations within this thesis:

- Local losses of throttles and connections including the entire geometry
- Chamber behaviour
- Overall hydraulic behaviour of a surge tank
- Degassing behaviour of a bubble regime by performing multiphase simulation
- Visualisation of flow behaviour in surge tanks with multiphase simulations

3D-numerical simulations herein were conducted by applying the RANS (Reynolds-Averaged Navier-Stokes Equations) turbulence modelling approach [135]. The basis of this concept was first proposed in 1895 by *O. Reynolds* [136]. In 1897 *Boussinesq* introduced the concept of eddy viscosity [137]. The first turbulence model was developed by *Prandtl* in 1925 introducing the turbulent mixing length. Further developments of *Prandtl* (1945) established the first one-equation turbulence model proposing a transport equation for the turbulent kinetic energy as a basis for modern RANS modelling concepts [138].

More than 120 years of development of the representation and simulation methods of turbulent flows have led to apply comprehensive approaches for solving various problems of flows. Indeed, the development is strongly coupled with the developments of computer technologies in order to increase the complexity and accuracy by finer resolution, decreasing the modelling demand and increasing the direct part of the flow simulation. This evolution is not at its end and will be continued for many more decades since the nature of turbulence is highly stochastic and takes place at the molecular level of the flow medium.

The software used in this thesis is *ANSYS CFX* in various versions to analyse 3D flow behaviour and local loss evaluation. The simulations were conducted mainly utilising the shear stress turbulence model (SST) [139] [140]. In case of significant rotational flows such as at outflows of throttles, that are attached in a significant angle to circular shaped tunnels, a curvature correction factor is applied [141]. The character of a restricted jet flow into a circular pipe geometry usually introduces complex rotational flows that may be difficult to be captured by two-equation turbulence models.

The comparison of 3D-numerical simulations to physical model tests are found to sufficiently solve the surge tank design demands. A limit of 3D-numerical simulations is the accurate prediction of air bubble production by intruding jets. Thus, multiphase simulations are needed to be interpreted carefully, especially the transition zone of free surface flow and air intruding waterfalls.

INVESTIGATION METHODS

Transient 3D-numerical simulations can reveal the complex, time dependent shapes and behaviour of jets generated by throttles. Figure 5-24 and Figure 5-25 show different time steps of a transient jet through an orifice throttle, visualised by the specific 15 m/s flow velocity envelope in a RANS simulation. The restricted jet flow is finally a diffuser flow problem and thus unstable. This instability leads to a fluctuating jet and a slightly fluctuating throttle loss. An oscillating jet may also touch the pipe wall with higher flow velocities as for power plant operation. The material resistance has to be determined in an interdisciplinary approach and influences the lining decision (see chapter 6.2).

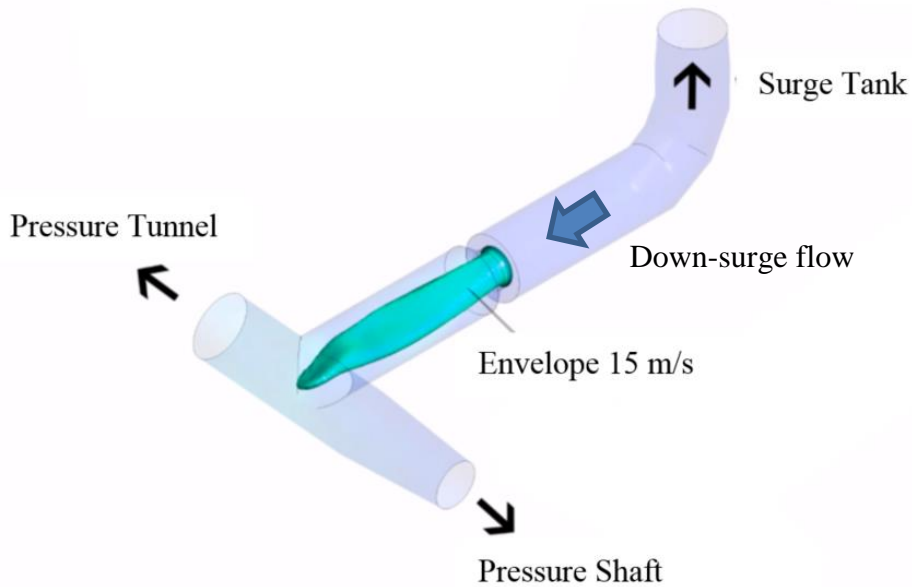


Figure 5-24: Transient 3D-CFD Simulation throttle jet, time point 1

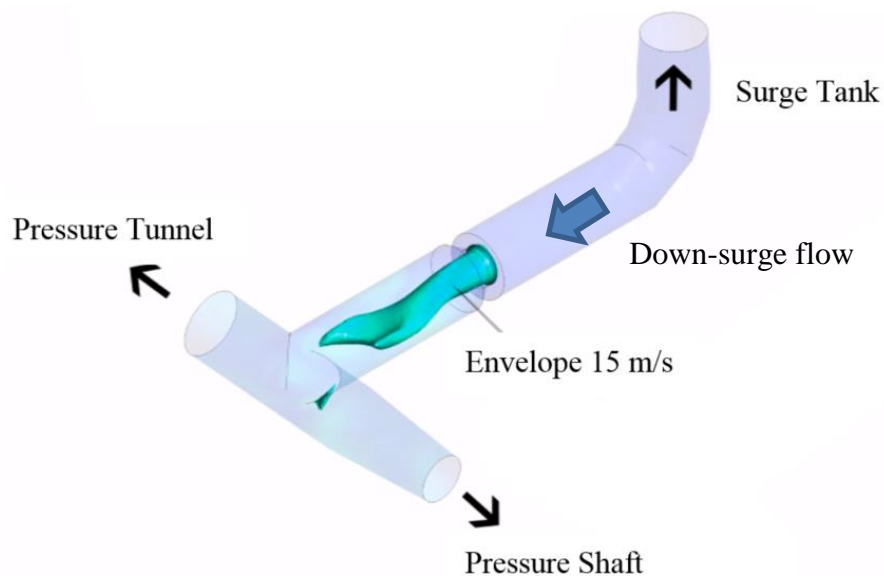


Figure 5-25: Transient 3D-CFD Simulation throttle jet, time point 2

5.4 Hybrid Modelling – Physical Model Test and 3D-CFD

Hybrid modelling is the extension of the physical modelling with numerical methods. In case of surge tanks, 3D-CFD simulations are referred here. Physical full model tests are usually limited to the Froude similitude representing gravity forces. In case of surge tanks, this is straightforward to represent the surface waves in the chambers. An advantage of 3D-CFD simulations of the full surge tank structure or parts of it is the fact that they can be done in prototype scale 1:1, which reveals additional hydraulic aspects such as:

- Vortex formation with proper Weber number [142]
- Air bubble behaviour may be simulated in terms of 3D-CFD applying multiphase approaches [106], [143]
- Waterfall behaviour [43]

Currently it is not possible to directly model the air intrusion capturing all physical phenomena generated by a water jet by means of 3D-numerical simulations within an engineering approach. However, multiphase models are available to describe the behaviour of air bubbles in a water flow [141]. Figure 5-26 shows the options for hybrid modelling of a surge tank in case of the *Atdorf* surge tank. With 3D-numerical simulations, extensions of the physical model test investigation are possible. Swirl flows are scaled usually by similitude of the Weber number. Air bubble degassing with two-phase simulation is applied by a design bubble de-aeration, or the jet impact of the waterfall. The described aspects can be investigated in a partial model applying the results from 1D-numerical simulations as boundary conditions.

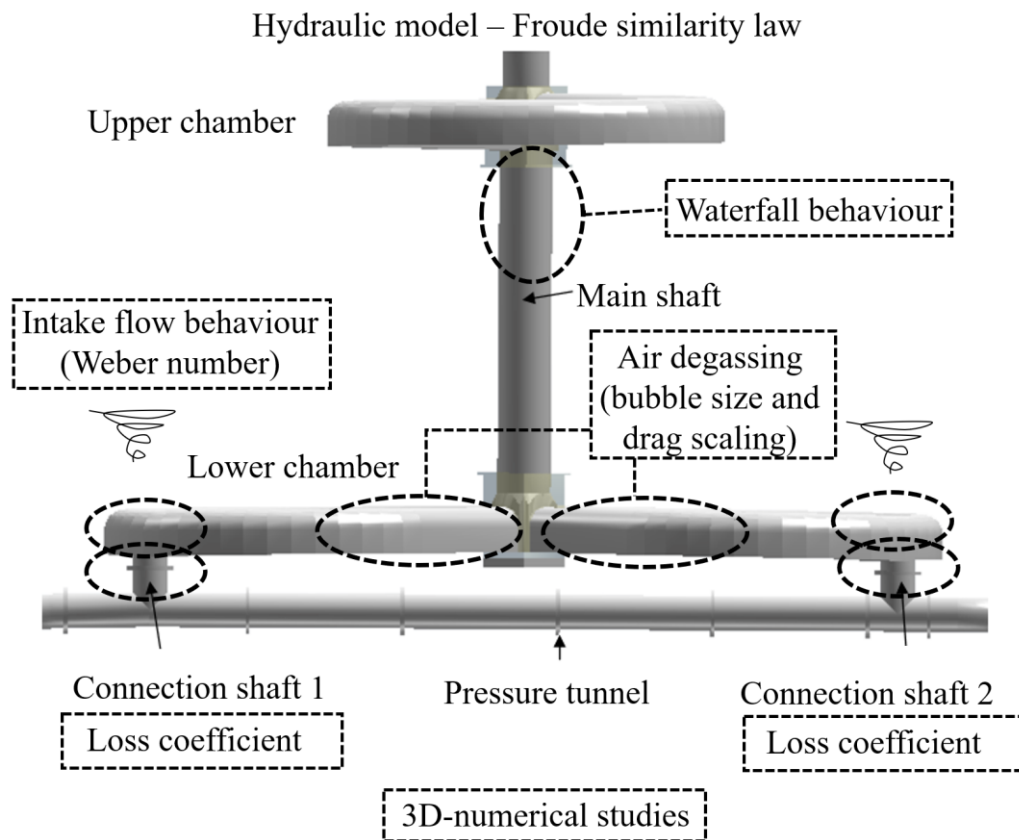


Figure 5-26: Hybrid modelling options in addition to a physical model test of a surge tank, modified from (Richter [142])

INVESTIGATION METHODS

Figure 5-27 shows the superficial water flow in the 3D-numerical simulation of the *Atdorf* surge tank. The simulation visualises the situation with free surface in the lower chamber while water discharges from the upper chamber as a waterfall. This waterfall represents the differential effect of the upper chamber. The simulation, as additional investigation tool to the physical model test (Figure 5-28) significantly improves the evaluation of variant studies of details as well as for variants of general concepts in order to improve the design or pre-check the functionality.

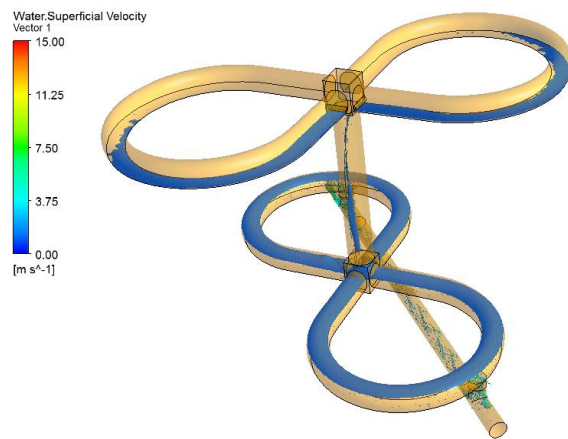


Figure 5-27: 3D-numerical simulation of the surge tank *Atdorf*, (Richter [106])



Figure 5-28: Physical model of the surge tank *Atdorf* in the hydraulic laboratory, (Richter [106])

In case of the *Atdorf* surge tank investigations of an air core vortex was observed for the most unfavourable outflow from the lower chamber into the pressure tunnel (Figure 5-29). Since the model test was operated in Froude similitude the air-filled core can be expected worse if scaled up to prototype, since the influence of the surface tension of the water tends to close an air-filled core in the scaled model test. Applying the Weber similitude law this effect can be studied more in detail. By applying a 1:1 scaled 3D-CFD simulation this challenge in the physical model test can be gapped. For the specific problem several variants with guide walls were tested, a wall that equally divides the flow into the shaft was found to be the best solution (Figure 5-30).

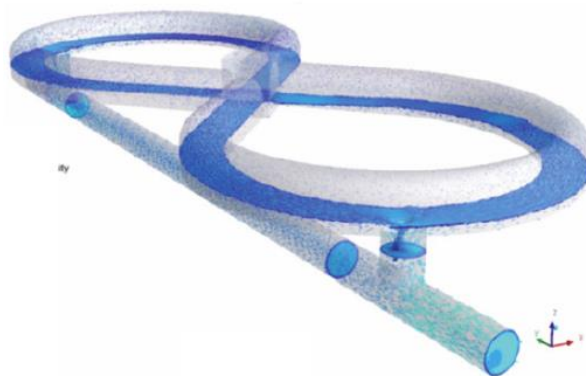


Figure 5-29: Lower chamber with vortex core at high discharge from lower chamber to pressure tunnel, (Richter [106])

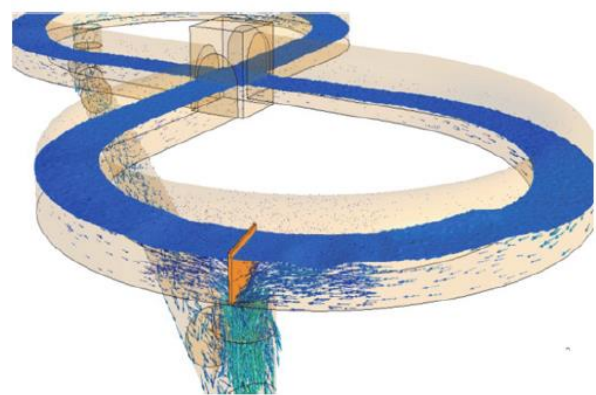


Figure 5-30: Wall in lower chamber dividing the flow from both sides of the chamber and avoiding the vortex (Richter [106])

INVESTIGATION METHODS

Figure 5-31 shows the discharge through the vertical connection into the pressure tunnel with the air-filled vortex at maximum discharge event and the vortex suppressing wall in the physical model test. Figure 5-32 shows the guiding wall in the small-scale test that divides the flow from the two branches of the lower chamber without creating an air-filled vortex. The small firefighter is in 1:40 scale showing the size of a human, the scale in Figure 5-32 shows the altitude of the structure in m a.s.l.

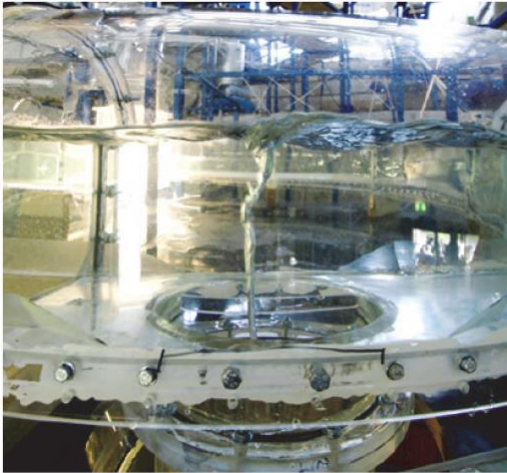


Figure 5-31: Vortex flow in connection shaft at maximum discharge due to resonance load-case, (Richter [106])

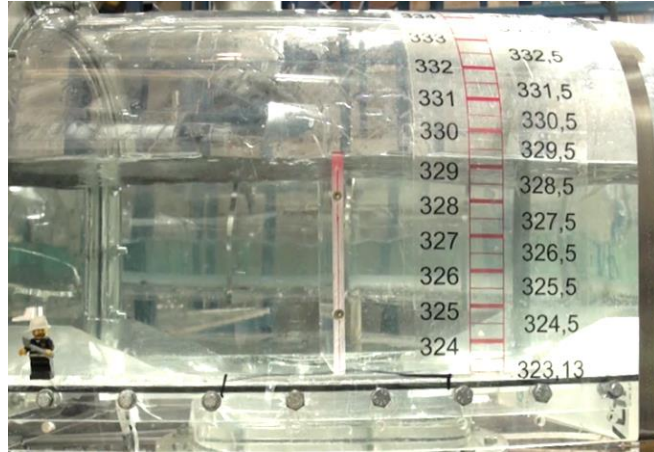


Figure 5-32: Avoided vortex flow for maximum transient design flow, wall that divides the flow from both lower chamber sides within the loop branch, (Richter [106])

The investigated example highlights the benefit of hybrid modelling the flow vectors and transient flow behaviours with 3D-numerical simulations. The simulations can be done independently from hydraulic scale factors and thus allow to overcome similitude law restrictions, such as the influence of the water surface tension or also the air bubble degassing in combination with the complex water flow (see chapter 6.8.6).

5.5 Prototype Measurements

During the commissioning of the pumped storage plant *Obervermuntwerk II* measurements in the surge tank were undertaken by Illwerke AG. Those were compared with the results of the numerical and physical modelling [45], see chapter 6.9.

6. RESULTS AND DISCUSSION

This chapter describes the approaches and the results of the hydraulically investigated surge tanks. Derived design tools as well as the boundary conditions for hydraulic surge tank design approaches such as relevant load-case scenarios are described, as well as structural aspects such as surge tank lining, air cushion surge tanks and its proposed application in Alpine regions. The chapter surge tank upgrade discusses the issues of efficiently upgrading existing surge tanks. New developments for surge tanks are presented such as semi-air cushion surge tanks and storage tunnel surge tanks. Surge tank details are described to underline the design of structural features that improve the hydraulic behaviour. The chapter about waterfalls investigates this specific phenomenon and its mitigation by a developed waterfall-dampening device. The final sub-chapter presents the validation of the investigated surge tank *Krespa* by prototype measurements.

6.1 Load-case Scenarios

Load-case scenarios for transient hydraulic events are developed, both for water hammer events and mass oscillation cases. Within this thesis, the focus is especially on the latter aspect to define the loadings for the surge tank design. The water hammer design load is bound to the mass oscillation aspects, since it focuses on the interaction of the transient behaviour of the machine and the water mass in the penstock, in combination with the acceleration reaction of the surge tank. The mass oscillation is characterised by low frequency amplitudes; the water hammer transients are defined with high frequent oscillation demanding high time resolution in numerical simulations. It is finally necessary to combine the surge tank design with low and high frequency pressure transients. However, the first steps in surge tank design may be assumed by applying linear machine loading and unloading boundary conditions and lower time step resolution to investigate the filling and emptying processes of surge tank structures. For final design, combined simulations with capturing the low and the high frequency pressure pulses are indispensable.

The aims of comprehensive 1D-numerical simulations for the surge tank design are to:

- A) Find the maximum water level in the surge tank shaft respectively the most severe surge in an upper chamber at the aeration structure.
- B) Find the minimum water level in the surge tank shaft respectively the lowest transient water level in the surge tank due to outflow.
- C) Evaluate the maximum pressure at the surge tank base.
- D) Evaluate the minimum pressure at the surge tank base: The crown of the pressure tunnel is the level that should not be allowed to show atmospheric sub-pressure in order to securely avoid macro cavitation that may be triggered by a severe transient event in the machines, and thus cause a secondary pressure surge with very high-pressure pulses.
- E) Check the stability criterion for the most unfavourable conditions with the lowest head at the maximum constant power output. Grid code requirements for pre-qualification of control services may be considered for this check.

For the transient design, high-head hydropower schemes and pumped storage hydropower plants that involve pump units show different demands for the surge tanks. Significant differences are found between the demands of tailrace surge tanks and headrace surge tanks.

Depending on the length of the associated pressure tunnel as well as the influences of the machines demand for different aspects such as a pump trip or a load rejection in generating mode. Those two phenomena have the opposite flow acceleration demands between headrace surge tank and tailrace surge tank. A major effect on the hydraulic surge tank and power waterway designs are caused by the machinery concept. Pelton turbines have the advantage that defined closings are possible even for severe load rejection events due to the function of deflectors. Francis turbines cannot be disconnected to the flow as quickly as Pelton turbines, therefore demands for the surge tank design might be higher for such machines regarding particular aspects in case of turbine load rejections or unloading events that may be controlled more specifically by utilising Pelton turbines. Reversible Francis pump turbines may react due to hydraulic self-blocking of the runner in case of load rejection and rotational acceleration much quicker (see chapter 5.2.2). This effect is triggered by the so-called S-shape instability. The ability of changing the flow from turbine mode to pumping mode influences the required reaction of the surge tank. For pump turbines this time is accounted around several minutes. Ternary machine units with separate pumps and turbines allow immediate or even overlapping operating change between pumping mode and generating mode. Fast changes between turbine mode and pump mode is also given by variable speed pump turbines that utilise frequency converters. The most unfavourable time point for loading or unloading is found shortly before the peak discharge in the pressure tunnel. The larger the section area of the main shaft the more the unfavourable point of load change differs from the time of peak discharge. For the simulations done for the current thesis the switching events were defined manually. In the design phases of a surge tank, the manual selection has the advantage of direct interpretation of the transient behaviour. The load-case input parameters may follow the accorded design safety philosophy (see chapter 3.7).

6.1.1 Headrace Surge Tanks

For headrace surge tanks the maximum up-surge is generated by an emergency shut down after load rejection in resonance of the mass oscillation or by cyclic loading between turbine mode and pump mode. At the same time, it needs to be distinguished to evaluate the maximum pressure at the surge tank base that most likely corresponds with the load-case at highest up-surge. The resonance case depends on the machinery concept, e.g. if a transition between pump and turbine operation is achievable in a short time or even overlapping. The minimum water level is generated by a full reloading of the machines in turbine generation at most unfavourable back flow situation from the surge tank to the upper reservoir. Load-cases with cyclic shifting between pump mode and turbine mode may also lead to the minimum water level in the surge tank.

RESULTS AND DISCUSSION

The following load-cases for headrace surge tank design are suggested to be checked for high-head schemes and pumped storage schemes with pump turbines:

- 1) Maximum up-surge and maximum pressure at the surge tank base, load-case at capacity level in upper reservoir:
 - a) For HPPs
Resonance case in turbine mode at capacity level in the upper reservoir, with: Loading, unloading, reloading and an emergency shutdown (ESD) at most unfavourable time point.
 - b) For flexible PSH
Resonance case with cyclic switching between turbine and pump mode at capacity level in the upper reservoir, considering: Loading and unloading of the turbines, subsequent loading of the pumps, unloading of the pumps, reloading of the turbines with subsequent full loading of the pumps at most unfavourable time point.
 - c) For fixed speed PSH
Depending on the time demand to switch between pump and turbine mode, it has to be distinguished between case (a) respectively (b) above.
- 2) Minimum level in surge tank and minimum pressure at surge tank base, load-case at draw down level in upper reservoir:
 - a) For HPPs
Resonance case; turbine mode with loading, unloading, reloading at the most unfavourable time point.
 - b) For fixed speed PSH
Synchronous pump start-up with synchronous full trip; at the most unfavourable time point before the peak discharge to the reservoir after acceleration of pressure tunnel flow or full pump trip at steady-state pump flow.
 - c) For flexible PSH
Loading and unloading of the pumps; subsequent loading of the turbines, unloading of the turbines, reloading of the pumps with subsequent full loading of the turbines at most unfavourable time point.
For minimum pressure at the surge tank base and the connected tunnel section to the pressure shaft a comparison with a full pump trip load-case is advisable.
- 3) Water hammer interference load-case.
At reservoir capacity level; turbines are synchronously unloaded to no load operation and subsequently reloaded followed by an ESD that causes a pressure pulse in addition to the previous unloading.
- 4) Load-case of unexpected closing of inlet/outlet gate at reservoir;
Such events may happen and are suggested to be investigated and prevented. Measures of structural damage mitigation is suggested to be considered that a surge is guided back into the reservoir. A structural example is realised at the high-head scheme *Sellrain-Silz* [144].

6.1.2 Tailrace Surge Tanks

Flow interruptions by ESDs or sudden load rejections in tailrace surge tanks lead to quick discharge fluctuation and may trigger negative pressures and severe water hammer events [145]. The tailrace surge tank shows opposite effects between pump mode operation and turbine mode operation in comparison to headrace surge tank in sense of filling (up-surge) and emptying (down-surge). In general, tailrace surge tanks need a lower free surface cross-section area to achieve the stability criterion due to stabilising effect of the tailrace discharge. This criterion is more significant for short tailrace tunnels as described by *Svee* (1970) [65]. Due to generally lower counter pressure on the tailrace side of a power cavern the tailrace surge tank needs to be located in significant closer distance to the units as the headrace surge tank.

The following load-cases for tailrace surge tank design are proposed to be checked for high-head and pumped storage schemes with pump turbines:

- 1) Maximum up-surge and pressure at surge tank base, load-case at capacity level in lower reservoir:
 - a) For HPP
Resonance load-cases of full turbine loading followed by full unloading at the most unfavourable time to no load operation, followed by full reloading at most unfavourable point, to achieve the highest up-surge in resonance mode; assuming low friction with safety margin.
 - b) For flexible PSH
Resonance case cyclic switching between turbine and pump mode at capacity level in the lower reservoir, with: Loading and unloading of the turbines, subsequent loading of the pumps, unloading of the pumps, reloading of the turbines with subsequent full loading of the pumps at most unfavourable time point and subsequent full pump trip, that reverses the flow to suddenly fill the surge tank.
 - c) For fixed speed PSH
Depending on the time demand to switch between pump and turbine mode, it has to be distinguished between (a) or (b) above.

- 2) Minimum water level and pressure at surge tank base, load-cases at draw down level in lower reservoir:
 - a) For HPP:
Resonance load-cases of full loading followed by full unloading at most unfavourable time to no load operation followed by full reloading at most unfavourable point. Subsequently followed by an emergency shutdown of all units synchronously to achieve the lowest down-surge level of the surge tank and minimum pressure events in the tailrace pipe and tunnel system, assuming low friction with safety margin.
 - b) For fixed speed and flexible PSH:
Synchronous load rejection at full load turbine operation assuming that at least one unit encounter blocked guide vanes that may lead to severe low-pressure events to be captured by structural design of the tailrace system and the surge tank [146].

RESULTS AND DISCUSSION

- c) For fixed speed and flexible PSH with uneven length of draft tube pipes between the units and the surge tank:

Load rejection with delayed time between the units as an asynchronous event [145]. 1D-numerical software such as *SIMSEN* allow for automated input to check various delayed load rejection cases that lead to water hammer interference. This aspect plays a role at any tailrace manifolds with asymmetric distances after Francis or pump turbine units and can be skipped by designing symmetrical distances from each unit to the surge mitigating device such as foreseen at the *Gouvães* tailrace surge tank [147]. Safety margins are suggested since exact water hammer velocities are difficult to estimate.

- 3) Load-case of unexpected closing of inlet/outlet gate at reservoir. Measures of structural damage mitigation is suggested to be considered that a surge is guided back into the reservoir.

6.2 Surge Tank Lining

This chapter briefly discusses the aspects of lining for pressure tunnels and for surge tanks in specific.

Surge tanks must be watertight and structurally stable. Thus, lining of surge tanks may be necessary in many cases. Depending on the ratio of overburden and internal water pressure, rock quality and demands on water tightness, surge tanks are unlined, concrete lined (with or without reinforcement), lined with pre-stressed concrete lining or a steel lining. Pre-stressed lining may be passively pre-stressed such as utilising grouting injections or actively pre-stressed concrete lining utilising pre-stressing cables. Surge tank shafts or chambers need to be steel-lined if the overburden is not sufficiently bearing the maximum internal pressures. In particular, the minimum rock stress (σ_3) needs to be above the maximum internal pressure to be unlined. The minimum rock stresses need to be measured in-situ. FEM simulations may be utilised to study the stressed based on the local topography. The topography may have a major impact on the stress situation as describe by *Broch* (1984) [148].

In Alpine rock situations such as in Austria the rule of thumb to choose steel liners in pressure tunnels is a ratio of 1:1 (overburden: maximum internal pressure) [94]. This ratio considers that the rock-mass has a higher density than water but also may have weakness zones and non-active topography to act with sufficient counter pressure. Thus, the higher density of rock is the safety value. In Norway the rule of thumb allows even lower overburden versus maximum internal pressure as in Alpine region due to (i): high rock-mass quality and (ii): horizontal pre-stressing from the glacial period. Descriptions can be found by *Palmström* and *Broch* (2017) [96] and cited literature therein. Also, some pressure tunnels may be constructed without steel liner, even though the dynamic pressure is above the overburden. High horizontal pressures generate high minimum rock stress values as for e.g. the pressure tunnel at the HPP *Langenegg*, in Austria [149]. This is the advantage of placing pressure tunnels with high overburden. To keep the water tightness at such pressure tunnels with sufficient minimum stresses but internal pressure above the *Walch's limit* a plastic foil is used [150]. Another example that utilises plastic foil is the pressure shaft and pressure tunnel of the pumped storage scheme *Kühtai*, a high-head facility without surge tank [100]. This foil is placed as outside layer behind the concrete lining that bears the compression forces by the pre-stressing due to grouting. The plastic foil can gap concrete crack widths of the foils thickness [94]. Owing to the high rock-mass quality, pressure tunnels and surge tanks are usually unlined in Norway and allow to utilise the rock as confinement material, resulting in very economic constructions. In combination with high-heads and significant precipitation Norway can produce vast amounts of energy from economic hydropower. This economic hydropower is defined by very high ratios of EROI that is the ration between the output energy of operation time and the invested energy to construct the production unit (see chapter: 2.2). One may notice that unlined pressure tunnels always carry the risk of rock falls or partial collapse, and even the best rock-mass has faults and weaker zones. Rock falls may be triggered by too fast water emptying that is associated with steep gradients of pore pressures. An overview of major failures in Norwegian unlined Pressure shafts and tunnels is given by *Pantheni and Basnet* (2016) [151].

Pre-stressing methods were already used by grouting measures at the *Catskill* water supply pressure tunnel for New York City [152]. *Mühlhofer* [153] describes in 1921 the positive action of groundwater table and grouting injection found at the *Catskill* pressure tunnel. The pre-

RESULTS AND DISCUSSION

stressing was further improved by *Kieser* 1943 [154]. The state-of-the-art method in Austria is the TIWAG grout injection pre-stressing method developed by *Lauffer* and *Seeber* during the construction of the *Kaunertal* high-head scheme (commissioned in 1964) [155]. The applied investigation methods have been further improved by modern materials and techniques. In addition to this method the TIWAG radial press as in-situ rock properties measuring method was used to develop an in-situ dimensioning concept for pressure tunnels together with the graphical method; the *Seeber*-diagram [156], [157], [100], [158], [159].

The lining demand of surge tanks corresponds with the concerns regarding the positioning of this structure. Figure 6-1 shows the example of the original surge tank of the *Kaunertal* HPP, that was in operation between 1964-2016. The lower chamber is exposed to less overburden as maximum internal pressure due to relatively flat mountain gradient. Usually, the need is to place the surge tank as close as possible to the pressure shaft. Thus, the lower chamber may have no sufficient overburden to act as a counter rock-mass abutment. This demands for reinforced concrete lining or steel lining. Whereas the disadvantage of reinforced concrete is that the reinforcement needs cracks to be activated that is in contrast to the tightness demand. The cracks can be distributed by comprehensive reinforcement. Actively pre-stressed reinforcement was used for the *Lünerseewerk* surge tank shaft [154].

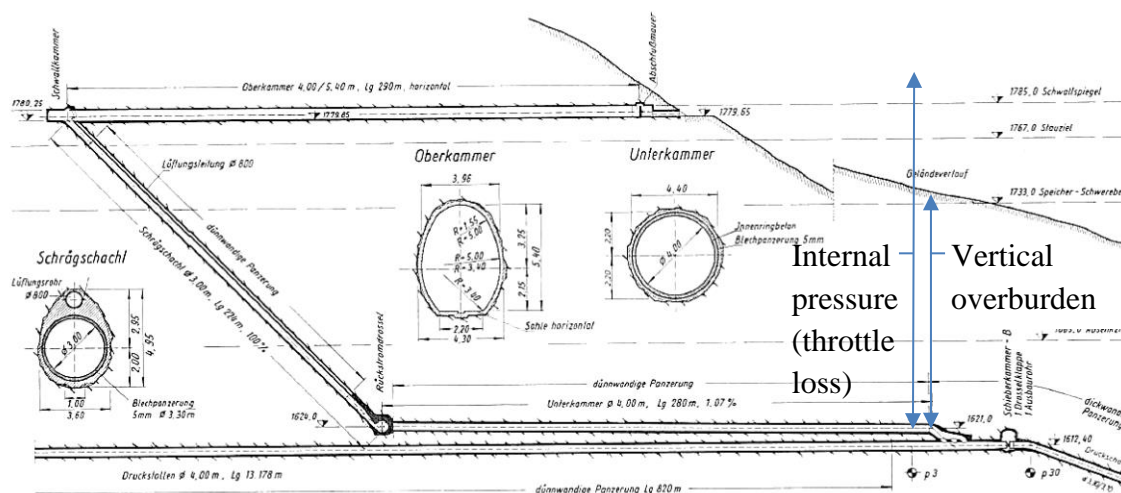


Figure 6-1: Chamber surge tank HPP *Kaunertal* (surge tank in operation from 1964 - 2016) [82]

At the *Hattelberg* surge tank for the *Malta Main Stage* high-head and pumped storage scheme the positioning demand was found to encounter insufficient rock properties, that could not be solved with grouting and demanded steel lining placing after first plant commissioning [160]. It can be noted that the positioning of surge tanks is mainly defined by other demands of the power waterway and the hydroelectric scheme itself. Applying free surface surge tanks at the transition of the headrace pressure tunnel and pressure shaft respectively pressure pipe penstock may likely show challenging geological situations that need to be handled. On the one hand surge tanks need to be close to the penstock to allow sufficient reaction time, but on the other hand this position is also close to the surface that has a higher likelihood of:

- Altered rock
- Less rock confinement
- Lower mountain water table
- Low minimum stress (σ_3)

RESULTS AND DISCUSSION

Tailwater surge tanks may have less of these positioning linked issues owing to usually higher overburden and thus higher stresses at these locations. The solution of an air cushion surge tank has the advantage of higher overburden and more freedom in choosing the best position, as proven in Norway. The advantage of the Norwegian approach is to analyse the rock quality by in-situ radial hydro jacking tests during the construction to choose the best cavern and surge tank position [161]. In contrast to that, the Austrian method utilises the radial-press to determine the in-situ rock stresses developed by *Seeber* [159]. Another method is the uniaxial plate jacking test [162]. Additionally, the Norwegian method requires flexible construction contracts to specifically decide onsite where to finally place the surge tank. This is a vital structural advantage of the unlined design approach [70], [148], [163], [164]. The unlined rock design concept in Norway also requires sand traps, that are placed after the surge tank before the transition to the pressure shaft. Thus, these sediment trapping devices are not affected by the amplified mass oscillation discharges. The sand traps are pressurized and thus, more complex than usual free surface flow sand traps [98]. Norwegian sand traps are usually designed to capture about 1 – 2 mm grains [97]. In case of the *Tonstad* high-head scheme and other schemes in Norway the unlined tunnels were excavated by drill and blast method, keeping parts of the material on the tunnel invert to allow having roads for construction works. This material was not removed, in order to enable quick commissioning. The tunnels were hydraulically designed to allow the grains to remain on the ground by sufficient low flow velocities. With an increased flexible operation demand these sediments are more likely to be transported [109].

Lining efforts may also be a need in association with air cushion chambers. For PSH *Obervermuntwerk II* a variant of an air cushion surge tank was studied, but not realised due to high expected lining efforts and concerns about air management for long filling times in case of maintenance [108]. For new large high-head and pumped storage schemes the large surge tanks are also increasingly demanding comprehensive lining or positioning strategies.

Due to high flow velocities and the static demands of Borda mouth-piece equipped throttles, those need be made of steel. High flow velocities on walls may result from restricted jet flow. For clean water *Momber* and *Kovacevic* (1993) [165] show that flow velocities have to be significantly above 100 m/s to damage a C20/25 concrete probe by erosion. This reference shows that for sufficiently clean water no abrasion on concrete walls can take place. The evaluation of fine sediment contents in high velocity throttle jets acting on concrete walls may demand for further research. In contrast to abrasion and erosion *Tzanakis et. al.* [166] quantify the cavitation problem that induces local peak velocities of up to 1000 m/s and local peak pressures of 1000 MPa due to micro jets created by the collapsing cavity.

6.3 Air Cushion Surge Tanks

Air cushion surge tanks respectively closed surge tanks are often utilised for water hammer protection in water transportation pipelines and water distribution systems, in combination with pumps [167]. Hydropower schemes demand for a specific stability criterion to safely apply air cushion surge tanks. Steel lined pressurized air chambers were used to mitigate water hammer effects in pipe systems and power waterways already in the early days of hydroelectric plants but insufficient stability properties caused problems. The stability aspect for closed surge tanks and a specific open-air surge tank case that has caused oscillation issues was the reason for the dissertation of *Thoma* (1910). *Thoma* derived the stability criterion for open air surge tanks. This work combined the pressure mitigation and stability aspect in one structure: The surge tank. The solution of the stability criterion of pressurized air chambers for hydropower plants was described by *Svee* (1972) [67]. The advantage of ACST systems are listed in the following:

- Possibility of a direct connection between the power cavern and the reservoir by reducing the excavation volumes of tunnelling
- Minimising the hydraulic losses due to minimised pressure tunnel length
- Economic benefits by minimised penstock length that mitigates the need for steel liner
- Due to lower kinetic energy in a short penstock the water hammer pressure can be reduced, or a higher flexibility can be obtained
- The short distance allows very fast response times of pressure waves, this increases the stability of the system
- No extra access to the surge tank for excavation and aeration is necessary
- No sudden penstock breaches due to breakage can occur, because the pressure shaft is significantly deeper covered in the mountain as conventional pressure shafts

The crucial demands for ACST design are:

- The ratio of maximum internal pressure to minimal rock-mass stress (σ_3) to avoid hydraulic fracturing
- Providing low permeability of the rock-mass to minimise air loss

Additional facilities demanded in order to provide proper operation of ACST:

- Air supply pipes and air release pipes
- Compressor station
- A small pump that slightly increases the pressure of headrace water to establish a water curtain for protection against air losses, if necessary [168]
- Possibly a valve to separate the ACST to the pressure tunnel to allow short interval inspection of the pressure tunnel [52]

In Norway ten air cushion chambers were built up to now, nine are successfully in operation, as shown in Table 6-1, also the latest air cushion chambers in China and Vietnam are listed. The Surge tank at *Taffjord K5* air cushion surge tank failed by rock overstress after the head was increased by heighting the water surface level of the upper reservoir. Until this system change the air cushion surge tank with very high internal pressure and water curtain was successfully in operation [169].

RESULTS AND DISCUSSION

Table 6-1: Air cushion chambers in Norway [164], China [170] and Vietnam [171]

HPP	year	Rock type	Total Volume [m ³]	Water Surface Area [m ²]	Air pressure [MPa]	Ratio head/overburden *)	Experience
<i>Driva (NOR)</i>	1973	Banded gneiss	6,600	111	4.2	0.5	No air leakage
<i>Jukla (NOR)</i>	1974	Granitic gneiss	6,200	129	2.4	0.7	No air leakage
<i>Oksla (NOR)</i>	1980	Granitic gneiss	18,100	235	4.4	1	Air leakage <5 Nm ³ /h
<i>Sima (NOR)</i>	1980	Granitic gneiss	10,500	173	4.8	1.1	Air leakage <2 Nm ³ /h
<i>Osa (NOR)</i>	1981	Gneissic granite	12,000	176	1.9	1.3	Intensive injections
<i>Kvilldal (NOR)</i>	1981	Migmatic gneiss	120,000	260-370	4,1	0.8	Pressurized water curtain
<i>Tafford⁺ (NOR)</i>	1981	Banded gneiss	2,000	130	7.8	1.8	Pressurized water curtain
<i>Brattset (NOR)</i>	1982	Phyllite	9,000	89	2.5	1.6	Air leakage 11 Nm ³ /h
<i>Ulset (NOR)</i>	1985	Mica gneiss	4,800	92	2.8	1.1	No air leakage
<i>Torpa (NOR)</i>	1989	Meta siltstone	14,000	95	4.4	2	Pressurized water curtain
<i>Dagangou (CHN)</i>	2000		4,396	78	3.8 - 4.2		Steel-lined
<i>Ziyili (CHN)</i>	2004		11,927	90	3.8 - 4.3		Water curtain
<i>Xiaotiandu (CHN)</i>	2006		22,540	138	3.35 - 4.35		Water curtain
<i>Upper Kon Tum (VNM)</i>	2018		14,900	1000	5.67-5.9		Steel lining
*) Ratio of maximum head in the ACST compared to overburden +) ACST failed by a hydraulic fracturing due to storage level upgrade							

Nm³/h ... Standard cubic meter per hour (under atmospheric pressure)

RESULTS AND DISCUSSION

The first functioning large air cushion chamber in a rock cavern was built 1973 for the *Driva* high-head hydropower plant. The power plant is located in a Norwegian valley with very steep topography. A classical solution would have had the drawbacks of a road to an open-air surge tank and high efforts for a slightly inclined tunnel construction. A direct pressure tunnel from the power cavern to the reservoir with an open-air surge tank would have needed an uneconomic large shaft with 900 m height, showing also issues with the stability demands [172]. Thus, it was found that an unlined rock chamber with 5000 m³ of compressed air was the most economical solution [68].

The installation of pressurized water curtains was found to be an appropriate technique to minimise air leakage. This technology is described by *Kjørholt and Broch* (1992) [168]. For the utilisation boreholes are drilled above the ACST and operated with pressurized water. The water is controlled by a pump and measurement facilities to allow a constant water pressure in the boreholes that is approximately 20 m w.c. above of the static pressure inside the ACST [169]. The water in the boreholes creates a counter pressure to leaking air, and instead of air leakage small amounts of water leak into the ACST. Well realised grout curtains may be installed before the water curtain. The technology has been successfully utilised in locations with unsatisfied high permeability of rock at the hydro power plants *Torpa* and *Kvilldal*. The ACST *Brattset* constructed in Phyllite rock has a sufficient low hydraulic conductivity of $9,8 \cdot 10^{-9}$ [m/s] [164]. This shows that ACST not necessarily have to be constructed in highest quality granite only. Steel lined ACST can also provide high resistance regarding air loss but higher costs have to be considered as if unlined.

The benefit for dimensioning the size of closed-surge tanks via the Svee stability criterion is the definition of the polytropic coefficient. This can be either 1.0 [-] for isothermal or 1.4 [-] for adiabatic behaviour. *Vereide et.al. 2015* [71] describe measurements at power plants in Norway to capture the polytropic coefficient. From that work it can be concluded, that for slow reaction of the closed surge tank a sufficient thermal energy exchange with the rock is observed and thus shows an isotropic behaviour. In case of quick loading of the pressurized air and heating process an adiabatic behaviour is measured and can be applied in the simulations. The mass oscillations can be seen as a quick loading event that produces heat due to compression but insufficient heat exchange keeps it to behave as an adiabatic system. The findings of *Vereide et.al.* show, that for quick compression of air cushion chambers, as it happens in hydropower plants in case of mass oscillation and water hammer protection the polytropic coefficient of 1.4 [-] is sufficient. For slow compression, if two separate hydraulic reservoirs are connected by valve opening an isothermal behaviour has to be applied [71]. For closed surge tanks, protecting pumping stations for fresh water systems no stability criterion has to be provided. An extensive study of the polytropic behaviour in closed surge tanks and potential optimisations in sizing is provided by *Van der Zwan et.al. (2015)* [173].

6.3.1 Existing Air Cushion Chambers for Alpine Adaptions

In the Alpine region no air cushion chamber exists yet in the high-pressure part of the power plant. Two exist in tailrace systems at *Kopswerk II* PSH and at the *Albulawerk*, HPP. Both power stations are equipped with a Pelton turbine. At the *Albulawerk* in Sils, Switzerland a heightening of the tailrace reservoir would have submerged the Pelton turbine. This was prevented by applying pressurized air into the open-air outflow system of the Pelton turbine [81]. Also, at *Tafford* power plant in Norway air cushions are utilised to operate Pelton turbines independently from the tailwater level and even below [174]. This feature allows to place Pelton turbines as deep as possible to use the full head. Thus, an up-surge in the tailrace surge tank is possible by pressure increase above the axis of the Pelton wheel without interrupting the operation capability.

At the pumped storage power plant *Kopswerk II* a tailrace ACST was installed to allow a deeper positioning of the Pelton turbine in order to use the additional head when the lower reservoir is at drawdown level. The production equipment consists of a vertical ternary machinery arrangement with a Pelton turbine, a motor generator and a pump. The pressurized system also allows a compact and short vertical distance between turbine and pump. This arrangement enables a hydraulic short circuit and thus a completely free regulation of the pumping mode operations, in order to provide negative regulation for the grid. The shifting time between 100 % turbine mode to 100 % pump mode is only 20 s [118]. Since the commissioning of this power plant, the high flexibility of the machines was proven due to their advantageous ability to balance the grid volatility [175]. The pressurized air cushion in the tailrace tunnels of the Pelton wheels are equipped with steel liners in the air exposed parts of the tunnel shape (wall and crown).

At the upgraded power plant *Dießbach*, Austria several industrial pumps were placed to possibly pump water up to an existing reservoir. To capture the transients in case of pump trip closed-surge tanks are used [28].

6.3.2 Proposed Possible Arrangement of Alpine ACST

This paragraph discusses how a possible use of alpine ACST may look like. Alpine geology differs in some important points from Norwegian mountain boundary conditions. Norwegian rock-mass consists mainly of high-quality gneisses and granites. This fact enables a very economic tunnelling excavation progress. Additionally, very bad quality rock may appear in fault zones and shear zones in-between good rock sections. A major advantage in Norway is the glacial pre-stressing that increases significantly the available horizontal stress in many regions. Especially the position of ACST's and unlined high-pressure tunnels and shafts take advantage of this fact, because the facilities can be placed closer towards the mountain surface. This favourable positioning is possible due to tectonically horizontal pre-stresses of the Caledonian mountain range [176]. Due to a general lack of pre-stressing in Alpine regions it is necessary to place the facilities deeper underground. Following this, the access tunnels to the power caverns are longer. Sophisticated rock evaluation regarding stress analysis and jacking tests are crucial investigations.

RESULTS AND DISCUSSION

Figure 6-2 shows the comparison between a classical Alpine high-head pressurized water conveyance system to a Norwegian pressurized system with an air cushion chamber and the potential advantage of a shorter connection.

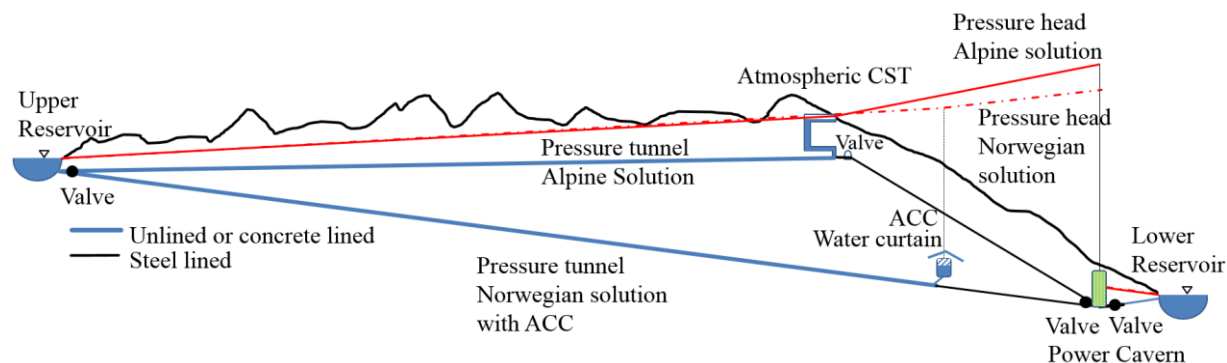


Figure 6-2: General comparison of longitudinal section of pressurized water conveyance system for a classic Alpine solution with and open-air surge tank and a Norwegian solution with an air cushion surge tank

Figure 6-3 shows the comparison between a classic Alpine high-head pressurized water conveyance system to an adapted Alpine system with an air cushion surge tank. In difference to Figure 6-2 the air cushion chamber has to be situated to locations that offer a sufficient overburden compared to maximum head inside the pressurized air chamber. Alpine regions do not show such favourable horizontal pre-stresses as the Caledonian mountain range.

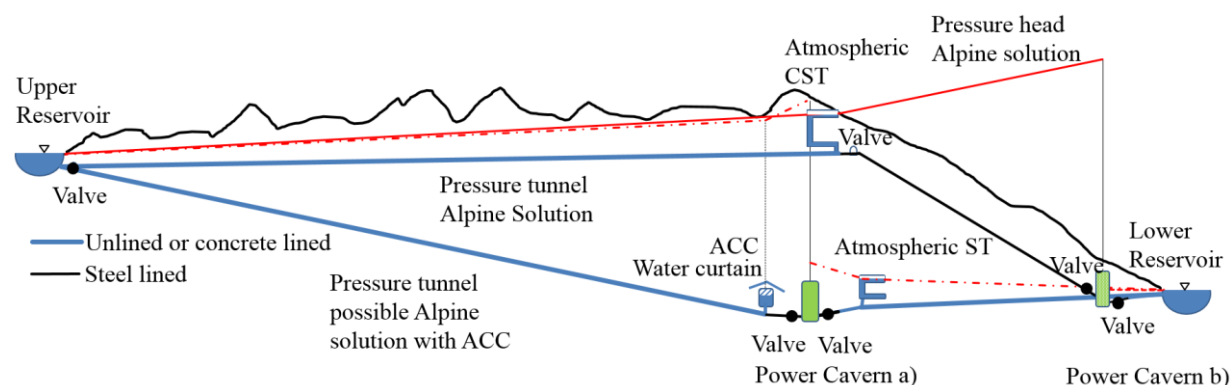


Figure 6-3: General comparison of longitudinal section of pressurized water conveyance system regarding a classical Alpine solution and an adapted solution with an air cushion chamber for Alpine regions (Richter [177], modified)

For the *Obervermuntwerk II* PSH an ACST was initially investigated to serve as surge tank on the headrace side. The quick response of ACST to the hydraulic system would have been beneficial (starting and stopping both machines simultaneously within 30 seconds), but high costs of sealing with steel and also high time efforts regarding filling of the chamber with pressurized air were found to have higher negative impact on costs and maintenance interruption [108].

6.3.3 Challenges with Air Cushion Surge Tanks

The application of air cushion chambers may be well evaluated and be applied to utilise the advantages of low water inertia and construction benefits. But one has to consider the aspects to be handled such as:

- Filling times of pressurized air for very large air cushion chambers such as the one in *Kvilldal* with about 80,000 m³ at about 40 bar
- Careful emptying of pressurized air
- Additional installations for air management to counterbalance air losses
- Measures for air leakage protection
- Risk of blow-outs

The air is under high pressure and must be kept inside, in case of maintenance a quick release and refilling should be possible. However, until now this may be very time-consuming. Improvements, such as placing a closing device to allow inspections of the pressure shaft without emptying the ACST and high-pressure pre-grouting in early excavation stage are proposed by *Ødegaard* and *Vereide* (2018) [52]. *Rathe*, (1975) describes the practical design and reasons of the first ACST at *Driva* HPP in Norway [68]. *Goodall* (1988) describes 20 years of experience with air cushion chambers in Norway [178].

6.4 Surge Tank Upgrade

Hydropower plants provide renewable primary energy and are constructed to operate for a very long period of time. They utilise a natural monopoly; no second plant can use the same energy potential in the same catchment. During the lifetime, power plants may face changed demands that may affect several boundary conditions for their operation. Such changes may have hydrological, economic or operational reasons. Operational adaptations are linked to changing demands of the power market. In Austria the concession of water rights is usually given for 90 years. For re-commissioning, power plants usually receive a comprehensive rehabilitation. In many cases power plants are requested to allow higher discharges for the operation, either machines need to be upgraded, higher inflow need to be possible or the power market requests for more flexible operation. For high-head schemes or pumped storage power plants the challenges are to adapt the upgrades in a proper manner, especially when long power waterways are affected. Pressure tunnels demand for high efforts if rehabilitated or upgraded. Due to high costs and time efforts such demands lead to new tunnels. However, surge tanks may be upgraded more efficiently as if tunnels are expanded, since construction works can be done separately. This results in a shorter interruption of the operation that is needed to construct the connection from an expanded surge tank to the power waterway.

Further examples of upgrades of existing power plants by adapting the surge tank are realised in the power plant *FMHL+*, the upgrade of a high-head scheme to a flexible pumped storage scheme in Switzerland [179]. Also, the refurbishment of the hydropower scheme *Gondo* in Switzerland was improved by surge tank upgrade and elaborated throttle design studies [180].

6.4.1 Case Study of Surge Tank Upgrade

As an example of an ongoing surge tank upgrade investigation at *Tonstad* HPP the research project *Flexible Sand Traps (FlekS)* is conducted with the contribution of the author [98], [109], [181]. *Tonstad* HPP is a 960 MW high-head scheme in the south of Norway producing around 3.8 TWh/a. The first operational stage was commissioned in 1968 (320 MW), the second in 1971 (in total 640 MW) and the third in 1982 (in total 960 MW). The power plant has a nominal discharge of 250 m³/s and a nominal head of 430 m. It consists of 5 turbines, three parallel penstocks, three parallel surge tanks and three parallel sand traps after the surge tanks. The original headrace tunnel was kept in the original design. The upgrade in 1982 was successful regarding the increase of the power output for the power plant. Due to higher friction losses in the tunnel the minimum drawn down level in the upper reservoirs was increased. Within the five decades of operation also the power markets have changed. The increase of power interconnections in the vicinity of the *Tonstad* HPP and the Norwegian electricity grid in general to the continental European grid allow significant trade of electricity, and offers flexibility options as well as flexibility demands. The grid frequency has worsened by the associated increased connection to fluctuating renewable sources and the shutdown of thermal units. Thus, increasing flexibility of power and frequency regulation is needed for the Nordic grid in order to restore the grid frequency to 50 Hz [182]. Especially the integration of vast amounts of renewable sources have changed the demands and boundary conditions of the electrical system from a submission oriented to a yield-oriented market situation since renewable sources are not projectable. In general, it has increased the demand of flexible operation of hydropower plants. In contrast to Austrian surge tanks most surge tanks in the

RESULTS AND DISCUSSION

world, also in Norway were not designed for resonance load-cases of the mass oscillation as discussed in chapter 3.7. Therefore, the lower chambers were originally designed as start-up chambers but not as chambers to capture unfavourable reloading after unloading events. Even though resonance load-cases may occur very seldom, any damage or even potential damage is not desirable. Due to the change of operation and an increased flexibility unfavourable resonance events may become more likely. At *Tonstad* power plant, free surface flow events in the pressure tunnel were documented with undesirable consequences [109]. A countermeasure that is in the meantime installed, is a digital twin with control feedback loop of the power plant scheme [183]. Due to the unlined power waterway and the gravel left on the invert, sand traps were constructed right after the surge tank shafts. These sand traps are an important principle of the Norwegian hydropower plant design. In combination with the installation of new turbine governors the power plant has been operated more flexible, but resulted in some problems due to higher transients and amplified mass oscillations in the surge tanks. Gravel was reported to be flushed to the turbines. In addition, high pressure on the downstream side of the reservoir intake gates was observed and caused uncertainties regarding the structural safety of the gates. These problems have resulted in restrictions on operation and economical loss due to repair and reduced power production revenue [109]. To minimize the danger of free surface flow in the sand traps a predictive control system was installed in 2014. This included a real-time simulation of the transients of the power plant with the software *LVTrans* [132]. The simulation predicts new correct set-points for the governor and other adjustments that are necessary to stay within given limits of water levels in the surge tank [182]. Figure 6-4 shows the overview of the surge tank situation and geometry. The open-air chamber surge tanks were constructed fully unlined except the gate section. The sand traps are integrated in the power waterway after the surge tanks. The sand traps are operated fully pressurized. The flow section of one sand trap has a standard cross-section of about 100 m², to settle sand and gravel particles by decreased flow velocity. Sand trap no. 1 and no. 2 were investigated by comprehensive hydraulic model tests in Trondheim in 1967 [184]. However, sand trap no. 3 was attached without additional model testing. Basic principles of the original sand traps were applied, but not all in detail. The lower chamber no. 3 was directly included in the power waterway and also the access tunnel was attached some 30 m apart from the rack. Sand trap no. 3 was 3D laser scanned. These results are included in Figure 6-4 and show the unlined rock pattern [185].

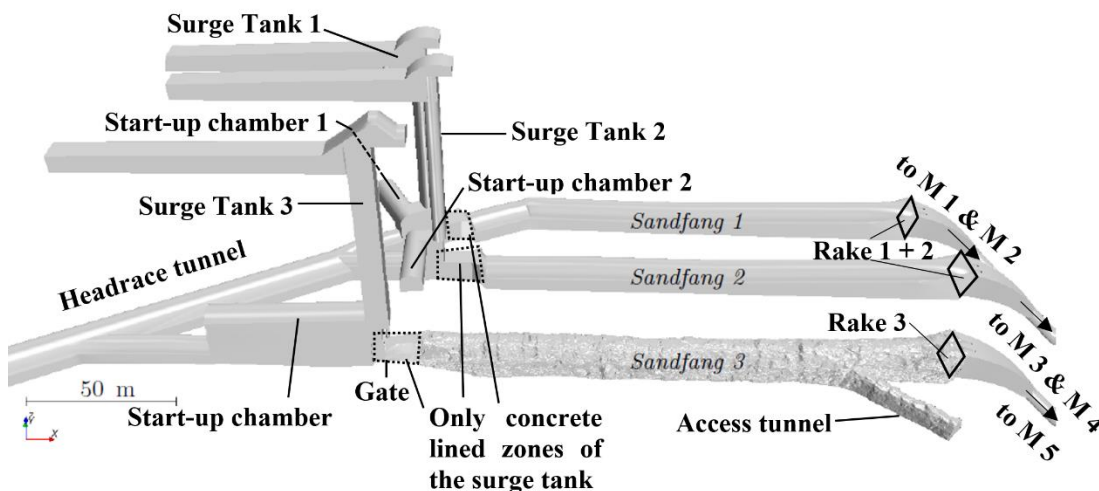


Figure 6-4: Layout of the *Tonstad* surge tank (figure from [186], modified)

RESULTS AND DISCUSSION

The following measures have been undertaken by interdisciplinary approaches to investigate the surge tank no. 3 and to apply the aspects for research activities (selection by the awareness of the author):

A) Control devices improvements

- Installing brook intake measurements
- Installing new governors with set point improvements [182]
- Applying a digital twin system to allow predictive control and improve operational aspects [183]

B) Hydraulic investigations

- Ph.D. thesis and several master theses for investigating the flow behaviour of the particular sand trap [186], [187]
- 3D-laser scan of the sand trap no. 3 [185]
- Master thesis at NTNU to investigate surge tank devices such as throttles [188]
- Investigating and improving the sand grain trapping with 3D-numerical particle tracking simulation and introducing flow calming devices in the diffuser [98]
- Upgrade investigations of the surge tank by an additional lower chamber [110]
- Construction of a physical model at NTNU to test diffuser variants and improve sand trap functionality (ongoing research)

6.4.2 Attached Additional Chamber

The challenge of upgrading a surge tank of a power plant during operation is that operational interruptions are the most expensive cost factor. Thus, it is very beneficial to construct new chambers and connect those in a short power production interruption. In case of the *Tonstad* surge tank system three chambers are available that can be separately closed by a gate device at the main riser. The proposed variant by the author is to attach a single large lower chamber that provides water for all machines and all separate surge tanks. Figure 6-5 shows a possible constructive solution studied and drawn by *Sterner* (2018) [110] to upgrade the complex surge tank system by adding a single additional lower chamber that serves also for the other surge tanks that are hydraulically connected. The curved design of the attached chamber is associated with the need for sufficient overburden that are given at the proposed location.

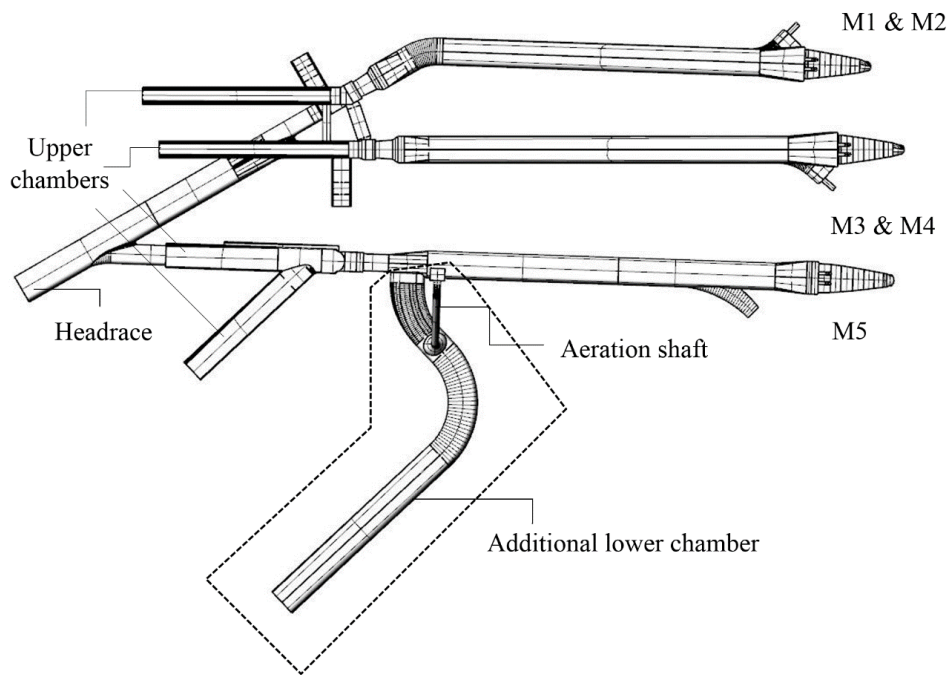


Figure 6-5: Tonstad surge tank with proposed attached additional lower chamber, ground view (Stern [110], modified)

For the upgrade investigation, no additional upper chamber is needed, since the existing ones can capture the proposed upgrade of 25 % discharge for the emergency shut-down. Figure 6-6 depicts the front view of the proposed principal solution with the attached lower chamber on the left and the three existing surge tanks on the right. An aeration shaft of the lower chamber is necessary; it connects the crown of the extension with a small chamber near the access gallery to the upper chamber.

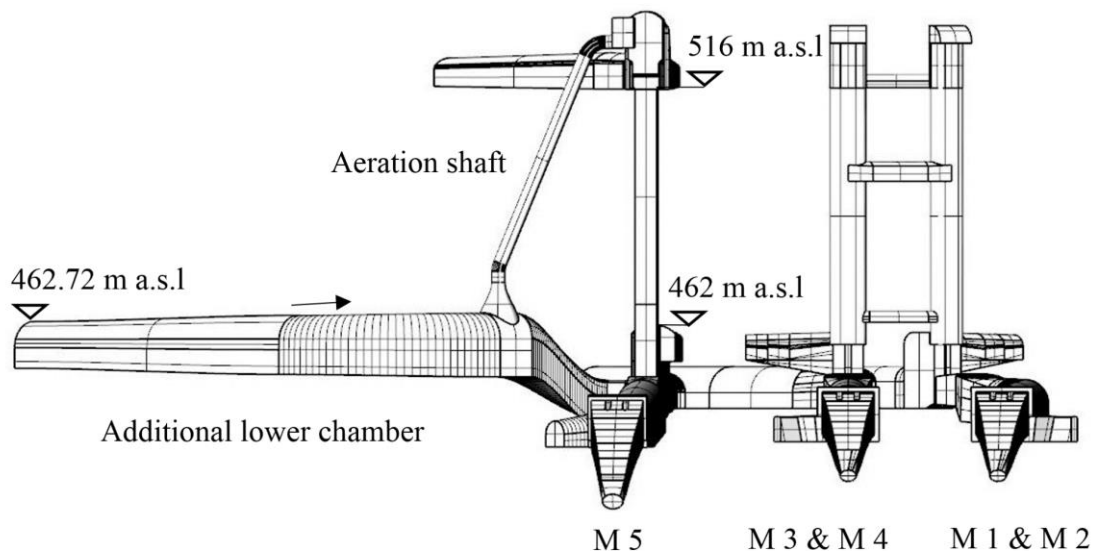


Figure 6-6: Layout of Tonstad surge tank with proposed attached additional lower chamber, front view (Stern [110], modified)

The investigation of Stern (2018) [110] show the operability of the proposal by the author of semi-closed surge tanks as a possibility for upgrade of surge tanks and as an additional feature for new large chamber surge tanks to minimise the volume demand (see chapter 6.5).

6.5 Semi-Air Cushion Surge Tank Proposal

The author proposes to utilise semi-air cushion respectively semi-closed surge tanks by introducing crown throttles in lower chambers. This construction traps air by a controlled manner at the crown and delays the filling by a small air pipe. This pressure rise by the air compression at the crown can be noted as an additional feature to improve the differential effect. The construction is semi-closed since the air is released and not fully trapped and compressed.

The investigations for the *Tonstad* surge tank upgrade [110] have revealed in principal the possibility of a semi-closed surge tank as a new type of surge tank.

Surge tanks with slightly inclined chambers face the situation of entrapped air in the lower chamber at the filling process during a mass oscillation event due to delayed air escape. Figure 6-7 visualises this aspect in a 3D two-phase simulation (air and water) for the 8-loop chamber surge tank of the *Atdorf* PSH. Since the air requires volume, the water level in the main shaft rises earlier. Thus, the associated pressure at the surge tank base at this point is higher than generated in a 1D-numerical simulation. For the prototype this behaviour is beneficial since it increases the hydraulic safety of the surge tank design. However, this correlation exemplarily visualises the idea behind the semi-air cushion surge tank. In contrast to the observed air compression at the *Atdorf* surge tank, semi-air cushion surge tanks release the air more controlled and can trap significantly more air to amplify the effect.

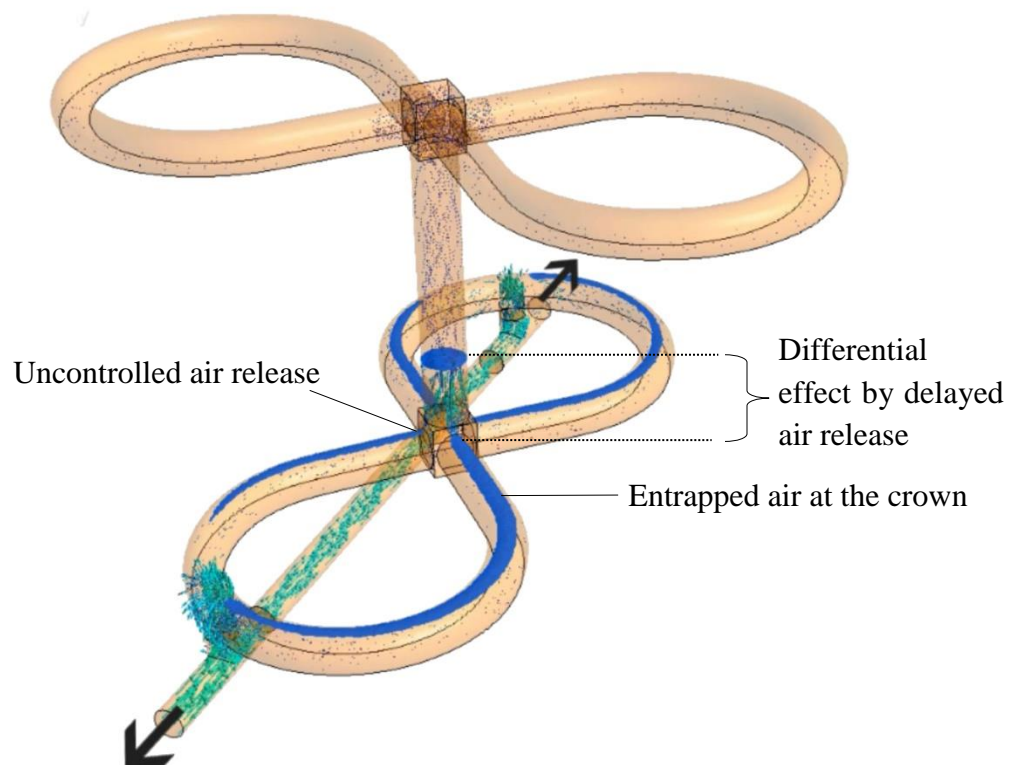


Figure 6-7: 3D-numerical study of up-surge in 8-loop shape surge tank for the *Atdorf* PSH project

Nicolet et. al. (2018) [189] report and measure the fluctuating behaviour of air release in chambers. This effect indeed leads to local pressure peaks, but is not measured at the surge tank base. Thus, it can be concluded that the local pressure surges are dissipated.

RESULTS AND DISCUSSION

Figure 6-8 shows a schematic longitudinal section of the proposal for a semi-air cushion surge tank. A crown throttle is introduced; it separates a significant amount of volume at the crown section of the chamber. In case of an up-surge the trapped air behind the throttle compresses and is forced through a small pipe that acts as a throttle and prevents the fast filling of the crown section with water. In the meantime, the shaft fills with water and represents the pressure increase on the system. The volume behind the crown throttle is slowly replaced by air. The compressed air is forced out through the de-aeration pipe. Thus, the compressed air section acts as it would be an upper chamber due to the increased pressure equivalent to the water level in the upper chamber of the surge tank.

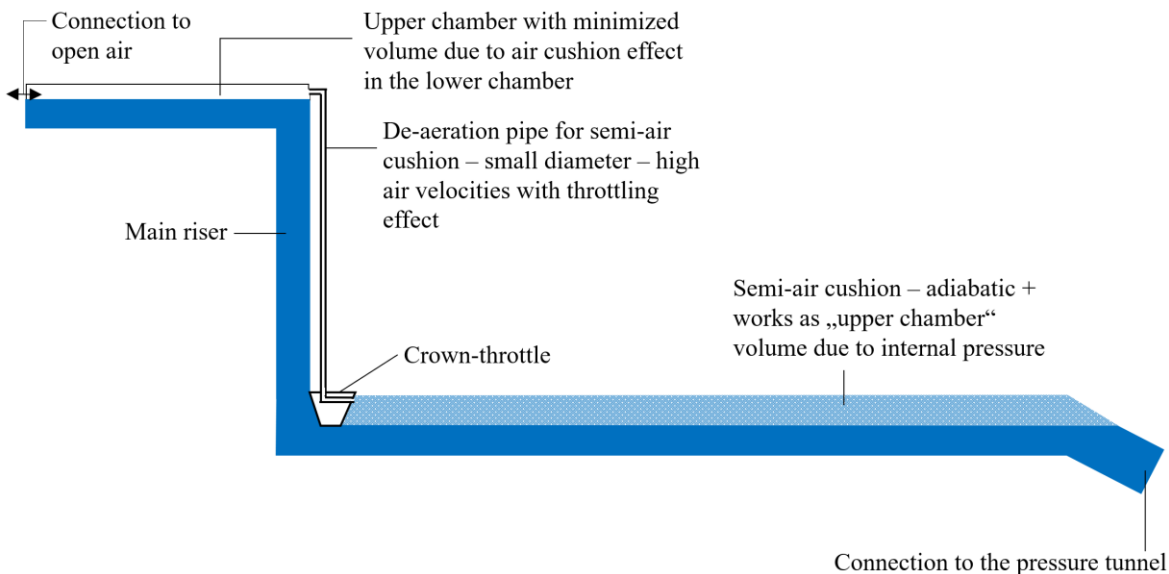


Figure 6-8: Layout of the semi-closed surge tank design with crown throttle

Figure 6-9 shows the suggested principle of a surge tank extension for *Tonstad* power plant with a minimised shaft and the absence of an upper chamber for the surge tank extension, since the stability criterion and the demanded water volume in case of emergency shut-down are given by the existing surge tank system.

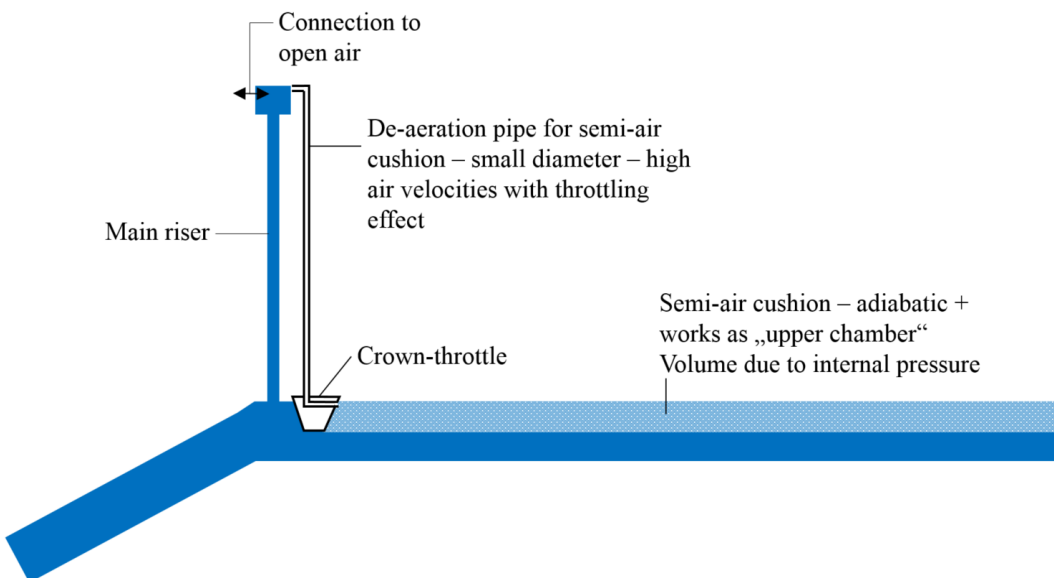


Figure 6-9: Layout of a proposed *Tonstad* surge tank expansion with proposed attached additional lower chamber and suggested development of semi-air cushion, schematic longitudinal section

RESULTS AND DISCUSSION

Figure 6-10 shows the principle of the semi-closed surge tank system in which the lower chamber is throttled by a hydraulic throttle at the bottom and an air throttle at the crown that restricts the air discharge by a small diameter. The surge tank is in principle a differential surge tank with a quick riser and a storage shaft. Waterfalls only occur from the upper chamber into the storage shaft. The quick riser provides sufficiently low water inertia for water hammer reflection. The additional value of the semi-air cushion is that in the filling phase the lower chamber is pressurizing at an early stage. This creates an early counter pressure to dampen the mass oscillation, but also provides water to replace the released air. This effect mitigates the upper chamber volume demand. A secondary effect is that also a lower pressure level at down-surge event is possible. This mitigates the lower chamber volume demand due to the throttled differential riser.

Semi-closed surge tanks are proposed for upgrades of existing systems as explained in 6.4.2 as well as for new schemes with the need of fast water hammer reaction as demanded for pump turbines at full pump trip events and full load rejections.

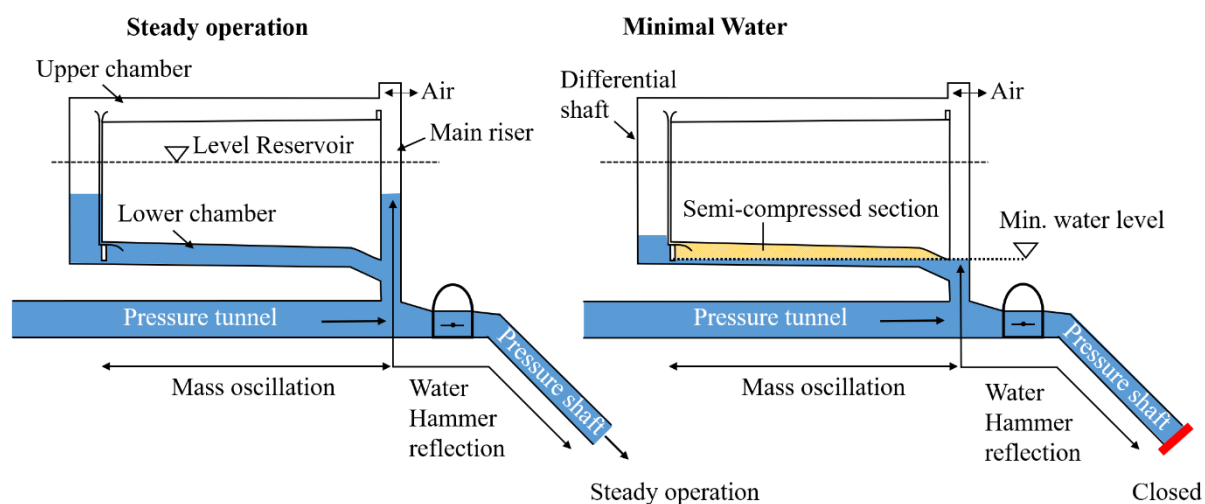


Figure 6-10: Layout of the semi-closed surge tank design for steady operation and at state of minimal water level

Sterner (2018) [110] investigated with the supervision of the author the behaviour of the semi-air cushion on a proposed extension of the *Tonstad* surge tank. The investigations were done to find a possible aeration and de-aeration structure in combination with a crown throttle. Figure 6-11 shows the *Tonstad* surge tank with expansion chamber at the time point of down-surge of the surge tank with extended semi-closed surge tank. The water level in the lower chamber is shown for the region in front of the crown throttle (unthrottled air pipe) and behind the crown throttle (throttled air pipe). The significant water volume behind the throttle is the benefit of the differential effect of the compressed air section. The small de-aeration pipe provides a throttling effect during the filling process with increased counter pressure acting on the whole headrace system. This effect increases the effectiveness of the chamber surge tank in terms of efficient volume utilisation.

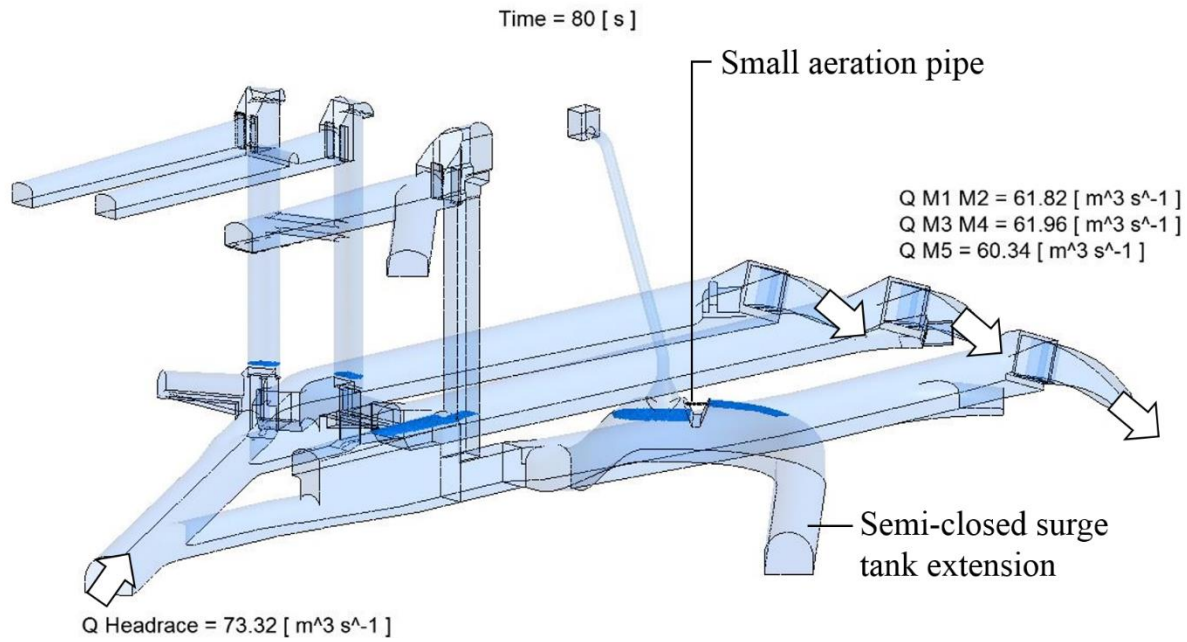


Figure 6-11: Layout of *Tonstad* surge tank with proposed attached additional lower chamber and suggested development of semi-air cushion at time point of down-surge – no separate air pipe (*Sterner* [110], modified).

Figure 6-12 shows the time point of up-surge in the proposed surge tank extension with a semi-closed chamber. The pressurized air is released in mixture with water of the aeration shaft. The simulations showed that separate aeration pipes of the pressurized section and the atmospheric section were needed. In the case of the pilot study with the extension, no additional upper chamber was required, since a discharge upgrade can be captured by existing upper chambers in combination with the semi-air cushion section that also acts as an upper chamber. The high velocities in the aeration shaft indicate rough air release conditions and this is not desired. Therefore, a separate air release pipe is proposed for the general layout.

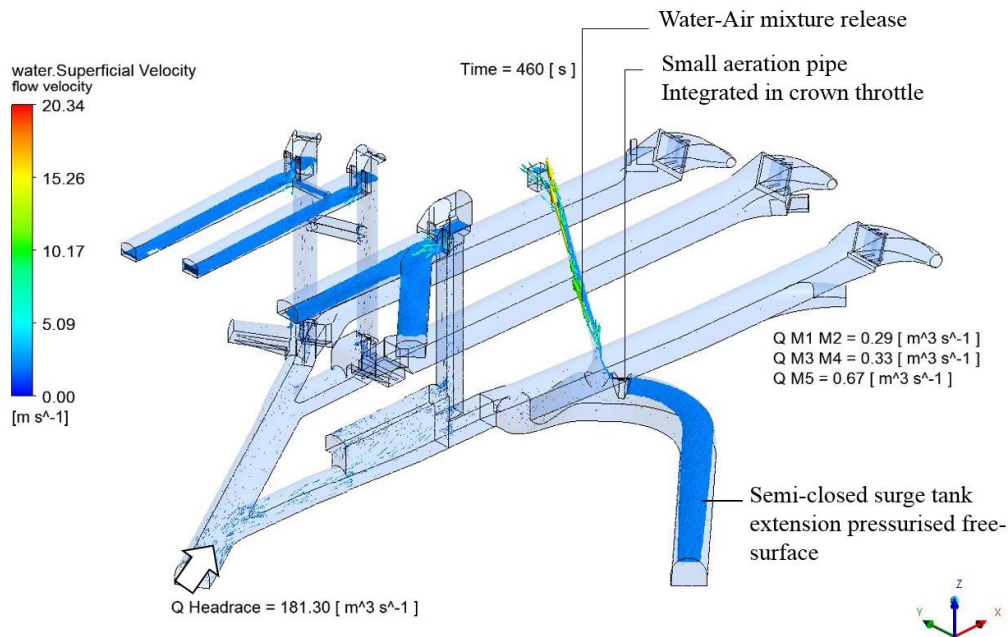


Figure 6-12: Layout of *Tonstad* surge tank with proposed attached additional lower chamber and proposed development of semi-air cushion at time point of up-surge, water-air mixture → Separate air shaft suggested (*Sterner* [110], modified)

RESULTS AND DISCUSSION

Figure 6-13 visualises the semi-air cushion with separate water shaft and air release shaft. In contrast to Figure 6-12 it was found that a much smoother water rise is possible in a small pipe while the pressurized air is released in a separate pipe that also acts as the throttling device. Figure 6-13 shows the utilisation of the lower chamber in the functionality of the upper chamber due to the pressurized air cushion that is replaced by the filling water. The pressurized air creates a head difference that can be tuned by the pipe diameter design.

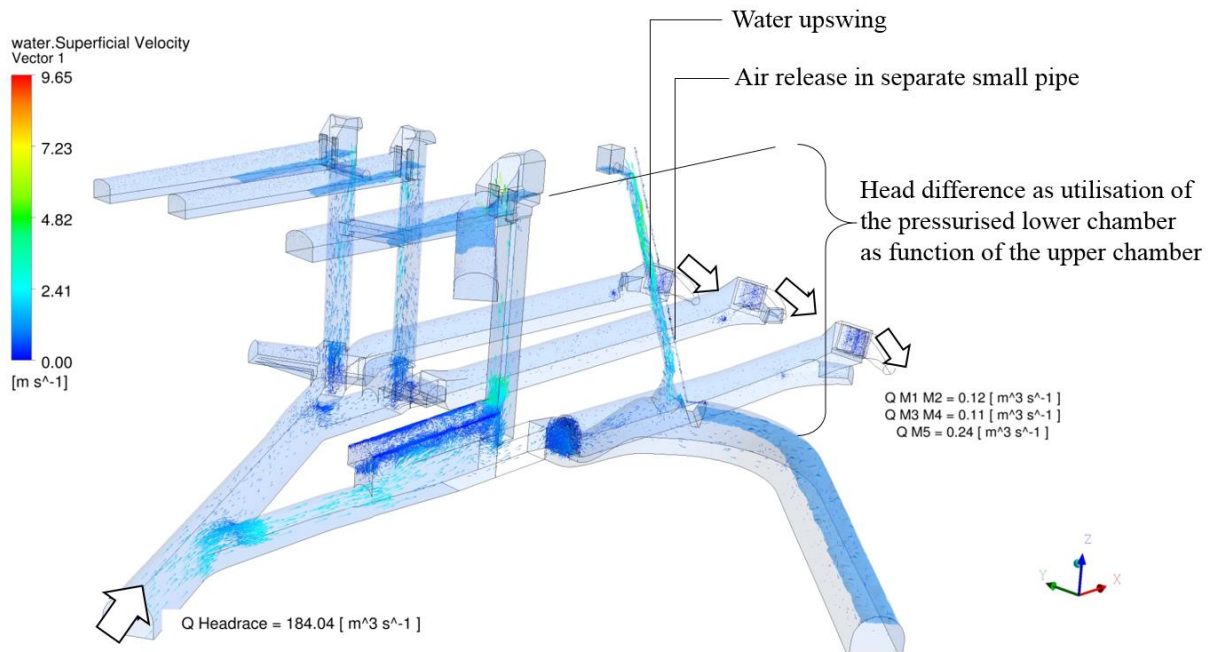


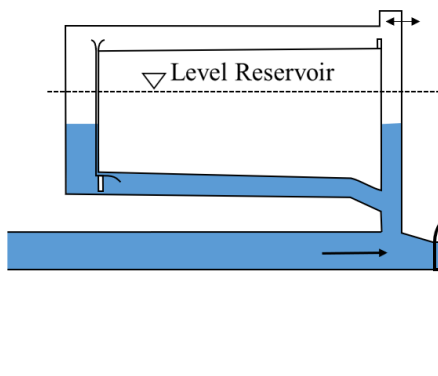
Figure 6-13: Layout of *Tonstad* surge tank with proposed attached additional lower chamber and suggested development of semi-air cushion at time point of up-surge with a separate air pipe (*Sterner* [110], modified)

6.5.1 General Proposal of Semi-Closed Surge Tanks

This chapter describes a general approach of utilising semi-closed surge tanks. Figure 6-14 to Figure 6-27 visualise schematically the proposed functionality of the semi-closed surge tank from steady operation followed by unloading and reloading events in resonance and subsequent emergency shut-down.

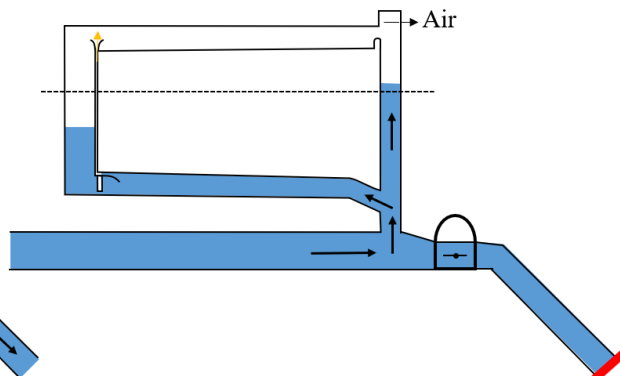
Sequence (1) to (4) show the surge tank behaviour from steady operation to back flow situation after unloading.

1) Steady-state operation



Steady operation

2) Stop of the machine discharge →
Up-surge in small riser



Closed

Figure 6-14: Steady-state operation as starting condition, with water level in the surge tank below the reservoir level

Figure 6-15: Unloading event of the turbines indicated as closed pressure shaft

3) Highest water level for 1st up-surge
→ Start of backswing – discharge = 0
at the time increment

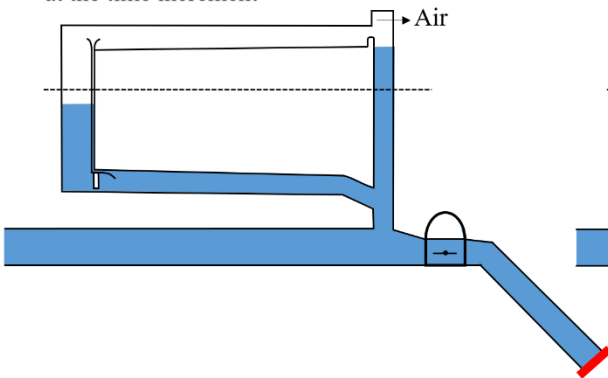


Figure 6-16: Up-surge due to water mass oscillation → inflow surge tank

4) Utilising of additional ΔH to already significant differential effect before reaching lower chamber

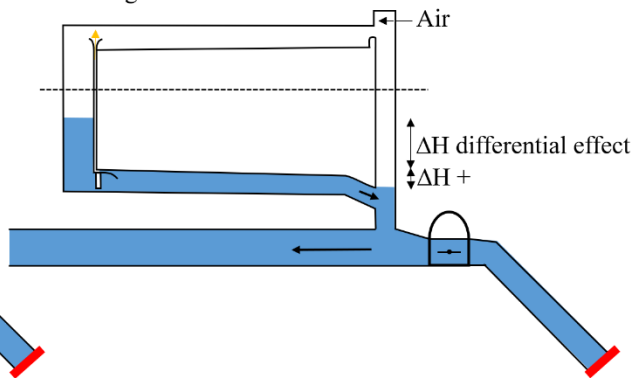
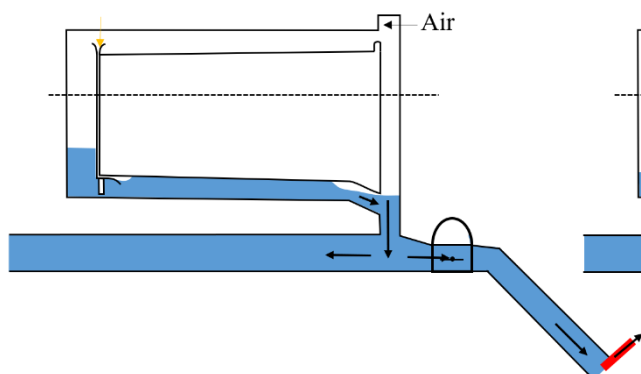


Figure 6-17: Subsequent backflow triggered by previous up-surge → outflow surge tank

RESULTS AND DISCUSSION

Sequence (5) to (8) visualise the reloading at unfavourable back flow to subsequent unloading.

5) Reloading - Start of discharge
lower chamber air inflow



6) Reaching low level in lower chamber

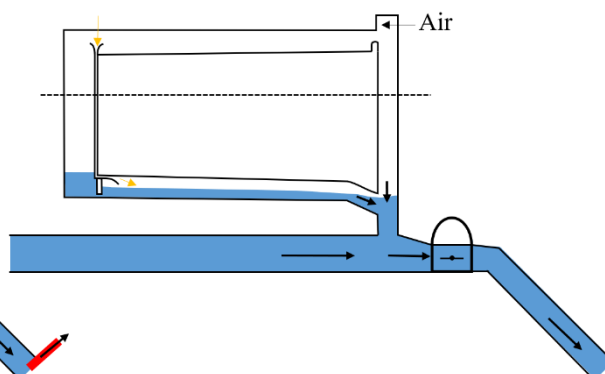


Figure 6-18: Amplified down-surge related to reloading of machines → lower chamber feeds the discharge, aeration shaft prevents cavitation and allows efficient outflow of the lower chamber, throttled outflow of the differential riser acts as decoupled reservoir for efficient surge tank behaviour to accelerate the water mass in the pressure tunnel

Figure 6-19: Outflow of surge tank allows acceleration of the pressure tunnel

7) Unloading in resonance → up-surge

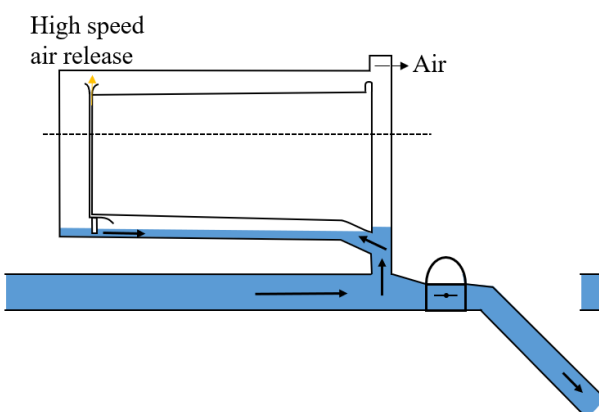


Figure 6-20: Starting of backflow after minimum water level in surge tank

8) Up-surge in small riser
Start compressing of the semi-air cushion

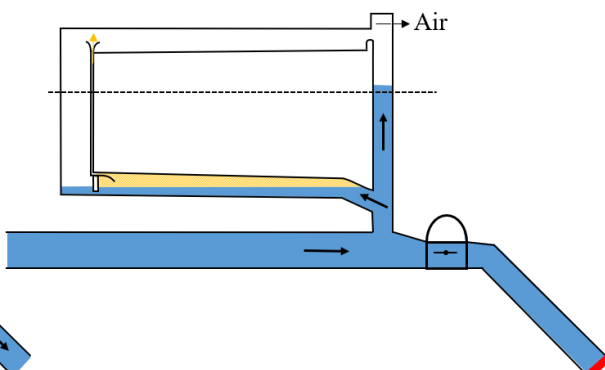


Figure 6-21: Unloading of turbines with activation of air cushion in lower chamber by throttled air release in small pipe

RESULTS AND DISCUSSION

Sequence (9) to (12) visualise the up-surge due to unloading in resonance and subsequent reloading.

9) Start of overflow in the upper chamber

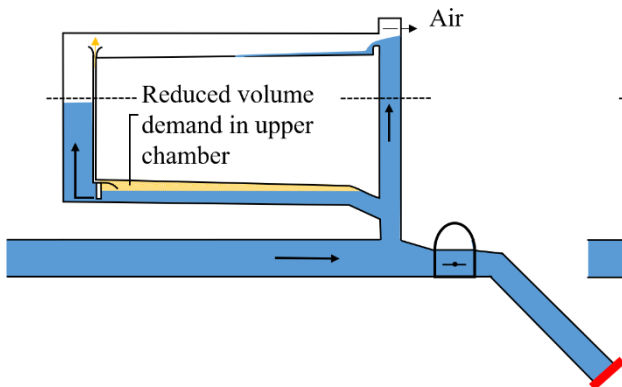


Figure 6-22: Up-surge and overflow event of the small riser, effect of delayed air release in lower chamber comparable to upper chamber filling

10) Maximum filling for this generic load case, time point of no discharge → water fall and air intrusion

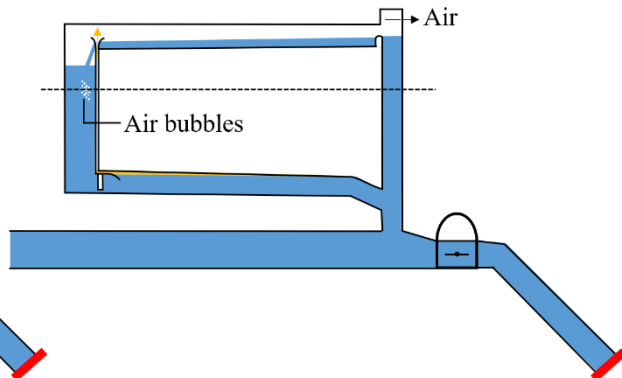


Figure 6-23: Filling of the surge tank facility reaching high filling and providing sufficient safety volume

11) Reloading in resonance - two direction outflow of the surge tank

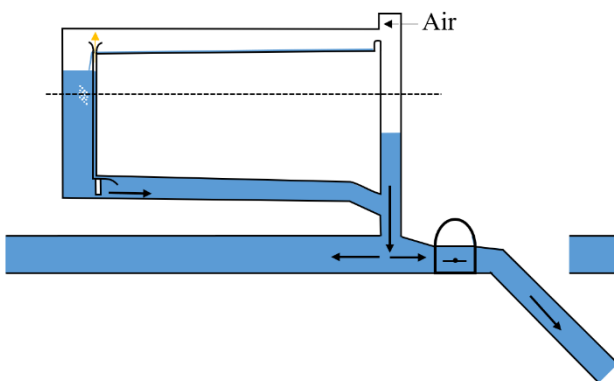


Figure 6-24: Reloading of the machines in generation mode, quick reaction of the small riser mitigating water hammer and supplying water

12) Start of emptying lower chamber – de aeration of bubbles – sufficient water in the storage riser

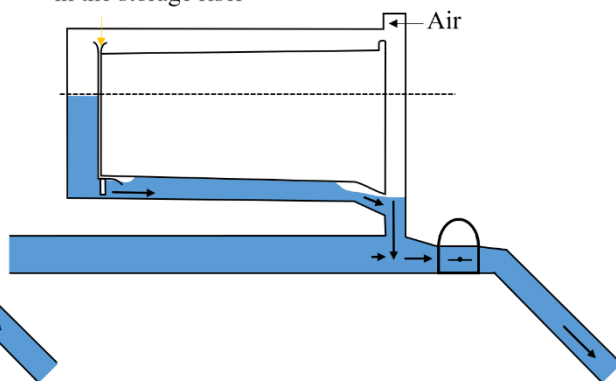


Figure 6-25: Quick creation of air pockets in the lower chamber from both sides

RESULTS AND DISCUSSION

Sequence (13) to (14) show the most unfavourable lowest water level in the lower chamber after resonance event and the subsequent refilling with creation of the partial air cushion in the surge tank.

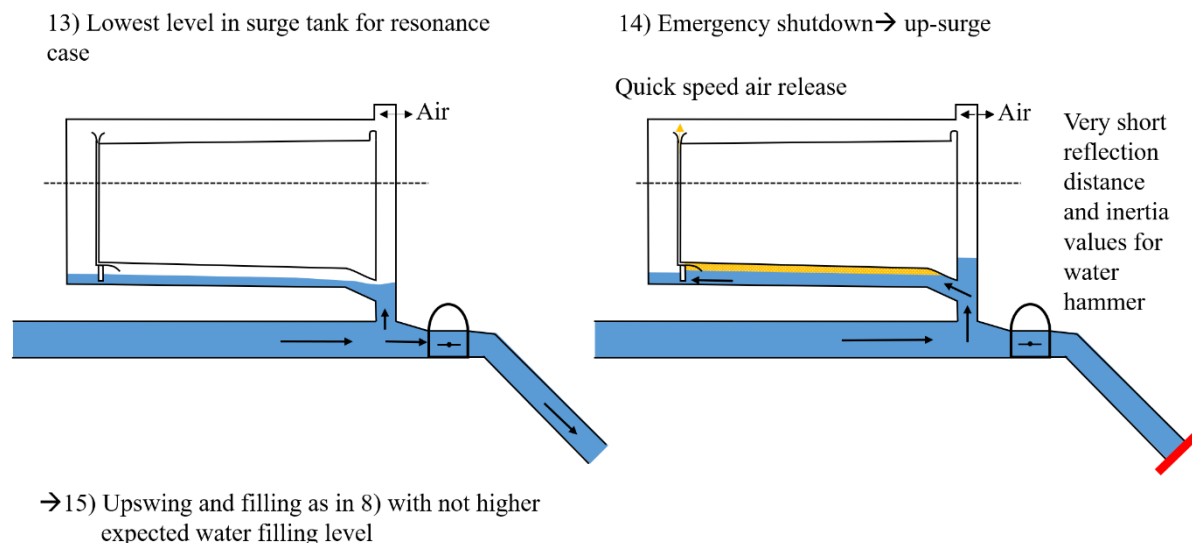


Figure 6-26: Lowest level in lower chamber with safety volume and minimum free surface flow to avoid hydraulic jump and air intrusion

Figure 6-27: Backflow and subsequent up-surge at emergency shut down in mass oscillation resonance

For prototype applications, semi-closed surge tanks request further investigations. The air ventilation system needs to be proven for thermodynamic states to avoid freezing due to high-pressure gradients. A high potential for application may be upgrades of existing surge tanks by implementing a crown throttle and a throttled aeration shaft to improve the capability for resonance load-cases. Also, large surge tanks with large chambers may be significantly improved by implementing crown throttles to create a semi-closed surge tank behaviour.

6.5.2 Design Process of Semi-Closed Surge Tanks

The following points express the proposed path to evaluate the possibility of implementing semi-air cushion chambers for specific sites:

- Preliminary design; 1D-numerical simulations.
- Detailed design of 3D flow behaviour; two-phase 3D-numerical simulations to evaluate the water and the air behaviour. The compression of air leads to significant temperature gradients that need to be studied.
- Final physical hydraulic check; physical small-scale model test with two factors scaling (Froude and compressed air); such scaling can be done with an extra air volume tank as utilised for *Kopswerk II* PSH physical modelling as described by *Larcher et.al.* (2006) [118].

Required for 1D-simulations are special semi-air cushion modules in addition to existing 1D air cushion representations, that allow the aeration and de-aeration through a throttled pipeline including thermodynamic effects. More tests and evaluations are needed to study the behaviour of this new surge tank approach.

6.5.3 Thermodynamic Effect

Two-phase flow 3D-CFD simulations with temperature terms were carried out to study the effect of the transient compressing of the air cushion that has a throttled outflow. It was found by Vereide *et. al.* (2015) [71] that a fully adiabatic behaviour can be assumed for short term pressuring as it occurs in air cushion chambers. This aspect can also be applied on the semi-closed surge tank approach with the pressurized chamber sections, since it is just for short time. Thus, it is not relevant for heat flux into the rock-mass or the lining. An important issue is the sudden expansion of air at the end of the de-aeration pipe that leads to significant cooling of the air temperature. This effect may freeze some portion of saturated water in the air and further specific test and careful design is required for final practical use. This demands carefully rounded pipe inlet respectively outlet designs.

6.6 Storage-Tunnel Surge Tank

This chapter describes the aspects of surge tanks that allow tunnels to operate both for free surface flows as well as in pressurized flows to optimise the hydraulic performance and multifunction of hydro power and hydraulic energy storing schemes. The aspects are also relevant for large storage cavern array systems in combination with underground pumped hydropower plants to optimise the volume use.

In specific cases, upstream reservoirs may be usefully enlarged by the storage volumes of the tunnel systems. Such multipurpose conveyance systems may be applied at storage hydropower plants, run-of-river power plants or pumped storage hydropower plants. For small or mid-sized hydropower plants, the storage-tunnel can improve the performance regarding the production and grid regulation operations. Also, hydropeaking surges in rivers may be at least partially transferred to the storage-tunnel. Additionally, to headrace tunnels, tailrace tunnels may be adapted. For pumped storage hydropower plants with long tunnel infrastructure, storage-tunnels can be utilised for volume optimisation. For sufficient power production at free surface flow, storage-tunnels have to offer adequate heads on the turbines. To achieve this, the inclination should be as small as possible. This inclination can be determined specifically for each site and may be between 0.1 % to 0.2 % [190]. The topic was presented and published at 19th International Seminar on Hydropower Plants, Vienna 2016 [191]. Based on the studies of *Wechtitsch* (2014) [190] a 1D-numerical model in *Wanda* was applied to capture storage-tunnel flow behaviour. The model utilises free surface pipe elements that neglect air effects. A realised project in Austria by *Widmann et.al.* (2015) [192] utilises the benefits of the storage-tunnel design with increased flexibility operation options for mid-sized hydropower schemes. *Berg et.al.* (2019) [193] describes a storage-tunnel concept for a power plant in Norway including typical Norwegian brook intakes into the design.

Since 2014 the mid-sized hydropower plant with storage-tunnel project *Stanzertal* is successfully in operation in Austria [192]. Usually, conveyance tunnels provide an insignificant amount of water compared to the reservoir sizes, thus a clear defined one-phase system with water has been usually the goal of the power waterway design. The main concerns regarding changing conditions between free surface flow and pressurized flow are addressed as the:

1. Behaviour of intruded air bubbles or accumulated air,
 - Sudden release in upstream intakes
 - Air behaviour at transition from tunnel to pressure shafts
2. Water hammer reflection
3. Prevention of column separation

Regarding the above-mentioned aspects, following solutions are proposed:

- Air must not be released by a blow-out upstream and not be transported to the turbines respectively pumps.
- A de-aeration shaft installed directly after the main inlet prevents sudden air releases [192]. The protection against air bubbles or air core swirl flows into the pressure shaft avoids air problems in the machines.

- Air intrusion can be avoided if no waterfalls or hydraulic jumps occur at the transition from the pressure tunnel into the pressure shaft. Sufficient precautions and an adequate surge tank design fulfils these requirements.
- Regarding water hammer reflection, the free surface or captured air is seen to be positive, because it reflects water hammer pulses. The danger of column separation can be avoided by providing an appropriate surge tank construction.

A main advantage of a storage-tunnel concept may be utilised by integrating this at run-of river power plant sites with long conveyance tunnels and high discharges and low or medium heads. Such systems demand for large diameters to keep the mass oscillation stability criterion. By designing a storage-tunnel concept this may lead to beneficial use of the surge tank as storage and utilising the tunnel both as a free-flow and a pressurized conveyance system.

Storage-tunnels can be integrated in water conduit systems of a hydropower plant to support flexible peak production in combination with compensating the size of basins if required, in respect to the environmental demands regarding surge mitigation.

6.6.1 Storage-Tunnel Surge Tank Operation

For turbine start-up the storage-tunnel surge tank has to provide sufficient water in the lower chamber at a very deep level. For a shut-down event the chambers need to capture the water volume and dissipate the kinetic energy of the water in pressure tunnel by generating a counter head. The dissipation can be provided by a hydraulic throttle and the corresponding up-surge. For all possible start-up times, column separation or macro-cavitation must not appear at the transition of the pressure tunnel to the pressure shaft. To allow sufficient safety regarding this aspect the pressure tunnel is widened in the pressure tunnel section before the transition.

RESULTS AND DISCUSSION

Figure 6-28 shows the schematic sketch of the storage-tunnel surge tank design concept. In respect of a deep position of the lower chamber, the water level is designed to allow various free surface levels in the conveyance tunnel respectively pressure tunnel. The hydraulic system is to be designed to allow resonance load-cases for mass oscillation. For run-of river schemes an unfavourable unloading-reloading in resonance may be sufficient. This means no further need to investigate resonance load-cases such as suggested for pumped storage schemes.

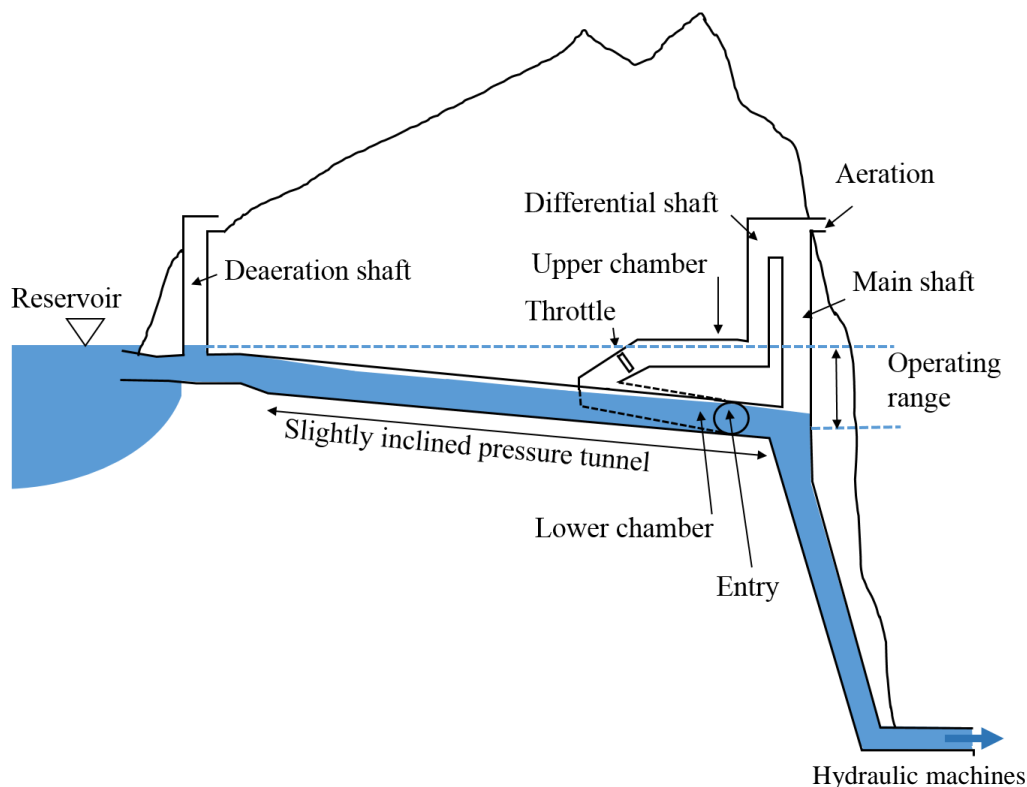


Figure 6-28: Schematic layout of a run-of river power plant with storage-tunnel and storage-tunnel surge tank, direct water intake design (Richter [194])

In case of shut-off events the differential design of the surge tank dissipates the kinetic energy of the water in pressure tunnel by overflow from the main shaft into the differential shaft controlled by the throttle loss. The combined effect of the throttle and the overflow height defines the maximum pressure at the surge tank base regarding the mass oscillation. The upper chamber is directly connected to the lower chamber via the differential throttle. The two chambers are constructed as inclined tunnels. The tunnel sizes are defined by the needs of the mass oscillation for the design load-cases and the stability criterion. The chambers can be constructed from the same access. The upper chamber significantly reduces the backflow of the water from the surge tank to the reservoir due to its low position above the maximum level in the reservoir. The throttle is necessary to dampen the discharge into the upper chamber through the lower chamber. Thus, the throttle is recommended to be a differential throttle with higher resistance for the inflow respectively the up-surge direction. The throttle needs to be designed for an optimised diameter that allows sufficient volume in the upper chamber in case of a sudden shut-off, in order to avoid a filling of the differential shaft. The throttle itself has an insignificant impact to the water hammer design [195]. To allow the escape of air, the throttle has an air pipe, that is placed at the crown of the tunnel section at the throttle's position as it is shown in Figure 6-30.

RESULTS AND DISCUSSION

Figure 6-29 explains an adaption of the explained design above with an additionally syphon that bridges a valley or other obstacles between the inlet and the storage-tunnel itself. The syphon is always pressurized. The air flow for the storage-tunnel is provided by the deaeration shaft at the beginning of the storage-tunnel.

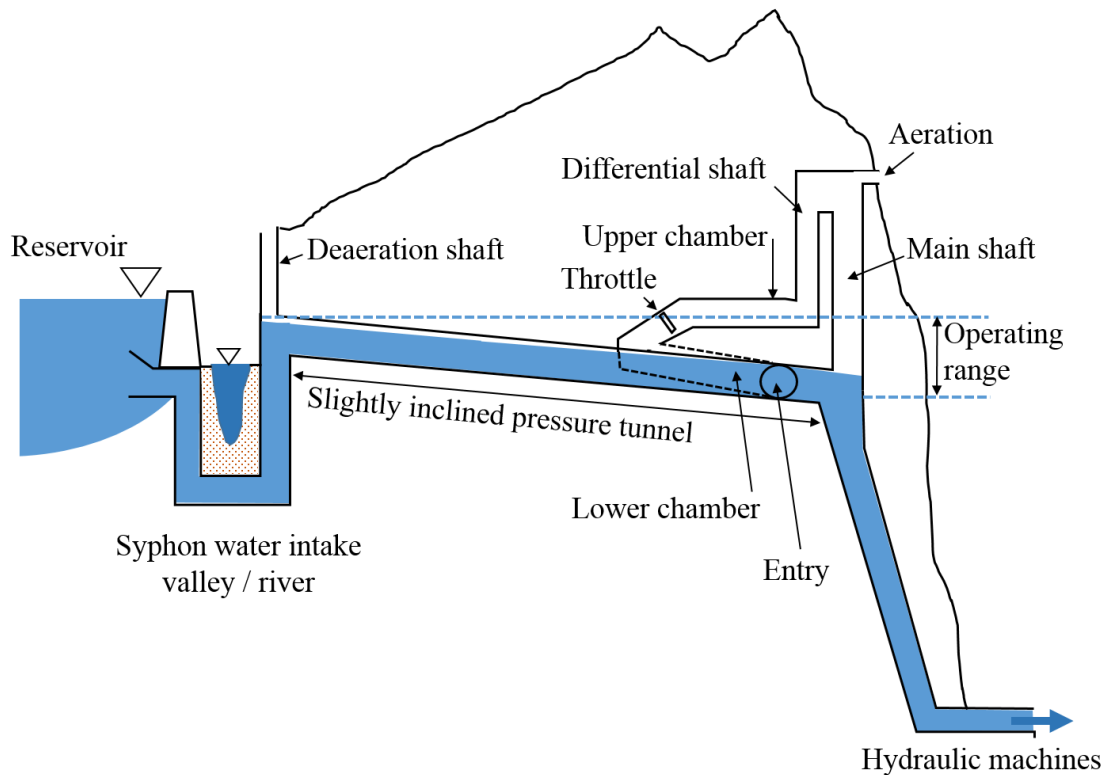


Figure 6-29: Schematic layout of a run-of-river power plant with storage-tunnel and storage-tunnel surge tank, siphon water intake design (Richter [191])

The water hammer will be mainly reflected in the main shaft of the surge tank. The main shaft is designed without a throttle and is located very close to the pressure shaft.

Since it is possible that the flow conditions in the storage-tunnel change from free surface flow to pressurized flow, it is very likely that air is trapped at the top of the tunnel. This air has on the one hand a positive effect regarding dampening of pressure pulses but on the other hand tends to move, according to the local hydraulic situations. Therefore, a shaft is placed to provide de-aeration close to the inlet structure at the reservoir to avoid blow outs at the inlet construction or racks.

RESULTS AND DISCUSSION

Figure 6-30 shows the horizontally arranged differential throttle in the pumped storage hydropower scheme *Obervermuntwerk II*. This throttle design is principally comparable for a suggested throttle design to be applied for storage-tunnel surge tanks. The asymmetric design in this specific case provides a hydraulic loss factor of about 2.8 [-] with a significant down-surge loss in relation to the up-surge direction. The pipes are installed at the crown to provide de-aeration of the hydraulic system and at the invert to allow de-watering of the surge tank in case of maintenance.

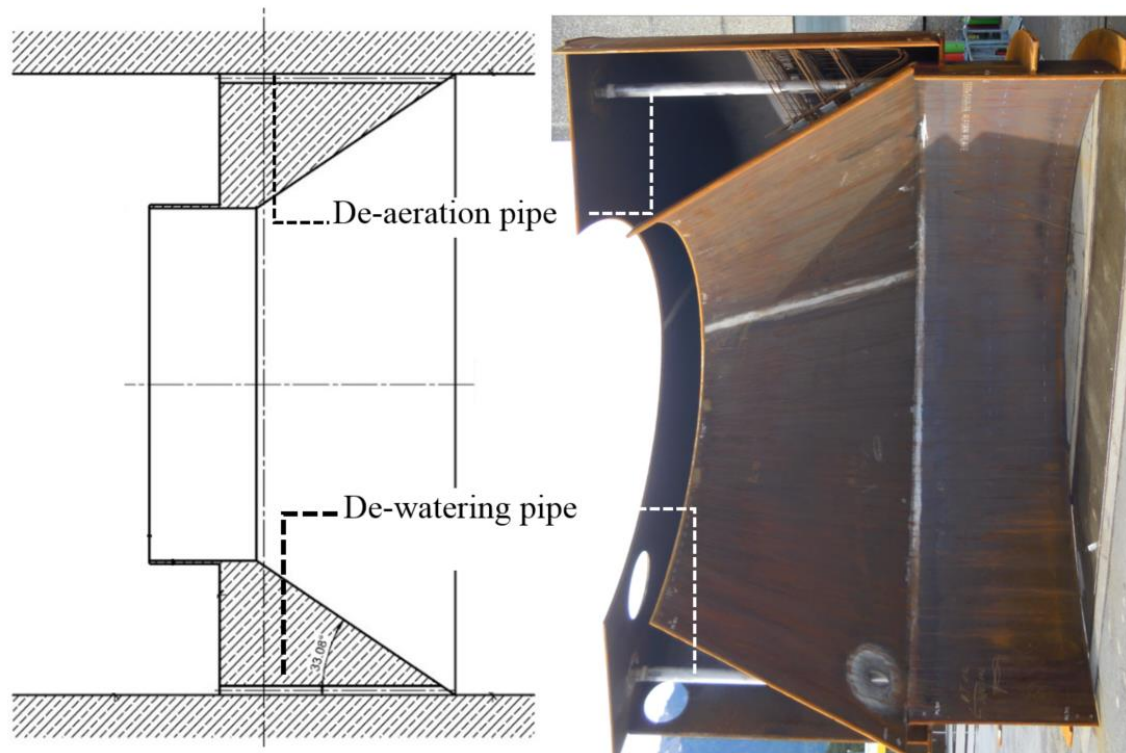


Figure 6-30: Example of a differential throttle with a de-aeration and a de-watering pipe in horizontal arrangement for the pumped storage power plant *Obervermuntwerk II* [44] (Lazer, (modified), picture: courtesy of Illwerke AG)

6.6.2 Stability Criterion for Storage-Tunnel Surge Tanks

Hydropower plants with small or medium heads, large discharges as well as long tunnels demand for large horizontal surge tank section areas to fulfil the stability criterion. This may appear at run-of river power plants with long power waterway tunnels. The water levels of such power plants do not vary significantly. A slightly inclined storage-tunnel allows high power output at free surface flow in the storage-tunnel. The chambers of the storage-tunnel surge tank are designed for the stability criterion. Therefore, a free surface flow has to be provided for all operational cases in the chamber areas especially in the connection tunnel between the two surge chambers. But also, the lower and the upper chamber can be accounted for the stability purpose, integrated to all other design load-cases.

6.6.3 Case Study Simulation for a Storage-Tunnel Surge Tank

This chapter briefly describes the simulation and design study of a storage-tunnel surge tank facility. The remaining hydropower potential in regions with already high shares of hydropower exploitation may demand solutions to optimise the value of such hydroelectric facilities. Places with the necessity of long tunnel infrastructures may be constructed with storage-tunnel surge tanks as the example below is desired to indicate.

6.6.3.1 Stability Criterion

The 1D-numerical simulations were conducted with *V4.3* to investigate a generic scheme, demonstrating the practical applicability. A most unfavourable load-case of machine start-up is simulated by utilising 3D-numerical simulations.

The experiences by the author of applied research of small-scale physical model tests with hybrid modelling of surge tanks were used to calibrate the 1D-numerical simulations of the generic case. Especially in the lower surge tank chamber, transitions between pressurized and free surface flow regimes appear to be complex, since air is suddenly released. The experiences from filling lower chambers in Austrian surge tanks show a robust behaviour. The layout criteria are applied to the storage-tunnel surge tank design.

The pilot case simulation is conducted to compare load-cases for start-up and shut-off events as well as stability events. As roughness parameter the Strickler coefficient K_{ST} [$m^{1/3}/s$] is applied as a basic value for the simulations. The following power plant dimensions are generic and defined for case simulation:

- Gross head: 60 m
- Design discharge: 140 m^3/s
- Length of storage-tunnel: 15 000 m, $D = 8.0$ m, $K_{ST} = \text{variable}$
- Gross storage volume: 754 000 m^3
- Power capacity: 67 MW
- Pressure shaft: $L = 80$ m, $D = 6$ m, $K_{ST} = 110 m^{1/3}/s$

Tunnel alternative A): tunnel – without concrete lining $K_{ST} = 55 \text{ m}^{1/3}/\text{s}$ (TBM drilled, lined with shotcrete)

- Needed stability area regarding the Thoma criterion:
with factor 1.0 [-]: 325 m²,
with factor 1.5 [-] (usually adapted): 488 m²
- Needed stability area regarding the Svee criterion [65]: 433 m²

Tunnel alternative B): tunnel – with concrete lining $K_{ST} = 85 \text{ m}^{1/3}/\text{s}$

The roughness of a concrete lined tunnel is defined by the Strickler coefficient of $K_{ST} = 85 \text{ m}^{1/3}/\text{s}$. This comparison assumes the same diameter for the concrete lined tunnel as well as the unlined tunnel. The following stability areas are demanded:

- Needed stability area regarding the Thoma criterion:
with factor 1.0 [-]: 777 m²,
with factor 1.5 [-]: 1166 m²
- Needed stability area regarding the Svee criterion [65]: 833 m²

The comparison of both tunnel configurations shows, that the stability criterion regarding the Svee criterion requires smaller surge tank areas than utilising the Thoma stability criterion with the suggested empiric safety factor of 1.5 [-] by *Jaeger* [64]. The efficiency of the hydraulic machines is assumed to be constant. Due to the slight inclination and the free surface flow in storage-tunnels, especially for run-of river power plants the internal pressures are very small. For storage-tunnel surge tanks with differential effects for a short period of time, higher pressures are generated. For specific tunnel situations with sufficient geological conditions, an unlined tunnel can provide several advantages such as:

- Additional storage volume,
- A smaller stability criterion as well as
- Construction and economic advantages.

Since a storage-tunnel surge tank offers a complex geometry with variable horizontal sections a comprehensive 1D-numerical stability analysis with free surface pipe elements is demanded.

6.6.3.2 Simulation of the Storage-Tunnel Surge Tank

A generic case study is conducted regarding the operation of a storage-tunnel surge tank. A storage-tunnel is defined with an internal diameter of $D_i = 7.0 \text{ m}$, Length $L=14.5 \text{ km}$ with an inclination of 0.11% and a design turbine discharge $Q_A = 140 \text{ m}^3/\text{s}$. This example should highlight a case where a run of river power plant is diverted in a quite large long tunnel utilising a relatively small head. By applying a storage-tunnel surge tank several advantageous aspects compared to conventional design can be addressed:

- Active utilisation of surge tank volume to meet stability criterion,
- Utilisation of significant volume of the tunnel for flexible operation,
- Storage reserve for surge mitigation.

RESULTS AND DISCUSSION

Figure 6-31 shows the specific time frame at 300 s of the 1D-numerical simulation with a graphical visualisation of the surge tank. It shows the outflow of the surge tank separated by an asymmetric throttle between lower chamber and upper chamber. The 1D-numerical simulation utilises free surface pipe elements to model the headrace tunnel and the surge tank. This throttle was tuned to allow best possible balance between the water capturing of the lower chamber and the water flow retardation due to the energy dissipation at the throttle with a higher up-surge loss compared to the down-surge local loss. The challenge was to balance the discharge through the throttle and the discharge over the surge shaft with the overflow. This way the upper chamber is filled from two sides. The headrace tunnel faces partial emptying starting from the surge tank and surface waves in filling process when the surge tank fills.

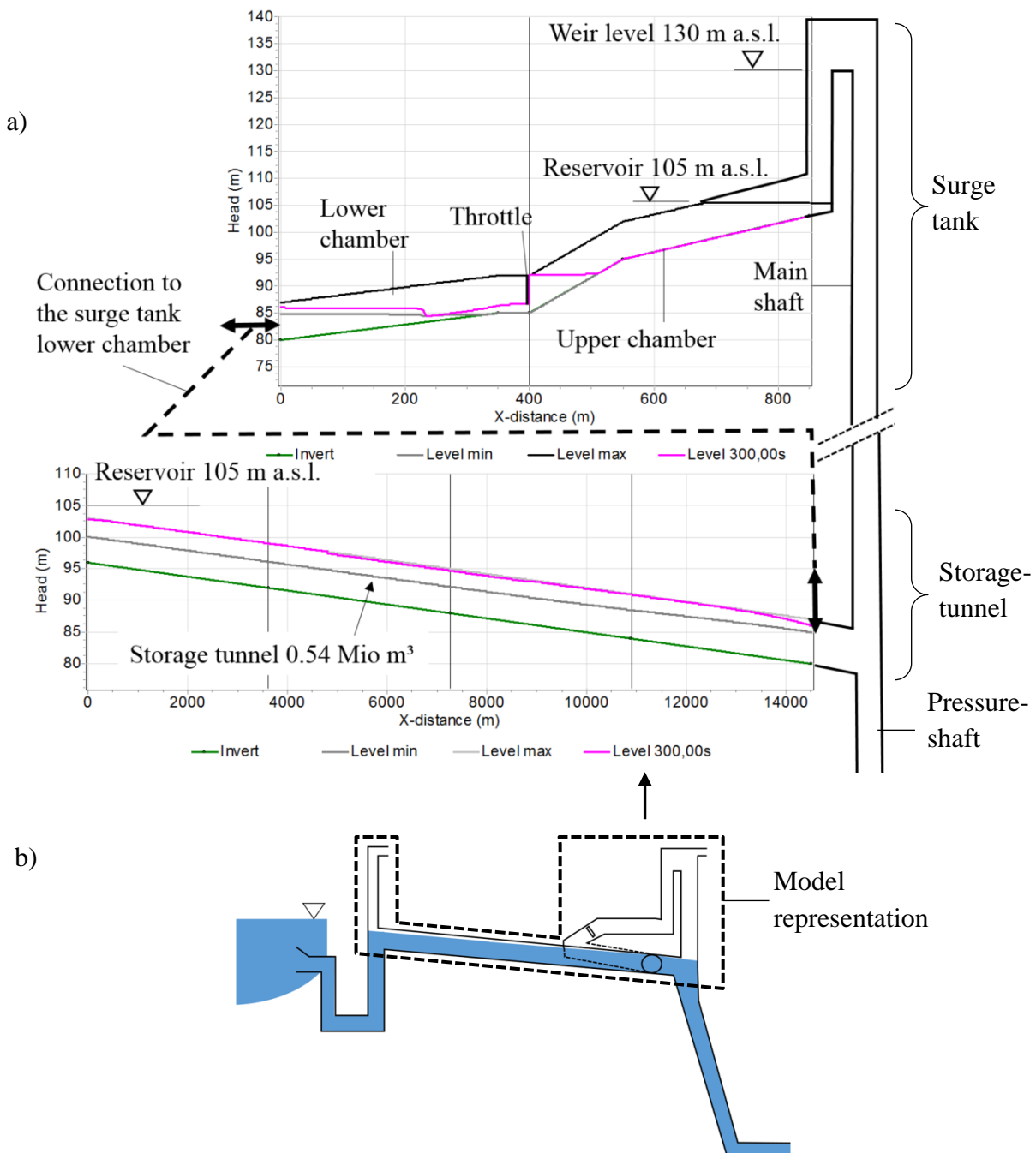


Figure 6-31: (a) 1D-numerical simulation screen shot with the arrangement of the storage-tunnel design using free surface pipe elements in the software *Wanda V4.3*; (b) system scheme indicating the part represented in the 1D-numerical simulation in (a) (Richter [191], modified)

RESULTS AND DISCUSSION

Figure 6-32 shows the screenshot of the 1D simulation with a total time of 8000 s, the start-up in 60 s to conduct 140 m³/s through the pressure shaft. 95 m³/s are withdrawn from the inlet; the difference is utilised by the storage-tunnel reservoir. After the shutdown of the units at 4500 s, the discharge from the inlet refills the storage-tunnel. The timeframe of 300 s links to Figure 6-31.

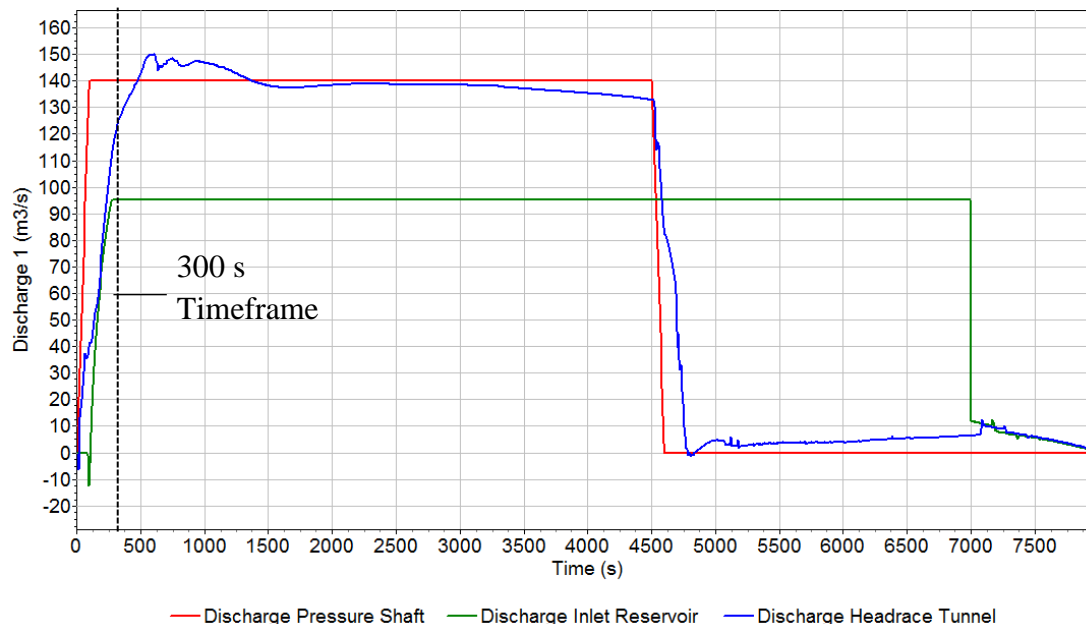


Figure 6-32: Load-case of operation start in the pressure shaft with 140 m³/s in 60s (Richter [191], modified)

Using 1D-numerical simulations, the behaviour of the storage-tunnel surge tank including the capturing of the free surface flow can be studied and the size of the surge tank can be designed for the relevant load-cases. The system is started linearly to the design discharge Q_A within 60 s. The throttle at the end of the lower chamber generates a differential effect due to a 1:3 ratio between down-surge and up-surge loss factor. The lower chamber is connected at the same elevation as the storage-tunnel. This allows a start-up with free surface flow in the tunnel system without column separation. A de-aeration of the lower chamber through the throttle is necessary and simulated in a simplified manner in the 1D simulation. This de-aeration is applied by a pipe at the crown of tunnel through the throttle section. Further comparison such as multiphase 3D-numerical simulations and physical model tests are important for specific cases. An increased diameter of the tunnel before the transition to the power shaft as visualised in Figure 6-33 is necessary to avoid flow separation and a waterfall at the transition to the pressure shaft. The transition at this location shows a free surface in the tunnel and a pressurized flow in the shaft. The conventional tunnel diameter design is not sufficient since the acceleration of the water mass at the time of creating the free surface is changing due to the significant difference by a factor of 100 [-] due to the difference of the pressure wave information (~ 1000 m/s) and free surface wave information (~ 10 m/s). At closing or shut-off, air is captured in the pressure tunnel system and needs to escape by the aeration shaft after the inlet to avoid blow outs. Waiting times for re-opening may be considered specifically.

Hybrid modelling for specific design is demanded. The benefits of such storage-tunnel systems can be the utilisation of water mass of surge mitigation from an ecological point of view and increased flexibility for economic point of view. Both aspects are in close relation to improve resource efficient hydropower applications.

RESULTS AND DISCUSSION

Figure 6-33 shows the result from a 3D-numerical simulation of the pilot case storage-tunnel surge tank with a geometry as shown in Figure 6-34 and Figure 6-35. The turbines were started-up within 60 seconds.

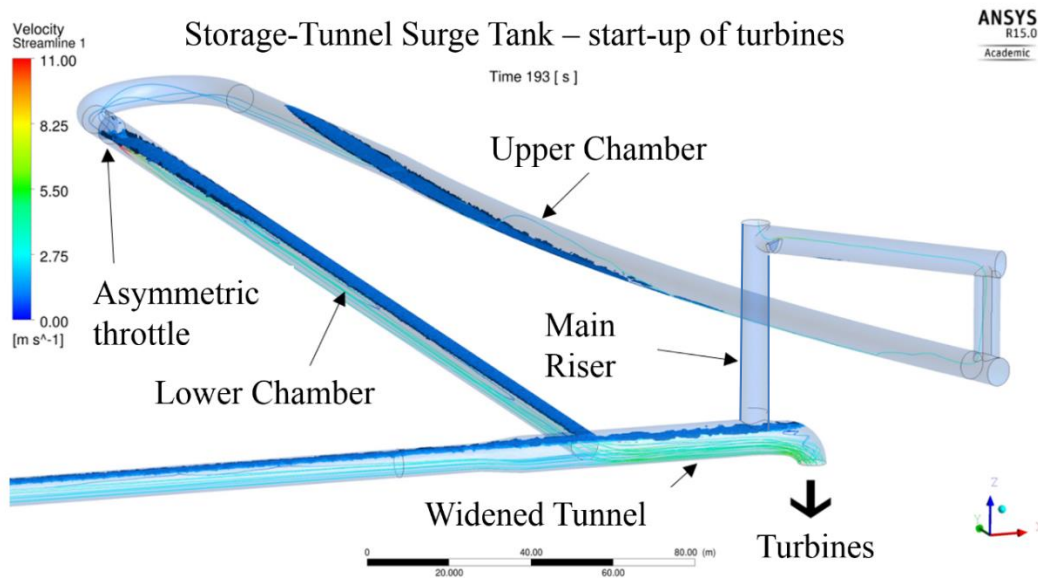


Figure 6-33: CFD Simulation for start-up of pilot case system – free surface flow in tunnel and surge tank – widened tunnel section before the drop into the pressure shaft (Richter [191])

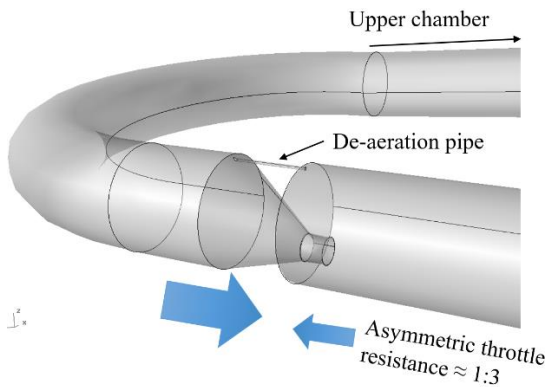


Figure 6-34: Asymmetric throttle with de-aeration pipe, detail (Richter [191])

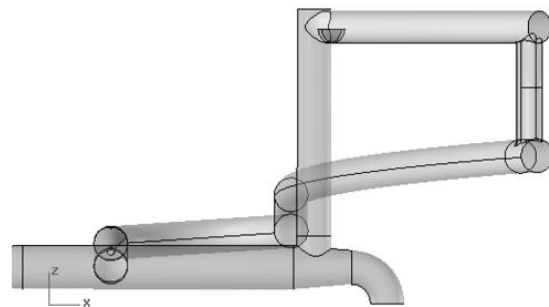


Figure 6-35: Front view of the storage-tunnel surge tank (Richter [191])

Regarding the hydraulic dimensioning of the storage-tunnel surge tank the following parts were designed by 1D and 3D-numerical transient simulations:

- Lower chamber for the most unfavourable opening load-case without column separation in the storage-tunnel and a sufficient emptying of the upper chamber regarding the throttle diameter
- The pressure tunnel diameter before the pressure shaft is recommended to be enlarged to avoid column separation at free surface flow situations
- Upper chamber for the most unfavourable shut-down load-case in adjustment with the throttle dimensioning
- Horizontal water surface area in the surge tank chamber regarding the stability criterion relating to the maximum pressure at the surge tank base

6.7 Surge Tank Details

This chapter discusses the specific technical details for surge tanks that were investigated both numerically and in physical model tests:

- 1) The differential throttle as a mass oscillation damping device.
- 2) A novel device to mitigate the effects of waterfalls in a specific surge tank shaft such as air intrusion depth; the waterfall-dampening device.
- 3) Behaviour of long upper chambers.

6.7.1 Throttle Design

A hydraulic throttle (respectively orifice respectively diaphragm) can significantly improve the mass oscillation behaviour of a surge tank. This includes a decreased volume demand for the surge tank as well as improved machine operability that increases the flexibility of the power plant. The throttle is designed for a specific surge tank in order to improve its distinct hydraulic behaviour. The connection pipe and all bends account with additional losses that influence the mass oscillation and may be added to the specific throttle loss in terms of the 1D-numerical simulation. Hydraulic losses of throttles are always a combination of the geometry before and after the particular device itself. The actual loss is created mainly by a Borda-Carnot local loss type, that is created downstream of the throttle. This illustrates that even symmetric orifice throttles may generate asymmetric losses. Throttles increase the pressure head at the surge tank base in case of up-surge (for CSTs as soon as the lower chamber is filled, Figure 6-37). At down-surge the hydraulic loss created by the restricted flow through the throttle decreases the head acting on the pressurized flow in the hydraulic system. This differential effect of the throttle dampens the mass flow in the tunnel system, mitigates the volume demand of the surge tank and decreases the excavation expenses of this construction. Throttles are a simple and effective way to generate a beneficial differential effect. The throttles need to be designed specifically for each hydraulic system. Throttled surge tanks have to be checked for:

- Acceleration of the water mass in the surge tank
- Capturing of the water hammer
- Avoiding macro cavitation in the adjacent pipe system
- Need of aeration shaft for cavitation prevention
- Need of deaeration pipe for the filling case
- Maximum water jet velocity hitting concrete walls
- Simple geometry for construction
- Need of dewatering pipes
- Prevention of vortex flow
- Resultant forces on abutment

Hydraulically a throttle is designed for specific:

- Up-surge loss coefficient
- Down-surge loss coefficient

RESULTS AND DISCUSSION

Throttles create a jet by the flow restriction. The jet dissipates in the water of the subsequent pipe. This can be hydraulically seen as a sharp diffuser and thus a hydraulic unsteady effect by a fluctuating jet. It may result also in a hydraulic loss that shows a fluctuating value. Strong flow restrictions in combination with high velocity differences between the involved pipes and structures may result in higher relative loss fluctuations. In absolute values these fluctuations are small. The fluctuations are also related to the stochastic nature of diffuser flows.

Exact steady local losses are not able to be guaranteed and will always show a certain range. Thus, it is recommended to design surge tank throttles with some loss margin in order to meet with the safety design philosophy.

Figure 6-36 and Figure 6-37 show the principal positions of throttles in surge tanks. Throttles may be placed in the connection shaft or tunnel to the surge tank (Figure 6-36) or in the bottom of the main riser for chamber surge tanks (Figure 6-37).

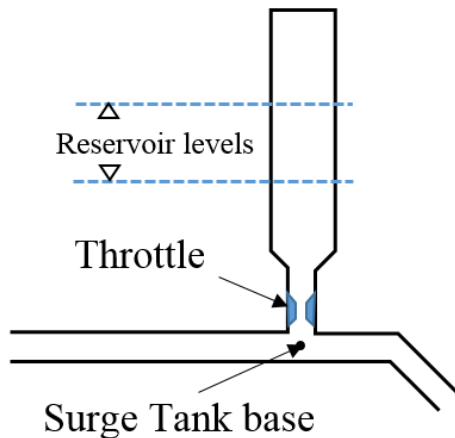


Figure 6-36: Throttle position at transition from pressure tunnel to surge tank (symmetric orifice throttle, shaft surge tank)

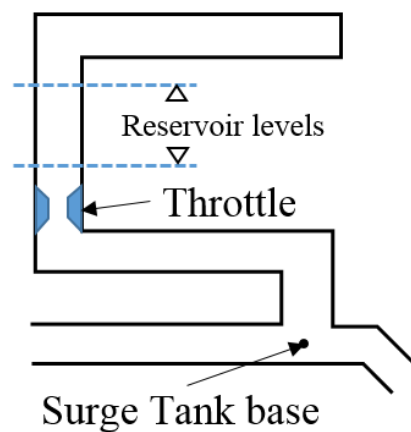


Figure 6-37: Throttle position at transition from lower chamber to main shaft (symmetric orifice throttle, chamber surge tank)

Hydraulic throttles may improve the governor stability of the surge tank [196]. *Li & Brekke* [66] conclude that throttled surge tanks may allow smaller safety factors regarding the stability criterion. Additionally, crown throttles may be utilised to enable semi air cushion surge tanks as described in chapter 6.5.

6.7.2 Orifice Throttle

Orifice throttles represent simple geometric designs that consist of symmetrical structural flow contraction. The local loss is basically generated by Borda-Carnot type head loss. If symmetrical flow restrictions are placed in a straight pipe with fully developed straight flow, then the head loss is symmetrical in both flow directions. Usually in surge tanks fully symmetrical hydraulic losses are hardly possible since structural boundary conditions such as bends or different pipe diameters are present. Especially the pressure tunnel diameter differs from the pressure shaft diameter and this utilises a different Borda-Carnot loss coefficient. Further studies of orifice throttles were investigated by *Gabl* [197] and *Adam* [198].

6.7.3 Differential Orifice Throttle

Differential orifice throttles feature significant hydraulic asymmetrical loss coefficients between up-surge and down-surge. This allows primarily to minimise the net volume demand. Essential for the differential throttling effect is the Borda mouthpiece introducing an amplified local loss in the associated flow direction (Figure 6-38).

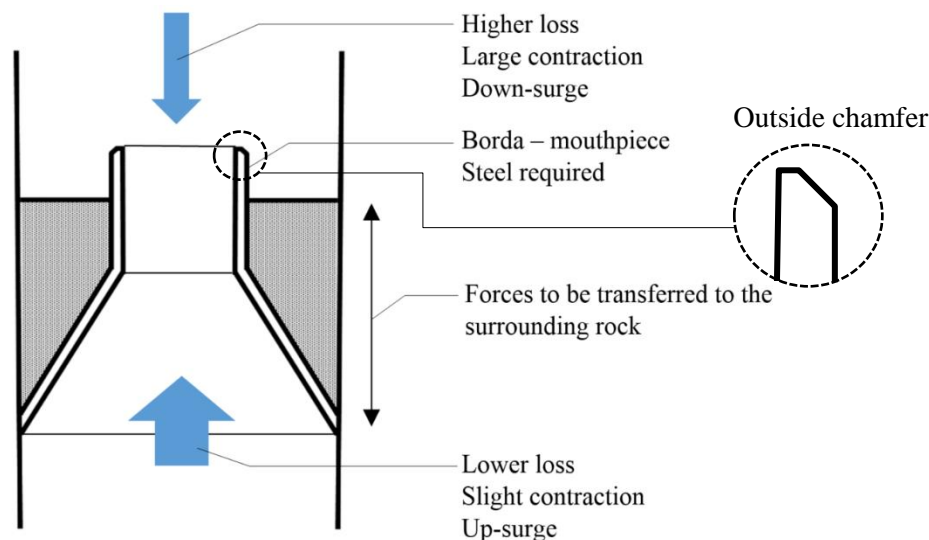


Figure 6-38: Differential orifice throttle definitions

Figure 6-39 visualises the complex down-surge flow regime at the *Burgstall* surge tank throttle. The flow is efficiently restricted by the throttle and enters an enlarged pipe combined with a 90° elbow. Due to the fluctuating jet the down-surge loss factor shows a slight transient variation. For 3D-numerical simulations it was found that the average value of a transient simulation gave the best approximation [116]. Figure 6-39 shows that the riser has a smaller diameter than the lower chamber and thus this diameter ratio additionally influences the local loss ratio between the up-surge and the down-surge. Regarding this aspect, no general maximum loss ration value for differential orifice throttles can be given.

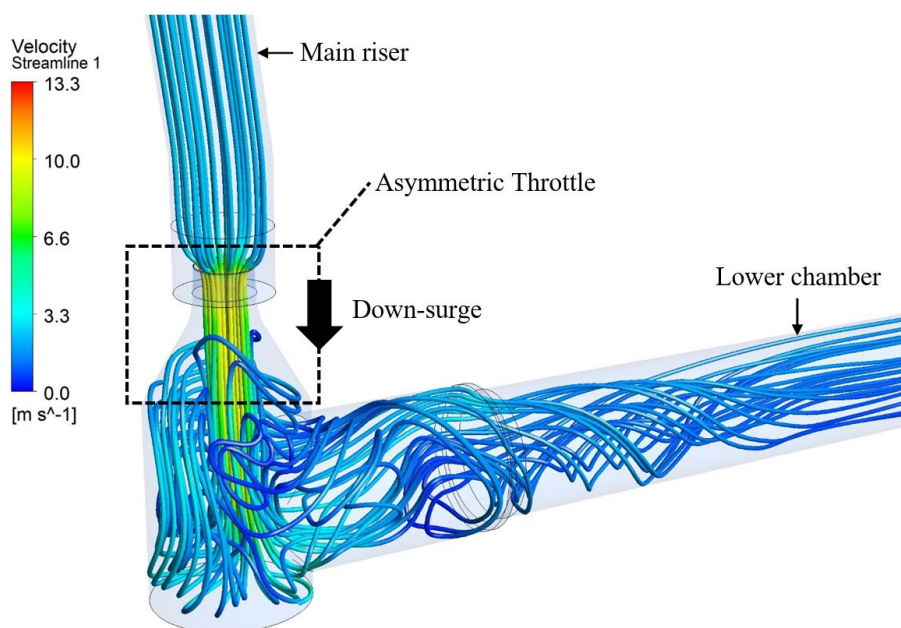


Figure 6-39: Down-surge situation at certain time step at complex asymmetric orifice throttle

RESULTS AND DISCUSSION

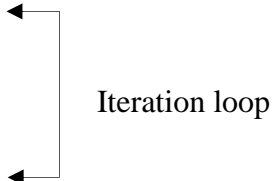
The loss ratio region is between: 1.0 – 4.0 [-]. It is influenced by:

- Diameter ratio of the pipes before and after the throttle
- Dimensions of the Borda mouthpiece
- Steel thickness of the throttle
- Chamfer detail of the throttle entrance
- Approach flow
- Length of the pipes before and after the throttle
- Position of the throttle (at centre or off-centre)

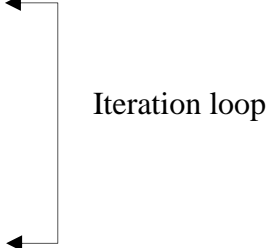
Table 6-2 visualises the approach of the investigation procedure for a differential throttle design. First, 1D-numerical simulations of the mass oscillation are undertaken, possibly with rigid column approach, to check the restricting head loss. This can be either limited by up-surge (maximum pressure) or down-surge (cavitation). Then, a reasonable assumption for the head loss ratio is applied. The defined local losses are defining the geometry of the throttle for down-surge and up-surge. These are checked and fine-tuned by 3D-numerical simulations of the losses. The numerically designed throttle is proven by a physical small-scale model test. By adapting an appropriate safety factor, the physical small-scale model test may be spared. For 3D-numerical throttle design only, the author suggests a value of about 20 % loss variation in both direction towards the more unfavourable and thus, safe side.

Table 6-2: Throttle development procedure

Rough geometry variation iteration process

1. 1D-numerical simulations
 2. Geometry variation
 3. 3D-numerical simulations
head loss evaluation
 4. Result: Principal shape of the throttle
- 
- Iteration loop

Fine-tuning of throttle geometry

5. 3D-CFD → head loss up-surge and
down-surge
 6. 3D Geometry diameter variation
 7. Physical small-scale model test for
hydraulic proving
 8. Result: final throttle geometry
- 
- Iteration loop

6.7.4 Differential Vortex Throttle

The highest possible differential loss factor can be achieved by differential vortex throttles. Vortex throttles were introduced by *Thoma* (1930) [199]. The first vortex throttle for a hydropower scheme was constructed at the HPP *Kaunertal* in Austria commissioned in 1964 (replaced 2016). Figure 6-40 visualises the 3D geometry of the differential vortex throttle. A ratio of 1:50 was possible between up-surge and down-surge loss [82] [200]. This specific vortex throttle was the first of its kind in such dimensions. It was originally designed for and still popular used for water piping systems [201]. The differential vortex throttles for high-head hydropower schemes were improved by *Heigerth* [83], against cavitation issues and equipped with a lower loss ratio of 1:20. This is still very high compared to differential orifice throttles. Such high ratio throttles are in operation in several high-head schemes in Austria such as HPP *Gerlos II*, HPP *Mayrhofen*, PSH *Rosshag*, PSH *Malta-Mainstage* [202].

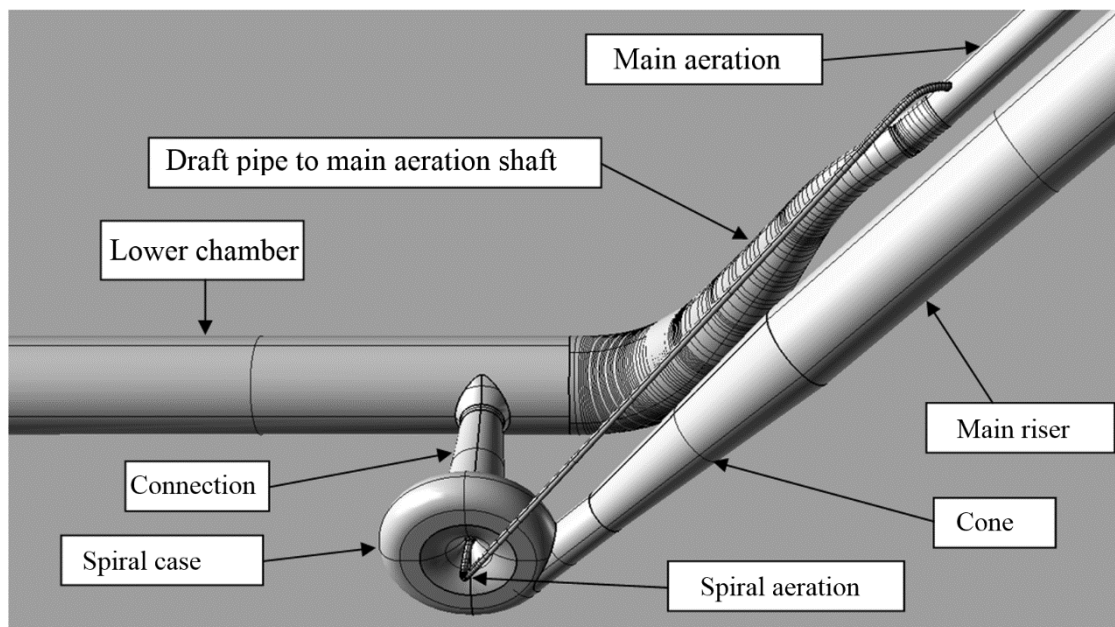


Figure 6-40: Differential vortex throttle geometry, HPP *Kaunertal* (*Richter* [1])

RESULTS AND DISCUSSION

Figure 6-41 visualises the down-surge with high loss factor due to the vortex flow. In contrast to a Francis turbine spiral case the vortex throttle consists of a torus with constant flow section and without any guide vanes. The “draft tube” at the vortex throttle is applied in the centre of the torus. This design leads to self-blocking of the outflow from the shaft creating the high loss but also to heavy pressure transients [117]. For very sharp hydraulic design as for the original HPP *Kaunertal* high pressure fluctuations and flow internal micro cavitation effects were observed. The aeration shaft into the centre of the spiral was effectively dampening the induced noise and forces. In 2016 the surge tank of HPP *Kaunertal* was replaced by a new surge tank utilising a differential orifice throttle [203].

Due to the pressure fluctuations, the high construction effort and the limit of scalability to larger constructions of vortex throttles it is advisable to prefer best valuated orifice throttles for a surge tank design allowing flexible hydropower operation.

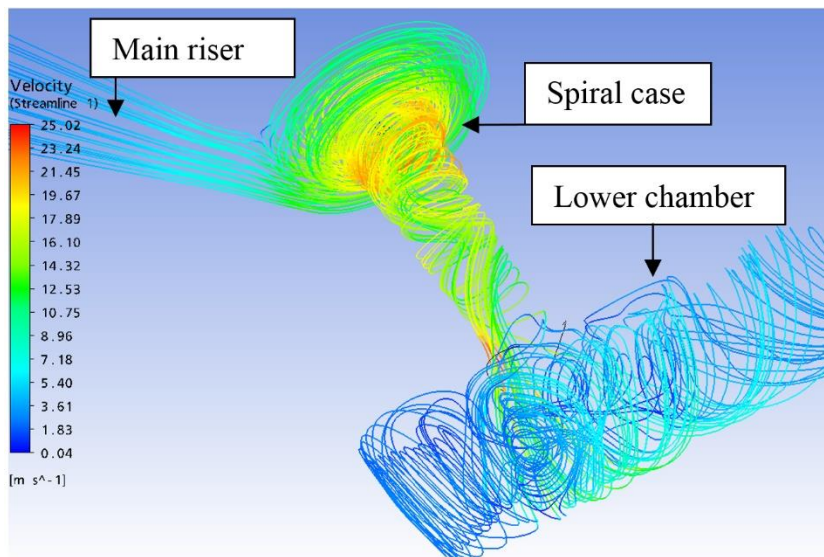


Figure 6-41: Down-surge of the *Kaunertal* vortex throttle of 15 m³/s, transient 3D-numerical simulation, snapshot at specific time point (*Richter* [1])

6.7.5 Aeration Shaft

In order to avoid cavitation, especially macro cavitation (column separation), chamber surge tanks with strong throttles in down-surge directions may be equipped with aeration pipes. For the *Kaunertal* vortex throttle (1964) a complex aeration pipe system was installed (Figure 6-42). In this case, the pipes mitigated cavitation effects as well as provided air directly into the spiral case that was dampening the pressure fluctuations. The pipe that was aerating the lower chamber was later filled with cement and found not to be necessary. Tests with filling the throttle aeration pipe have resulted in unacceptable pressure pulsations and thus stated that this aeration pipe is absolutely needed [204].

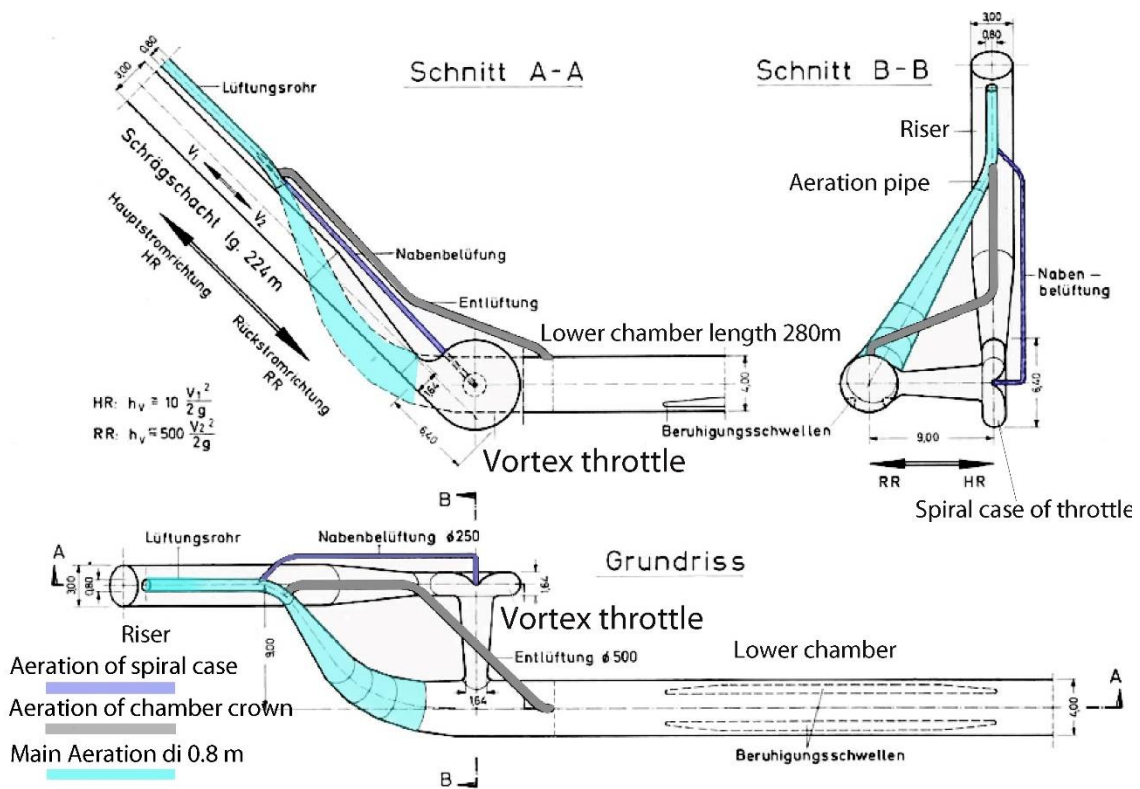


Figure 6-42: Aeration shaft system for *Kaunertal* HPP vortex throttled chamber surge tank (*Seeber*, 1970 [82] modified)

Figure 6-43 shows the placing of an aeration shaft in a chamber surge tank to avoid macro cavitation. The aeration pipe length is driven by the arising local pressure drop (velocity head) of the throttle at outflow and the corresponding water level in the riser (pressure). In view of this fact the aeration pipe length does not necessarily enter the upper chamber. Certain pipe diameters are recommended to allow proper maintenance work ($D_i \geq 1.2$ m).

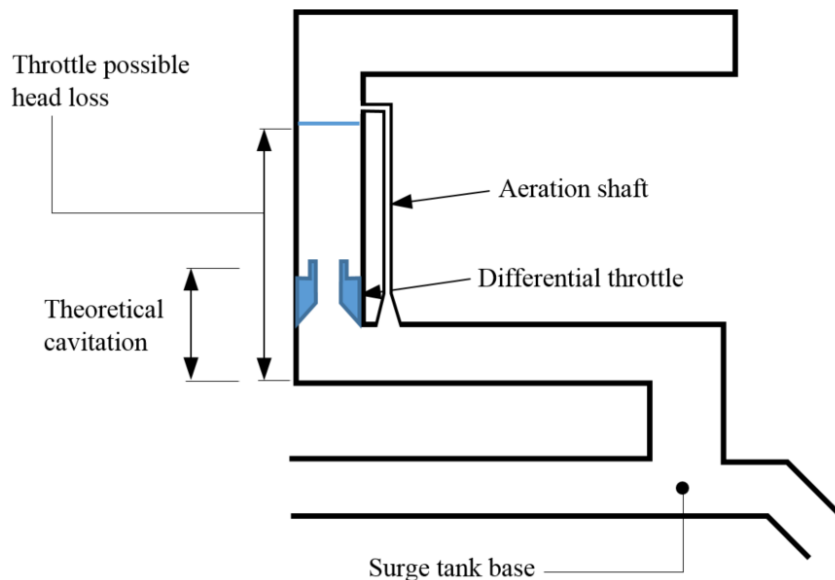


Figure 6-43: Aeration shaft for chamber surge tank

6.7.6 Flow Direction Aspects for Throttle Losses

To further improve the local loss ratio of differential orifice throttles an angle at the connection to the pressure tunnel may be applied. The angle with more direct flow to the turbines and sharp edge for backflow situation generates a lower loss at the outflow to the units and a higher loss for backflow situations of the mass oscillation. Figure 6-44 and Figure 6-45 show a generic surge tank arrangement of 30° attached connection tunnel in plan view. Figure 6-44 shows the outflow of the surge tank towards the units, this direction creates less dissipation as for the back-flow situation in Figure 6-45 with a higher head loss of 23 % due to this arrangement. The lower loss to the units may also be an advantage for pump trip load-cases, whereas a quick outflow of the surge tank to the pressure shaft is in favour to mitigate low pressure situations

The simulations were conducted at a numerical scale model of 1:30 and discharges realising Reynolds numbers of about 10^6 [-] in the outflow pipe.

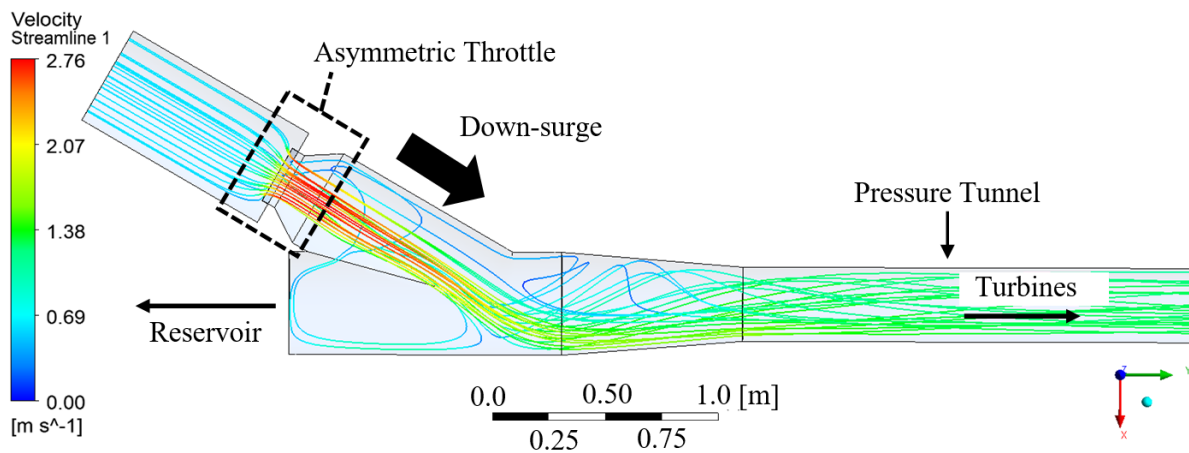


Figure 6-44: Throttle alignment with lower loss factor in turbine flow direction as for backflow to the reservoir, numerical simulation in scale 1:30, plan view (Richter [117])

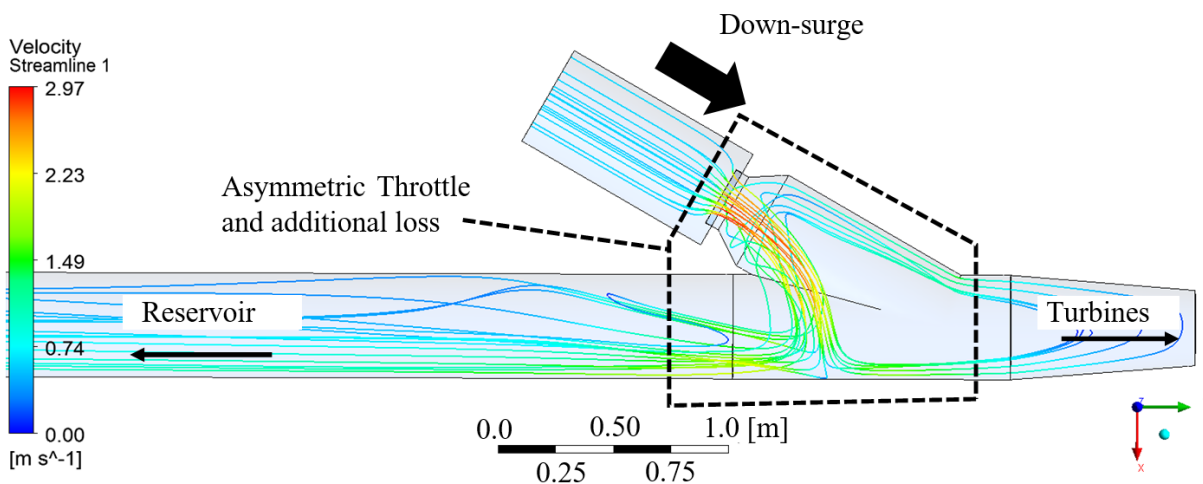


Figure 6-45: Throttle alignment with higher loss factor for backflow direction as for the flow direction to the units, numerical simulation in scale 1:30, plan view (Richter [117])

6.7.7 PIV Measurements of a Throttle

This chapter describes the PIV investigations of a vertically aligned asymmetrical orifice throttle in a two-chamber differential surge tank for up-surge direction. The work described in this chapter was partly published *Richter et. al. (2012)* in [205]. Figure 6-46 shows the geometry of the investigated surge tank with the position of the throttle and the 3D geometry. The PIV measurements were compared with 3D-numerical simulations.

For modelling the turbulence in the 3D-numerical comparison, Reynolds averaged Navier Stokes equation (RANS) implementations were applied with SST and $k-\varepsilon$ models. Aside from the calculations of the loss coefficients, the prediction of velocity profiles at parts of the particular surge tank was an important aspect. The reason for the investigations were a variant study of the throttle placing and the distance of the throttle to the wall of the main riser. Velocity concentrations were considered to touch the main riser lining. In the case study, a concrete wall after the throttle up-surge direction is close to the main jet of the throttle and thus, created high flow velocities. Figure 6-46 shows the throttle alignment in the surge tank.

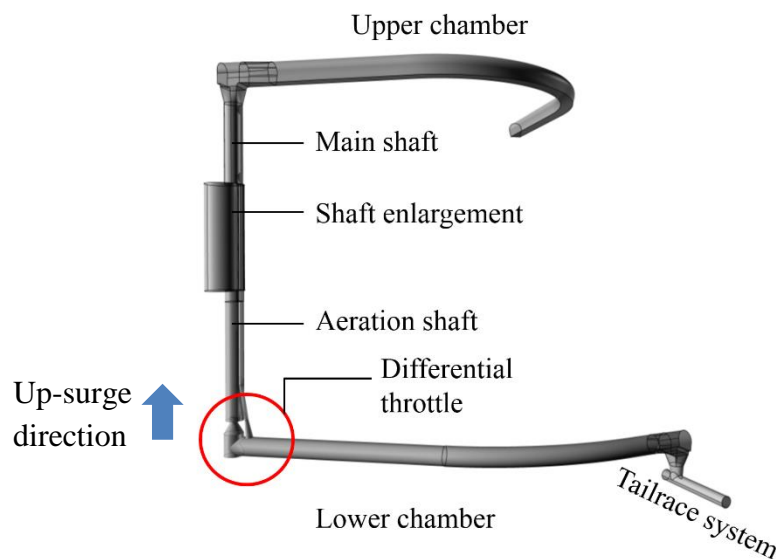


Figure 6-46: Two chamber tailrace surge tank for PIV investigations (*Richter [205]*)

To investigate the effect of the up-surging jet on the lining of the main shaft and in particular for the integrated aeration shaft, parts of the surge tank were constructed in acrylic glass at a scale factor 1:25. The throttle and lower chamber were constructed in stainless steel. For practical reasons the surge tank was positioned horizontally. Gravitational forces were found to be negligible for the throttle investigations. To avoid distortions (astigmatism) of the laser light by the curvature of the circular shaft a small basin was attached to the shaft and filled with water to provide a plane surface. This basin had rectangular walls whose surface was parallel to the velocity plane investigated with the PIV. This accounts for almost the same refraction indices for acrylic glass and for water to capture a non-distorted image [119]. For the purpose of the seedings to be reflected in the laser sheet the natural turbidity of water of the hydraulic laboratory in Graz was utilised, as described by *Dobler (2012)* [119]. The reflected seeding on the laser sheet was captured with a high-speed camera.

RESULTS AND DISCUSSION

Figure 6-47 illustrates the positions of plane 1 and plane 2 to measure the velocity field by the means of the PIV. Figure 6-48 sketches the section of the main shaft where the flow is reduced by the aeration shaft. The analysis was applied to determine the influence of the high flow velocities onto the affected parts of the construction. Figure 6-49 visualises the experimental equipment of the PIV-device. The laser sheet covers plane 1 and plane 2 measurements in the flow section. The size of the planes was restricted due to the opening angle of the laser sheet. The high-speed camera is positioned orthogonally to the laser sheet. To compare the flow velocities in this plane, 3D-numerical simulations were conducted.

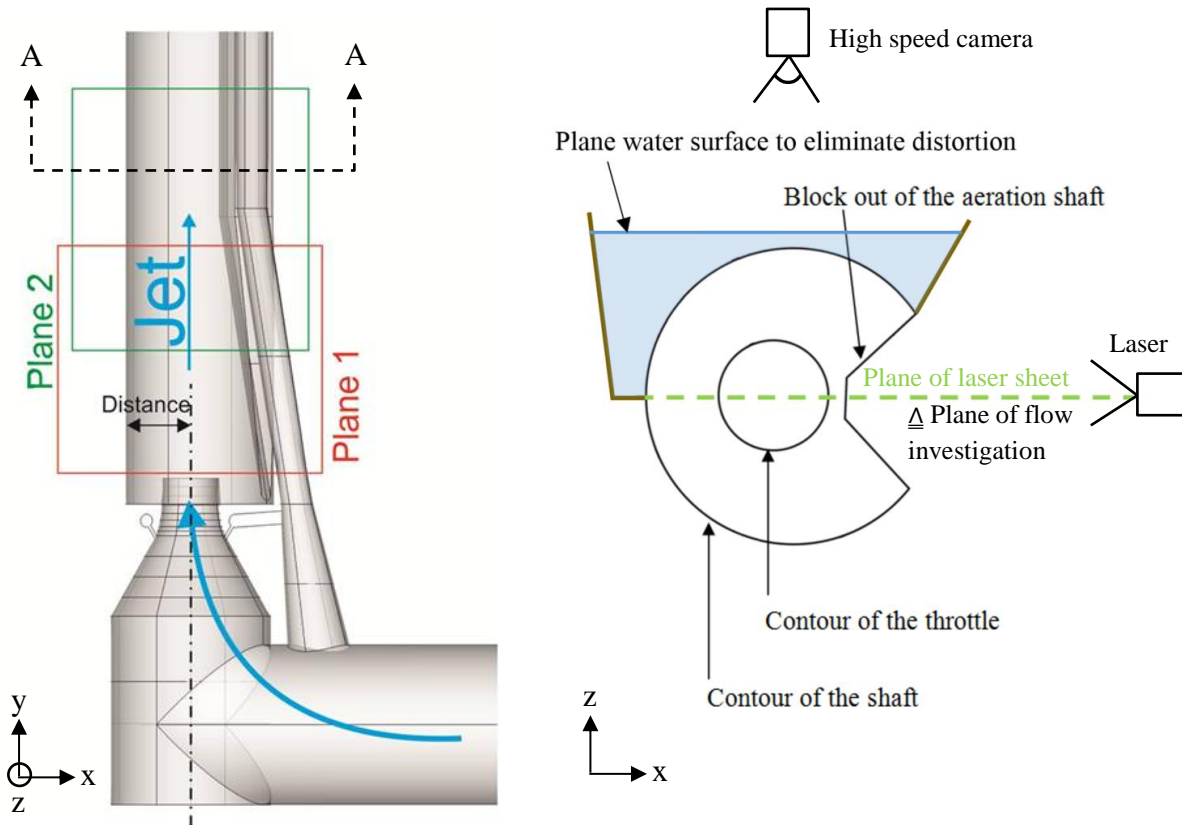


Figure 6-47: Measurement planes of the PIV investigations (Dobler [205], modified)

Figure 6-48: Section A-A of the main shaft and plan view of the throttle (Dobler [205], modified)

RESULTS AND DISCUSSION

Figure 6-49 visualises the PIV setup within the PIV housing. Since the used laser represents class 4 intensity the investigated section was housed by this safety housing.

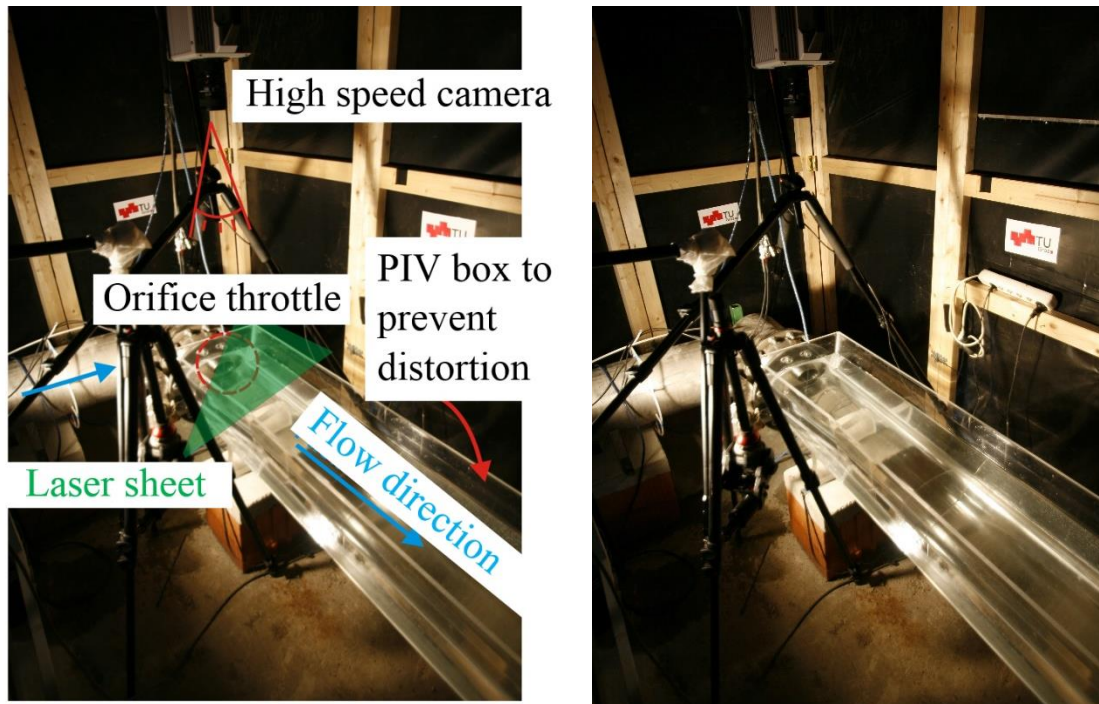


Figure 6-49: PIV setup surrounded by the PIV box for safety reasons (*Richter*) [205]

Figure 6-50 shows the detail of the green laser sheet after the throttle outlet with the water basin placed on top of the circular pipe to allow a horizontal water surface for a perpendicular flow field visualisation to avoid distortion due to the curvature of the circular pipe geometry.

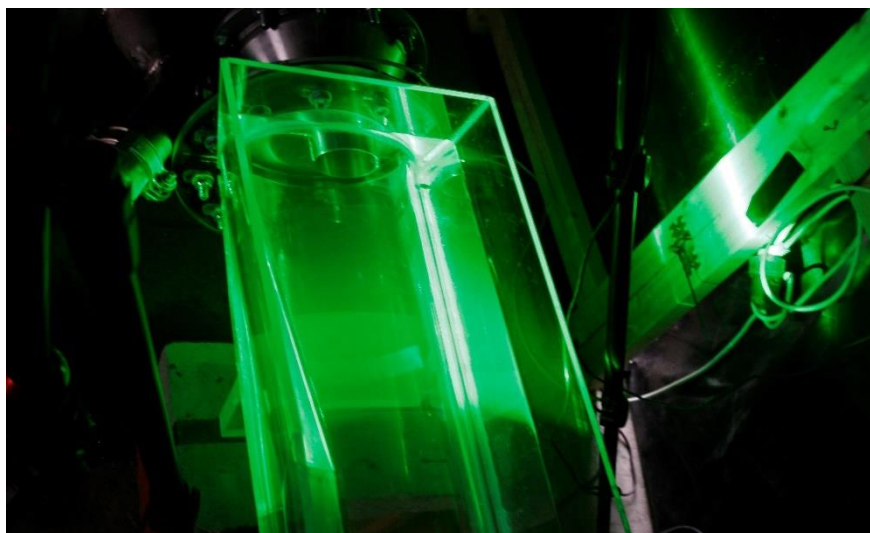


Figure 6-50: PIV laser sheet at throttle outlet (*Richter*)

Figure 6-51 and Figure 6-52 represent the mean velocities for one data set each (10.000 pictures). The investigated load-case refers to an up-surge situation. The time step between two pictures is 500 μ s, respectively 0.5 ms.

RESULTS AND DISCUSSION

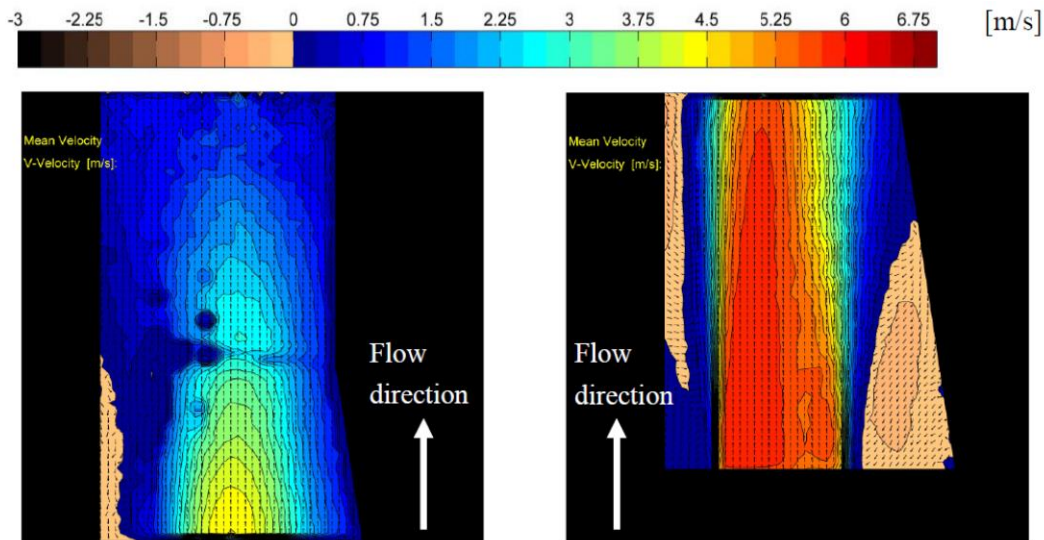


Figure 6-51: Average flow velocity over 5 seconds (model scale), plane 2 of PIV measurement (Dobler [205])

Figure 6-52: Average flow velocity over 5 seconds (model scale), plane 1 of PIV measurement (Dobler [205])

Figure 6-53 visualises the flow of the 3D-numerical simulation in model scale as investigated with PIV with the steady-state solver of *Ansys CFX*. In direct comparison to that, the results of the transient flow simulation with *Ansys CFX* of the prototype scale is shown in Figure 6-54. In general, a comparability can be stated. But significant flow pattern differences are visible especially the higher rate of disturbances near the edge. Diffusor jets such as in throttles are never stable and thus need to be simulated with a transient approach as also stated above in this thesis. Subsequently also throttle losses are always varying slightly by some percentage of loss factor amplitude.

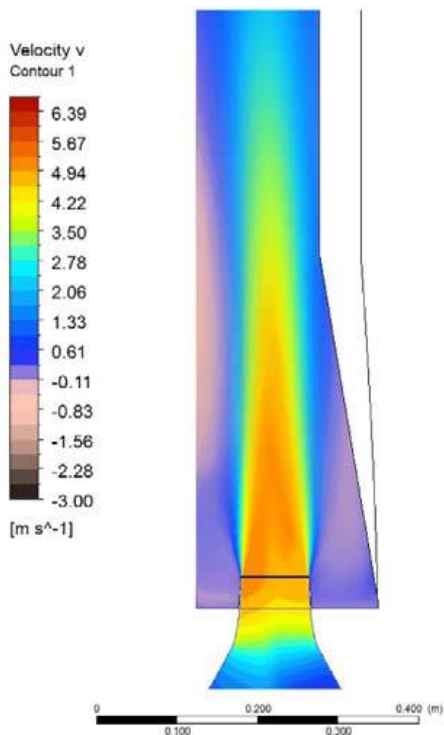


Figure 6-53: Average flow velocity in steady-state CFD calculation of the model test regarding the same boundary conditions as for the PIV measurements (Richter [205])

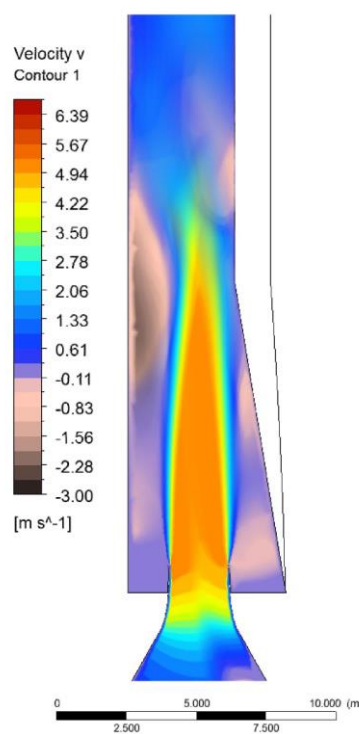


Figure 6-54: Average flow velocity in transient CFD calculation of the prototype regarding the same boundary conditions as in the model test (Dobler [205])

RESULTS AND DISCUSSION

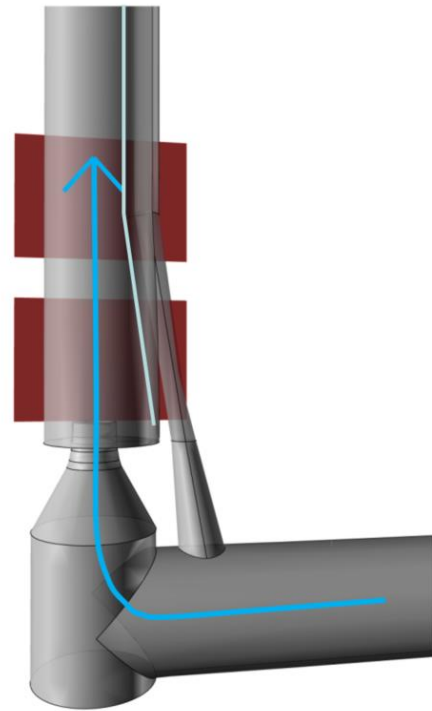
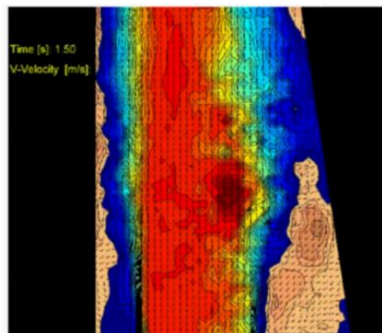
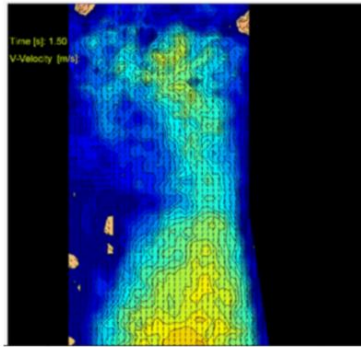
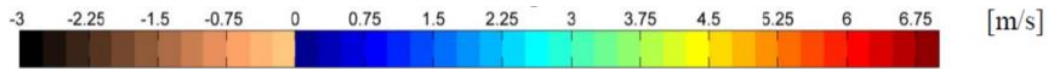


Figure 6-55: PIV result: Distribution of the up-surge flow at time step 1.5 s (Dobler [205])

Figure 6-56: Schematic description of the measurement planes 1 and 2 (Dobler [205])

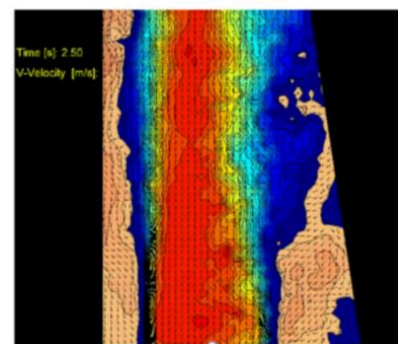
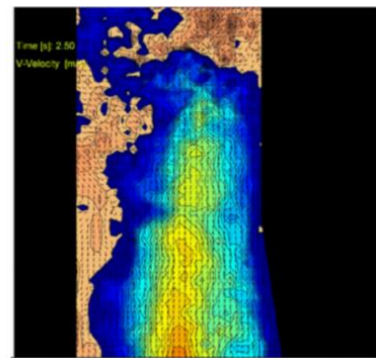
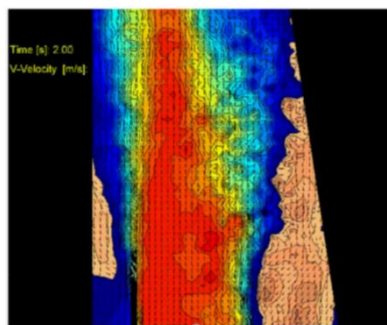
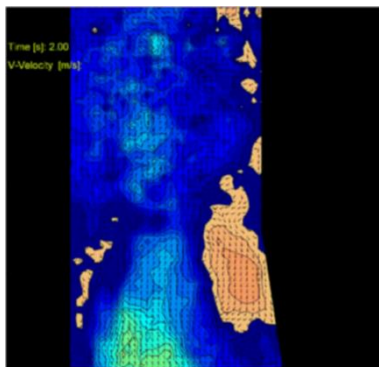


Figure 6-57: PIV result: Distribution of the up-surge flow at time step 2.0 s (Dobler [205])

Figure 6-58: PIV result: Distribution of the up-surge flow at time step 2.5 s (Dobler [205])

RESULTS AND DISCUSSION

Figure 6-55, Figure 6-57, Figure 6-58 and Figure 6-59 show the transient flow behaviour of the throttle outflow dissipation zone at different time steps after the 90° bend. The laser sheet is placed in two sections (Figure 6-56). Figure 6-59 and Figure 6-60 show the PIV measurements in comparison to the transient 3D-numerical simulation. The figures show that the tip of the jet is highly fluctuating and. The transient 3D-numerical simulations show a comparable result representing the jet dissipation.

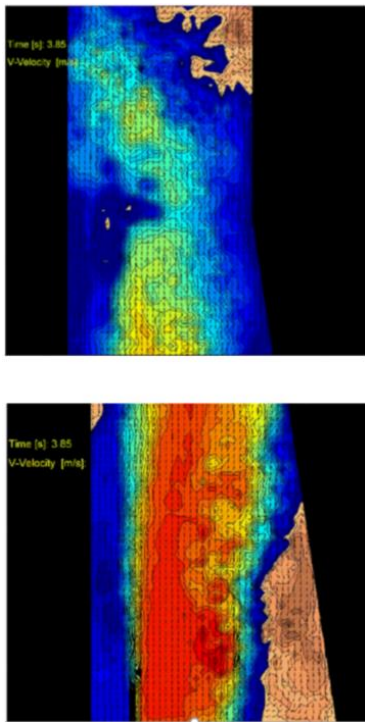


Figure 6-59: PIV result: Distribution of the up-surge flow at time step 3.85 s (*Dobler [205]*)

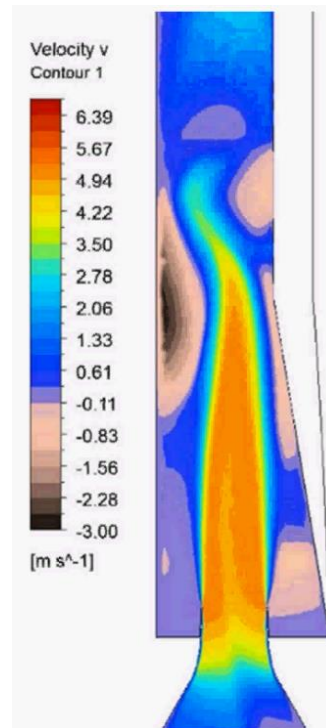


Figure 6-60: 3D-CFD transient simulation model scale equal boundary conditions as PIV model test measurement (*Dobler [205]*)

6.7.8 Long Upper Chambers - Hydraulic Behaviour

This chapter describes the transient flow behaviour studied for the long upper chamber of the *Krespa* surge tank and the looped upper chamber of the *Atdorf* surge tank.

Upper chambers are slightly inclined free surface flow tunnels. In contrast to lower chambers the occurrence of pressurized flow has to be avoided. The filling and emptying process is mainly driven by the inclination and the length of the tunnel. Since a higher inclination influences the gravity centre of the upper chamber it effects the mass oscillation and thus the volume demand of the surge tank. The steeper, the more volume is needed. At the end wall of the surge tank respectively at the aeration structure, a reflection of free surface waves takes place. The aeration structure has to prevent any overflow out of the surge tank system. Upper chambers in Austria are designed with sufficient reserve volume, even for extreme resonance load-cases [55]. The emptying process of the upper chamber will basically be accompanied by a waterfall at a specific time step. In superposition with the reflected wave, the waterfall will have a specific maximum impact. The wave reflection can be minimised by structural precautions such as steps or beams [206]. Moreover, an optimised inclination improves this behaviour. In case of the *Krespa* surge tank an inclination of 1.5 % was found to improve the surge wave behaviour with minimum reflection intensity and no flow blocking of the tunnel (Figure 6-61) [43]. This specific upper chamber has a length of 311 meters and an internal diameter of 7.0 m for a circular profile. It is filled with about 210 m³/s at peak inflow. An ideal inclination (variant B in Figure 6-61) could be evaluated by 1D- and 3D-numerical simulations. The inclination was confirmed by physical model tests. Additional deflectors were investigated (variant C). In case of the pilot study the deflectors were not found to be necessary. But for other chambers with significant surge effects deflectors may improve the transient filling. The demand for deflectors is to dissipate differentially by utilising higher losses at inflow and lower losses at outflow. Thus, the deflectors hydraulically perform best if constructed as segmental structures at the walls as “ears”, to keep undisturbed outflow for low water levels. A proposed deflector design is visualised in Figure 6-62.

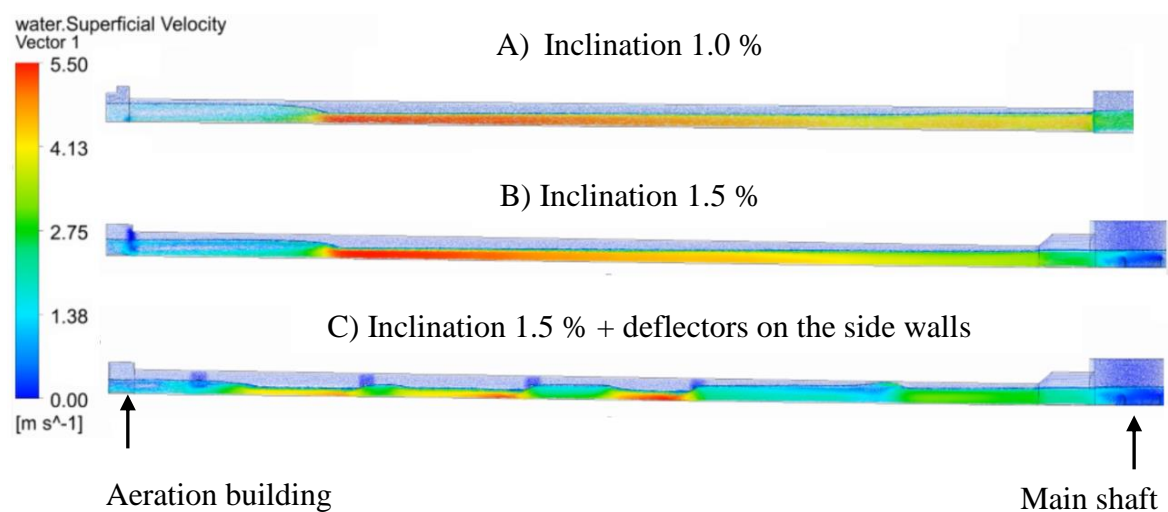


Figure 6-61: Filling of specific long upper chamber with surge reflection at aeration building with slope inclination of 1.0 %, 1.5 % and 1.5 % plus additional deflectors at the side walls (Richter [207])

RESULTS AND DISCUSSION

Figure 6-62 shows the filling and emptying improved by dissipators that are attached on the sidewalls. The dissipators only dissipate the flow above a certain level, allowing undisturbed and non-delayed outflow of the long chamber for low water levels. The dissipator design allows vehicles to drive through. The obstacles allow an equal water surface in transient filling. This feature was numerically tested in simulation prototype scale. It clearly shows the demands of dissipation and undisturbed emptying at low water levels in the upper chamber to avoid accumulating effects in case of resonance upper chamber load-cases. The dissipators are not attached in the front part of the upper chamber, in order to not create a flow blocking.

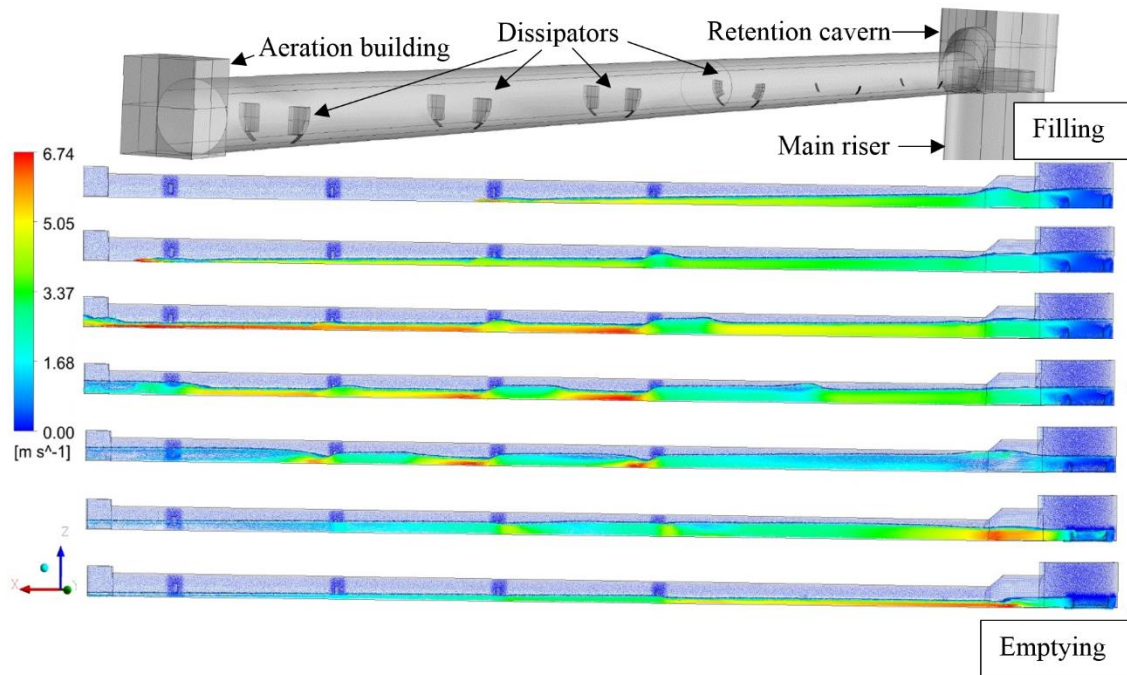


Figure 6-62: Long chamber filling and emptying improved by sidewall dissipators (*Richter* [117])

Some very large hydraulic power waterways may demand for very large surge tanks such as the investigated case study of the *Atdorf* PSH tailrace surge tank. This provides a gross surge tank volume of over 130,000 m³. The net water demand depends significantly on the design approach and may be much lower, since an upper chamber must not overflow and thus air volume has to be included as specifically defined. Lower chambers may additionally contain the demanded water at their invert to provide sufficiently low water velocity to avoid hydraulic jumps with undesirable air intrusion in case of outflow. A common longitudinal inclination of the invert is about 1.0 %. This is usually sufficient for the outflow. Especially, if a lower chamber is very long and large amounts of water have to be provided to the system a comprehensive design with adjusted inclination improves the hydraulic behaviour. Thus, a minimum water level is demanded to allow for sufficient flow capacity and can be quantified as dead water in sense of not active water volume for the mass oscillation. Especially for slightly inclined chambers with outflow at small water depths high velocities and unfavourable hydraulic jumps may occur. Such effects would intrude air into the system, which is unwanted.

The case study of surge tank *Krespa* shows an example of a very compact lower chamber design with three attached branches and large diameters of $3 \times D_i = 7.0$ m, that are vertically enlarged to 9.0 m and conical decreasing at the connection to the main riser. This inclination at the crown and the invert allows both a deaeration in case of up-surge event and a dewatering in case of

RESULTS AND DISCUSSION

unfavourable design down-surge. The chamber length is 70 m. Due to the large cross section the water level rises and falls very slowly allowing a high outflow capacity and avoiding any hydraulic jump. Thus, it is possible to design the chambers for complete emptying and avoiding dead water volumes. In this particular case the long connection shaft to the pressure tunnel serves as hydraulic safety volume. New surge tanks for large hydro schemes that contain significant water inertia to overcome in the power waterways may need to be designed uniquely for optimised volume demand. Surge tanks facilities are applied according to the needs of the specific demands of the power plants.

Figure 6-63 shows a detail of the upper chamber connection to the main riser of the *Atdorf* surge tank with flow retardation structure to improve the differential effect, a toy person in scale is visualizing the prototype size.

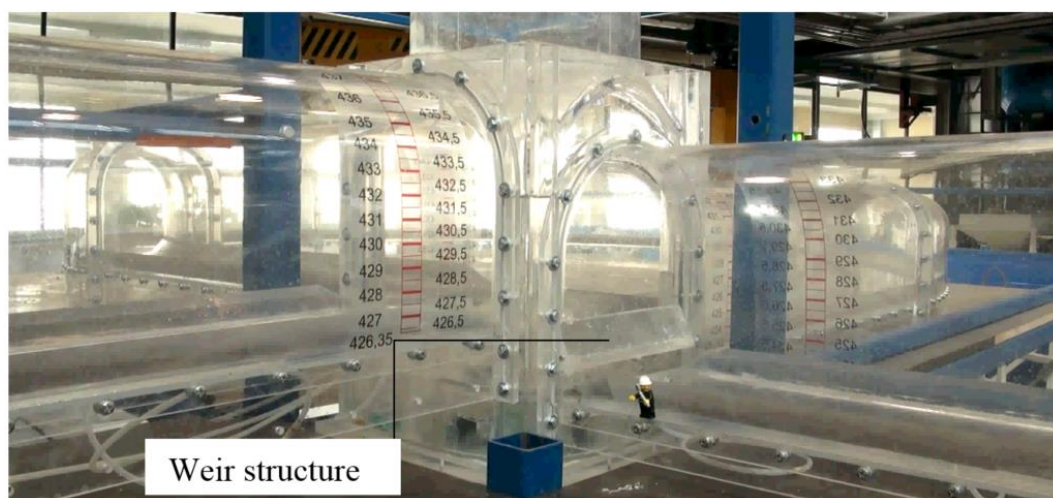


Figure 6-63: Chamber connection to the main riser for *Atdorf* surge tank model (scale factor 1:40), scaled human (*Richter* [106]))

RESULTS AND DISCUSSION

In case of the PSH *Atdorf* surge tank, a four-chamber arrangement, 8-loop shaped, both upper and lower chamber were tested. The two 8-loop shape chambers have four overflows into the main shaft. The entrance level of a single loop is lower as the exit level due to the helix geometry. Consequently, no filling surge is reflected at a structure but two confronting surge waves. This allows a moderate outflow of the upper chamber with a free surface flow and without large reflection waves [142]. Waterfalls intrude a massive amount of air into the main shaft. If the surge tank is designed with a moderate length flow-through lower chamber (about half of the chamber length) air bubbles can escape to the crown of the lower chamber.

Figure 6-64 shows the 3D-numerical simulation of the filling of the 8-loop upper chamber from two sides. The filling leads to an effective dissipation of the free surface flow to generate an equal filling without significant free surface waves of the long chamber. The observations from the 3D-numerical simulations were validated by the physical model test.

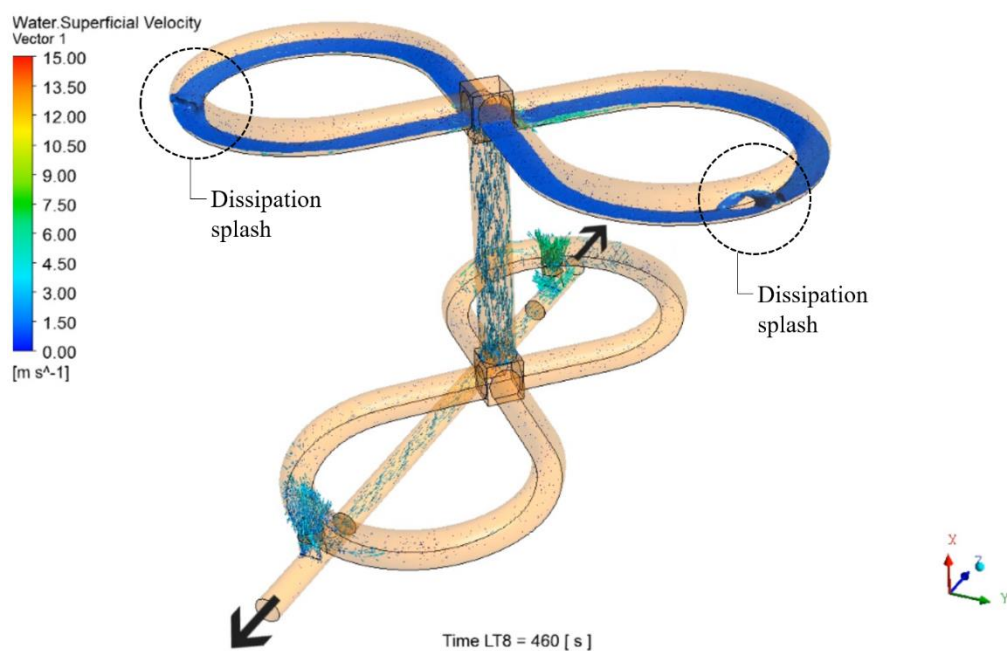


Figure 6-64: 3D-numerical simulation of the surge tank PSH *Atdorf*, upper chamber filling (Richter [142])

Long chambers may generate complex surface waves that must not lead to overflow or spilling at the aeration construction, thus a deflection plate is an effective structure to guide the waves back into the chamber (Figure 6-65). Figure 6-66 a) to d) visualises the functionality of the deflection plate at a transient filling of a curved long upper chamber. The surge wave is amplified by its flow into the chamber and splashes on the confining wall creating a significant vertical up-surge that is redirected by the plate into the chamber as a spill protection. The toy person, placed directly on the deflection plate, indicates the scale of the physical model test, in the particular case 1:25.

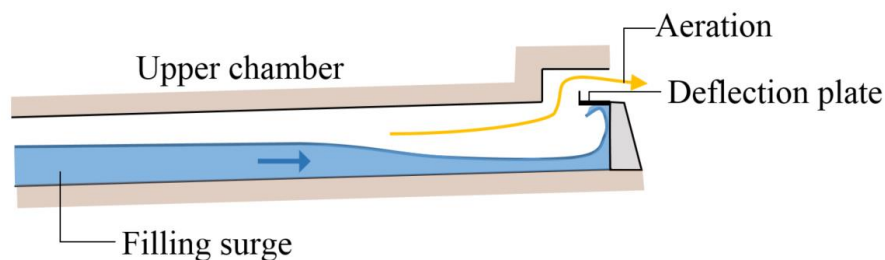
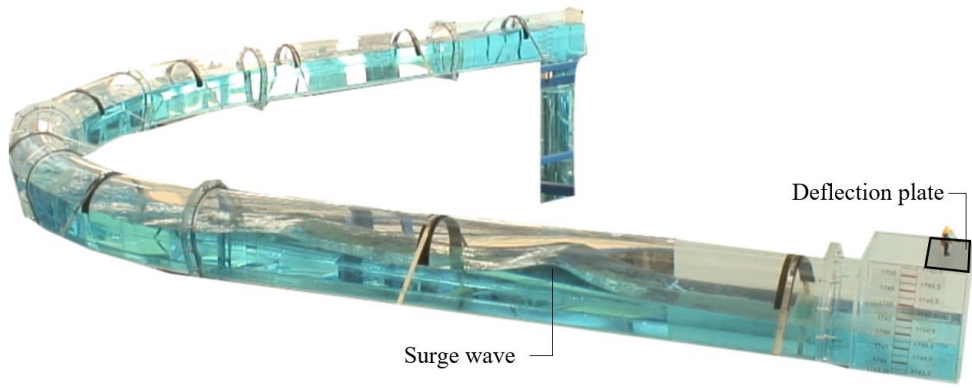
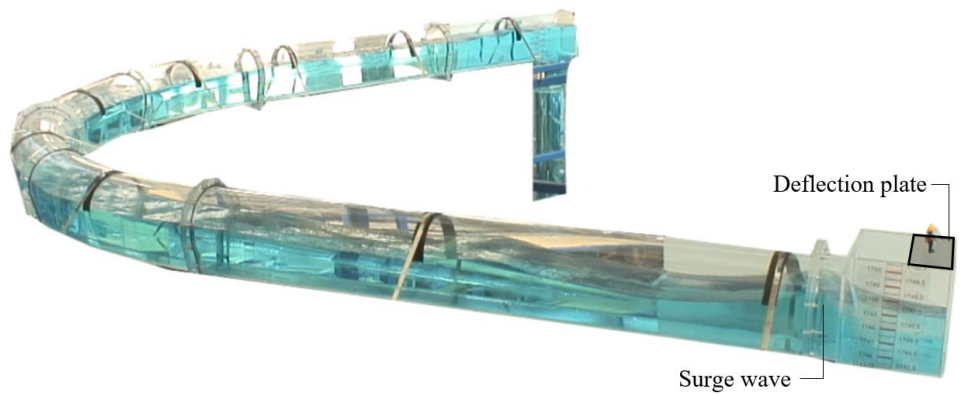


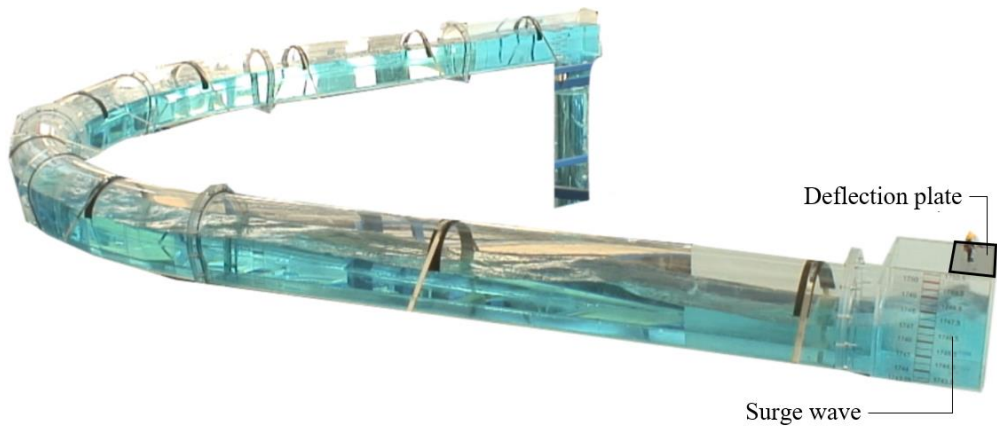
Figure 6-65: Long chamber spill protection by deflection plate



a) Long chamber spill protection by deflection plate, advancing surge wave



b) Long chamber spill protection by deflection plate, advancing surge wave



c) Long chamber spill protection by deflection plate, advancing surge wave, up-surge at wall

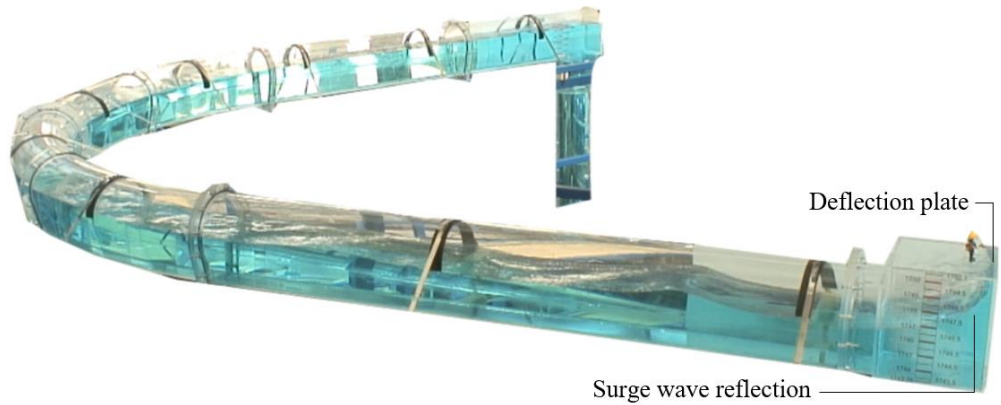


Figure 6-66: d) Long chamber spill protection by deflection plate, surge deflection by the plate (*Richter*)

6.8 Waterfalls in Surge Tanks

Waterfalls in surge tanks occur at upper chambers designed as slightly inclined free surface flow tunnels. These chamber constructions are filled at up-surge events. At the subsequent emptying of the chamber, the free surface discharge capacity will not fulfil the flow demand regarding the mass oscillation at a certain point. At this point of time, the flow separates at the transition from the shaft to the upper chamber and causes a waterfall. Concerning the mass oscillation, the separation functions as a dampening due to the retention of water in the upper chamber. Therefore, this is beneficial for the surge tank design. The dampening reduces the volume demand of the surge tank. Usually, the volume reduction will be more significant for the design lower chamber load-cases. Because of reduced time with full head in the surge tank after the filling event.

The challenge of a waterfall is the air intrusion into the water in the shaft. Air bubbles should not accumulate in the pressure tunnel or reach the machines. Figure 6-67 shows the situation of flow separation in the surge tank with waterfall and air intrusion. Figure 6-67 shows the principle of the de-aeration in the lower chamber if it is a flow through design. Air accumulates at the crown of the lower chamber and can then escape back into the riser. Model test investigations show, that a crown inclination of 2.0 % leads to a good behaviour for de-aeration. In comparison to that, Figure 6-68 visualises a surge tank with improved outflow of the upper chamber. The waterfall will still appear but less intensive. The head of the surge tank is ΔH higher than for the surge tank with separation. This ΔH additionally accelerates the backswing from the surge tank to the upper reservoir. Subsequently the outflow of the surge tank will be higher as the damped one with the waterfall. This will result in a higher volume demand and more complex geometry. If in resonance load-cases at drawdown level the upper chamber partly fills, the separation can significantly improve the dampening of the mass oscillation. In case of large surge tanks, this effect is very important to be utilised. Figure 6-68 visualises a smoother transition of the upper chamber into the main shaft. This may mitigate the waterfall appearance but cannot completely avoid it.

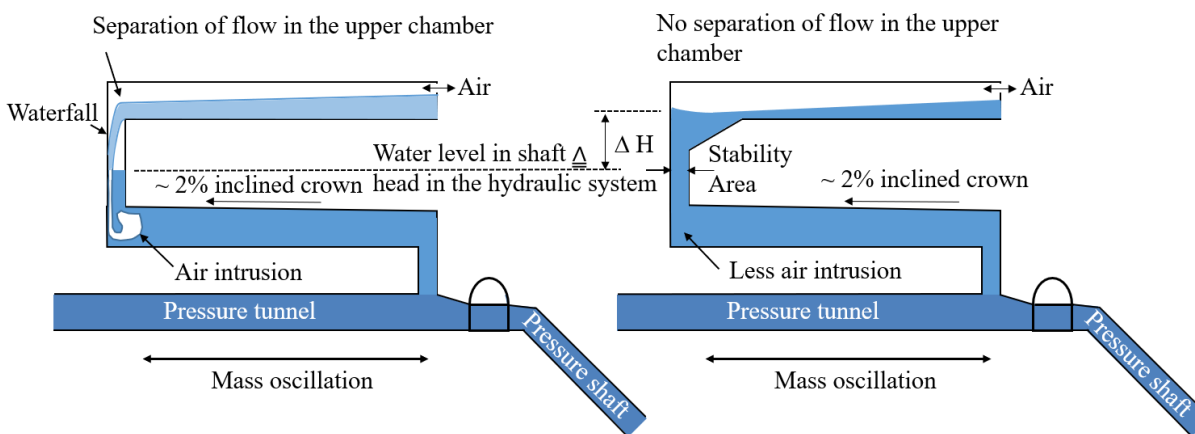


Figure 6-67: Chamber surge tank with flow separation and waterfall intruding air into the water cushion (scheme). Positive regarding mass oscillation dampening.

Figure 6-68: Chamber surge tank with mitigated flow separation due to outflow optimization (scheme). Less separation is negative regarding mass oscillation dampening.

RESULTS AND DISCUSSION

For any kind of upper chambers made as tunnels, a flow separation may appear. Chambers would need to be very steep to avoid waterfalls and thus would lose the upper chamber effect and would need more excavation volume. A compact upper basin with steeply inclined inverts may allow emptying without waterfall, such as visualised in Figure 6-69 and Figure 6-70. However, such an upper basin also requires more volume as a well-designed upper chamber allowing a waterfall. The advantage of design in Figure 6-70 compared to Figure 6-69 is the direct water hammer reflection in the shaft.

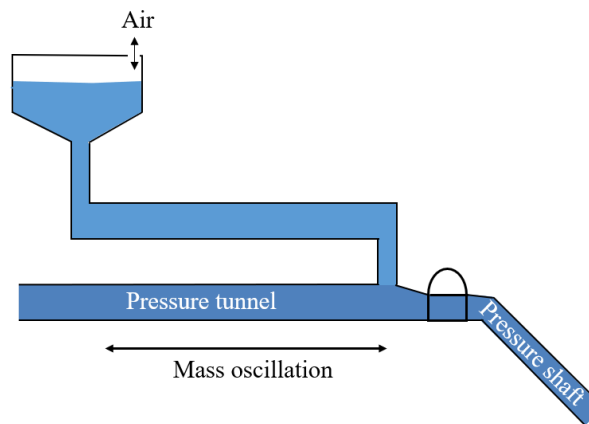


Figure 6-69: Compact upper chamber to avoid waterfall occurrence, with lower chamber inertia

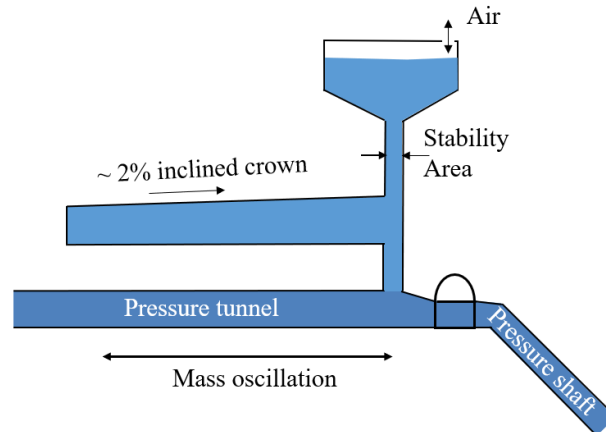


Figure 6-70: Compact upper chamber to avoid waterfall occurrence, without lower chamber inertia

6.8.1 Air Bubble Entrainment

In case of the *Krespa* surge tank the air bubble behaviour was intensively studied to predict the impact of the design waterfall case. These studies, in addition to the conclusions made by the physical model test of the *Atdorf* surge tank were the basis for the development of the waterfall-dampening device described in section 6.8.7. In the following, the creation of air entrainment is briefly discussed. Two ways of possibilities to entrain air by a plunging jet into a water body are described by *Danciu* [208]:

1. Between the rough wavy boundary of the jet and the waves at the surface of the water body air pockets are trapped (Figure 6-71)
2. At jet submergence into the water small air pockets are created that collapse with high frequency and are dragged down into the water (Figure 6-72)

The buoyancy force and the drag forces act on the air bubbles. The bubbles are also deformed such as compressed or expanded, thus the forces on single bubbles are varying very significantly. For the air intrusion depth, it is not possible and not meaningful to evaluate a single bubble. Essentially the maximum intrusion depth is investigated. Studies for the surge tank behaviour are made by utilising literature and via 3D-numercial simulations. In addition, coalescence (confluence of colloidal particles) causes the merging of small single bubbles into larger bubbles. This reduces the surface area, causing larger bubbles to rise faster. On the one hand, the lower surface generates less friction loss, and on the other hand, a larger volume creates a larger buoyancy component. However, this positive effect is neglected in the consideration of the degassing studies for surge tanks.

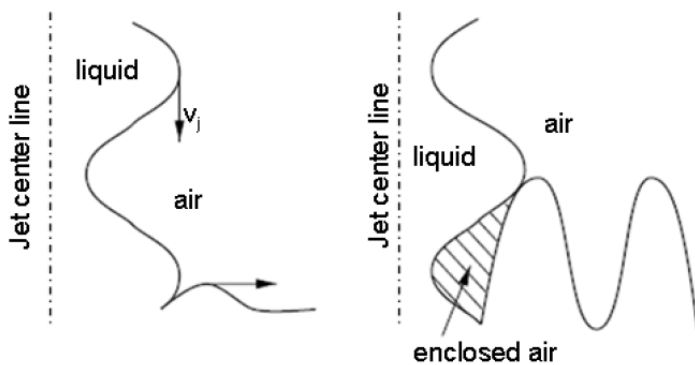


Figure 6-71: Air entrainment mechanism (1), inclusion of air packets by contact of wave peaks of the water cushion and the jet (figure from *Danciu* [208])

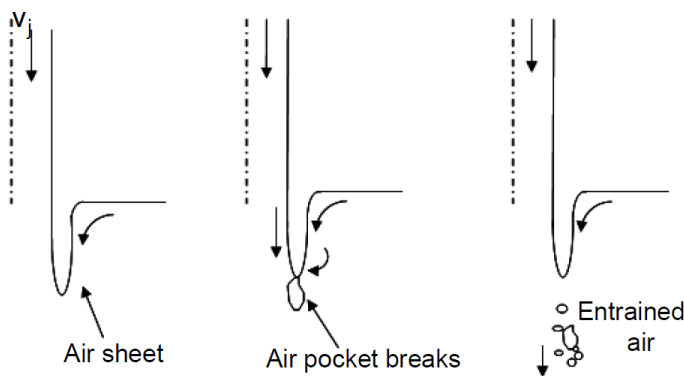


Figure 6-72: Air entrainment mechanism (2), inclusion of air packets due to surface tension effects (figure from *Danciu* [208])

RESULTS AND DISCUSSION

The goal of the surge tank design is to find robust solutions for a complex issue such as air bubble behaviour. The following list explains the most important processes of air intrusion by waterfalls in surge tanks and the de-aeration mechanisms. It identifies also aspects that are not considered for the surge tank design, for reasons of providing a conservative engineering approach.

- Vertical impulse of the jet; most important negative component
- Vertical terminating velocity of the single bubble; most important positive component
- Single-bubble compression; negative because of decreased terminating velocity component; not considered in simplified approach; covered by safety factors
- Solution of air in the water; positive; not considered
- Coalescence; positive; not considered
- Rotational flows; negative; can be very complex and therefore difficult to calculate. At *Kopswerk II* a flow calming rack was designed to mitigate the rotation flow for this aspect [209]
- Deformation of the single bubble; negative in principle; not considered, because hardly detectable
- Separation of the jet and formation of water packages; positive, not considered for design cases because the falling height is too small for the separation of the entire waterfall. However, this effect provides security in load-cases with a low water level in the riser shaft with high falling heights of the waterfall.

The waterfall in a surge tank will be an aerated jet at a certain falling height, depending on the discharge and on the Rayleigh-Taylor instability [210]. The jet will disperse into large and small packages of water that hit the water surface like bullets. It is assumed that the air intrusion mechanism (2) is formed by dragged cavities that enclose air and are being pushed into the water body (Figure 6-73) [208].

Water packages create voids in the water cushion which quickly close, but producing air pockets forming the bubbles. Considering the more unfavorable air intrusion depth by a demolished jet means to start from a lower penetration depth than a continuous jet. Rather large flows at relatively small drop height tend to be the worst case for the air intrusion depth. This aspect is the reason for the design waterfall case used for the specific waterfall-dampening device for the *Krespa* surge tank (Chapter: 6.8.7).



Figure 6-73: Air bubble intrusion mechanism of a single jet (*Danciu* [208])

6.8.2 Numerical Simulation of Waterfalls

This chapter describes the waterfall simulation approach for the pilot surge tank *Krespa*. To find the design waterfall load-case for the mass oscillation events, different reservoir heights were investigated regarding resonance flow in the pressure tunnel. A crucial influence for the waterfall for long single chambers is the reflected surge wave at the rear wall of the chamber. The design value is the reflected surge wave back to the edge entering the main shaft. A major question was, if either low drops with high waterfall discharge or high drops with low waterfall discharges are more unfavourable regarding the air intrusion depth. By the investigations, it was finally concluded that low drops with high discharge are representing the suggested design approach. Low dropping heights are associated with higher discharges, since the chamber is still quite full, and thus higher values of water-air interaction boundary size. This leads to higher quantities of relative air transported by the impulse of water jet and jet velocity compared to the situation with high dropping heights and less water quantity. Therefore, a design drop height between 3.0 to 5.0 m was defined for the specific waterfall load-case. This event was furthermore investigated both in physical small-scale model tests and 3D-numerical simulations. Figure 6-74 shows the 1D-numerical simulation of the surge tank with long upper chamber in the case of a reflected surge wave at the upper chamber. At the peak discharge of the upper chamber a waterfall of about 84 m³/s occurs and drops into the shaft. By accounting for smooth tunnel friction, implemented in the mass oscillation simulation, this value contains a sufficient amount of safety. The free surface flow was simulated with free surface pipe elements in a 1D-numerical simulation approach and was confirmed by the physical model test.

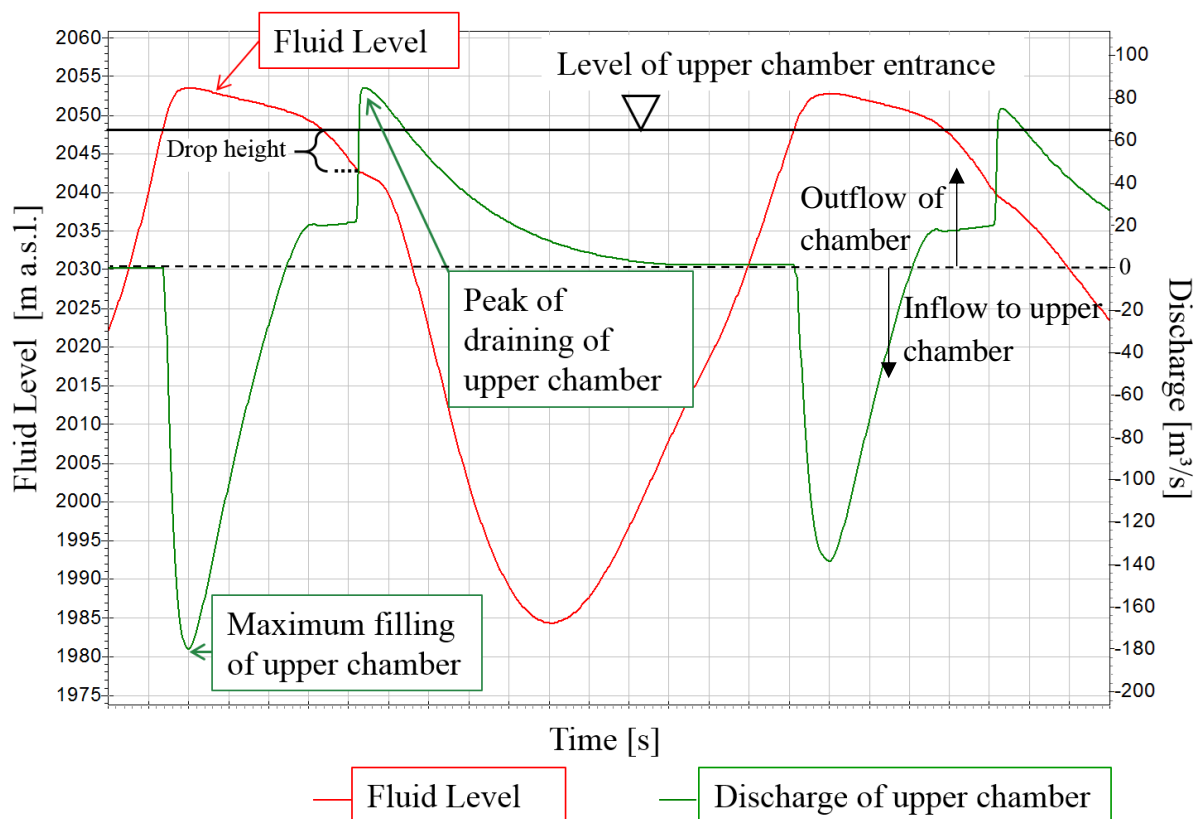


Figure 6-74: 1D-numerical simulation of the upper chamber behaviour for the waterfall occurrence at the *Krespa* surge tank (Richter [43])

RESULTS AND DISCUSSION

The 3D-numerical simulations were done to investigate the maximum air intrusion depth, since the air bubble behaviour is not represented by Froude similitude physical model tests. In addition, the physics of the air entrainment itself cannot yet be modelled directly with the help of 3D-numerical simulations utilising the RANS approach for an engineering approach. The aim of the calculations was both the representation of the transient flow as well as the hydraulic behaviour of the waterfall dropping into the shaft. To find the maximum air intrusion depth, the velocities of the dissipating jet in the water are compared with literature values of the terminating velocity of air bubbles. Design assumption: As design air bubble terminating velocity a value of 0.2 m/s was chosen. It can be assumed that the maximum intrusion depth of the waterfall is in balance of the terminating velocity of the bubbles versus the degrading waterfall jet, also reaching the same value of 0.2 [m/s] [211]. The jet degradation in the air and the effects of the density impact of the bubble flow are neglected for this specific 3D-numerical investigation, since this was technically not possible to simulate this with the given computational power and resolution. The method can therefore be seen as an engineering approach. The results of the simulations were compared with the data of the air intrusion depths for water jets given by *Ervine and Falvey and Falvey* [212]. To investigate the further behaviour of the air bubbles after these are pushed downwards by the water jet at the maximum depth a kinetic coupling of the flow properties of the mass oscillation process in the surge tank was applied by a 1D approach. Therefore, the terminating velocity of the air bubbles and the downward velocity in the main shaft were compared to find the maximum possible downward drag of air bubbles. The waterfall discharge was modelled by transient 3D-numerical simulations. Figure 6-75 shows a particular timestep with the intruding water fall of 63 m³/s and a falling height of 15 m and a measuring plane 62 m below the water surface. The boundary conditions were given by the results of the 1D numerical simulation, imposed as free surface flow in the upper chamber and the outflow of the main riser.

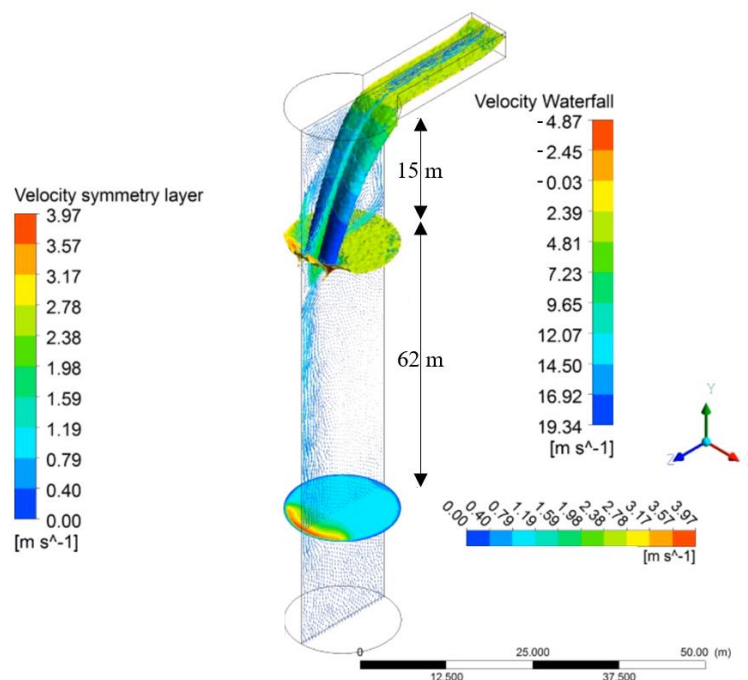


Figure 6-75: 3D-numerical waterfall investigations without dampening device (*Richter* [43])

The jet intrusion depth was visualised by the flow velocity fields in the symmetry layer of the main shaft. Figure 6-75 indicates the velocities of the waterfall that has reached 19.34 m/s when

RESULTS AND DISCUSSION

entering the water surface at the certain simulation time. The horizontal layer in the shaft shows an increased vertical down-warded velocity of 3.97 m/s, indicating the intruding water fall and due to high local velocities also an intrusion of air bubbles. The 3D-numerical simulation (Figure 6-77) visualises the outflow of the upper chamber creating the plunging jet by column separation. The 3D-numerical simulation in Figure 6-77 shows the waterfall with the not-to-scale air bubble representation. This behaviour may lead to a significant underestimation of an air intrusion depth in Froude similitude model tests. Figure 6-78 shows the 1D-numerical time plot of the water level in the surge tank (red line) and the steadily degrading water level at the upper chamber crest (green line).



Figure 6-76: Waterfall in physical model test without dampening device (*Richter* [43])

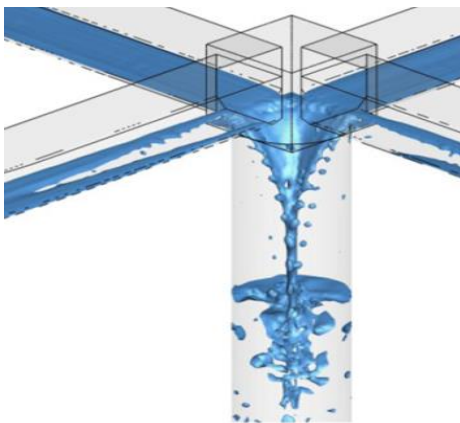


Figure 6-77: 3D-numerical simulation, visualising the waterfall occurrence with flow separation at upper chamber (*Dobler* [106])

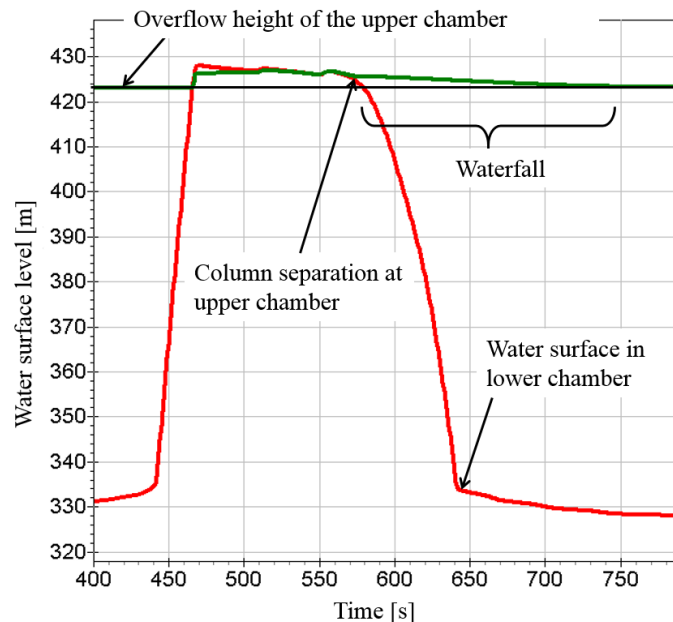


Figure 6-78: 1D-numerics including the separation of columns and waterfall discharge into shaft, water level surge tank (red line) and water level at upper chamber crest (green line), (*Richter* [106])

6.8.3 Criterion of Similitude of Air Intrusion

Air bubbles are not directly scaled in the physical Froude scaled model test, the bubbles are represented too large in terms of the model scale factor. A higher buoyancy of the individual bubble is the reason of quicker terminating velocity. In principle, it can be assumed that air bubbles are pushed into the water body by the water jet down to the water depth where the balance between the terminating velocity of the bubble and the penetration speed of the jet is given [211]. From this comparison, it can be concluded that the air penetration depth of a vertical water jet in the Froude scaled model test is too small. The factor of discrepancy can be quantified by the Froude velocity factor. For the surge tank *Krespa*, this results in an air penetration ratio of $\sqrt{30} = 5.48$ [-] between model test and prototype. With this factor, the penetration depth of air bubbles in the prototype can be estimated from the model experiment with a vertical waterfall.

6.8.4 Terminating Velocity of Air Bubbles

For the air terminating velocity, a design bubble diameter of 6.0 mm diameter was used in the presented investigations. It refers to a local minimum of air bubble terminating velocity (Figure 6-79). The 6.0 mm bubble refers to a terminating velocity of 0.2 m/s. This is more conservative as the 0.25 m/s suggested by *Ervin and Falvey* [212].

Figure 6-79 shows the air terminating velocity of single bubbles in distilled and contaminated water. It can be seen that air bubbles rise faster in distilled water than in contaminated water. It can be assumed that the water conditions for the pilot case surge tank are somewhere between the two lines. It can also be seen that air bubbles up to 1.0 to 2.0 mm diameter are also captured with the terminating velocity of 0.2 m/s. Thus, the value of 0.2 m/s contains a safety aspect.

The local minimum for air bubbles in the order of 6.0 mm results from the deformability of their shape and the resulting reduced terminating velocity. Images of the high-speed camera on the physical surge tank model show that air bubbles in this size range are very deformable.

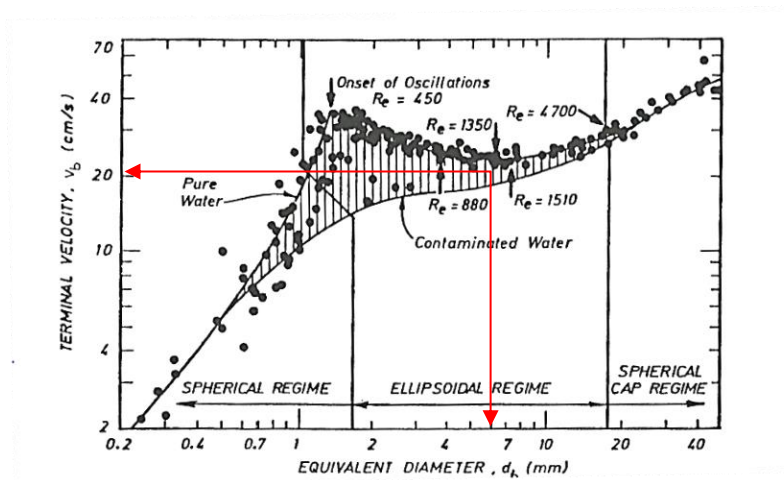


Figure 6-79: Terminating velocity of a single air bubble (figure from [213])

6.8.5 Methods for Determining the Air Penetration Depth

This chapter describes how to assess the air intrusion depth for a waterfall in a surge tank.

For the determination of the penetration depths of circular water jets, which are determined under laboratory conditions, many publications are available, such as *Clanet and Lasheras* (1997) [211]. For their investigations, which were carried out under laboratory conditions, the extrapolated value for waterfalls with considerably larger jet diameters is discussed.

Related investigations are presented by *Ervine and Falvey* [212]. In this case, both the behaviour of the jet in the air and its dissipation in the water are considered. Important for the determination of the air penetration depth is a diagram with data from *Vigander* [212], which were compared in the following with the results of *Clanet and Lasheras* [211].

Until now, it was not possible to use 3D-numerical methods to model the physical process of entraining air by a plunging jet penetrating free water surface. Therefore, the findings from the literature study were used to obtain information about an air penetration depth directly from a 3D-numerical flow simulation that calculates the water jet velocity decay in the water. Two-phase simulations were performed, with the waterfall forming the jet accelerated by gravity, falling into a sinking water level in the surge tank due to transient mass oscillation (see chapter: 6.8.2).

6.8.5.1 Equation of *Clanet and Lasheras*

The determination approach developed by *Clanet and Lasheras* [211] describes a relationship between the jet diameter, the jet velocity, a 12.5 ° aperture angle of the penetrating jet, and the design bubble size. The equations are proposed for the average penetration depth and a maximum penetration depth, considering fluctuations.

$$\frac{H_B}{D_{\text{jet}}} = \frac{1}{2 \tan \alpha_{\text{jet}}} \frac{v_{\text{jet}}}{u_B} \quad (6-1)$$

$$\frac{H_B}{D_{\text{jet}}} = \frac{1 + \tan \alpha_{\text{jet}}}{2 \tan \alpha_{\text{jet}}} \frac{v_{\text{jet}}}{u_B} \quad (6-2)$$

Equation (6-1) describes the mean or standard air bubble penetration depth and equation (6-2) the air penetration depth considering fluctuations.

H_B	...	Air bubble penetration depth
D_{jet}	...	Jet diameter entering the water cushion
α_{jet}	...	Opening angle of a waterfall jet dissipating in the water
v_{jet}	...	Jet velocity at water surface
u_B	...	Terminating velocity of a single bubble

The investigations of *Arch* (2008) [143] show an average terminating velocity of about 0.19 m/s, that was determined in tailwater canals of Pelton turbines. This corresponds well to the 6.0 mm bubble diameter approach of 0.2 m/s.

RESULTS AND DISCUSSION

It should be noted that the terminating velocity may be significantly influenced by turbulence or rotational flow. Under such boundary conditions the problem becomes more complex. For investigations on a shaft of a surge tank with a large shaft cross section ($D_{\text{shaft}} / D_{\text{waterfall}} < 10$) these influences are neglected.

6.8.5.2 Experimental Air Intrusion Depth by Ervine and Falvey

The determination of air intrusion depth developed by *Ervine and Falvey* (1987) [212] describes the influence of the degree of turbulence of the ruptured jet in free fall and the theoretical angle of the dissipating jet in the water. The design of the final air penetration depth of a jet or a waterfall can be determined using the diagram in Figure 6-80. On the x-axis, the ratio of the velocity of the penetrating jet and the air terminating velocity is given. By intersecting with an upper measured value, the ratio of the air penetration depth to the jet diameter can be determined. If the jet or waterfall diameter is known, this results in the penetration depth of the air bubbles. The jet diameter can be estimated by the continuity condition.

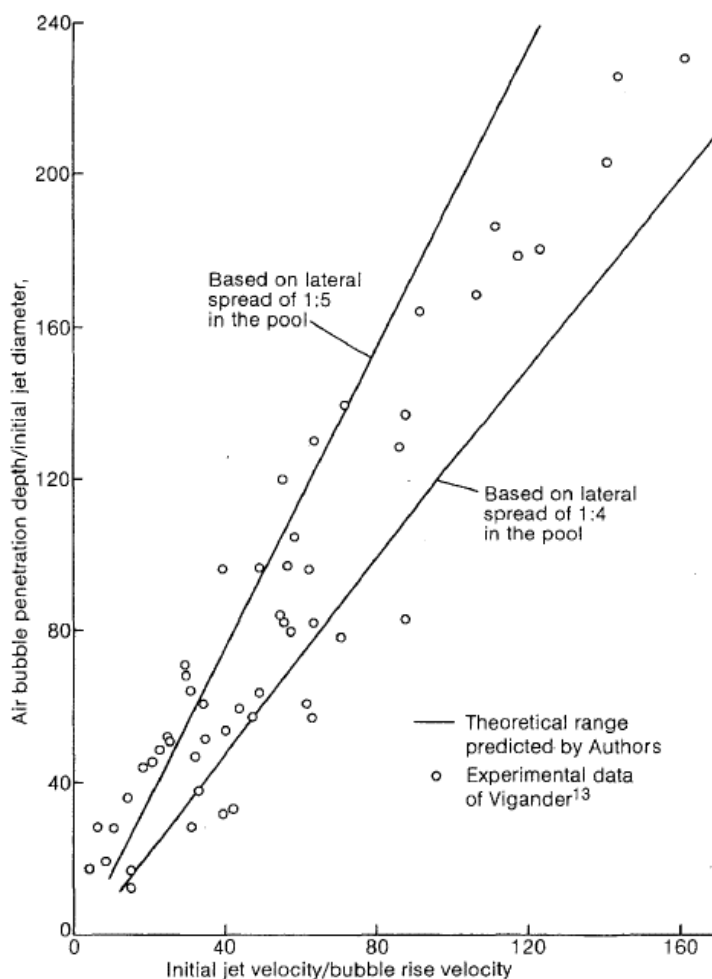


Figure 6-80: Air intrusion depth in an unconfined pool with bubble terminating velocity of 0.25 m/s, key figure of the *Ervine and Falvey* publication, (figure from [212])

6.8.5.3 3D-Numerical Simulation of Waterfalls

Up to now, it has not been possible to directly model the air bubble intrusion process utilising a multiphase 3D-numerical simulation. However, single-phase 3D-numerical simulations are able to predict the intrusion depth for vertical jets. The relevant information from the 3D simulations is the decay of the jet velocity in the water by dissipation. The intrusion depth is given at the balance of the terminating velocity of the design bubble and the associated velocity of the jet.

Clanet and Lasheras [211] describe the balance of the terminating velocity of the single bubble and the downward velocity of the jet in the water. The air bubbles are injected as deep as the velocity of the penetrating jet has decreased due to the dissipation in the water to that of the bubble terminating velocity. This criterion was used to compare the air intrusion depth with the results of the 3D-numerical simulations. The acceleration of the waterfall is described via the *Toricelli* equation:

$$v_0 = \sqrt{2gH} \quad (6-3)$$

H ... Falling height [m]
g ... Gravity [m/s²]

After only a few meters of falling height, the waterfall is considerably accelerated. In combination with the jet diameter and the relationships (6-1) respectively (6-2) the air penetration depth can be calculated. The disadvantage is that the falling water, due to its physical properties, tends to concentrate in a compact jet. This behaviour and the dissipating jet in the water cushion are evaluated using two-phase 3D-numerical simulation.

The calculations are performed with *Ansys CFX*. Utilising a two-phase model with water and air temperature of 25 °C, the SST turbulence model, unstructured tetrahedral mesh, time step of 0.2 s, considering gravitation, standard free surface model, surface tension of 0.073 [N/m], Laplace Volume Fraction Smoothing (Figure 6-75).

6.8.5.4 Hydraulic Froude Scale Model

In the hydraulic model with Froude scaling, the flow velocity of the fluid is slower by the square root of the model scale factor. Air bubbles, which are formed through an intruding water jet, have a similar size as in the prototype with a diameter of about 5-6 mm. Thus, the same terminating velocity of the prototype is created in the hydraulic model test and is therefore relatively too fast. This is clearly on the unsafe side and has to be considered by appropriate assumptions.

RESULTS AND DISCUSSION

Figure 6-81 shows the comparison between the 1D-numerical simulation of the mass oscillation case that causes a waterfall into the main shaft of the surge tank *Krespa*. The first peak at around 90 seconds represents the maximum up-surge by starting the pumps; the second peak at around 325 seconds refers to the resonance load-case of shifting pumps and turbines at a specific time in order to maximize the acceleration of the flow in the pressure tunnel.

Due to a large diameter and high amounts of water at the waterfall a significant intrusion depth was found in the 3D-numerical evaluations as well as the waterfall calculations comparing with the literature [212]. The coupling of the intrusion depth with the velocities from the mass oscillation in the surge tank showed that structural precautions need to be taken into consideration in order to avoid air bubbles in the pressure tunnel. It was found that the influence from the lower chambers on the degassing behaviour of the shaft can be neglected.

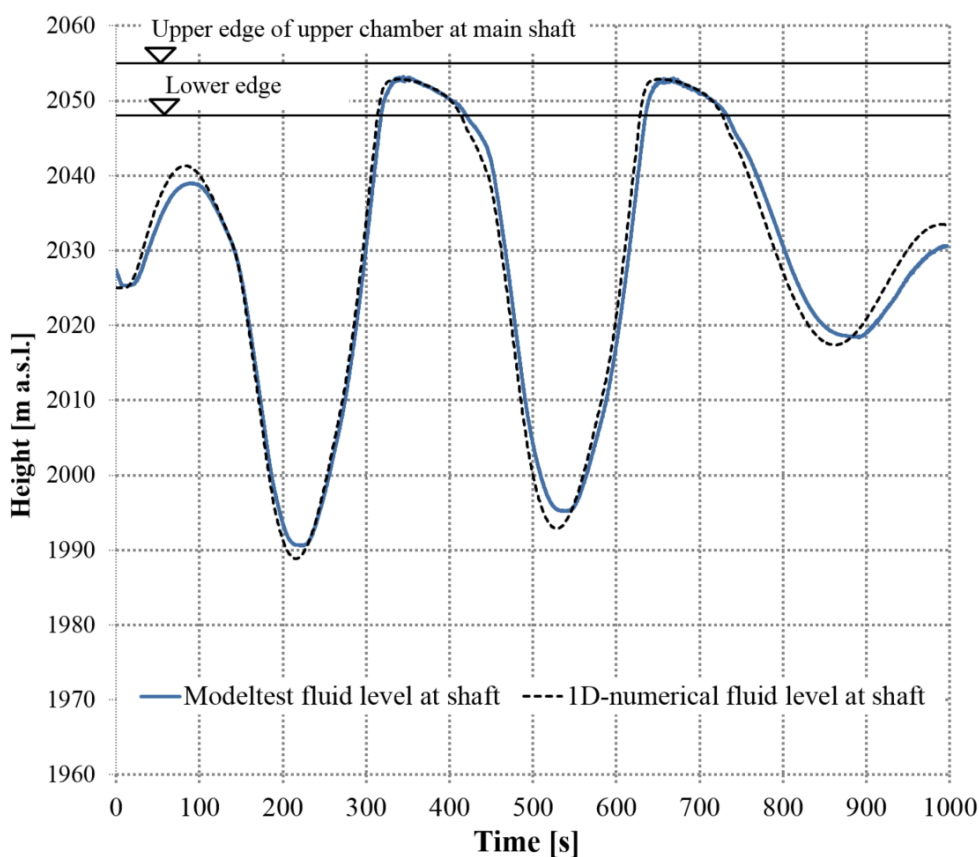


Figure 6-81: Comparison of the 1D-simulations and the physical model test of the waterfall design load-case (*Richter* [43])

RESULTS AND DISCUSSION

Figure 6-82 visualises the comparison of the evaluations of *Clanet and Lasheras* [211], *Ervine and Falvey* [212] and the results from the 3D-CFD simulations regarding the waterfall. The investigations of *Clanet* took place in laboratory size and show a linear relation between jet dimension and intrusion depth while the prototype scale measurement data from *Ervine and Falvey* [212] show a decrease of the intrusion depth with increasing jet velocities. The evaluated data from the 3D-numerical simulations for high velocity jets confirm the results in the range of the data according to *Ervine and Falvey* [212].

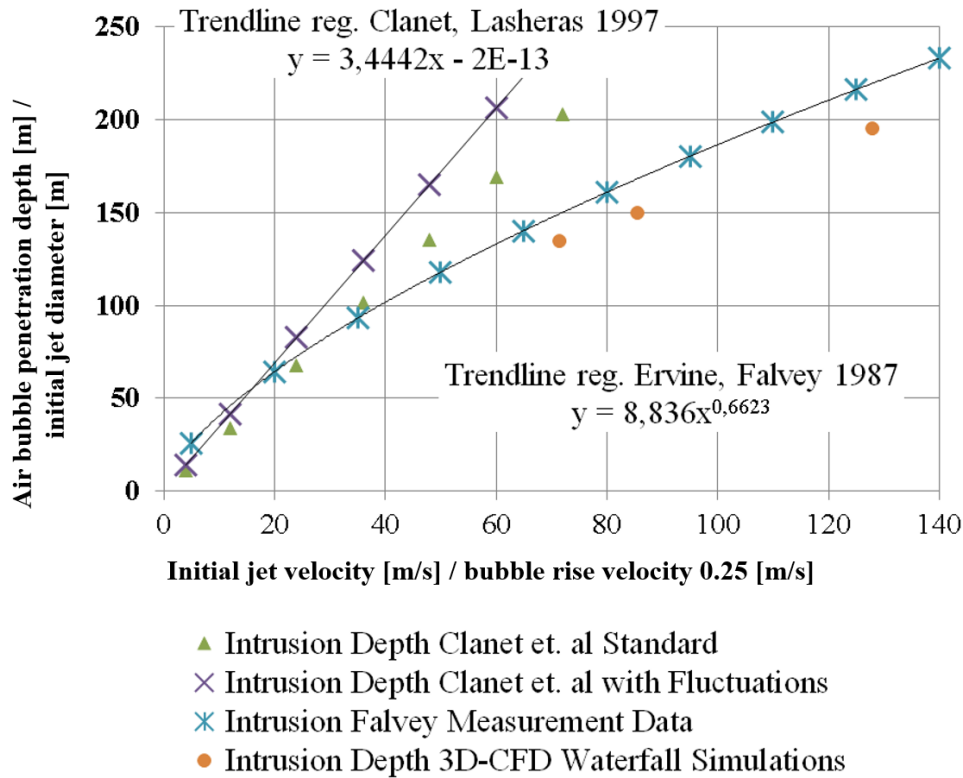


Figure 6-82: Evaluation of Air intrusion depth by water jet, Results from *Clanet and Laheras*, *Ervine and Falvey* and CFD simulations (*Richter* [43])

6.8.5.5 PIV Measurements of Air Intrusion Depth

PIV measurements were carried out to measure the bubble intrusion and terminating velocity in the Froude scale model to evaluate the theory and the air intrusion depth by utilising the hydraulic small-scale model of the surge tank *Krespa*. The investigations were done with and without the waterfall-dampening device by the Master theses of *Ruetz* (2014) [214] and *Urach* (2015) [215]. *Ruetz* did the investigations at a low drop height. *Urach* at a high drop height. For both investigations a rectangular, water filled PIV box was installed to compensate the refraction of the curved main shaft of the surge tank. The investigations of the waterfall into the surge tank were done at steady-state flow conditions. A main question was to evaluate the worst case that can appear in the specific prototype and in general surge tank waterfall situations. The two maximum cases of waterfall conditions were defined as described in section 6.8.7.

In contrast to the most unfavourable resonance load-cases defining the upper- and lower chamber design volume, these waterfall load-cases were in-between. Thus, the design level had to be found manually. PIV measurements were done in Froude scale physical model test investigation to evaluate the mitigated air intrusion depth by the waterfall-dampening device [214] and [215]. The plunging single jet creates a heavily disturbed water surface intruding significant amount of (Figure 6-83). Figure 6-84 visualises the results from PIV for the situation visible in Figure 6-83. It shows and confirms the instantaneous velocities for the up-warded flow and thus indicates the bubble terminating velocity and its reverse at about -0.2 m/s.

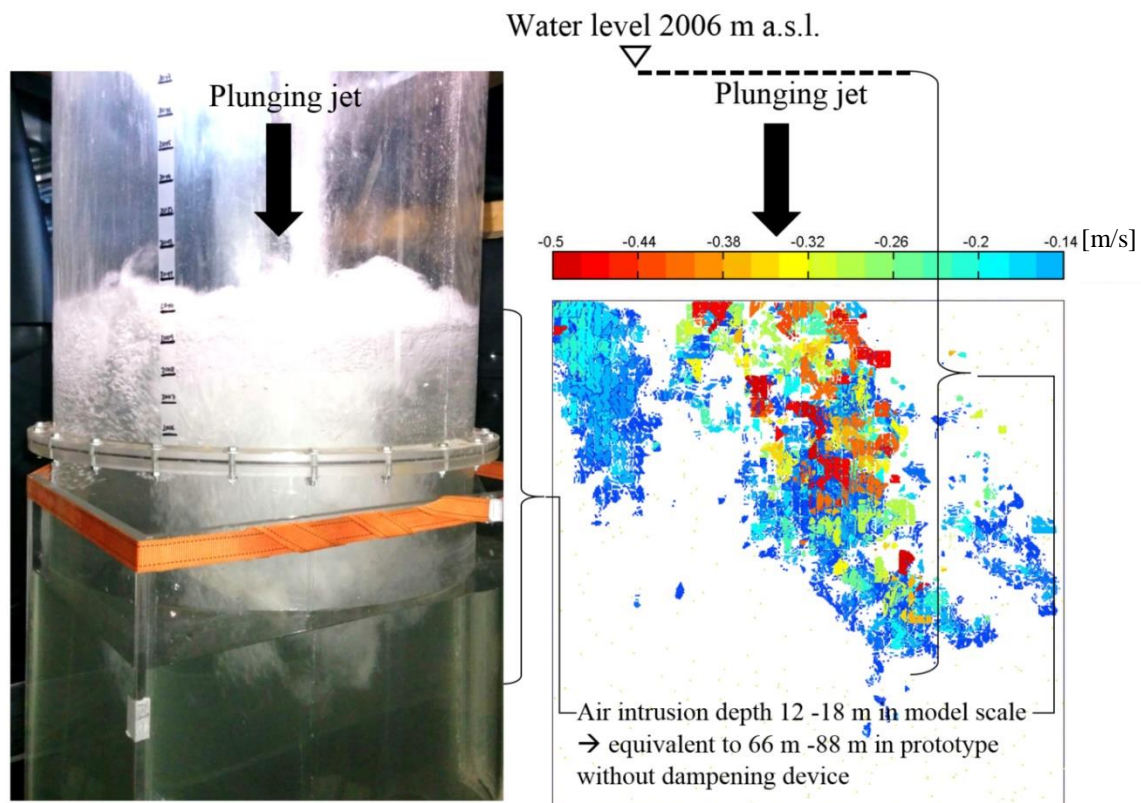


Figure 6-83: Air intruding plunging jet at physical model without dampening device (*Urach* [215], modified)

Figure 6-84: Terminal air bubble PIV velocity measurement at *Krespa* surge tank without dampening device (*Urach* [215], modified)

RESULTS AND DISCUSSION

Figure 6-85 visualises the result from the PIV measurements in the jet plane without the dampening device, representing the concentrated waterfall event. Figure 6-86 shows the air intrusion depth at the main shaft by utilised waterfall-dampening device that significantly mitigates the air intrusion depth by dividing a single concentrated jet into several defined small jets similar to a showerhead outflow.

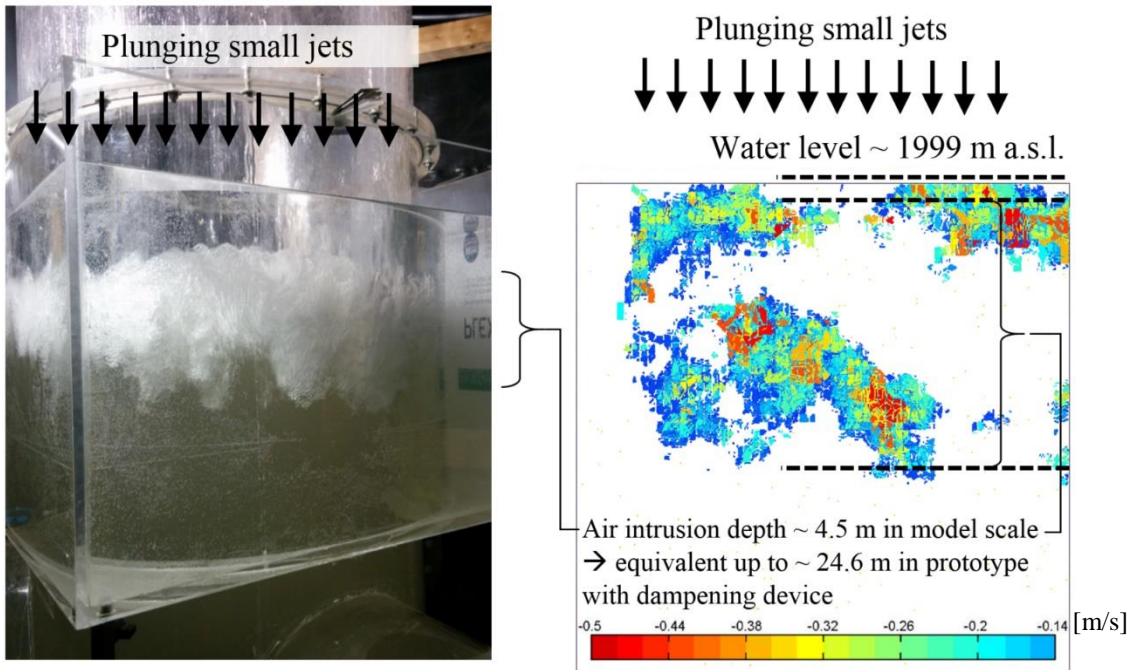


Figure 6-85: Air intruding plunging jet at physical model test with utilisation of the dampening device, (Urach [215], modified)

Figure 6-86: Terminal air bubble PIV velocity measurement at surge tank with dampening device, (Urach [215], modified)

RESULTS AND DISCUSSION

Figure 6-87 shows the PIV box with laser sheet in case of low drop water jets and the result of the PIV measurements at the maximum bubble intrusion depth for the particular case indicating the terminating velocities of the bubbles and the flow field in the section cut.

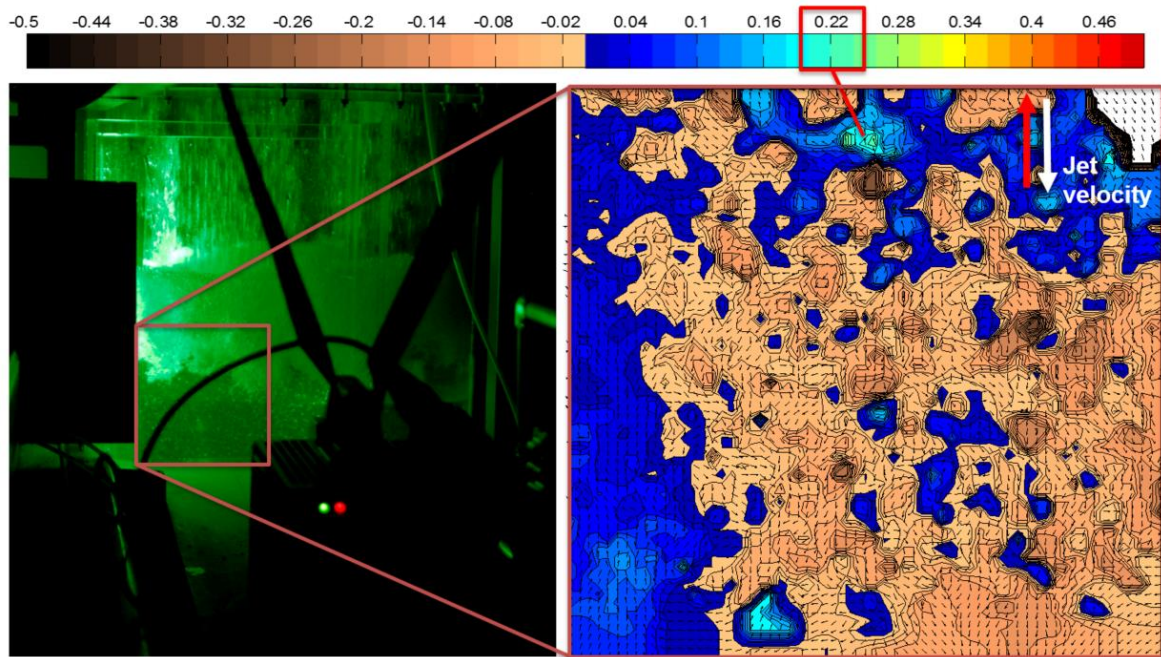


Figure 6-87: Terminal air bubble velocity at Krespa surge tank with the dampening device (*Ruetz* [214])

6.8.6 Air Detrainment in 3D-numerical Multi-phase Simulation Approach

This chapter briefly describes the approach of modelling the air bubble behaviour in terms of 3D-numerical simulations the *Atdorf* surge tank. Figure 6-88 shows the implementation of the terminating velocity of air bubbles in *Ansys CFX* compared to the measured terminating air bubble velocity from literature. Due to the non-spherical bubble shape of air bubbles for the size range between about 1.0 mm to about 10 mm the terminating velocity is decreasing. The *Grace Correlation* [216] accounts for this aspect in the software. A design bubble diameter of 6.0 mm was used and shows to be a useful design approach in a 3D-numerical simulation, since the terminating velocity of this bubble size has a local minimum and thus is conservative. Additionally, the drag force influences the bubble behaviour in the water. The approach applied is the *Schiller-Naumann* drag behaviour [217].

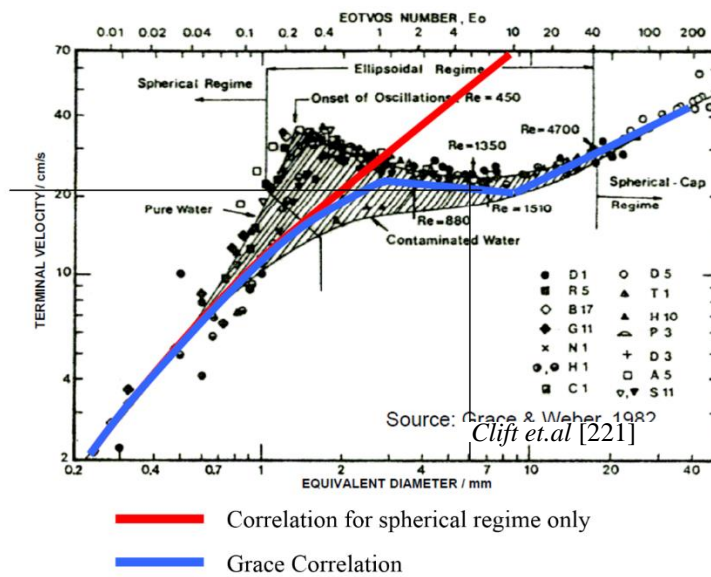


Figure 6-88: Terminating air bubble velocity, implementation in *Ansys CFX*, (figure from [216])

Since no direct air bubble production was found possible, the air bubble fraction is defined for the specific approaches in terms of the void fraction factor. For the surge tank *Atdorf* the air bubble fraction was defined for the investigations as 10 % in combination with the transient discharge in the shaft as a result from the 1D-numerical simulation for the design load-case with the maximum discharge through the lower chambers (Figure 6-89).

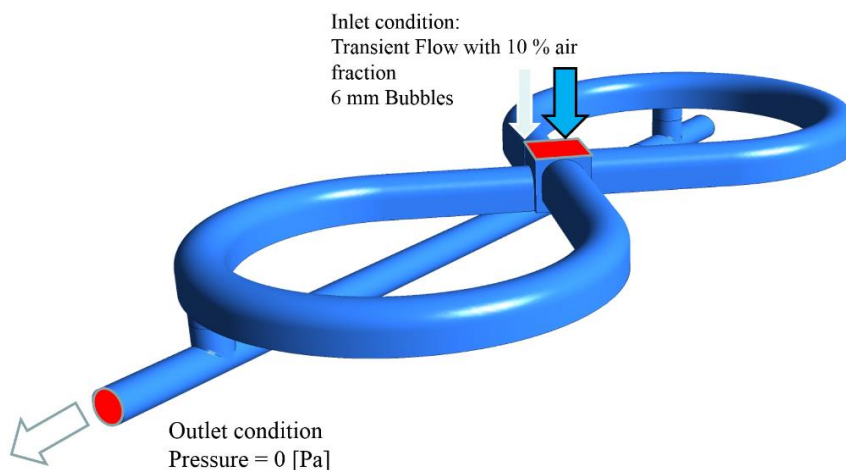


Figure 6-89: Boundary conditions for the numerical model, (*Richter* [106])

3D-numerical simulation in comparison with model test

Figure 6-90 shows the lower chamber connection point with the main shaft at time of significant air bubble production by the waterfall from the upper chamber. The air bubbles behave significantly more beneficial in the model test scale, compared to the prototype scale. The bubbles itself are not scaled in size and thus show the unscaled terminating velocity. The comparison with the degassing process in the model test made this behaviour visible by the 3D-numerical simulations in the same amount and quality.

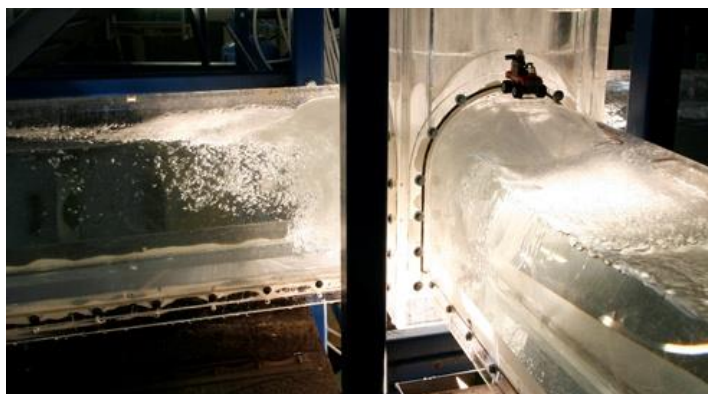


Figure 6-90: Degassing in lower chamber *Atdorf* tailrace surge tank, physical model test scale 1:40 (*Richter* [218])

Figure 6-91 shows the instantaneous time associated to the model test in Figure 6-90. The multiphase 3D-CFD simulation was calculated with the 6 mm diameter design air bubbles, terminating in the 8-loop shape lower chamber. The free surface of the water in the lower chamber was not possible to be reproduced in a stable multiphase numerical simulation. The accumulation of air by terminating bubbles is indicated by the air volume fraction value of 1.0 [-]. The air bubbles are dragged by the turbulent flow. An amplifier for long travel distances of air bubbles are rotational flows. Thus, flow calming or flow orientation devices improve the deaeration behaviour. For the chamber de-aeration such a construction was not needed.

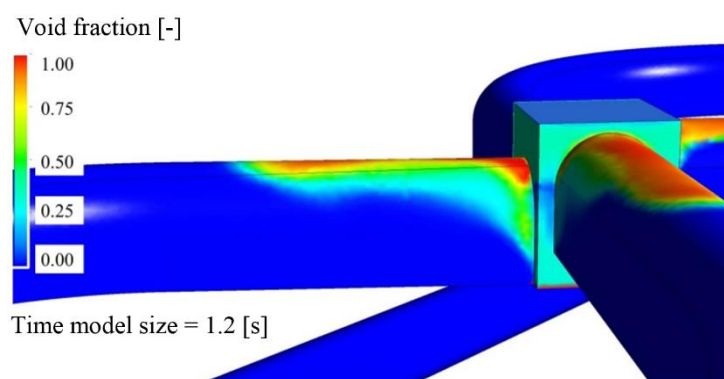


Figure 6-91: Degassing in lower chamber of the *Atdorf* surge tank, model test 1:40 in 3D-numerical two-phase simulation at model time 1.2 s, (*Richter* [218], modified)

Investigations regarding air bubble detrainment in Pelton turbine tailwater channels including prototype measurements and 3D-CFD simulations were carried out by *Arch* (2008) [143].

6.8.7 Waterfall-Dampening Device

For the *Krespa* surge tank a waterfall-dampening device was hydraulically developed by the author to mitigate the intrusion depth of air bubbles induced by a waterfall. In principle, the waterfall-dampening device forces the water flow from the upper chamber into sufficiently small vertical water jets that are in sum able to capture discharge of the design waterfall. The device transforms a large jet into numerous small water jets, comparable to a showerhead. This spreads the impact on a larger section of the shaft. The data developed waterfall-dampening device for surge tank *Krespa*:

- 368 vertical holes $D_i = 180$ mm
- 64 horizontal holes $D_i = 180$ mm
- Mitigation of intrusion depth by $2/3$, from about 75 m to about 24 m for worst expected event

In surge tanks with long chambers, several transient effects were investigated such as:

- Transient oscillation of the shaft
- Transient free surface wave behaviour of the chamber
- Large falling heights of the waterfall with low amount of water directly after flow separation in the upper chamber
- Low falling height of the waterfall with high amount of water

For certain surge tank layouts, a direct connection of the pressure tunnel with the upper chamber is the indicator for the necessity of waterfall investigations. In such cases the design load-case due to the maximum waterfall needs to be specified [43]. This load-case may differ from the upper chamber design load-case at resonance mass oscillation. The most unfavourable hydraulic situation for air intrusion can be detected by 1D-numerical simulations capturing the free surface flow behaviour in the upper chamber. The filling wave is reflected at the aeration structure at the end of the upper chamber. Following, two contrary resonance load-cases for the waterfall were basically investigated in the physical model test of the particular case after the pre-evaluation by 1D-numerical simulations:

- a) Water levels much below the capacity level in the upper reservoir → small waterfall discharges at high drops
- b) Water level slightly below the capacity level in upper reservoir → large waterfall discharges at low drops

At load-case (a) the surge wave will deeply fall into the main shaft due to time delay in the upper chamber free surface reflection. At load-case (b) the reflected flush will drop from low height onto the water surface of the main shaft. Investigations have shown that case (b) is the relevant situation for the evaluation of a design waterfall load-case. The reason for this is the mainly undisturbed water jet, thus the intrusion of air has the highest quantity. In addition, it occurs at the beginning of the down-surge period. To prevent a deep intrusion of air a waterfall-dampening device (Figure 6-92 and Figure 6-93) was proposed and tested for the headrace surge tank *Krespa* of PSH *Obervermuntwerk II* [43]. The device avoids the re-joining of the small waterfalls to larger jet formations and allows an appropriate air intrusion depth calculation depending on the design air bubble [212]. The dampening-device is situated in a cavern on top

RESULTS AND DISCUSSION

of the main shaft. The waterfall occurrence comes along with a differential effect affecting the pressure at the surge tank base. Thus, the separation of the flow in the upper chamber has a positive damping effect on the mass oscillation. The length of the upper chamber is limited by the demand of a complete draining before a subsequent oscillation fills the chamber again. In the case of the surge tank *Krespa* the widening of the main shaft at the transition to the upper chamber also improves the filling of the single chamber.



Figure 6-92: Waterfall damping device for Krespa surge tank, time at water column separation (*Richter*)



Figure 6-93: Waterfall damping device for Krespa surge tank, transformation of a large waterfall to defined smaller water jets (*Richter*)

The top widening of the main shaft, the retention gallery, houses the waterfall-dampening device (Figure 6-94). The device consists of a ring wall with circular holes and a bottom plate with circular holes. The air intrusion depth by the waterfall was significantly decreased.

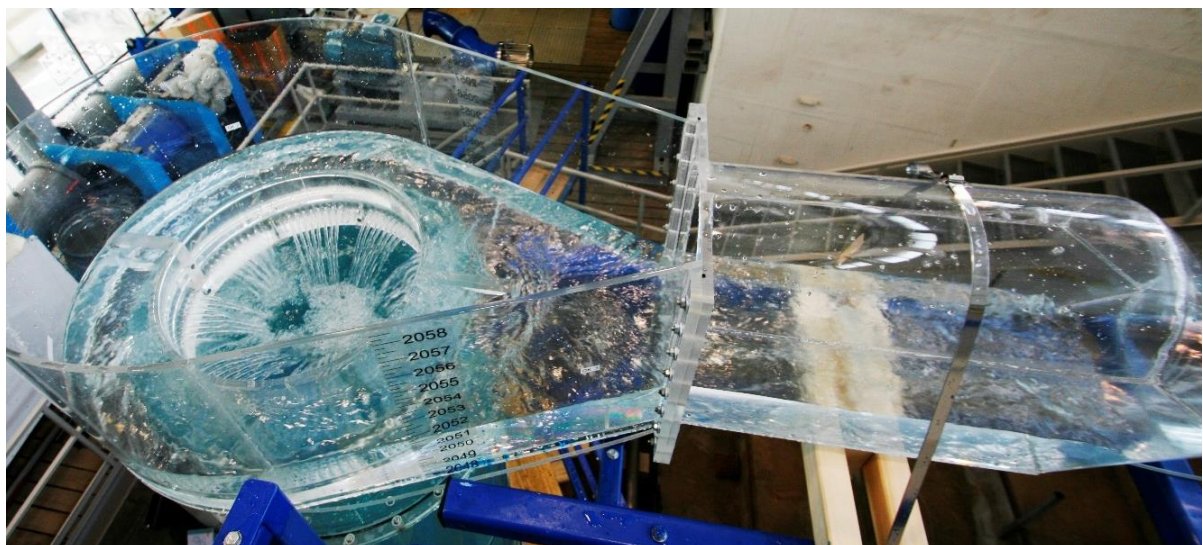


Figure 6-94: Waterfall-dampening device in the main shaft of *Krespa* surge tank (*Richter* [43])

RESULTS AND DISCUSSION

Figure 6-95 and Figure 6-96 show the geometry of the dampening device in plan view and section cut (plan drawing *Lazar* [114]).

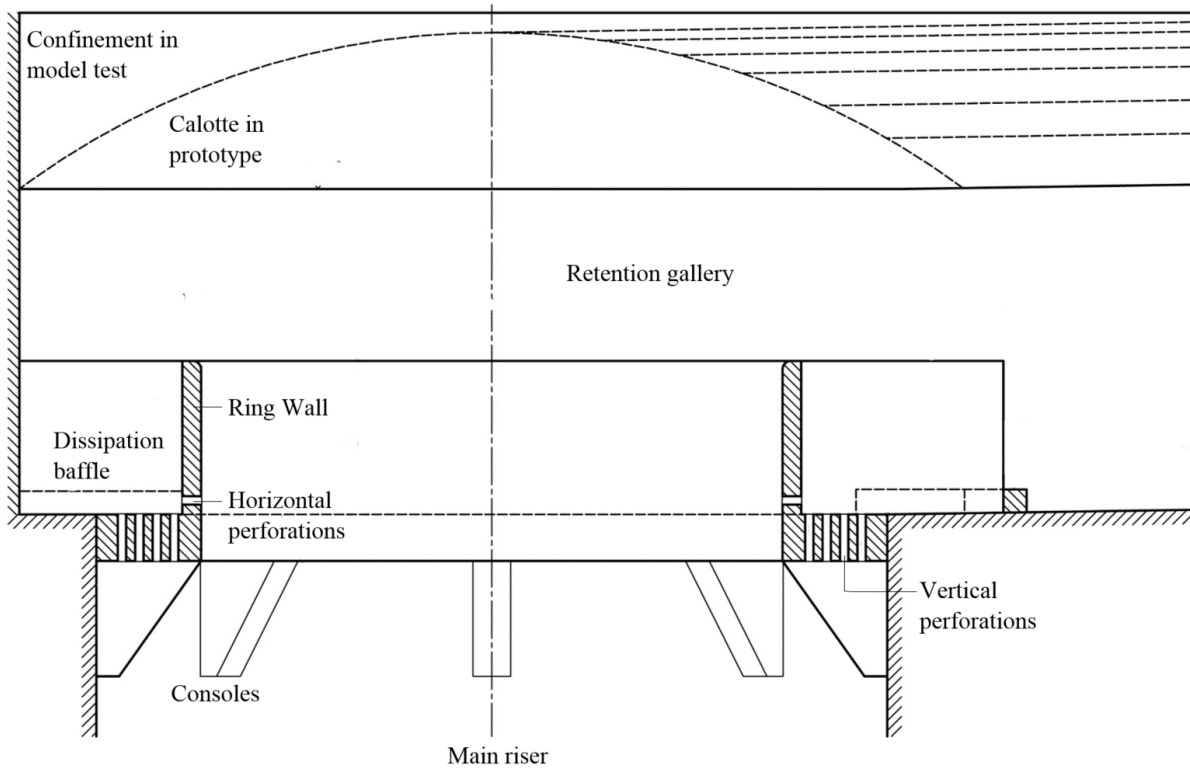


Figure 6-95: Waterfall-dampening device, section cut A-A (*Richter* adapted from *Lazar* [114])

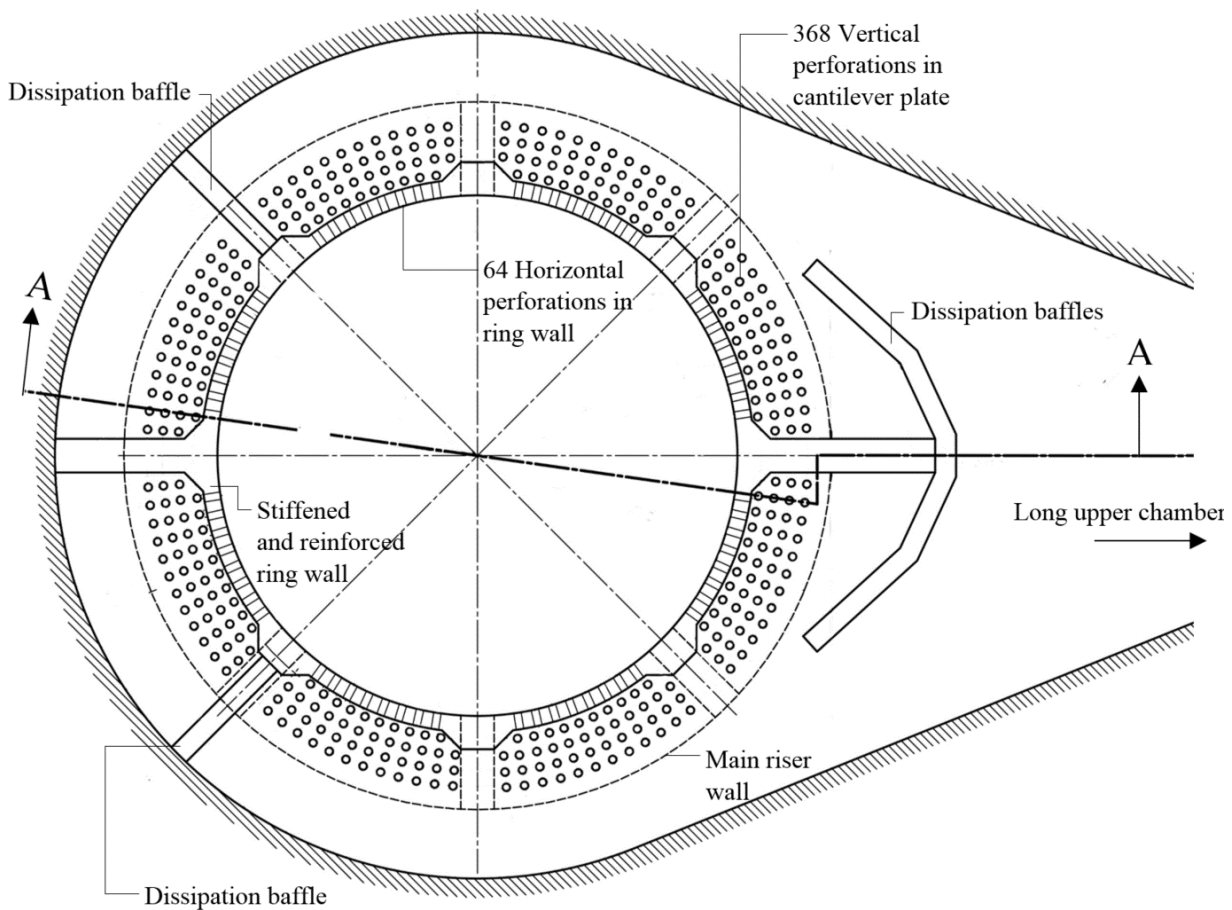


Figure 6-96: Waterfall-dampening device, plan view (*Richter* adapted from *Lazar* [114])

RESULTS AND DISCUSSION

Additionally, Figure 6-95 and Figure 6-96 indicate dissipation baffles that break the horizontal water flow coming from the upper chamber to equalise the discharge through the holes of the waterfall-dampening device. The prototype holes in the concrete of the dampening device for the *Krespa* surge tank are shown in Figure 6-97. The reinforced console bears the ring wall and the perforated cantilever plate. The perforations were finally constructed in manual construction work via blind formwork with mouth-widening to ensure the fixation (Figure 6-98).



Figure 6-97: Waterfall-dampening device, prototype of surge tank Krespa (courtesy of Illwerke AG)



Figure 6-98: Reinforcement and blind formwork of the perforation in the cantilever plate (footage of construction: [youtube.com: Obervermuntwerk II - viertes Baujahr 2017](https://www.youtube.com/watch?v=Obervermuntwerk-II-viertes-Baujahr-2017) [219])

6.9 Surge Tank Commissioning

In the phase of a power plant commissioning the surge tank concept is directly tested within the operability of the whole system in combination with the transient behaviour of the machinery. Real-time simulations of a power plant, parallel to the operational tests in sense of a digital twin may reveal the full overview of the surge tank behaviour in comparison with the design parameters and the real physics of the power plant. Online simulation receives the information of guide vane operation and the measurements provided from crucial power plant sections [179].

Thus, real-time simulation tools may not only be used to improve commissioning but may also allow valuable conclusions for surge tank design, machinery impact on transients and the roughness values of the power water conduits. Additionally, hydraulic altering and the detection of anomalies such as described by *Hachem and Schleiss* (2012) [220] may be detected.

The technology of digital twins, such as the *Hydro Clone* [189] shows high values to increase the economic and long-term operability of hydropower schemes to balance the wear off and allow best flexible operation modes in sense of predicted maintenance and predicted control. However, in the opinion of the author these applications do not substitute the advantages of hydropower layouts with robust surge tanks designed to capture resonance load-cases.

6.10 Prototype Measurements at Krespa Surge Tank

This chapter describes the results from the prototype measurement for a design load-case, conducted by Illwerke AG at the *Krespa* surge tank of the *Obervermuntwerk II* PSH compared with the 1D-numerical simulations. Further descriptions are discussed in *Wachter et.al. (2018)* [45]. The measurements confirm the hydraulic design of the surge tank and also the hydraulic function of the waterfall-dampening device within the mass oscillation response and the outflow behavior. Also, the upper chamber filling and emptying behavior was confirmed.

Figure 6-99 depicts the placed measurement equipment in the *Krespa* surge tank by Illwerke AG to observe the relevant pressures and the water level in the surge tank. Redundant measuring devices are utilising different techniques. Several pressure transducers are placed in the surge tank bottom and the lower chambers. A radar sensor is placed above the main shaft as well as two video cameras with light installations, observing the waterfall-dampening device and the rear part of the upper chamber.

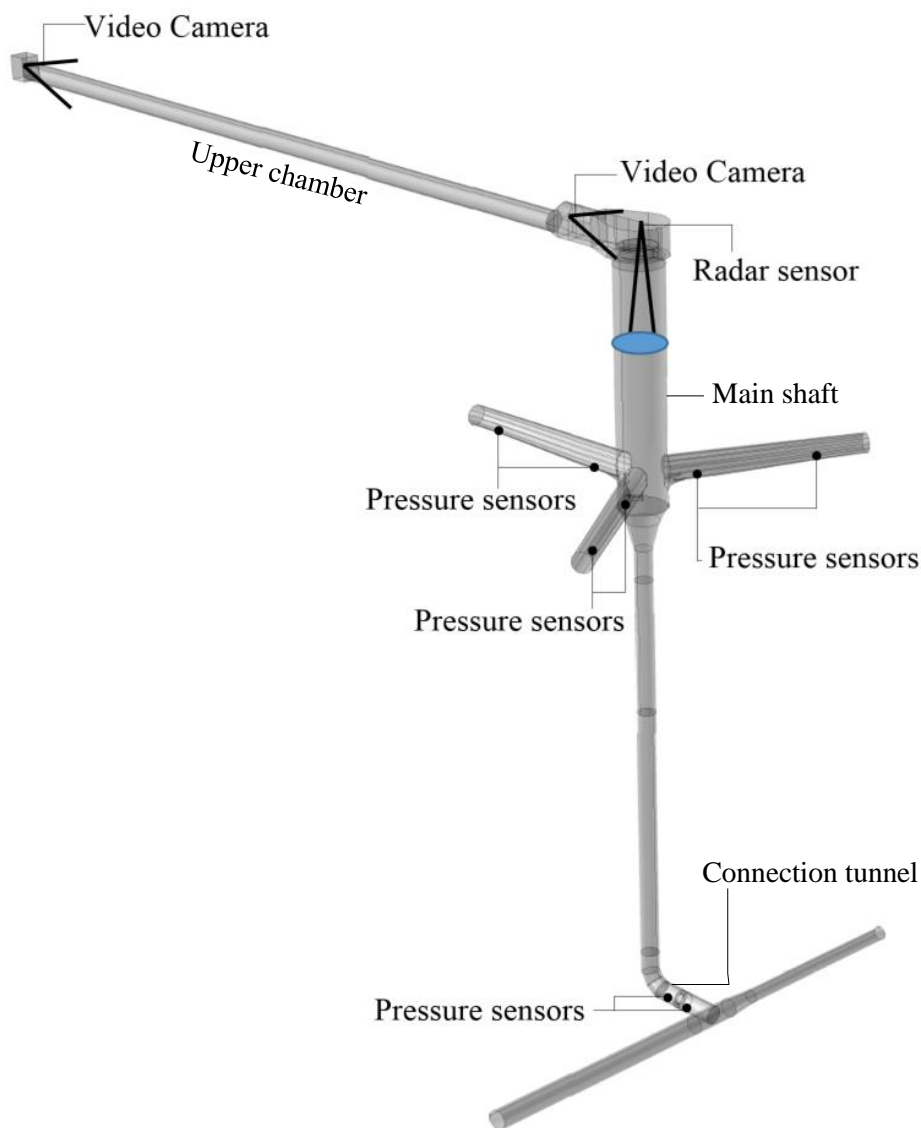


Figure 6-99: Measurement equipment for operational survey in the *Krespa* surge tank, installed by Illwerke AG

RESULTS AND DISCUSSION

Figure 6-100 shows the results for a one-unit operation in terms of the transient free surface level in the surge tank. The measurement data were compared with 1D-numerical simulation. The load-case contains the expected tunnel friction of $K_{ST} = 84 \text{ [m}^{1/3}/\text{s]}$ and the measured throttle loss from the physical model test

The thin dotted line shows the 1D-numerical simulated mass oscillation in good agreement with the prototype measurement (a). The thicker dotted line shows the 1D- numerical simulation with the equal machine discharge as the prototype case with reduced throttle loss.

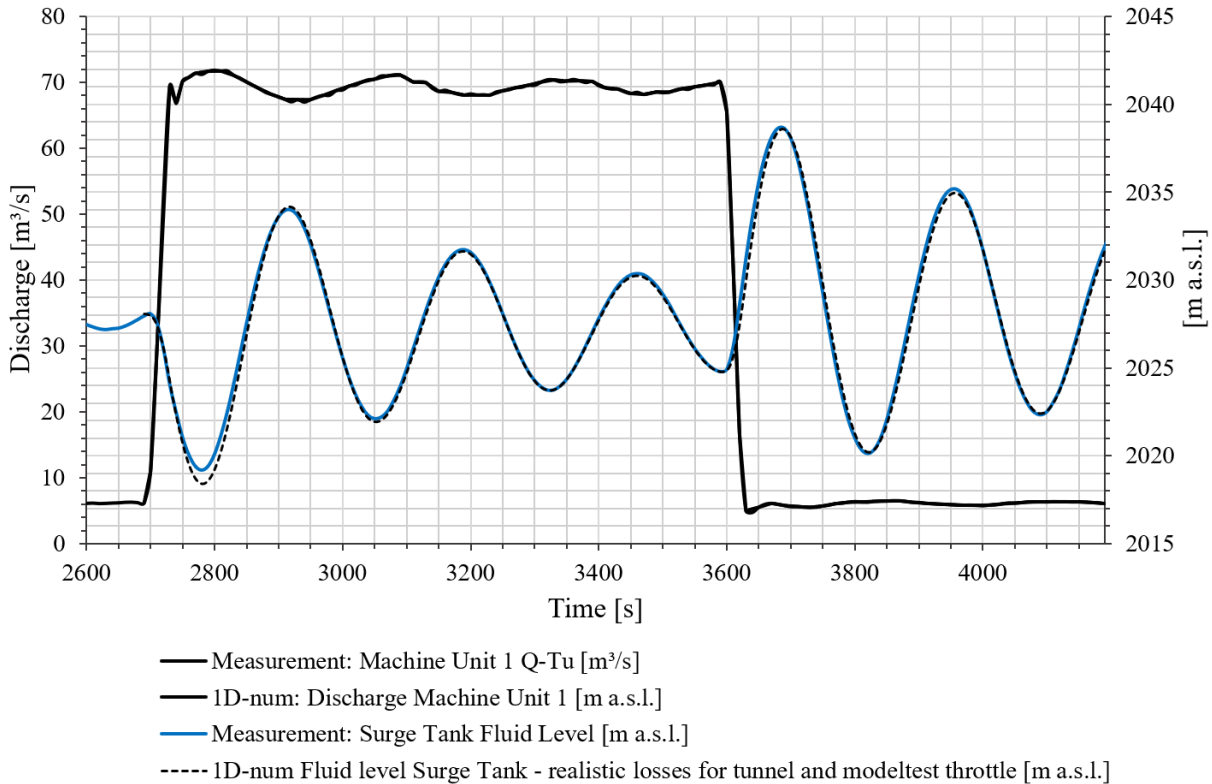


Figure 6-100: Comparison: 1D-numerical simulation and measurement of water level for 1-machine unit operation PSH *Obervermuntwerk II*, Headrace Di 6.8 m Surge Tank Di 17.0 Lines: Load-case prototype measurement versus simulation with expected and model test measured throttle losses (Richter [45])

RESULTS AND DISCUSSION

Figure 6-101 shows the prototype measurement with the included safety margins regarding the design discharge and the reduced hydraulic loss factors of 10 % for the local throttle loss based on the physical model test and the headrace tunnel friction factors. The green line shows the ideal linear 1D approach with 80 m³/s turbine discharge with loading and unloading in 30 s with the corresponding mass oscillation in the surge tank and reduced throttle loss. For this case the safety margin in the surge tank is visualised with additional 4 m for down-surge and 3.5 m for up-surge. Due to the large surface area in the main shaft of 227 m², a significant volume is provided.

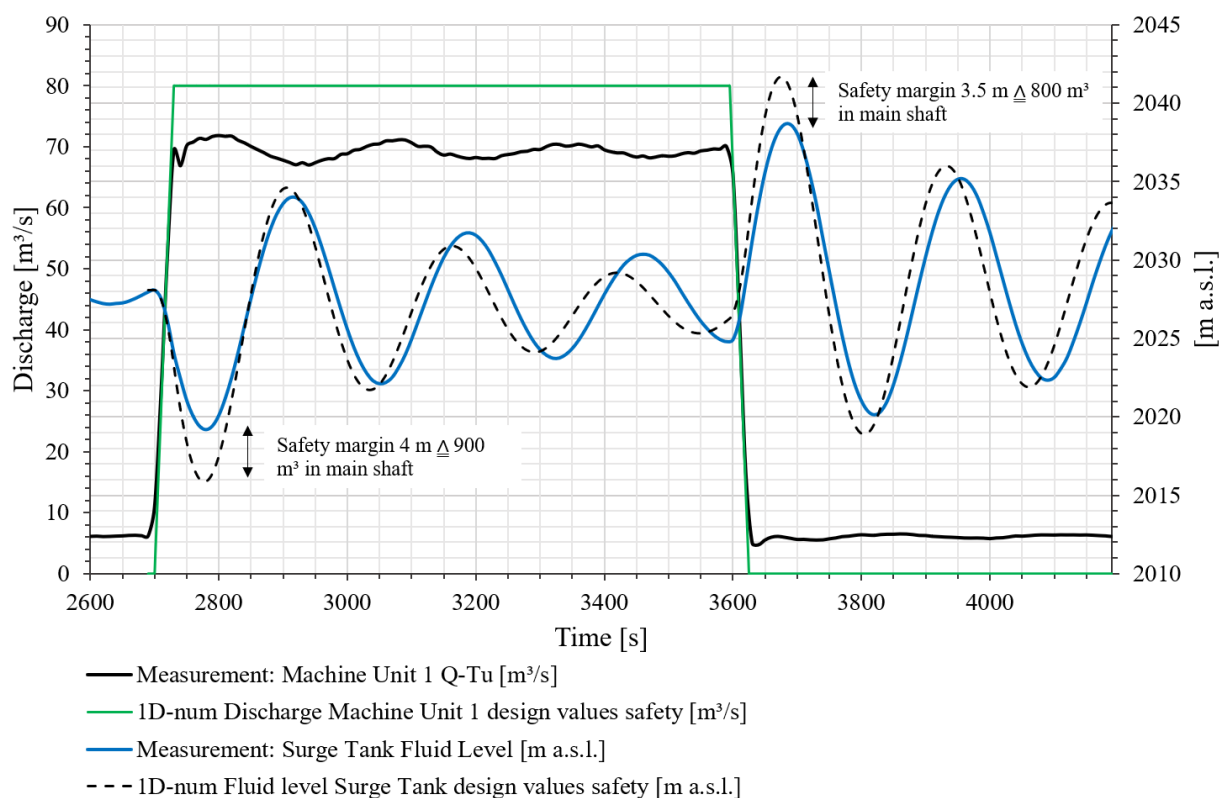


Figure 6-101: Comparison: 1D-numerical simulation and measurement of water level for 1-machine unit operation PSH *Obvermuntwerk II*, Headrace Di 6.8 m Surge Tank Di 17.0 Lines: Load-case prototype measurement versus simulation with expected headrace loss and 10 % reduced throttle loss; Load-case prototype ideal with 80 m³/s simulation with expected headrace loss and 10 % reduced throttle loss - design case, (*Richter* [45])

RESULTS AND DISCUSSION

Figure 6-102 shows a design load case event for two machine operation near the capacity level with a full pump mode start-up, followed by a switch to full turbine mode operation in 60 s back to 100 % pump mode within 60 s covering a full spread of 720 MW for this specific pumped storage plant for unfavourable hydraulic boundary conditions, in order to amplify the mass oscillation. Figure 6-102 shows the discharge of the units and the various measurement techniques in the surge tank; a pressure sensor in the connection tunnel, a pressure sensor in the lower chamber and the radar sensor above the main shaft. The radar sensor indicates the outflow and vanishes due to the water spray of the dissolving jets by the waterfall-dampening device. The load-case proves the functionality of the surge tank and also the hydraulic design of the waterfall-dampening device for a design outflow with surface waves from the upper chamber reflection.

The figure also shows the importance of different measuring techniques and the installation of various sensors, due for calibration and to apply a safety against sensor failures.

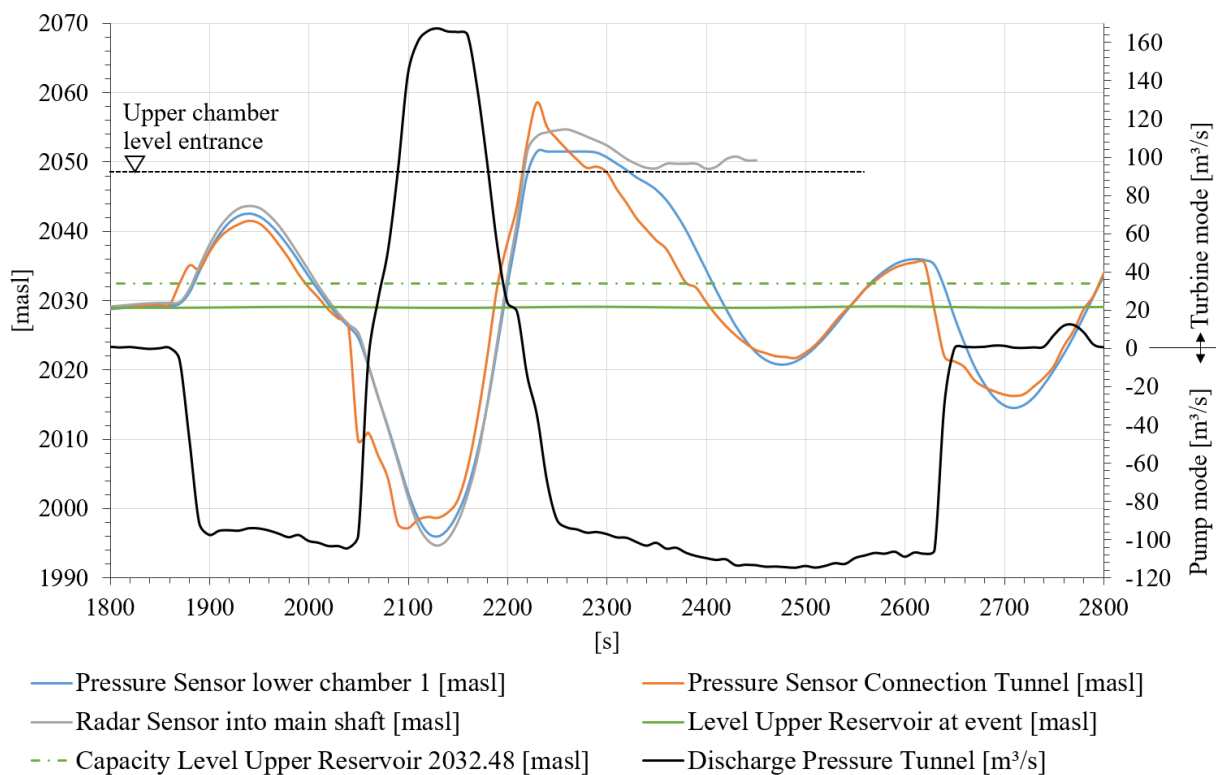


Figure 6-102: Resonance load-case event for 2-machine operation near capacity level of the upper reservoir, measurement of the surge tank *Krespa*, (*Richter* [45], modified)

RESULTS AND DISCUSSION

Figure 6-103 visualises the comparison of the 1D-numerical simulation with the prototype measurements for the design load-case as shown in Figure 6-102. Two lines from the 1D-numerical mass oscillation simulations with *WANDA* are compared with the measurements showing the pressure at the surge tank base and the water level. The difference describes the hydraulic effect of the differential throttle. The simulations show a very good comparability with the measurements of this design load-case.

A very smooth concrete lining friction was recalculated to a Strickler value of $K_{ST} 100 [m^{1/3} s^{-1}]$. The reason for this very smooth friction behaviour is believed first of course due to the good construction quality of the in-situ concrete tunnel lining, but also to the hydraulic design whereas all local losses and friction losses of the tunnel are summed and ideally superposed. Due to the overlapping of hydraulic losses by the demanded dissipation length after a restriction such as a bend or a diameter change or closing device, this superposition approach might over-estimate hydraulic losses. Thus, the conservative hydraulic design applying reduced friction values (smoother walls) in the tunnel has proven its purpose. In addition, the gained results of these measurements are a proof of the above discussed hydraulic design philosophy, suggesting conservative hydraulic design values (chapter 3.7).

The prototype measurements underline the importance of safety margins in surge tank design. For the specific plant, the safety margins in combination with the smooth lining finally show an economic design that is able to capture extraordinary load-cases improving the flexible opportunities of the scheme.

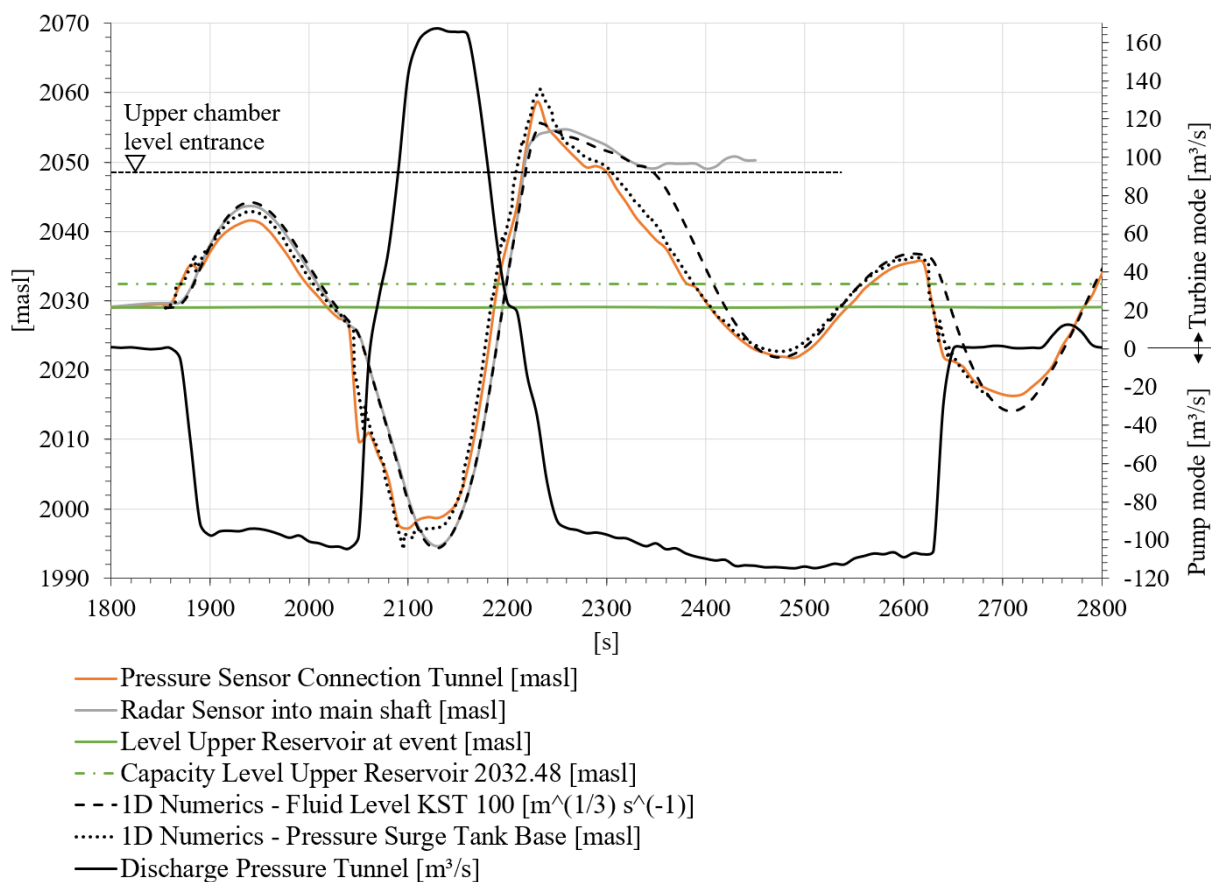


Figure 6-103: Comparison of the resonance load-case measurement of the surge tank *Krespa* and 1D-numerical simulation (*Richter* [45], modified)

7. SUMMARY AND OUTLOOK

Surge Tanks are key hydraulic structures for hydropower facilities that utilise pressure tunnel systems above a certain threshold of water inertia acting on the hydraulic machinery. Flexible hydropower schemes and pumped storage plants are key infrastructures for a renewable energy system. Surge tanks for new schemes are being constructed in increasingly larger sizes, demanding for more detailed investigations on hydraulic aspects such as differential effects and multiphase flow behaviour. The focus of the surge tank design is to provide safe and robust structures to control the mass oscillation of the pressurized water conduit systems. The mass oscillation is a consequence of the introduction of a free water surface in the surge tank that provides controllability to the hydraulic machine units and allows a significant pressure surge mitigation.

The approaches towards increasing shares of renewables, that are fluctuating energy sources by their nature and demands for flexible storage capacity in grid scale size, demand for capable storage facilities. Pumped storage hydropower schemes are proposed as the most beneficial and only mature large-scale electrical storage technology available today. Specific costs of pumped storage hydropower compared with other storage technologies show that pumped storage hydropower have very low specific energy related investment costs.

Surge tank case studies were investigated by means of physical scale model tests and numerical simulations. The investigated surge tanks are part of recent large pumped storage projects such as PSH *Atdorf*, PSH *Reisseck II* (surge tank *Burgstall*) and PSH *Obervermuntwerk II* (surge tank *Krespa*), as well as for the large high head scheme *Tonstad*. The two surge tanks *Krespa* and *Burgstall* were commissioned in the meantime and are successfully in operation. Prototype measurements of a design resonance load-case were investigated for the surge tank of the highly flexible electric energy storage scheme *Obervermuntwerk II*. These measurements were compared with the simulation results and could confirm the hydraulic design. Hydraulic safety approaches for the surge tank design is proposed and discussed for such applications in high-head hydropower schemes and pumped storage plants. Safety approaches are necessary, since transient hydraulic systems show deviations by their physical nature and possible imperfections as well as the demand to prevent extreme events such as water overflows of the system or complete emptying.

Waterfalls from upper chambers into surge tank shafts were studied for the surge tanks *Atdorf* and *Krespa*. Their consequences of air intrusion into the surge tank system as well as the prevention of air bubble transportation into the pressure tunnel system show their importance for the layout of large and flexible hydropower schemes. In surge tanks, waterfalls are created by flow separation in the upper chamber at a certain time at outflow. In a flow through lower chamber design, the air bubbles can rise to the crown and de-aerate back into the riser. But, flow-through lower chamber may also show unfavourably high inertia values. However, significant waterfalls also indicate efficient differential effects and thus, may be valuable for economic surge tank layouts. For surge tanks with long upper chambers and direct connected shafts to the pressure tunnels it is proposed to study the air bubble behaviour. In collaboration with Illwerke AG a comprehensive waterfall-dampening device was developed for the surge tank *Krespa* to mitigate the impact of a single large waterfall jet by dividing this into multiple vertical small jets with defined diameter. The mitigation of the waterfall significantly reduces

SUMMARY AND OUTLOOK

the air bubble intrusion depth by about 2/3 of the possible intrusion depth without a device. Such devices may be applied also for other types of shafts to significantly mitigate air intrusion. The waterfall-dampening device was successfully tested and proofed by prototype measurements during an unfavourable resonance design load case.

Air cushion surge tanks are discussed and summarised with their benefits and challenges. A new proposal of both surge tank upgrade and surge tank design is introduced: The semi-air cushion surge tank. It is derived and inspired by trapped air in the crown section of chamber surge tanks. Two-phase 3D-numerical simulations can visualise the positive effects for the mass oscillation of the semi-air cushion surge tanks. These facilities are constructed by adapting lower chambers by placing crown throttles, that are basically beams, trapping air in combination with small aeration pipes that control the air flow. The upgrade of the surge tank of the *Tonstad* hydropower plant was investigated by proposing an additional lower chamber that may also utilise a semi-closed surge tank by introducing a crown throttle providing hydraulic benefits for the design.

With respect to the transient behaviour of the throttle flow as a hydraulic diffuser, 3D-numerical simulations of the transient flow should be conducted with a transient loss coefficient that can be interpreted as an average factor with a constant value as input for 1D-numerical simulations. Imperfections of the structure and hydraulic deviations in the prototype-scale surge tank are recommended to be considered by a robust hydraulic safety philosophy. For final throttle design evaluation, a loss deviation of 10 % to 20 % may be considered at the design stage. For the throttle design 1D-numerical variant studies to find the most unfavourable load combination are straightforward. Surge tanks are strictly proposed without any moveable parts for the operation of the powerplant to ensure robustness. For hydraulic throttle design, based on 3D-numerical simulation only, an unfavourable loss deviation of 20 % is suggested.

A robust hydraulic safety philosophy is proposed, since no standard is yet available for surge tank design. It is advisable to conduct physical model tests additionally to 1D and 3D transient numerical simulations in order to capture the complex hydraulic behaviour and to avoid harmful load-cases in terms of economic design, as well as to provide a visual check. For the surge tank design for flexible hydropower schemes, hybrid approaches applying 1D-numerical and 3D-numerical as well as physical model tests are recommended.

A multiphase 3D-numerical approach was applied for de-aeration simulation and for a waterfall simulation for specific case studies. For this approaches several assumptions are necessary to be considered, since the physical behaviour of air intrusion by a plunging jet is not yet reproducible in a reliable way by 3D-numerical simulations. The comparison of the 3D-numerical simulations of the water fall with the physical small-scale test and design approaches from literature has shown meaningful results.

Suggestions for future work:

Several aspects for further research opportunities and an outlook for emerging aspects are listed below:

- Semi-air cushion surge tanks; for specific application comprehensive evaluation is necessary in terms of hybrid modelling and the development of a model implementation in a 1D-numerical code.
- Storage-tunnel surge tanks in combination with storage-tunnel applications; the thesis shows a design approach with key needs for optimised design. For specific applications, comprehensive investigations are suggested.
- The effect of fine sediment loaded high velocity throttle jets on concrete walls is an aspect that is suggested to be investigated further.
- Machine learning of surge tank design and high-head hydropower prospection.
- Implementation of digital twins to high-head schemes to tap the potential of monitoring of hydro power plants and to improve flexibility options. This technology may significantly improve the flexible operation and control of hydropower plants as well as the commissioning procedure, but should not replace the proven robust design philosophy.
- Ternary modelling in sense of expanding the hybrid modelling of numerical simulations and physical tests in combination with meta models. Meta models include vast simulation and modelling data to predict operational and maintenance demands of hydro power plants.

Solutions for an integrative decarbonised energy system transformation may lead to the conclusion that inefficient and carbon emitting combustion processes need to be substituted by an efficient, renewable, electricity powered economy. Such systems demand for highly efficient, economic electrical storages as well as for powerful grid control systems such as pumped storage hydropower. New or upgraded pumped storage schemes need comprehensive surge tanks to allow flexible and safe operation to achieve long-lifetimes.

8. BIBLIOGRAPHY

- [1] *W. Richter*, 3D-numerische Strömungssimulation von hydraulischen Rückstromdrosseln in Wasserschlossern (in German) 3D-CFD simulation of hydraulic differential throttles in surge tanks, Diploma Thesis, University of Innsbruck, Unit of Hydraulic Engineering, 2010.
- [2] *F. G. Pikel*, Kombination der Pumpspeichertechnologie mit thermischer Energiespeicherung (in German) Combination of the pumped storage technology with thermal energy storage, Graz: Master thesis, 2017.
- [3] *F. Pikel, W. Richter and G. Zenz*, Pumped storage technology combined with thermal energy storage – Power station and pressure tunnel concept, *Geomechanics and Tunnelling*, vol. 10, no. 5, pp. 611-619, 2017.
- [4] *F. Pikel, W. Richter and G. Zenz*, Wasserakku als innovativer Energiespeicher zur sektorgekoppelten Energieversorgung, in *Wasserbausymposium at Graz University of Technology*, 2017.
- [5] *F. Pikel*, Pumped Storage Hydroelectricity in Combination with Thermal Energy Storage, in *ICOLD 26th Congress*, Vienna, 2018.
- [6] *W. Füßl*, Oskar von Miller: 1855-1934 - Eine Biographie, C.H.Beck, 2005.
- [7] *European Commission*, Energy roadmap 2050, Publications Office of the European Union, Luxemburg, 2012.
- [8] *H. Stigler*, Grundlagen der Elektrizitätswirtschaft (basics of electrical industry), Graz: Script of the lecture, Graz University of Technology, 2008.
- [9] *T. Gobmaier, S. von Roon and D. Bernhard*, Markets for Demand Side Management, Graz, 2012.
- [10] *P. Konstantin*, Praxisbuch Energiewirtschaft, Energieumwandlung, -transport und -beschaffung im liberalisierten Markt, Springer Vieweg, 2013.
- [11] *H. Berndt, M. Hermann, H. D. Kreye, R. Reinisch, U. Scherer and J. Vanzetta*, TransmissionCode 2007; Network and System Rules of the German Transmission System Operators, Berlin: Verband der Netzbetreiber VDN, 2007.
- [12] *A. Lechner, J. Hell and R. Schürhuber*, Pumped Storage Contribution to Grid Inertia, in 18th Intern. Seminar on Hydropower Plants, Vienna, 2014.

BIBLIOGRAPHY

- [13] *S. Rehman, L. M. Al-Hadhrami and M. M. Alam*, Pumped hydro energy storage system: A technological review, *Renewable and Sustainable Energy Reviews*, vol. 44, no. <http://dx.doi.org/10.1016/j.rser.2014.12.040>, pp. 589-598, 2015.
- [14] *S. M. Schoenung and W. V. Hassenzahl*, Long- vs. Short-Term Energy Storage Technologies Analysis; A Life-Cycle Cost Study, Sandia Report, 2003.
- [15] *C. A. S. Hall*, *Energy Return on Investment*, Springer; ISBN-13: 9783319838328, 2018.
- [16] *C. A. Hall, J. G. Lambert and S. B. Balogh*, EROI of different fuels and the implications for society, *Energy Policy*, vol. 64, p. 141–152, 2014.
- [17] *R. Atlason and R. Unnthorsson*, Energy Return on Investment of Hydroelectric Power Generation Using a Standardised Methodology, *Renewable Energy*; doi.org/10.1016/j.renene.2013.12.029, vol. 66, pp. 364-370, 2014.
- [18] *H. L. Raadal, I. S. Modahl and T. H. Bakken*, Energy indicators for electricity production, CEDREN, ISBN: 978-82-7520-666-2, 2012.
- [19] *J. G. Lambert, C. S. Hall and S. Balogh*, EROI of Global Energy Resources: Status, Trends and Social Implications, UK -Department for International Development, DOI: [10.13140/2.1.2419.8724](https://doi.org/10.13140/2.1.2419.8724), 2013.
- [20] *J. G. Lambert, C. A. Hall, S. Balogh and M. Arnold*, Energy, EROI and quality of life, *Energy Policy*, vol. 64, pp. 153-167, 2014.
- [21] *M. Dale*, *Global Energy Modeling: A Biophysical Approach (GEMBA)*, University of Canterbury, Christchurch, New Zealand, 2010.
- [22] *C. J. Barnhart and S. M. Benson*, On the importance of reducing the energetic and material demands of electrical energy storage, *Energy & Environmental Science*; DOI: [10.1039/C3EE24040A](https://doi.org/10.1039/C3EE24040A), vol. 6, p. 1083–1092, 2013.
- [23] *M. A. Pellow, C. J. Emmott, C. J. Barnhart and S. Benson*, Hydrogen or batteries for grid storage? A net energy analysis, *Energy Environ. Sci.*, vol. 8, pp. 1938--1952, 2015.
- [24] *K. Hambaumer*, Shifting and storing renewable energy by pumped-storage hydropower plants for the power system in Germany (in German), Master Thesis, Graz University of Technology, 2017.
- [25] *F. Píkl, W. Richter and G. Zenz*, Großtechnische, wirtschaftliche und effiziente untertägige Energiespeicher; Large-scale, economic and efficient underground energy storage, *Geomechanics and Tunneling*, DOI: [10.1002/geot.201900007](https://doi.org/10.1002/geot.201900007), vol. 12, no. 3, pp. 251-269, 2019.

BIBLIOGRAPHY

- [26] *Agora Energiewende*, Agorameter, 2018.
- [27] *Agora Verkehrswende*, Agora Energiewende and Frontier Economics, The Future Costs of Electricity-Based Synthetic Fuels, 2018.
- [28] *Austrian National Committee on Large Dams*, Pumped Storage Hydropower in Austria, Graz: Graz University of Technology, 2018.
- [29] *M. Koch*, Überblick der Hochdruckanlagen in Österreich (in German), Overview of Austrian High-Head Power Plants, Bachelor Project, TU Graz, 2015.
- [30] *V. Jülch*, Comparison of electricity storage options using levelized cost of storage (LCOS) method, *Applied Energy*, no. 183, p. 1594–1606, 2016.
- [31] *IRENA*, Electricity Storage and Renewables: Cost and Markets to 2030, International Renewable Energy Agency, Abu Dhabi, 2017.
- [32] *B. Nykvist and M. Nilsson*, Rapidly falling costs of battery packs for electric vehicles, Nature Publishing Group. *Nature Climate Change.*, 2015.
- [33] *C. Nicolet, Y. Pannatier, B. Kawkabani, A. Schwery, F. Avellan and J.-J. Simond*, Benefits of Variable Speed Pumped storage Units in Mixed Islanded Power Network during Transient Operation., in *Hydro*, Lyon, 2009.
- [34] *T. Kunz, G. Sari, A. Schwery, R. Guillaume and J.-M. Henry*, Commissioning and operation of variable speed units at the 1000 MW Linthal pumped-storage plant, *Hydropower & Dams*, no. 5, pp. 50-58, 2017.
- [35] *E. Wikner*, Lithium ion Battery Aging: Battery Lifetime Testing and Physics-based Modeling for Electric Vehicle Applications, Thesis, Göteborg: Chalmers University of Technology, 2017.
- [36] *A. Thielmann and A. Sauer*, Gesamt-Roadmap Lithium-Ionen-Batterien 2030, Fraunhofer ISI, Karlsruhe, 2015.
- [37] *World Energy Council*, E-storage: shifting from cost to value Wind and solar applications, London, 2016.
- [38] *W. F. Pickard*, The History, Present State, and Future Prospects of Underground Pumped Hydro for Massive Energy Storage, *Proceedings of the IEEE*, DOI: 10.1109/JPROC.2011.2126030, vol. 100, no. 2, pp. 473 - 483, 2012.

BIBLIOGRAPHY

- [39] *K. Smith, A. Saxon, M. Keyser, B. Lundstrom, Z. Cao and A. Roc*, Life Prediction Model for Grid-Connected Li-ion Battery Energy Storage System, in American Control Conference, Seattle, 2017.
- [40] *V. Koritanov, T. Veselka, J. Gasper, B. Bethke, A. Botterud, J. Wang, M. Mahalik, Z. Zhou, C. Milostan, J. Feltes, Y. Kazachkov, T. Guo, G. Liu, B. Trouille, P. Donalek, K. King, E. Ela, B. Kirby, I. Krad and V. Gevorgian*, Modelling and Analysis of Value of Advanced Pumped Storage Hydropower in the United States, Argonne National Laboratory Report ANL/DIS-14/7, Argonne, Illinois, 2014.
- [41] *K. S. Lee*, Underground Thermal Energy Storage, London: Springer, DOI 10.1007/978-1-4471-4273-7, 2013.
- [42] *C. Nicolet, Arpe, J., and A. Rejec*, Influence of The Surge Tank Water Inertia on Pumped Storage Power Plant Transients in Case of Pump Emergency Shutdown, in 6 th International Meeting of the Workgroup on Cavitation and Dynamic Problems in Hydraulic Machinery and Systems, September 9-11, Ljubljana,, 2015.
- [43] *W. Richter, J. Schneider, G. Zenz and G. Innerhofer*, Hybrid Modelling and Development of a long Upper Chamber in a Surge Tank, Proceedings of Hydro Congress, Innsbruck, 2013.
- [44] *W. Richter, J. Schneider, G. Zenz, G. Innerhofer and G. Gökler*, Wasserschloss Obervermuntwerk II Anforderungen, Untersuchungen, Realisierung, in Wasserbausymposium, Wallgau, Germany, 2016.
- [45] *S. Wachter, G. Innerhofer, G. Gökler, L. Werle, W. Richter, J. Schneider and G. Zenz*, Obervermuntwerk II, Wasserschloss Krespa - Von der Theorie zur Praxis; Obervermuntwerk II, Surge Tank Krespa - from theory to practical application, in Wasserbausymposium, TU Graz, 2018.
- [46] *G. Garbrecht*, Wasserwirtschaftliche Anlagen des antiken Pergamon - Die Madradag Leitung -, Leichtweiss-Institut für Wasserbau der TU Braunschweig. Mitteilungen Heft 37, 1973.
- [47] *G. Garbrecht*, Meisterwerke antiker Hydrotechnik, Stuttgart: Leipzig: Teubner; Zürich, vdf-Hochschulverlag an der ETH, 1995.
- [48] *Cerjak et al.*, High Strength Steels for Hydropower Plants - Design Concepts - Pressure Conduits, Verlag TU-Graz, 2013.
- [49] *A. Bergant, A. Simpson and A. S. Tijsseling*, Water hammer with column separation: A historical review, Journal of Fluids and Structures, pp. 135-171, 2006.

BIBLIOGRAPHY

- [50] *D. Thoma*, Theorie des Wasserschlosses bei selbsttätig geregelten Turbinenanlagen (The theory of surge tanks for turbine installations equipped with governors, translated by Jan C. Van Tienhoven (1955), F.B. Campbell, Vicksburg), Dissertation, Kgl. Technische Hochschule zu München: R. Oldenbourg, 1910.
- [51] *W. Hudovernik*, Untersuchungen über die dynamische Druckbeanspruchung im Triebwassersystem von Hochdruck-Wasserkraftanlagen, Habilitation, Universität Innsbruck, 1987.
- [52] *H. Ødegaard and K. Vereide*, Air Cushion Surge Chambers - Three Proposals for Design Improvements (in Norwegian) Uforede Luftputekammer - Tre Forslag til Designforbedringer, in Fjellsprengningsdagen 2018, Oslo.
- [53] *J. Michaud*, Coups de bélier dans les conduits. Étude des moyens employés pour en atténuer les effets, Bulletin de, Vols. 3,4, pp. 56–64, 65–77, 1878.
- [54] *R. Johnson*, The Surge Tank in Water Power Plants, ASME, Volume 30, Pages 443-501, 1908.
- [55] *W. Richter, H. Knoblauch and G. Zenz*, Surge tank design in Austria: Dimensioning-philosophy for flexible hydropower, in Hydro Conference, Seville, 2017.
- [56] *ASCE*, Compendium of Pumped Storage Plants in the United States, New York, NY: Task Committee on Pumped Storage of the Hydropower Committee of the Energy Division of the American Society of Civil Engineers, 1993.
- [57] *W. Richter, G. Zenz, J. Schneider and H. Knoblauch*, Surge tanks for high head hydropowerplants - Hydraulic layout - New developments, Geomechanics and tunneling, vol. 8, no. 1, 2015.
- [58] *A. Schleiss*, Competitive pumped-storage projects with vertical pressure shafts without steel linings, Geomechanics and Tunneling, pp. Volume 6, No. 5, Page 456-463, 2013.
- [59] *T. Nielsen*, Transient Characteristics of high head Francis Turbines, Doctoral thesis, NTH Trondheim, 1990.
- [60] *T. Stein*, Drehzalregelung der Wasserturbinen, Schweizerische Bauzeitung, vol. 65, no. 39, pp. 531-535, 1947.
- [61] *S. Vogt-Svendsen*, Simulation Program for Stability Analysis of Hydropower Plants, Master Thesis, Norwegian University of Science and Technology, 2012.

BIBLIOGRAPHY

- [62] *R. Mader*, Untersuchung des Schwingverhaltens einer Oberwasserführung mit Druckluftwasserschloß anhand des Beispiels einer Hochdruckwasserkraftanlage, Dissertation, Technische Universität Graz, 1990.
- [63] *J. Giesecke and E. Mosonyi*, Wasserkraftanlagen, Planung, Bau und Betrieb, 5. Auflage: Springer Heidelberg, 2009.
- [64] *C. Jaeger*, Contribution to the Stability Theory of Systems of Surge Tanks, 1958.
- [65] *R. Svee*, Untersuchungen über die Stabilität bei Wasserkraftanlagen mit idealer Regelung, Mitteilungen Nr. 15 Institut für Wasserbau Technische Universität Graz, 1970.
- [66] *X. Li and H. Brekke*, Large amplitude water level oscillations in throttled surge tanks, Journal of Hydraulic Research, pp. 537-551, 1989.
- [67] *R. Svee*, Surge Chamber with an Enclosed, Compressed Air-Cushion, Proceedings of International Conference on Pressure Surges, Canterbury, England, pp. G2 15 - G2 24, 1972.
- [68] *L. Rathe*, An innovation in surge-chamber design, Water Power & Dam Construction, vol. June/July, pp. 244-248, 1975.
- [69] *E. Wylie and V. Streeter*, Fluid Transients, Ann Arbor, Michigan: Feb Press ISBN 0-9610144-0-7, 1983.
- [70] *K. V. Vereide*, Hydraulics and Thermodynamics of Closed Surge Tanks for Hydropower Plants, Doctoral theses at NTNU, Trondheim, 2016.
- [71] *K. Vereide, T. Tekle and T. Nielsen*, Thermodynamic Behavior and Heat Transfer in Closed Surge Tanks for Hydropower Plants, Journal of Hydraulic Engineering, ASCE, 2015.
- [72] *L. Pitorac, D. Bardini, K. Vereide and L. Lia*, The effect of brook intakes, downstream surge tanks and reservoir levels on surge tank stability, in BHR 13th International Conference on Pressure Surges, Bordeaux, 2018.
- [73] *H. Chaudhry, M. Sabbah and J. Fowler*, Analysis and Stability of Closed Surge Tanks, Journal of Hydraulic Engineering, vol. 111, no. 7, pp. 1079-1096, 1985.
- [74] *TIWAG*, 25 Jahre Tiroler Wasserkraftwerke A.G., Innsbruck, 1949.
- [75] *O. Rathkolb and O. Freund*, NS-Zwangsarbeit in der Elektrizitätswirtschaft der "Ostmark", 1938-1945, Böhlau Verlag, 2014.

BIBLIOGRAPHY

- [76] *Wikipedia* - price of oil, [Online]. Available: https://en.wikipedia.org/wiki/Price_of_oil [Accessed 28 July 2018].
- [77] *J. Torriti, M. G. Hassan and M. Leach*, Demand response experience in Europe: Policies, programmes, *Energy*, no. 35, p. 1575–1583, 2010.
- [78] *R. Mader and G. Gökler*, Kopswerk II, Luftmanagement einer Gegendruckturbine, in *Wasserbausymposium*, ETH, Zürich, 2008.
- [79] *R. Mader and G. Gökler*, Kopswerk II, Wasserführung, hydraulisches Design und transiente Vorgänge, in *Wasserbausymposium*, ETH, Zürich, 2008.
- [80] *R. Mader*, Lastkollektive für das Speicherkraftwerk KOPS II, in *Wasserbausymposium*, TU Graz, Graz, 2006.
- [81] *F. Meier, A. Németh and J. Vichr*, Luftdruck-Differentialwasserschloss als unkonventionelle Lösung beim Verbinden von zwei alten Hochdruckkraftwerken, in *Wasserbausymposium*, Graz, 1994.
- [82] *G. Seeber*, Das Wasserschloss des Kaunertalkraftwerkes der TIWAG, *Schweizerische Bauzeitung*, Heft 1, 1970.
- [83] *G. Heigerth*, Drossel- und Differential- Wasserschlösser von Regelkraftwerken mit freier Betriebsführung, *Dissertation*, TH Wien, 1970.
- [84] *N. Dahlbäck*, Flooding from surge in underground plants, a severe safety risk, in *Proceedings of Hydro conference*, Montreux, 2015.
- [85] *K. M. Hákonardóttir, G. G. Tómasson, J. Kaelin and B. Stefánsson*, The hydraulic roughness of unlined and shotcreted TBM-bored tunnels in volcanic rock: In situ observations and measurements at Kárahnjúkar Iceland, *Tunnelling and Underground Space Technology*, vol. 24, pp. 706-715, 2009.
- [86] *B. C. Viljoen and J. R. Metcalf*, Commissioning of the LHWP Delivery Tunnel: Overview of Work Done and Results Obtained, *Tunnelling and Underground Space Technology*, vol. 14, no. 1, pp. 37-57, 1999.
- [87] *J. Berlamont*, Friction Losses in Large-Diameter Pipes, *J. Pipeline Syst. Eng. Pract.*, vol. 6, no. 1, 2015.
- [88] *C. Jaeger*, *Fluid Transients in Hydro-Electric Engineering Practice*, Glasgow & London: Blackie, 1977.
- [89] *C. Jaeger*, *Technische Hydraulik*, Basel: Birkenhäuser, 1949.

BIBLIOGRAPHY

- [90] *C. Jaeger*, Italienische Messungen, Schweizerische Bauzeitung, vol. 108, no. 14, pp. 150-151, 1936.
- [91] *C. Dich and C. Barwart*, Headrace system of HPP Obervermuntwerk II – Geotechnical design and experience, Geomechanics and Tunneling, DOI: 10.1002/geot.201700032, vol. 10, no. 5, pp. 591-601, 2017.
- [92] *I. E. Idel'cik*, Handbook of hydraulic resistance 3rd Edition, CRC Press, 1994.
- [93] *D. S. Miller*, Internal flow systems, Bedford: BHRA, 1990.
- [94] *A. Vigl*, Script of lecture Pressure Tunnel Design - Module 3: Principles of Dimensioning, TU Graz, Vigl Consult, 2018.
- [95] *P.-E. Rønn and M. Skog*, New method for estimation of head loss in unlined water tunnels., Hydropower'97, 1997.
- [96] *A. Palmström and E. Broch*, The design of unlined hydropower tunnels and shafts: 100 years of Norwegian experience, Hydropower & Dams Issue, no. 3, pp. 72 -79, 2017.
- [97] *D. K. Lysne*, Sand transport and Sand Traps in Hydo Power Tunnels, in International Conferenc on Pumped Storage Development and its Environmental Effects, University of Wisconsin, Milwaukee, 1971.
- [98] *W. Richter, K. Vereide and G. Zenz*, Upgrading of a Norwegian pressurized sand trap combined with an open air surge tank, Geomechanics and Tunneling, p. DOI: 10.1002/geot.201700027, 2017.
- [99] *Ø. Solvik and E. Tesaker*, Floor paving in unlined hydropower tunnels, in Hydropower'97, Rotterdam, 1997.
- [100] *G. Seeber*, Druckstollen und Druckschächte, ENKE, 1999.
- [101] *R. D. Johnson*, The differential surge tank, ASCE Transactions No. 1324, pp. 760-805, 1914.
- [102] *W. Richter, K. Vereide and G. Zenz*, Optimizing surge tank layout for highly flexible hydropower, Hydropower & Dams, pp. 42-46, 2018.
- [103] *S. Kolb and V. Brost*, Neubauprojekt Pumpspeicherwerk Atdorf, Auslegung des hydraulischen Systems, Proceedings of Wasserbausymposium, TU Graz, 2012.

BIBLIOGRAPHY

- [104] *V. Brost, H. Reinhardt, A. Ruprecht, S. Kolb and J.-U. Wiesemann*, Dimensioning of the Tailwater System of the Pumped-Storage Plant Atdorf, Proceedings of 16th International Seminar on Hydropower Plants, Vienna University of Technology, 2010.
- [105] *W. Richter, J. Schneider, G. Zenz and S. Kolb*, Modellversuch Wasserschloss Atdorf, Proceedings of Wasserbausymposium, Graz University of Technology, 2012.
- [106] *W. Richter, J. Schneider, G. Zenz and S. Kolb*, Degassing of Air Bubbles in a Chamber Surge Tank,, Proceedings of 2nd European IAHR Congress, Munich, 2012.
- [107] *W. Richter, H. Knoblauch, G. Zenz and M. Larcher*, Transient Model Test of Surge Tank Reisseck 2, in 2nd IAHR European Conference, Munich, 2012.
- [108] *P. Meusburger and G. Gökler*, Pumped Storage Power Plant Obervermuntwerk II- Plant Layout and Study of different Surge Tank Design, in 18th Int. Seminar on Hydropower Plants, Vienna, 2014.
- [109] *K. Vereide, S. Bjørnar and G. Rolv*, Case study: Damaging effects of increasing the installed capacity in an existing hydropower plant, in BHR Pressure Surges, Dublin, 2015.
- [110] *L. Sterner*, 3D CFD Simulations for Tonstad Surge Tanks Upgrade, Master Thesis, Graz University of Technology, Graz, 2018.
- [111] *H. Kobus*, Wasserbauliches Versuchswesen, Stuttgart: Verlag Paul Parey, 1984.
- [112] *ASTRÖ*, Bericht - Drosselverluste der Rückstromdrossel Sellrain-Silz, not public, Graz, 1978.
- [113] *R. Klasinc, H. Knoblauch and T. Dum*, Power losses in distribution pipes, Fluid flow modelling, 1992.
- [114] *G. Zenz, J. Schneider, W. Richter and F. Lazar*, Modelbericht Wasserschloss Krespa - PSKW Obervermuntwerk II - Report of hydraulic scale model of surge Tank Krespa PSH Obervermuntwerk II, Institute of Hydraulic Engineering and Water Resources Management, Graz University of Technology, 2014, not published.
- [115] *B. Preißler*, Technische Hydromechanik Band 1, Berlin: Verlag für Bauwesen, 1980.
- [116] *M. Koch*, 3D-Numerische Simulationen der hydraulischen Verlustbeiwerte der asymmetrischen Drossel im Wasserschloss Krespa (in German) 3D Numerical Simulation of the Local Hydraulic Losses of the Asymetric Throttle in the Surge Tank Krespa, Master Thesis, TU Graz, 2016.

BIBLIOGRAPHY

- [117] *W. Richter, G. Zenz and K. Vereide*, Hydraulic design and modelling of large surge tanks, in BHR Pressure Surges, Dublin, 2015.
- [118] *M. Larcher, G. Heigerth, R. Klansinc, D. Mayr, R. Mader and G. Gökler*, Modelluntersuchung von Wasserschlosssystemen – Kopswerk II: Unterwassersystem in Gegedruckbetrieb, Wasserbausymposium TU Graz, 2006.
- [119] *W. Dobler*, Hydraulic Investigations of a Y-bifurcator, Dissertation TU Graz, 2012.
- [120] *F. Prášil*, Wasserschlossprobleme, Schweizerische Bauzeitung, vol. 51/52, 1908.
- [121] *A. Schoklitsch*, Spiegelbewegung in Wasserschlossern, Schweizerische Bauzeitung, vol. 81/82, 1923.
- [122] *A. Gardel*, Vereinfachte Berechnung von Wasserschlossern, Schweizerische Bauzeitung, vol. 75, no. 31, pp. 485-489, 1957.
- [123] *O. Schnyder*, Über Druckstöße in Rohrleitungen. (On water hammer in pipe lines.). (in German), Wasserkraft und Wasserwirtschaft, vol. 27, no. 5,6,8, pp. 49–54, 64–7,96, 1932.
- [124] *L. Bergeron*, Etude des variations de régime dans les conduites d'eau. Solution graphique générale. (Study on the steady-state variations in water-filled conduits. General graphical solution.) (in French), Revue Générale de l'Hydraulique, vol. 1, no. 1, pp. 12-25, 1935.
- [125] *C. Jaeger*, Théorie générale du coup de bélier, Paris: Dunod, 1933.
- [126] WANDA 4.2 User Manual, Deltares, 2013.
- [127] *C. Nicolet, F. Avellan, P. Allenbach, A. Sapin and J.-J. Simond*, New Tool for the Simulation of Transient Phenomena In Francis Turbine Power Plants, Lausanne: Proceedings of the Hydraulic Machinery and Systems 21st IAHR Symposium, 2002.
- [128] *C. Nicolet*, Hydroacoustic modelling and numerical simulation of unsteady operation of hydroelectric systems, Dissertation; École Polytechnique Fédérale de Lausanne, 2007.
- [129] *M. Guggenberber, F. Senn, J. Schiffer, H. Jaberg, C. Gentner, M. Sallaberger and C. Widmer*, Experimental investigation of the turbine instability of a pump-turbine during synchronization, Proceedings of 27 th IAHR Symposium on Hydraulic Machinery and Systems, 2014.

BIBLIOGRAPHY

- [130] *U. Ješe, V. Novotný and A. Skoták*, Development trends in the field of reversible pump-turbines - Study of pumping and generating mode off-design conditions, IOP Conf. Ser.: Earth Environ. Sci. 240 082009, pp. doi:10.1088/1755-1315/240/8/082009, 2019.
- [131] *Z. Zuo , H. Fan, S. Liu and Y. Wu*, S-shaped characteristics on the performance curves of pump-turbines in turbine mode – A review, Renewable and Sustainable Energy Reviews, vol. 60, pp. 836-851, 2016.
- [132] *B. Svingen*, Application of LabVIEW for dynamic simulation of Hydraulic piping systems, in Proceedings of 46th Conference on Simulation and Modeling, Trondheim, 2005.
- [133] *R. Rodic, J. Mlacnik, A. Rejec, M. Ivetic and M. Komel*, The hydraulic model study of the improvement of the surge tank at the Avce pumped storage plant, with an aeration pipe, Hydro Congress Innsbruck 2013, 2013.
- [134] *J. Arpe, C. Nicolet, P. Rodič and A. Rejec*, Experimental Investigation of Transient Behavior in the Surge Tank Physical Model of a Pumped-Storage Power Plant (PSPP), in 20th International Seminar on Hydropower Plants, Laxenburg & Vienna, 2018.
- [135] *T. Gatski and C. Rumsey*, Linear and Nonlinear Eddy Viscosity Models, in Closure Strategies for Turbulent and Transitional Flows, Cambridge , B.E. Launder, N.D. Sandham, Cambridge University Press, 2002, pp. 9-46.
- [136] *O. Reynolds*, On the Dynamical Theory of Incompressible Viscous Fluids and the Determination of the Criterion, Philosophical Transactions of the Royal Society of London, vol. 186, pp. 123-164, 1895.
- [137] *J. Boussinesq*, Théorie de l'écoulement tourbillonnant et tumultueux des liquides, Paris: Gauthier-Villars et Fils, Ded Comptes Rendus des Séances de L'Académie des Sciences, 1897.
- [138] *T. Baumann*, Turbulenzmodellierung von Strömungen niedriger molekularer Prandtlzahl, Karlsruhe, Dissertation Karlsruher Institut für Technologie (KIT), 2010.
- [139] *F. Menter*, Two-equation eddy-viscosity turbulence models for engineering applications, IAA-Journal, vol. 32, no. 8, pp. 269-289, 1994.
- [140] *F. Menter, M. Kuntz and R. Langtry*, Ten Years of Industrial Experience with the SST Turbulence Model, in Turbulence, Heat and Mass Transfer 4, Hanjalic K., Nagano J., Tummers M. (editors), Begell House, Inc , 2003.
- [141] *Ansys*, Ansys CFX-Solver Theory Guide, Canonsburg, PA: Ansys, Inc., 2011.

BIBLIOGRAPHY

- [142] *W. Richter, J. Schneider, G. Zenz and S. Kolb*, Hybrid Modelling of a Large Surge Tank, Proceedings of 17th International Seminar on Hydropower Plants, Vienna, 2012.
- [143] *A. Arch*, Luftein- und Austragsprozesse bei Anlagen mit Pelton-turbinen im Gegendruckbetrieb, Dissertation TU Graz, Graz, 2008.
- [144] *H. Drobir*, Wartungsfreundliche Lösung des Naßschachtnotverschlusses, Österreichische Wasserwirtschaft, vol. 45, no. 7/8, p. 213, 1993.
- [145] *Y. J. Fang and J. Koutnik*, The numerical simulation of the delayed load rejection of a pump-turbine powerplant, in 26th IAHR Symposium on Hydraulic Machinery and Systems, 2012.
- [146] *S. Pejovic, B. W. Karney and A. Gajic*, Analysis of Pump-Turbine S-Instability and Reverse Waterhammer Incidents in Hydropower Systems, in 4-th International Meeting on Cavitation and Dynamic Problems in Hydraulic Machinery and Systems October, 26-28, 2011, Belgrade, Serbia, 2011.
- [147] *W. Richter, G. Zenz, C. Nicolet, C. Landry, J. Vera Rodriguez and L. De La Torre Abietar*, Hydraulics of the Tail Race Surge Tank of Gouvães Pumped-Storage Hydropower, Wasserwirtschaft Extra, vol. S1, pp. 83-88, 2019.
- [148] *E. Broch*, Unlined high pressure tunnels in areas of complex topography, Water power and Dam construction , no. 11, pp. 21-23, 1984.
- [149] *R. Gerstner, E. Netzer and L. Vigl*, Long-term behaviour of pressure tunnels, Geomechanics and Tunnelling, no. 6, pp. 407-421, 2013.
- [150] *G. Seeber*, Möglichkeiten und Grenzen im Druckstollenbau, Schweizer Ingenieur und Architekt, vol. 89, no. 29, pp. 639-647, 1981.
- [151] *K. Panthi and C. Basnet*, Review on the Major Failure Cases of Unlined Pressure Shafts/Tunnels of Norwegian Hydropower Projects, Hydro Nepal Journal of Water Energy and Environment, vol. 6, no. 1, pp. 6 - 15, 2016.
- [152] *J. F. Sandborn and M. E. Zipser*, Grouting Operations, Catskill Water Supply, ASCE-Proceedings, vol. 1, 1920.
- [153] *L. Mühlhofer*, Theoretische Betrachtungen zum Problem des Druckstollenbaues, Schweizerische Bauzeitung, vol. 77/78, no. 21, 1921.
- [154] *A. Kieser*, Druckstollenbau, Wien: Springer Verlag, 1960.
- [155] *H. Lauffer*, Vorspanninjektionen für Druckstollen, Nr. Heft 7, 1968.

BIBLIOGRAPHY

- [156] *G. Seeber*, Power conduits for high-head plants, *Water Power & Dam Construction*, no. 6, pp. 50 - 54, 1985.
- [157] *G. Seeber*, Power conduits for high-head plants, Part two, *Water Power & Dam Construction*, no. 7, pp. 95-98, 1985.
- [158] *F. Eibl, M. Mähr and D. Vögele*, Automated rock strain measurements for the planned pumped storage plant Kühtai using the TIWAG-Radial Press, *Geomechanics and Tunnelling*, no. 5, pp. 31-39, 2012.
- [159] *G. Seeber*, I) Wirklichkeitsnahe Bemessung von Druckschachtpanzerungen II) Auswertungen von statischen Felsdehnungsmessungen, Dissertation, Technische Hochschule Graz, 1961.
- [160] *G. Seeber, W. Demmer and W. Finger*, Damages at Hattelberg Pressure Tunnel Caused by Extraordinary Natural Stresses (German - Die Schäden im Hattelber-Druckstollen als Folge eines außergewöhnlichen Primärspannungszustandes, in *ISRM Congress*, Montreux, 1979.
- [161] *E. Broch, T. S. Dalhø and S. E. Hansen*, Hydraulic jacking tests for unlined high pressure tunnels, in *Hydropower'97*, Balkema, Rotterdam, 1997.
- [162] *J. Kummerer and H. Stäuble*, Auswertungen Felsmechanischer Untersuchungen, gezeigt am Beispiel der Vorarbeiten für eine Kraftwerkskaverne, *Felsbau*, vol. 8, no. 4, pp. 167-174, 1990.
- [163] *E. Broch*, Die Entwicklung von nicht-ausgekleideten Hochdruckstollen und geschlossenen Schwallräumen mit Luftpolster in Norwegen, in *38. Salzburger Kolloquium für Geomechanik*, 1989.
- [164] *H. Kjørholt*, Gas Tightness of Unlined Hard Rock Caverns, Dissertation NTH Trondheim, 1991.
- [165] *A. Momber and R. Kovacevic*, Fundamental investigations on concrete wear by high velocity water flow, Elsevier, 1994.
- [166] *I. Tzanakis, D. Eskin, A. Georgoulas and D. Fytanidis*, Incubation pit analysis and calculation of the hydrodynamic impact pressure from the implosion of an acoustic cavitation bubble, *Ultrasonics Sonochemistry* 21, 866 - 878: Elsevier, 2014.
- [167] *I. Pothof and B. Karney*, Guidelines for Transient Analysis in Water Transmission and Distribution Systems, InTech DOI: 10.5772/53944, 2012.

BIBLIOGRAPHY

- [168] *H. Kjørholt and E. Broch*, The Water Curtain-a Successful Means of Preventing Gas Leakage from High-Pressure, Unlined Rock Caverns, Tunneling and Underground Space Technology, Vol.7 No.2 pp127-132: Pergamon Press, 1992.
- [169] *E. Broch*, Tunnels and Underground Works for Hydropower, Muir Wood Lecture, 2010.
- [170] *J. Hu, J. Zhang, L. Suo and J. Fang*, Advance in Research On Air Cushion Surge Chamber in Hydropower Plant, in ASME International Mechanical Engineering Congress and Exposition, Seattle, USA, 2007.
- [171] *T. Røse, A. Koksæter, K. Dalviken, O. Skuncke, B. Børresen and K. Vereide*, Design of an ACSC for Upper Kon Tum HPP, Proceedings of Hydro Asia, Danang, Vietnam, 2018.
- [172] *H. Brekke*, Stability Problems in High Pressure Tunnel Systems in Norwegian Hydro-Electric Power Plants, International Conference on Pressure Surges: BHRA, 1972.
- [173] *S. Van der Zwan, M. Toussaint, A. Alidai, I. W. M. Pothof and P. H. Leruth*, Thermodynamics of surge vessels, in 12th BHR Pressure Surges Conference, Dublin, 2015.
- [174] *H. Brekke*, Hydraulic Turbines Design, Erection and Operation, in Script, NTNU, 2001.
- [175] *P. Matt*, Just in Time - Kops II - als Antwort auf die Volatilität des Energiemarktes, in Wasserbausymposium Walgau TU München, 2010.
- [176] *B. Nilsen and A. Thidemann*, Hydropwer Development - Rock Engeneeing, Trondheim: Norwegian Insitute of Technology, Divison of Hydraulic Engineering, 1993.
- [177] *W. Richter, K. Vereide, J. Schneider, H. Knoblauch, L. Lia and G. Zenz*, Druckluft-wasserschläsöser für alpine Hochdruckwasserkraftanlagen, in Tagungsband Internationales Symposium 2014, ETH Zürich, 2014.
- [178] *D. C. Goodall, H. Kjørholt, T. Tekle and E. Broch*, Air cushion surge chambers for underground power plants, Water Power and Dam Construction, 1988.
- [179] *C. Nicolet, A. Béguin, J.-D. Dayer and J. Micoulet*, Hydraulic transient challenges for the upgrade of FMHL+pumped storage power plant from 240MW to 420MW, in IAHR, Kyoto, 2018.
- [180] *N. Adam, G. De Cesare, C. Nicolet, P. Billeter, A. Angermayr, B. Valluy and A. Schleiss*, Design of a Throttled Surge Tank for Refurbishment by Increase of Installed Capacity at a High-Head Power Plant, Journal of Hydraulic Engineering, vol. 144, no. 2, 2018.

BIBLIOGRAPHY

- [181] *K. Vereide, W. Richter, O. Havrevoll, L. Lia and T. Jacobsen*, Upgrading of Sand Traps in Existing Hydropower Plants, in Proceedings of Hydro Congress, Seville, 2017.
- [182] *B. Svingen and H. H. Francke*, Large and rapid set-point adjustment of hydro power plants using embedded transient hydraulic simulations of the plant as a model predictive method, in BHR Group, Pressure Surges, Dublin, 2015.
- [183] *K. Vereide, B. Svingen and T. Aarønes*, Digital Tvilling i Tonstad Kraftverk: Overordnet Regulator og Vannveisvern (in Norwegian), in Produksjonsteknisk konferanse, Oslo, 2019.
- [184] *F. Johansen*, Tonstad Kravtverk Sandfang - og Strømningsundersøkelser, Sintef, Trondheim, 1967.
- [185] *K. Bråtveit, L. Lia and N. Olsen*, An efficient method to describe the geometry and the roughness of an existing unlined hydro power tunnel, Energy Procedia 20 (2012) , p. 200 – 206, 2012.
- [186] *O. Brevik*, 3D numerisk modellering av deler av vassvegen til Tonstad kraftverk, Master thesis NTNU, Trondheim, 2013.
- [187] *K. Bråtveit*, Effects of load fluctuation on hydropower tunnels , in Doctoral Thesis, NTNU, Trondheim, 2015.
- [188] *D. Gomsrud*, Design of a Surge Tank Throttle for Tontad Hydropower Plant, Trondheim, Master Thesis,: NTNU - Norwegian University of Science and Technology, 2015.
- [189] *C. Nicolet, M. Dreyer, A. Béguin, E. Bollaert, S. Torrent and J.-D. Dayer*, Hydraulic Transient Survey at Cleuson-Dixence with Real-Time Hydro-Clone Monitoring System, Proceedings of Hydro Conference, Gdansk, 2018.
- [190] *R. Wechtitsch*, Modellierung von Stollenspeicher (in German) Modelling of Storage Tunnels, Master Thesis, Graz University of Technology, 2014.
- [191] *W. Richter, H. Knoblauch and G. Zenz*, Surge Tank Design for Storage-Tunnels, in 19th International Seminar on Hydropower Plants, Vienna, 2016.
- [192] *W. Widmann, T. Lebesmühlbacher, A. Eder and K. Knorpp*, Design and operation of the Stanzertal hydro power plant headrace tunnel as reservoir, in Hydro Congress, Bordeaux, 2015.
- [193] *T. Berg, E. Bårgard, L. Lia and W. Richter*, Headrace tunnels used as short-term reservoirs for hydropower, in Proceedings of HYdro Congress, Porto, 2019.

BIBLIOGRAPHY

- [194] *W. Richter, H. Knoblauch and G. Zenz*, Wasserschlossdesign für Stollenspeicher (in German) Surge tank Design for Storage-Tunnels, in Proceedings of: 18th Wasserbausymposium Obernach TU München , Wallgau, 2016.
- [195] *R. Prenner*, Design of Throttled Surge Tanks for High-Head Plants. Comparison of the Hydraulic Behavior of Several Throttle Types in a Straight Pipe During Pressure Wave Transmission, *Waterpower*, 1999.
- [196] *K. Vereide, B. Svingen, T. Nielsen and L. Lia*, The Effect of Surge Tank Throttling on Governing Stability, Power Control, and Hydraulic Transients in Hydropower Plants, *IEEE Transactions on Energy*, vol. VOL. 32 , no. NO. 1, 2017.
- [197] *R. Gabl*, Numerische und physikalische Untersuchung des Verlustbeiwertes einer asymmetrischen Düse im Wasserschloss, Dissertation, University of Innsbruck, 2012.
- [198] *N. J. Adam*, Characterization of hydraulic behavior of orifices in conduits, Doctoral Thesis: École Polytechnique Fédérale de Lausanne, 2017.
- [199] *D. Thoma*, Die Rückstromdrossel, *VDI-Zeitschrift*, vol. 74, 1930.
- [200] *J. Gspan*, Untersuchungen an der hydraulischen Rückstromdrossel von Wasser-schlössern, *Wasserwirtschaft* 69, Nr.12, 1979.
- [201] *F. Haakh*, Wirbelkammerdioden als Drosselorgan im Rohrleitungssystem, Berechnung des transienten Strömungsverhaltens, *Wasser Abwasser* Nr. 9, 2003.
- [202] *B. Huber*, Der Einfluß einer Rückstromdrossel auf die Transmission und Reflexion von Druckwellen, Dissertation , Technische Universität Wien, 1999.
- [203] *P. Bonapace*, Renewal of the pressure shaft and surge tank of the Kaunertal power station, *Geomechanics and Tunneling*, vol. 5, no. 5, 2012.
- [204] *TIWAG*, Technical report about the surge tank maintenance at Kaunertal HPP (unpublished), 2009.
- [205] *W. Richter, W. Dobler and H. Knoblauch*, Hydraulic and Numerical Modelling of an Asymmetric Orifice within a Surge Tank, 4th International Symposium on Hydraulic Structures, Porto, 2012.
- [206] *M. Larcher, H. Knoblauch, G. Heigerth, E. Wagner and P. Stering*, Instationäre Füll- und Entleervorgänge bei der Auslegung der Oberkammer des Wasserschlusses Limberg II, *Wasserwirtschaft* Nr.4 Pg. 107 - 109, 2010.

BIBLIOGRAPHY

- [207] *W. Richter, J. Schneider, H. Knoblauch and G. Zenz*, Behavior of Long Chambers in Surge Tanks, Proceedings of 18th International Seminar on Hydropower Plants, Vienna, 2014.
- [208] *D. Danciu*, Experimental Investigations on Air Entrainment under Impinging Jets, in 9th Ansys Multiphase Flow Workshop, Dresden, 2011.
- [209] *H. Sigg., A. Lais and P. Volkart*, Kopswerk II: Peltonturbinen im Gegendruckbetrieb, Modellversuche zur Entlüftungsproblematik., Proceedings of Wasserbausymposium TU Graz, vol. 46, no. 1, pp. 477-489, 2006.
- [210] *H. Kull*, Theory of the Rayleigh-Taylor Instability, Physics Reports (Review Section of Physical Letters), vol. 206, no. 5, pp. 197-325, 1991.
- [211] *C. Clanet and J. Lasheras*, Depth of penetration of bubbles entrained by a plunging water jet, University of California, San Diego, 1997.
- [212] *H. Falvey. D.A. Ervine*, Behaviour of turbulent water jets in the atmosphere and in plunge pools, Proc. Inst. Civ. Engineers, pp. 295-314, 1987.
- [213] *H. Kobus*, Air entrainment in free-surface flows, IAHR hydraulic structures design manual, Rotterdam: Ian R.Wood, 1991.
- [214] *M. Ruetz*, Particel Image Velocimetry (PIV) Messungen am Modellversuch Wasserschloss Krespa (in German), Particel Image Velocimetry (PIV) Measurements at the surge tank Krespa, Master Thesis, Graz University of Technology, 2014.
- [215] *T. Urach*, Modelluntersuchungen am Wasserschloss Krespa des PSKW Obervermuntwerk II (in German), Model Test investigations on the surge tank Krespa of the Obervermuntwerk II, Master Thesis, Graz University of Technology, 2015.
- [216] *Frank*, Eulerian Multiphase Flow Modelling: Phase Interaction Models, 9th Ansys Multiphase Flow Workshop Dresden, 2011.
- [217] *L. Schiller and A. Naumann*, Über die grundlegende Berechnungen bei der Schwerkraftaufbereitung, Zeitschrift des Vereines deutscher Ingenieure, p. Leipzig, 1933.
- [218] *W. Richter, J. Schneider, G. Zenz and S. Kolb*, Entgasung in einem Kammerwasserschloss, Wasserwirtschaft, no. 6, pp. 37-42, 2012.
- [219] *VKW Illwerke*, Youtube.com, Wiederin Film, 2017. [Online]. Available: <https://www.youtube.com/watch?v=UdTHVcs9WdM>. [Accessed 03 06 2019].

LIST OF FIGURES

[220] *F. Hachem and A. Schleiss*, Online Monitoring of Steel-Lined Pressure Shafts by Using Pressure Transient Signals under Normal Operation Conditions, *Journal of Hydraulic Engineering*, vol. 138, no. 12, pp. 1110-1118, 2012.

[221] *R. Clift, J. Grace and M. Weber*, *Bubbles, Drops and Particles*, Academic Press, 1978.

LIST OF FIGURES

Figure 2-1: Frequency control stages to stabilise the electrical grid, times to provide the pre-approved 100 % of the power (<i>Richter</i> , information from [9], [10]).....	27
Figure 2-2: “Mean EROI (and standard error) values for known published assessments of electric power generation systems (Note: the ranges of the values are much greater than the standard error). Values derived using known modern and historical published EROI and energy analysis assessments and values published by Dale (2010)” [21], (figure from <i>Lambert et. al.</i> [19])	29
Figure 2-3: ESOL _e ratios of energy storage in geologic, battery LIB (lithium-Ion), NaS (sodium sulphur), VBR (vanadium redox), ZnBr (zinc-bromine) flow batteries, (PbA (lead-acid) , and regenerative fuel cell systems (figure from [23])	30
Figure 2-4: Ideal electrical storage demand with PSH of extrapolated 100 % power production in Germany with basis years 2012 to 2017 (<i>Richter</i> , data from: [26]).....	32
Figure 2-5: Ideal electrical storage demand with PSH of extrapolated 100 % power production in Germany with basis years 2016 to 2017, detail (<i>Richter</i> , data from: [26]).....	33
Figure 2-6: Ideal power capacity demand for PSH equivalent storage demand of extrapolated 100 % power production in Germany with basis years 2012, to 2017 (<i>Richter</i> , data from [26]).....	34
Figure 2-7: Storage capacity in Austria [GWh] and filling level of the hydro storage [%], (from E-Control, Austria)	35
Figure 2-8: Specific capacity investments [€/kW] and gross heads [m] for selection of recent pumped storage schemes (P) Project in planning, (figure and data collected by <i>Richter</i>)	37
Figure 2-9: Specific investments €/kW versus €/kWh for selection of recent pumped storage schemes, (P) projects in planning, (figure and data collected by <i>Richter</i>)	39
Figure 3-1: Purposes and dependencies of surge tank design.....	49
Figure 3-2:General layout of a high-head hydropower plant with headrace surge tank system, indicating the oscillation regimes (<i>Richter</i> [57])	51
Figure 3-3: Longitudinal section of generic pumped-storage hydropower scheme with chamber surge tanks	52
Figure 3-4: Turbine discharge for ST with Thoma 1.0 and 1.5 shaft size.....	55
Figure 3-5: Shaft oscillation in ST with Thoma 1.0 and 1.5 shaft size	55
Figure 3-6: Turbine discharge for ST with Thoma 1.0 [-] not throttled and throttled and a not-throttled Thoma 1.5 [-] shaft size.....	56
Figure 3-7: Comparison of Svee stability area to Thoma stability area for tailrace conduit systems [65]	57
Figure 3-8: Large high-head and pumped storage schemes in Austria, development of power (P), design discharge (Q) and diameter of headrace tunnels (D) along one hundred years, as well as the planned <i>Atdorf</i> PSH scheme in Germany (<i>Richter</i> , data collection from [29]).....	60

LIST OF FIGURES

Figure 3-9: Internal water volume of pressure tunnels in selected Austrian and the planned PSH <i>Atdorf</i> in Germany schemes, chronological from left to right (<i>Richter</i> , data from [29])	64
Figure 3-10: Reloading after start-up and unloading, idealised 1D-numerical simulation of a generic system with rigid column simulation, without water hammer capturing (<i>Richter</i> [55])	67
Figure 3-11: Resonance load-case – multiple loading cases, idealized 1D-numerical simulation of a generic system representing with rigid column simulation, without water hammer capturing (<i>Richter</i> [55])	68
Figure 3-12: Table approach to convert Strickler friction into Darcy friction factor and sand grain roughness	70
Figure 3-13: Typical friction coefficients for tunnel and shaft liners in Strickler value k_{ST} [$m^{1/3}s^{-1}$] (source: lecture script A. <i>Vigl</i> 2018, modified).....	72
Figure 3-14: Generic shaft surge-tank design.....	73
Figure 3-15: Generic chamber surge tank design	74
Figure 3-16: Generic Johnson differential surge tank design (<i>Richter</i> [102])	75
Figure 3-17: Johnson differential surge tank at <i>Prutz-Imst</i> HPP in Austria (<i>Richter</i> [102])	75
Figure 4-1: Schematic section of the <i>Atdorf</i> pumped storage hydropower plant, not to scale (<i>Richter</i> [105]).....	77
Figure 4-2: Perspective view of surge tank <i>Atdorf</i> PSH, 8-loop shape upper and lower chamber (<i>Richter</i> [106])	78
Figure 4-3: Front view of investigated surge tank <i>Atdorf</i> PSH, two connection shafts to tailrace pressure tunnel (<i>Richter</i> [106])	78
Figure 4-4: Perspective view of the final <i>Atdorf</i> surge tank design with internal volume (<i>Richter</i> [106]).....	79
Figure 4-5: Top view of the final <i>Atdorf</i> surge tank design, indicating orientation and connection shafts	79
Figure 4-6: Systematic position of the <i>Burgstall</i> tailrace surge tank in the <i>Reisseck II</i> scheme (<i>Richter</i> [107], modified)	80
Figure 4-7: 3D geometry of the <i>Burgstall</i> tailrace surge tank (<i>Richter</i> [107])	80
Figure 4-8: Main shaft connection detail of the differential orifice throttle of <i>Burgstall</i> tailrace surge tank (<i>Richter</i> [107])	81
Figure 4-9: Visualisation of pumped storage scheme of the PSH <i>Obervermuntwerk II</i> [45] (modified)	82
Figure 4-10: Visualisation of the <i>Krespa</i> surge tank (<i>Richter</i> [44], modified).....	83
Figure 4-11: Water hammer reflection if flow-through lower chamber – initial variant	84
Figure 4-12: Water hammer reflection with direct shaft – final solution	84
Figure 4-13: General layout of <i>Tonstad</i> HPP scheme in southern Norway [98], (source: <i>Sira-Kvina</i>).....	85
Figure 4-14: <i>Tonstad</i> surge tank, perspective view (<i>Richter</i> , 3D model by <i>Sterner</i> [110]).....	86
Figure 5-1: Investigation evolution of hybrid modelling for waterfall aspect (1D-numerical simulation <i>Wanda</i> , 3D-CFD <i>Ansys CFX</i>)	87
Figure 5-2: Model test rig for differential throttle evaluation of <i>Krespa</i> surge tank (<i>Richter</i> [45], modified)	91
Figure 5-3: Pressurized model test setup for differential throttle evaluation of <i>Krespa</i> surge tank (<i>Richter</i> [114], modified)	92
Figure 5-4: Hydraulic losses in surge tank connection with differential throttle (<i>Richter</i> [114], modified)	93
Figure 5-5: Detail of the connection tunnel with the T-junction, the differential throttle, the conical bend	93
Figure 5-6: Up-surge loss discharge (<i>Richter</i> [114], modified).....	93
Figure 5-7: Down-surge loss discharge (<i>Richter</i> [114], modified).....	93
Figure 5-8: Local loss visualisation, 3D-flow zone, 1D approach flow zone (<i>Richter</i> after [115]).....	94

LIST OF FIGURES

Figure 5-9: Measurement sections and dissipation zone, PT (pressure tunnel), ST (surge tank), (<i>Richter</i> [114], modified).....	95
Figure 5-10: Differential orifice throttle small-scale model, (picture: <i>Richter</i>).....	95
Figure 5-11: Section cut of asymmetric throttle for physical test (figure and picture by <i>Richter</i> , [107] modified)	95
Figure 5-12: Scheme of a PSH design, boundary of 1D-numerical simulation, boundary of physical model test simulation for the <i>Atdorf</i> surge tank, (<i>Richter</i> [106]).....	96
Figure 5-13: Ground view of model test setting of PSH <i>Atdorf</i> surge tank investigation, (drawing by <i>Lazar</i> [105], modified).....	97
Figure 5-14: Prototype discharge at surge tank base	98
Figure 5-15: Model test discharge at surge tank base	98
Figure 5-16: Input discharge target compared with measured discharge at surge tank base at specific model test scale factor 1:25	98
Figure 5-17: Principle of PIV (<i>Dantec Dynamics</i>)	99
Figure 5-18: Small-scale surge tank model with reservoir, pressure tunnel, pressure shaft, surge tank and outlet valve (<i>Richter</i>).....	100
Figure 5-19: 1D-numerical model of <i>Krespa</i> surge tank with waterfall-dampening device in <i>WANDA</i> , (<i>Richter</i> [114]).....	103
Figure 5-20: 1D representation (area/height) of compact lower chamber in <i>Wanda</i> (<i>Richter</i> [114])	104
Figure 5-21: 3D geometry with horizontal section cuts of a lower chamber (<i>Richter</i> [114])	104
Figure 5-22: Typical Four-quadrant field characteristics with marked zones of instability, <i>Ješe et. al.</i> (2019) [130]	105
Figure 5-23: Effect of the S-shape zone for start-up and load rejection <i>Zuo et.al.</i> (2016) [131]	106
Figure 5-24: Transient 3D-CFD Simulation throttle jet, time point 1	109
Figure 5-25: Transient 3D-CFD Simulation throttle jet, time point 2	109
Figure 5-26: Hybrid modelling options in addition to a physical model test of a surge tank, modified from (<i>Richter</i> [142]).....	110
Figure 5-27: 3D-numerical simulation of the surge tank <i>Atdorf</i> , (<i>Richter</i> [106]).....	111
Figure 5-28: Physical model of the surge tank <i>Atdorf</i> in the hydraulic laboratory, (<i>Richter</i> [106])	111
Figure 5-29: Lower chamber with vortex core at high discharge from lower chamber to pressure tunnel, (<i>Richter</i> [106]).....	111
Figure 5-30: Wall in lower chamber dividing the flow from both sides of the chamber and avoiding the vortex, (<i>Richter</i> [106]).....	111
Figure 5-31: Vortex flow in connection shaft at maximum discharge due to resonance load-case, (<i>Richter</i> [106])	112
Figure 5-32: Avoided vortex flow for maximum transient design flow, wall that divides the flow from both lower chamber sides within the loop branch, (<i>Richter</i> [106])	112
Figure 6-1: Chamber surge tank HPP <i>Kaunertal</i> (surge tank in operation from 1964 - 2016) [82]	119
Figure 6-2: General comparison of longitudinal section of pressurized water conveyance system for a classic Alpine solution with and open-air surge tank and a Norwegian solution with an air cushion surge tank	125

LIST OF FIGURES

Figure 6-3: General comparison of longitudinal section of pressurized water conveyance system regarding a classical Alpine solution and an adapted solution with an air cushion chamber for Alpine regions (Richter [177], modified)	125
Figure 6-4: Layout of the <i>Tonstad</i> surge tank (figure from [186], modified).....	128
Figure 6-5: <i>Tonstad</i> surge tank with proposed attached additional lower chamber, ground view (Sterner [110], modified)	130
Figure 6-6: Layout of <i>Tonstad</i> surge tank with proposed attached additional lower chamber, front view (Sterner [110], modified)	130
Figure 6-7: 3D-numerical study of up-surge in 8-loop shape surge tank for the <i>Atdorf</i> PSH project	131
Figure 6-8: Layout of the semi-closed surge tank design with crown throttle	132
Figure 6-9: Layout of a proposed <i>Tonstad</i> surge tank expansion with proposed attached additional lower chamber and suggested development of semi-air cushion, schematic longitudinal section	132
Figure 6-10: Layout of the semi-closed surge tank design for steady operation and at state of minimal water level	133
Figure 6-11: Layout of <i>Tonstad</i> surge tank with proposed attached additional lower chamber and suggested development of semi-air cushion at time point of down-surge – no separate air pipe (Sterner [110], modified).	134
Figure 6-12: Layout of <i>Tonstad</i> surge tank with proposed attached additional lower chamber and proposed development of semi-air cushion at time point of up-surge, water-air mixture → Separate air shaft suggested (Sterner [110], modified)	134
Figure 6-13: Layout of <i>Tonstad</i> surge tank with proposed attached additional lower chamber and suggested development of semi-air cushion at time point of up-surge with a separate air pipe (Sterner [110], modified)	135
Figure 6-14: Steady-state operation as starting condition, with water level in the surge tank below the reservoir level	136
Figure 6-15: Unloading event of the turbines indicated as closed pressure shaft	136
Figure 6-16: Up-surge due to water mass oscillation → inflow surge tank	136
Figure 6-17: Subsequent backflow triggered by previous up-surge → outflow surge tank	136
Figure 6-18: Amplified down-surge related to reloading of machines → lower chamber feeds the discharge, aeration shaft prevents cavitation and allows efficient outflow of the lower chamber, throttled outflow of the differential riser acts as decoupled reservoir for efficient surge tank behaviour to accelerate the water mass in the pressure tunnel	137
Figure 6-19: Outflow of surge tank allows acceleration of the pressure tunnel	137
Figure 6-20: Starting of backflow after minimum water level in surge tank	137
Figure 6-21: Unloading of turbines with activation of air cushion in lower chamber by throttled air release in small pipe	137
Figure 6-22: Up-surge and overflow event of the small riser, effect of delayed air release in lower chamber comparable to upper chamber filling	138
Figure 6-23: Filling of the surge tank facility reaching high filling and providing sufficient safety volume	138
Figure 6-24: Reloading of the machines in generation mode, quick reaction of the small riser mitigating water hammer and supplying water	138
Figure 6-25: Quick creation of air pockets in the lower chamber from both sides	138

LIST OF FIGURES

Figure 6-26: Lowest level in lower chamber with safety volume and minimum free surface flow to avoid hydraulic jump and air intrusion	139
Figure 6-27: Backflow and subsequent up-surge at emergency shut down in mass oscillation resonance.....	139
Figure 6-28: Schematic layout of a run-of river power plant with storage-tunnel and storage-tunnel surge tank, direct water intake design (<i>Richter</i> [194]).....	143
Figure 6-29: Schematic layout of a run-of river power plant with storage-tunnel and storage-tunnel surge tank, siphon water intake design (<i>Richter</i> [191])	144
Figure 6-30: Example of a differential throttle with a de-aeration and a de-watering pipe in horizontal arrangement for the pumped storage power plant <i>Obervermuntwerk II</i> [44] (<i>Lazer</i> , (modified), picture: courtesy of Illwerke AG)	145
Figure 6-31: (a) 1D-numerical simulation screen shot with the arrangement of the storage-tunnel design using free surface pipe elements in the software <i>Wanda V4.3</i> ; (b) system scheme indicating the part represented in the 1D-numerical simulation in (a) (<i>Richter</i> [191], modified)	148
Figure 6-32: Load-case of operation start in the pressure shaft with 140 m ³ /s in 60s (<i>Richter</i> [191], modified)	149
Figure 6-33: CFD Simulation for start-up of pilot case system – free surface flow in tunnel and surge tank – widened tunnel section before the drop into the pressure shaft (<i>Richter</i> [191]).....	150
Figure 6-34: Asymmetric throttle with de-aeration pipe, detail (<i>Richter</i> [191]).....	150
Figure 6-35: Front view of the storage-tunnel surge tank (<i>Richter</i> [191]).....	150
Figure 6-36: Throttle position at transition from pressure tunnel to surge tank (symmetric orifice throttle, shaft surge tank).....	152
Figure 6-37: Throttle position at transition from lower chamber to main shaft (symmetric orifice throttle, chamber surge tank).....	152
Figure 6-38: Differential orifice throttle definitions	153
Figure 6-39: Down-surge situation at certain time step at complex asymmetric orifice throttle	153
Figure 6-40: Differential vortex throttle geometry, HPP <i>Kaunertal</i> (<i>Richter</i> [1]).....	155
Figure 6-41: Down-surge of the <i>Kaunertal</i> vortex throttle of 15 m ³ /s, transient 3D-numerical simulation, snapshot at specific time point, (<i>Richter</i> [1])	156
Figure 6-42: Aeration shaft system for <i>Kaunertal</i> HPP vortex throttled chamber surge tank (<i>Seeber</i> , 1970 [82] modified).....	157
Figure 6-43: Aeration shaft for chamber surge tank	157
Figure 6-44: Throttle alignment with lower loss factor in turbine flow direction as for backflow to the reservoir, numerical simulation in scale 1:30, plan view (<i>Richter</i> [117])	158
Figure 6-45: Throttle alignment with higher loss factor for backflow direction as for the flow direction to the units, numerical simulation in scale 1:30, plan view (<i>Richter</i> [117]).....	158
Figure 6-46: Two chamber tailrace surge tank for PIV investigations (<i>Richter</i> [205])	159
Figure 6-47: Measurement planes of the PIV investigations (<i>Dobler</i> [205], modified)	160
Figure 6-48: Section A-A of the main shaft and plan view of the throttle (<i>Dobler</i> [205], modified)	160
Figure 6-49: PIV setup surrounded by the PIV box for safety reasons (<i>Richter</i>) [205].....	161
Figure 6-50: PIV laser sheet at throttle outlet (<i>Richter</i>).....	161
Figure 6-51: Average flow velocity over 5 seconds (model scale), plane 2 of PIV measurement (<i>Dobler</i> [205])	162
Figure 6-52: Average flow velocity over 5	162

LIST OF FIGURES

Figure 6-53: Average flow velocity in steady-state CFD calculation of the model test regarding the same boundary conditions as for the PIV measurements (<i>Richter</i> [205])	162
Figure 6-54: Average flow velocity in transient	162
Figure 6-55: PIV result: Distribution of the up-surge flow at time step 1.5 s (<i>Dobler</i> [205])	163
Figure 6-56: Schematic description of the measurement planes 1 and 2 (<i>Dobler</i> [205])	163
Figure 6-57: PIV result: Distribution of the up-surge flow at time step 2.0 s (<i>Dobler</i> [205])	163
Figure 6-58: PIV result: Distribution of the up-surge flow at time step 2.5 s (<i>Dobler</i> [205])	163
Figure 6-59: PIV result: Distribution of the up-surge flow at time step 3.85 s (<i>Dobler</i> [205])	164
Figure 6-60: 3D-CFD transient simulation model scale equal boundary conditions as PIV model test measurement (<i>Dobler</i> [205])	164
Figure 6-61: Filling of specific long upper chamber with surge reflection at aeration building with slope inclination of 1.0 %, 1.5 % and 1.5 % plus additional deflectors at the side walls (<i>Richter</i> [207])	165
Figure 6-62: Long chamber filling and emptying improved by sidewall dissipators (<i>Richter</i> [117])	166
Figure 6-63: Chamber connection to the main riser for <i>Atdorf</i> surge tank model (scale factor 1:40), scaled human (<i>Richter</i> [106])	167
Figure 6-64: 3D-numerical simulation of the surge tank PSH <i>Atdorf</i> , upper chamber filling (<i>Richter</i> [142])	168
Figure 6-65: Long chamber spill protection by deflection plate	168
Figure 6-66: d) Long chamber spill protection by deflection plate, surge deflection by the plate (<i>Richter</i>)	169
Figure 6-67: Chamber surge tank with flow separation and waterfall intruding air into the water cushion (scheme). Positive regarding mass oscillation dampening.	170
Figure 6-68: Chamber surge tank with mitigated flow separation due to outflow optimization (scheme). Less separation is negative regarding mass oscillation dampening.	170
Figure 6-69: Compact upper chamber to avoid waterfall occurrence, with lower chamber inertia	171
Figure 6-70: Compact upper chamber to avoid waterfall occurrence, without lower chamber inertia	171
Figure 6-71: Air entrainment mechanism (1), inclusion of air packets by contact of wave peaks of the water cushion and the jet (figure from <i>Danciu</i> [208])	172
Figure 6-72: Air entrainment mechanism (2), inclusion of air packets due to surface tension effects (figure from <i>Danciu</i> [208])	172
Figure 6-73: Air bubble intrusion mechanism of a single jet (<i>Danciu</i> [208])	173
Figure 6-74: 1D-numerical simulation of the upper chamber behaviour for the waterfall occurrence at the <i>Krespa</i> surge tank (<i>Richter</i> [43])	174
Figure 6-75: 3D-numerical waterfall investigations without dampening device (<i>Richter</i> [43])	175
Figure 6-76: Waterfall in physical model test without dampening device (<i>Richter</i> [43])	176
Figure 6-77: 3D-numerical simulation, visualising the waterfall occurrence with flow separation at upper chamber (<i>Dobler</i> [106])	176
Figure 6-78: 1D-numeric including the separation of columns and waterfall discharge into shaft, water level surge tank (red line) and water level at upper chamber crest (green line), (<i>Richter</i> [106])	176
Figure 6-79: Terminating velocity of a single air bubble (figure from [213])	177
Figure 6-80: Air intrusion depth in an unconfined pool with bubble terminating velocity of 0.25 m/s, key figure of the <i>Ervine and Falvey</i> publication, (figure from [212])	179

LIST OF FIGURES

Figure 6-81: Comparison of the 1D-simulations and the physical model test of the waterfall design load-case (<i>Richter</i> [43]).....	181
Figure 6-82: Evaluation of Air intrusion depth by water jet, Results from <i>Clanet and Laheras, Ervine and Falvey</i> and CFD simulations (<i>Richter</i> [43]).....	182
Figure 6-83: Air intruding plunging jet at physical model without dampening device, (<i>Urach</i> [215], modified)	183
Figure 6-84: Terminal air bubble PIV velocity measurement at <i>Krespa</i> surge tank without dampening device, (<i>Urach</i> [215], modified).....	183
Figure 6-85: Air intruding plunging jet at physical model test with utilisation of the dampening device, (<i>Urach</i> [215], modified).....	184
Figure 6-86: Terminal air bubble PIV velocity measurement at surge tank with dampening device, (<i>Urach</i> [215], modified).....	184
Figure 6-87: Terminal air bubble velocity at <i>Krespa</i> surge tank with the dampening device, (<i>Ruetz</i> [214]).....	185
Figure 6-88: Terminating air bubble velocity, implementation in <i>Ansys CFX</i> , (figure from [216]).....	186
Figure 6-89: Boundary conditions for the numerical model, (<i>Richter</i> [106])	186
Figure 6-90: Degassing in lower chamber <i>Atdorf</i> tailrace surge tank, physical model test scale 1:40 (<i>Richter</i> [218])	187
Figure 6-91: Degassing in lower chamber of the <i>Atdorf</i> surge tank, model test 1:40 in 3D-numerical two-phase simulation at model time 1.2 s, (<i>Richter</i> [218], modified)	187
Figure 6-92: Waterfall damping device for <i>Krespa</i> surge tank, time at water column separation (<i>Richter</i>).....	189
Figure 6-93: Waterfall damping device for <i>Krespa</i> surge tank, transformation of a large waterfall to defined smaller water jets (<i>Richter</i>).....	189
Figure 6-94: Waterfall-dampening device in the main shaft of <i>Krespa</i> surge tank (<i>Richter</i> [43])	189
Figure 6-95: Waterfall-dampening device, section cut A-A (<i>Richter</i> adapted from <i>Lazar</i> [114]).....	190
Figure 6-96: Waterfall-dampening device, plan view (<i>Richter</i> adapted from <i>Lazar</i> [114])	190
Figure 6-97: Waterfall-dampening device, prototype of surge tank <i>Krespa</i> (courtesy of Illwerke AG).....	191
Figure 6-98: Reinforcement and blind formwork of the perforation in the cantilever plate (footage of construction: youtube.com: Obervermuntwerk II - viertes Baujahr 2017 [219]	191
Figure 6-99: Measurement equipment for operational survey in the <i>Krespa</i> surge tank, installed by Illwerke AG	193
Figure 6-100: Comparison: 1D-numerical simulation and measurement of water level for 1-machine unit operation PSH <i>Obervermuntwerk II</i> , Headrace Di 6.8 m Surge Tank Di 17.0 Lines: Load-case prototype measurement versus simulation with expected and model test measured throttle losses (<i>Richter</i> [45])	194
Figure 6-101: Comparison: 1D-numerical simulation and measurement of water level for 1-machine unit operation PSH <i>Obervermuntwerk II</i> , Headrace Di 6.8 m Surge Tank Di 17.0 Lines: Load-case prototype measurement versus simulation with expected headrace loss and 10 % reduced throttle loss; Load-case prototype ideal with 80 m ³ /s simulation with expected headrace loss and 10 % reduced throttle loss - design case (<i>Richter</i> [45]).....	195
Figure 6-102: Resonance load-case event for 2-machine operation near capacity level of the upper reservoir, measurement of the surge tank <i>Krespa</i> (<i>Richter</i> [45], modified)	196
Figure 6-103: Comparison of the resonance load-case measurement of the surge tank <i>Krespa</i> and 1D-numerical simulation (<i>Richter</i> [45], modified).....	197

LIST OF TABLES

Table 2-1: Examples of dynamic market options at EEX [9].....	28
Table 2-2: Qualitative comparison matrix between Li-ion batteries and PSH	40
Table 2-3: Advantages of pumped storage hydropower [40]	41
Table 3-1: Data of example high-head HPP.....	55
Table 3-2: HPPs in Austria and the planned <i>Atdorf</i> PSH scheme in Germany with their schematic surge tank concepts (selection), (<i>Richter</i> [57] (modified).....	61
Table 3-3: Friction value conversion Strickler (K_{ST} [$m^{1/3}/s$])– Darcy Weisbach (f or λ [-]) – equivalent sand grain roughness (K_S [mm]) after Colebrook-White.....	70
Table 4-1: Key numbers of <i>Atdorf</i> PSH	78
Table 4-2: Key numbers of <i>Reisseck II</i> PSH [28].....	81
Table 4-3: Key numbers of <i>Obervermuntwerk II</i> PSH [28]	82
Table 4-4: Key numbers of <i>Tonstad</i> HPP (source: <i>Sira-Kvina</i>)	86
Table 5-1: Dimensionless numbers for hydraulic model tests.....	88
Table 6-1: Air cushion chambers in Norway [164], China [170] and Vietnam [171]	122
Table 6-2: Throttle development procedure	154